SANDIA REPORT

SAND2013-2388
Unlimited Release
Printed May 2013

Nuclear Power Plant Cable Materials: Review of Qualification and Currently Available Aging Data for Margin Assessments in Cable Performance

Mathew C. Celina, Kenneth T. Gillen, and Eric R. Lindgren

Prepared by
Sandia National Laboratories
Albuquerque, New Mexico 87185 and Livermore, California 94550

Sandia National Laboratories is a multi-program laboratory managed and operated by Sandia Corporation, a wholly owned subsidiary of Lockheed Martin Corporation, for the U.S. Department of Energy's National Nuclear Security Administration under contract DE-AC04-94AL85000.

Approved for public release; further dissemination unlimited.

Sandia National Laboratories

Issued by Sandia National Laboratories, operated for the United States Department of Energy by Sandia Corporation.

NOTICE: This report was prepared as an account of work sponsored by an agency of the United States Government. Neither the United States Government, nor any agency thereof, nor any of their employees, nor any of their contractors, subcontractors, or their employees, make any warranty, express or implied, or assume any legal liability or responsibility for the accuracy, completeness, or usefulness of any information, apparatus, product, or process disclosed, or represent that its use would not infringe privately owned rights. Reference herein to any specific commercial product, process, or service by trade name, trademark, manufacturer, or otherwise, does not necessarily constitute or imply its endorsement, recommendation, or favoring by the United States Government, any agency thereof, or any of their contractors or subcontractors. The views and opinions expressed herein do not necessarily state or reflect those of the United States Government, any agency thereof, or any of their contractors.

The views, opinions and recommendations expressed herein are those of the authors subject to currently available information that may neither be comprehensive nor accurate in all aspects.

Printed in the United States of America. This report has been reproduced directly from the best available copy.

Available to DOE and DOE contractors from
U.S. Department of Energy
Office of Scientific and Technical Information
P.O. Box 62
Oak Ridge, TN 37831

Telephone: (865) 576-8401
Facsimile: (865) 576-5728
E-Mail: reports@adonis.osti.gov
Online ordering: http://www.osti.gov/bridge

Available to the public from
U.S. Department of Commerce
National Technical Information Service
5285 Port Royal Rd.
Springfield, VA 22161

Telephone: (800) 553-6847
Facsimile: (703) 605-6900
E-Mail: orders@ntis.fedworld.gov
Online order: http://www.ntis.gov/help/ordermethods.asp?loc=7-4-0#online

SAND2013-2388
Unlimited Release
Printed May 2013

Nuclear Power Plant Cable Materials: Review of Qualification and Currently Available Aging Data for Margin Assessments in Cable Performance

Mathew C. Celina, Kenneth T. Gillen
Materials Characterization Dept. 1819

Eric R. Lindgren
Advanced Nuclear Fuel Cycle Technology Dept. 6223

Sandia National Laboratories
P.O. Box 5800
Albuquerque, New Mexico 87185, U.S.A.

Abstract

A selective literature review was conducted to assess whether currently available accelerated aging and original qualification data could be used to establish operational margins for the continued use of cable insulation and jacketing materials in nuclear power plant environments. The materials are subject to chemical and physical degradation under extended radiation-thermal-oxidative conditions. Of particular interest were the circumstances under which existing aging data could be used to predict whether aged materials should pass loss of coolant accident (LOCA) performance requirements.

Original LOCA qualification testing usually involved accelerated aging simulations of the 40-year expected ambient aging conditions followed by a LOCA simulation. The accelerated aging simulations were conducted under rapid accelerated aging conditions that did not account for many of the known limitations in accelerated polymer aging and therefore did not correctly simulate actual aging conditions. These highly accelerated aging conditions resulted in insulation materials with mostly 'inert' aging processes as well as jacket materials where oxidative damage dropped quickly away from the air-exposed outside jacket surface. Therefore, for most LOCA performance predictions, testing appears to have relied upon heterogeneous aging behavior with oxidation often limited to the exterior of the cable cross-section – a situation which is not comparable with the nearly homogenous oxidative aging that will occur over decades under low dose rate and low temperature plant conditions.

The historical aging conditions are therefore insufficient to determine with reasonable confidence the remaining operational margins for these materials. This does not necessarily

imply that the existing 40-year-old materials would fail if LOCA conditions occurred, but rather that unambiguous statements about the current aging state and anticipated LOCA performance cannot be provided based on original qualification testing data alone. The non-availability of conclusive predictions for the aging conditions of 40-year-old cables implies that the same levels of uncertainty will remain for any re-qualification or extended operation of these cables. The highly variable aging behavior of the range of materials employed also implies that simple, standardized aging tests are not sufficient to provide the required aging data and performance predictions for all materials. It is recommended that focused studies be conducted that would yield the material aging parameters needed to predict aging behaviors under low dose, low temperature plant equivalent conditions and that appropriately aged specimens be prepared that would mimic oxidatively-aged 40- to 60- year-old materials for confirmatory LOCA performance testing.

This study concludes that it is not sufficient to expose materials to rapid, high radiation and high temperature levels with subsequent LOCA qualification testing in order to predictively quantify safety margins of existing infrastructure with regard to LOCA performance. We need to better understand how cable jacketing and insulation materials have degraded over decades of power plant operation and how this aging history relates to service life prediction and the performance of existing equipment to withstand a LOCA situation.

Executive Summary - Key Conclusions and Recommendations

Previous reports on aging and loss of coolant accident (LOCA) performance of polymeric cable and insulation materials under radiation-thermal-oxidative conditions, as encountered during their application in nuclear power plants, have been reviewed. Existing data were examined to establish whether long-term degradation under these environmental conditions is a concern and whether the evolving oxidative material aging is sufficiently covered within the original LOCA cable qualification testing (IEEE Std. 323-1974 standard and guidance in Regulatory Guide 1.89). This review addresses the question whether any remaining operational margins could be determined and whether predictions could be made that would suggest satisfactory LOCA performance of 40- to beyond 40-year-old materials. The following opinions, conclusions and recommendations are provided:

- We believe there is an unresolved discrepancy between (1) the complexity of polymer degradation and knowledge gained in the field of 'polymer aging' and (2) the more engineering-based testing approaches incorporated into standardized methods for lifetime prediction purposes of many polymeric materials. Limited highly accelerated testing methods using a few data points and relying on linear Arrhenius-type extrapolations do not always reproduce homogeneous degradation processes and do not accommodate mechanistic changes, and irregular temperature dependencies, which originate from polymer-specific material properties under oxidative radiation exposure conditions (i.e. "inverse temperature phenomena", where effective degradation proceeds faster at lower than prescribed high testing temperatures). This means that for some materials exposed to highly accelerated aging conditions, the predicted aging state and associated performance are insufficiently understood. Further research is needed to better understand the aging behavior, LOCA performance and potential remaining margins for non-diffusion-limited oxidation (DLO) aged cables that would mimic specimens under plant conditions.

- For those reasons, we believe that a single, rapid accelerated test method, as applied in IEEE Std. 323-1974, for lifetime simulation of a multitude of materials with different aging characteristics involves identification of unsubstantiated assumptions about the prevailing degradation pathways and perceived material aging state which creates uncertainty for subsequent LOCA performance interpretation. The IEEE Std. 383-2003 recognizes limitations subject to material-specific features such as DLO, dose rate and synergistic effects, but besides emphasizing considerate approaches, does not offer detailed guidance on how to address these issues for lifetime prediction purposes.

- Qualification testing conducted according to the IEEE Std. 323-1974 does not provide, in most cases, predictive values for long-term low temperature, low dose rate plant operating conditions. The IEEE Std. 323-1974 qualifies new materials by a high temperature, high dose rate LOCA simulation. This approach has some intrinsic limitations. A pre-aged material state is not a requirement but is recommended to be considered as an evaluation of a specific design and application. It is recognized that ongoing aging is part of environmental exposure and that materials qualification should be addressed by additional operating experience and analysis as part of ongoing qualification requirements.

- Optional additional test margins, as described in IEEE Std. 323-1974, with slightly higher temperature, pressure or radiation exposure applied do not translate into additional margins

for extended lifetime purposes since appropriate scientific methods do not exist for extrapolation of mostly inert aging tests to long-term oxidative aging.

- Neither qualification testing nor previous accelerated aging studies have satisfactorily dealt with 'inverse temperature' phenomena, where for some cable materials it has been shown that aging processes proceeded much faster than expected at typical operating plant conditions.
- Under highly accelerated dose rate and/or temperature conditions, cable insulations will often experience essentially 'inert aging,' whereas cable jackets will experience only partial oxidation with the equilibrium oxidation at the air-exposed outside jacket surface dropping to lower or non-existent values with depth. This contrasts with what occurs in the plant environment, where equilibrium oxidation proceeds throughout both the insulation and jacket materials.
- Under oxidative plant conditions, some jacketing materials may provide sufficient protection, thereby reducing oxidation rates for interior cables, which could then potentially age under inert-dominated conditions. Additional data are required to confirm if such trends exist and under what conditions qualification testing could provide guidance for cable assemblies for predictive purposes. Similarly, in situations where cables are permanently protected in inert N_2 environments, qualification testing and previous accelerated aging studies will have some extrapolative value for performance and margins. However, some additional lower temperature, lower dose rate data would offer more confidence in such situations.
- Based on a review of data for CSPE, CP, XLPO, EPR/EPDM (defined in 'acronyms') materials from published reports and our experience with these materials, we conclude that margins for reasonably confident lifetime simulations cannot be established. This interpretation was obtained from a review of estimated oxidation rates under thermal and combined radiation-thermal conditions, estimated permeability for thermal conditions, and a comparison of the estimated importance of DLO under long-term NPP aging conditions versus highly accelerated sequential or combined aging conditions.
- The non-availability of critical data for quantification of current aging state, LOCA behavior and lifetime prediction implies caution for any re-qualification or extended operation of these materials. The highly variable aging behavior of the range of materials employed also implies that the current methodology for aging tests cannot deliver the required aging data and performance predictions with an emphasis on unusual individual material behavior.
- While cable performance in oxidative environments may be satisfactory, and additional margins may exist, they cannot be readily predicted or validated from existing qualification and aging studies, as those data sets do not provide all of the necessary information required for model input. Some guidance on cable aging behavior under plant conditions can be obtained from existing data, but for many materials and conditions additional measurements will be required to establish appropriate predictive capabilities.
- Satisfactory LOCA performance of oxidatively aged cables currently in plant use may occur, but it should not be assumed based on original qualification testing. An 'inert'

versus oxidative pre-aged state of the material could affect LOCA performance to a degree that is currently not quantified.

- While cable lifespans may well exceed current licensed lifetimes under operational conditions, predictions of extended operational life must be treated with cognizance that the uncertainty bounds are not quantified.

Recommendations:

- Initiate an aging study for a number of representative materials from operating plants with a focus on plant-equivalent low dose rate, low temperature oxidative exposure conditions to obtain oxidation rates, oxygen permeation, and rate predictions as a function of depth. Couple such experiments with trends in mechanical properties. Use such data as input for newly developed FE models to enable DLO predictions for circular geometries and complex cable assemblies. Gain an understanding of material oxidation sensitivities at these conditions.

- Develop new dose to equivalent damage (DED) analytical models that will utilize measurements of effective oxidation rate and DED data trends from combined radiation-thermal environments. Such an approach may enable predictions based on multi-parameter fits to comprehensive data sets and may accommodate deviations from linear Arrhenius behavior or constant DED failure level assumptions. It may also simulate dose rate effects and changes in oxidation levels for equal mechanical property damage as a function of temperature, i.e. when inverse temperature effects prevent linear extrapolations.

- Investigate opportunities for wear-out aging studies involving aged plant specimens. Assess current material aging state by acquiring samples from nuclear power plants (NPPs) and applying wear-out aging or condition evaluations. By conducting accelerated aging of field-aged specimens, probe for fractional damage and information on remaining margins. Such approaches would have to rely on a clear definition of past and future environmental conditions (dose rate, total dose, temperature, and oxygen availability). Since some of these materials are subject to inverse temperature phenomena enhanced temperature exposure will be problematic as an avenue for further acceleration.

- For LOCA planning purposes and preparation of ‘pre-aged’ specimens, acquire additional model input data first and validate aging models. Conduct appropriate measurements to yield additional oxidation parameters that will enable model development and well-characterized and suitable samples to be prepared prior to any additional cable aging studies and LOCA exposure testing.

- Conduct new LOCA performance tests using lesser thermal and radiation acceleration factors to produce more homogeneously aged material specimens with an oxidative aging history that would closely mimic plant environments.

- Raise awareness of these issues in the community dealing with polymer aging, lifetime prediction, performance assessments and testing standards related to NPP materials. Recognize that the issues discussed here have implications for current aging state of these materials and re-qualification or lifetime extension requirements.

Scope of this Review

This study was initiated by the NRC. Sandia National Laboratories was tasked to examine the existing research data and original qualification testing methods for cable insulation and jacketing materials used in nuclear power plants. The opinions presented in this study should provide a perspective on the technical gaps associated with the original cable qualification approaches and the consequences of the currently known aging behavior of these materials on lifetime prediction and operational margins. Of key interest was whether the existing literature and our current knowledge of the degradation processes under radiation-thermal-oxidative conditions could be used to establish additional margins for a re-qualification of these materials as part of extended plant operation. Where problems were perceived, we were asked to emphasize the existing knowledge gaps and suggest additional research efforts that should provide more guidance on how cables may age and any remaining operational margins.

The NRC projected that aging trends published in a number of previous studies, as discussed in this report, coupled with better defined environmental conditions from over 40 years of operation in existing NPPs should provide guidance for establishing additional operational margins or demonstrate the existing limitations in our collective aging knowledge. This study defines the challenges in correlating often severe accelerated aging conditions, as applied in the IEEE Std. 323-1974 cable qualification testing, with the actual radiation-thermal-oxidative environmental conditions encountered in the plant environment. High dose rate conditions as applied within the IEEE Std. 323-1974 test regime results in mostly inert aging mechanisms especially for cable insulations, whereas during plant use, cable jackets and insulations will typically age under oxidative degradation processes. Of particular note is whether sufficient knowledge exists to define additional performance margins under low dose rate, low temperature oxidative conditions. This study intends to critically examine qualification testing approaches, the key existing literature reports dealing with predictive aging of cable materials, and our interpretation of the most likely aging scenarios for lifetime simulation purposes.

Acknowledgements

We acknowledge the help of Angela Dayile and Nicholas Giron with some editorial tasks for the preparation of this report. Adam Quintana is recognized for improved visualization models of aging trends in combined radiation-thermal environments and DLO behavior. The lead author thanks Ken Gillen for dedicating some of his retirement time to the preparation of this document and his lifelong commitment to a scientific approach and thoroughness in the complex field of polymer degradation. We also acknowledge Fred Gelbard who assisted as the project manager and financial administrator. NRC financial support for this study is gratefully recognized. This report went through a detailed review by the NRC prior to publication that resulted in challenges to some of the author's opinions, clarifications and additional comments.

Contents

Executive Summary - Key Conclusions and Recommendations ..... **iii**

Scope of this Review ..... **vi**

Report Overview ..... **ix**

Table of Figures ..... **x**

Table of Tables ..... **xvii**

Acronyms ..... **xviii**

1 Lifetime Prediction of Polymeric Materials in Radiation-Thermal-Oxidative Environments **1**

1.1 Introduction to Accelerated Aging Studies and Lifetime Prediction 1
1.2 Discussion of Lifetime Prediction Approaches and Models 3
1.2.1 Degradation and Lifetime Prediction of Cable and Jacketing Materials 5
1.2.2 Accelerated Aging as Relevant to Cable Lifetime Prediction 9
1.3 Performance Predictions from Highly Accelerated Qualification Conditions versus Actual Conditions Encountered in the Plant 16
1.4 Comments on Margin Assessments 18
1.5 Accelerated Aging Studies and LOCA testing: The Key Message from other Studies 21
1.6 Wear-out Aging Study to assist in Margin Determination 24
1.7 Complications Introduced by Inverse Temperature Behavior 27

2 Literature Review of Previous LOCA Testing Approaches and Recommendations **31**

2.1 LOCA Testing Overview 32
2.2 LOCA Testing Issues 34
2.2.1 Radiation dose-rates during LOCA tests 34
2.2.2 Dose rate recommendation 36
2.2.3 Simultaneous vs. sequential testing and air flow during LOCA 36
2.2.4 LOCA test sequence recommendation 38
2.2.5 Oxygen enrichment for aging acceleration 38
2.3 Summary 39

3 Estimates of Margins in Past and Future Aging Simulations of Safety-related Cables **41**

3.1 Introduction 41
3.2 Effects of Oxidation on Cable Degradation 41
3.3 Diffusion-Limited Oxidation (DLO) Modeling 47
3.4 Estimates of Oxidation Rate for Thermal Aging Conditions 51
3.4.1 Chlorosulfonated Polyethylene (CSPE) Jackets 51
3.4.2 Chloroprene (CP) Cable Jackets 54
3.4.3 Crosslinked Polyolefin (XLPO) Cable Insulation Materials 57
3.4.4 EPR/EPDM Cable Insulation Materials 64
3.5 Estimates of Oxidation Rate for Combined Radiation plus Thermal Aging Conditions 67
3.5.1 Chlorosulfonated Polyethylene (CSPE) Jackets 68

3.5.2 Chloroprene (CP) Cable Jackets 71
3.5.3 Crosslinked Polyolefin (XLPO) Cable Insulation Materials 72
3.5.4 EPR/EPDM Cable Insulation Materials....75
3.6 Estimates of P_{Ox} under Thermal Aging Conditions 77
3.7 Estimates of the Importance of DLO for Selected Aging Conditions 80
3.8 Estimation of DLO Effects under Long-Term Ambient Nuclear Power Plant Aging Conditions 81
3.9 Estimation of DLO Effects under the High Acceleration Sequential Aging Conditions used in Historic Qualifications....83
3.10 Estimation of DLO Effects under the Combined Environment Conditions used by Jacobus [68-70] 88
3.11 Development of Combined Environment Aging Conditions for Future Experiments 92
3.12 Inverse Temperature Effects 96
3.13 Conclusions of Margin Assessments 99

4 Recommendations for New Research Activities....101
4.1 Approach towards Additional Aging Studies 101
4.2 Targets for Aging Model Development and Expected Impact 103
4.3 Discussion of Required Future Work 105

5 Conclusions....109

6 Background of our SNL R&D Team 113

7 References....115

Report Overview

This report is structured into four sections:

(1). An overview and discussion of radiation-thermal-oxidative degradation phenomena and accelerated engineering-based testing for lifetime prediction purposes of cable insulation and jacketing materials in NPP environments. (Responsible author: M. Celina)

(2). A literature review of previous LOCA testing methods and variations in these accelerated testing protocols. A perspective on the definition of 'pre-aged specimens' and subsequent LOCA conditions. Recommendations for a more appropriate LOCA testing approach and preparation of more suitable 'pre-aged specimens' to be conducted as part of an additional experimental program. (Responsible author: E. Lindgren)

(3). A literature review of existing cable aging data to evaluate the specific oxidative degradation parameters that are currently available. These data are needed for model input and lead to predictions of differences between historical LOCA testing regimes and the aging condition of existing cable materials. This assessment includes an approach towards the quantification of the uncertainties associated with any margin classification. It includes a critical evaluation of the results from previous studies that would qualify to serve as model input, with recommendations on additionally required information where significant knowledge gaps exist. (Responsible author: K. T. Gillen)

(4). Recommendations for an experimental program that will yield a better understanding of the underlying behavior of cable insulation and jacketing materials under low dose rate, low temperature oxidative conditions encountered in nuclear power plant environments. This includes a discussion of the required experimentally-derived parameters that would allow for the development of new models for long-term aging behavior and performance predictions. In parallel, wear-out aging studies on existing materials (i.e. 40 year-old samples) could be conducted to establish more confidently the operational margins of existing materials. Future work should involve a clear definition of the operational boundaries and environmental conditions (dose rate, total dose, temperature, and oxygen availability) throughout the cable's history and establish the expected exposure conditions for future plant operation. (Responsible author: M. Celina)

Table of Figures

Page

Figure 1a, b. DED and TED plot versus dose rate for E_a = 80 kJ/mol for a theoretical set of parameters defined above. 11

Figure 2. Corresponding fractional degradation, i.e. the thermal (predominant at low dose rates) and radiative components (at high dose rates) of the combined degradation process. 12

Figure 3a, b. The effective oxidation rate for the combined degradation process. For 50°C at low dose rates (left Figure) the rate approaches 3.17e-13 mol/g-s, i.e the thermal only conditions . For high dose rates (right Figure) the rate settles on 1e-9 mol/g-Gy as defined for the situation that was modeled. 12

Figure 4a, b. DED and TED plot versus dose rate for E_a = 50 kJ/mol for a theoretical set of parameters discussed above. 13

Figure 5. Corresponding fractional degradation, i.e. the thermal (predominant at low dose rates) and radiative components (at high dose rates) of the combined degradation process. 13

Figure 6a, b. DED and TED plot versus dose rate for E_a = 100 kJ/mol for a theoretical set of parameters discussed above. 14

Figure 7. Corresponding fractional degradation, i.e. the thermal (predominant at low dose rates) and radiative components (at high dose rates) of the combined degradation process. 14

Figure 8a, b. DED and TED plot versus dose rate for E_a = 80 kJ/mol for the theoretical set of parameters discussed above, but a radiative oxidation rate of 1e-8 mol/g-Gy. 14

Figure 9. Corresponding fractional degradation, i.e. the thermal (predominant at low dose rates) and radiative components (at high dose rates) of the combined degradation process. 15

Figure 10a, b. DED and TED plot versus dose rate for E_a = 80 kJ/mol for the theoretical set of parameters discussed above, but with failure defined as 1e5 Gy. At 50°C with an identical thermal rate of 3.17e-13 mol/g-s failure at thermal only conditions will therefore occur at 10 years. Note: Oxidative failure will now occur at 0.32% oxidation consistent with a 5 times lower total dose for identical radiative oxidation rate of 1e-9 mols/g-Gy. 15

Figure 11. Corresponding fractional degradation, i.e. the thermal (predominant at low dose rates) and radiative components (at high dose rates) of the combined degradation process. 16

Figure 12. Hypothetical results illustrating the types of dose-rate effects which can occur in radiation-aged polymeric materials: the dose to equivalent damage (DED) is plotted versus the dose rate (R). The curve labeled Inert (T_1 + R) gives results for samples aged in inert atmospheres at temperature, T_1, this curve must asymptotically approach the isochrone (labeled Inert – T_1 only) appropriate to inert aging in a thermal-only environment. The curves with air substituted for inert have identical meaning for aging in air environments. At high dose rates, diffusion-limited oxidation effects can become important, resulting in the eventual approach of the air results to the inert results (Figure reproduced from [23]) 20

Figure 13. Visualization of different oxidation degradation profiles as a function of dose rate for equal deposited doses (0.5 MGy) where x equals normalized position (thickness of 2 mm) and oxygen is present on the left side of the specimen. At low dose rates the material is uniformly oxidized. At the high dose rate of 10 kGy/h the oxidation is limited to the surface, the total amount of oxidized material across the specimen is less than 2.5% of that generated at 1 Gy/h. At 10 and 1 kGy/h the material is mostly irradiated under inert degradation conditions, i.e. no oxidation effects occur within the interior. 23

Figure 14. Oxidation rates and DED properties for Brandrex XLPO insulation material.... 29

Figure 15 (Left). Comparison of elongation results versus aging time at 150°C for an Okonite chloroprene (CP) jacket in an oxygen-containing environment (air) versus aging under inert conditions. 43

Figure 16 (Right). Comparison of elongation results versus aging time at 138°C for a Samuel Moore Dekoron chlorosulfonated polyethylene (CSPE) jacket in an oxygen-containing environment (air) versus aging under inert conditions (surrounding atmosphere of argon). 43

Figure 17. Comparison of elongation results versus aging time at 150°C for an Anaconda Flameguard ethylene propylene rubber (EPR) insulation in an oxygen-containing environment (air) versus aging under inert conditions..... 43

Figure 18 (Left). Tensile elongation results versus aging time at 100.9°C in air for an Anaconda Flameguard ethylene propylene rubber (EPR) insulation..... 44

Figure 19 (Right). Density profile results for the Anaconda Flameguard ethylene propylene rubber (EPR) insulation after the various indicated aging times at 100.9°C. 44

Figure 20. (Left) Density profile results for the Anaconda Flameguard ethylene propylene rubber (EPR) insulation after the various indicated aging times at ~170°C comparing aging in air versus aging in nitrogen. 45

Figure 21. (Right) Elongation results versus total aging dose for a Brandrex XLPO cable insulation aged at 200 Gy/h plus 22°C in air and in nitrogen. 45

Figure 22. (Left) Normalized elongation results versus total aging dose for an Anaconda Flameguard EPR cable insulation aged under the indicated radiation aging conditions. 46

Figure 23. (Right) Normalized tensile strength results versus total aging dose for an Anaconda Flameguard EPR cable insulation aged under the indicated radiation aging conditions. 46

Figure 24. Density profile results for the Anaconda Flameguard ethylene propylene rubber (EPR) insulation after radiation aging at 870 Gy/h in air versus aging in nitrogen. 46

Figure 25. Oxidation relative to the reference oxidation rate at the air-exposed surface plotted against the reduction in the dissolved oxygen concentration for the values of β_{ref} indicated on the plot. 48

Figure 26 (Left). Relative dissolved oxygen concentration versus relative position across sheet samples with air on one side and β_{ref} = 1 under air partial pressure conditions. Curves are shown for various values of α. 50

Figure 27(Right). Relative oxidation rate versus relative position across sheet samples with air on one side and β_{ref} = 1 under air partial pressure conditions. Curves are shown for various values of α. 50
Figure 28 (Left). Relative dissolved oxygen concentration versus relative position across sheet samples with air on one side and β_{ref} = 30 under air partial pressure conditions. Curves are shown for various values of α. 50
Figure 29 (Right). Relative oxidation rate versus relative position across sheet samples with air on one side and β_{ref} = 30 under air partial pressure conditions. Curves are shown for various values of α. 50
Figure 30 (Left). Tensile elongation results for a Samuel Moore CSPE cable jacketing material. 52
Figure 31 (Right). Time-temperature superposition of the elongation results from Figure 30 at a 70°C reference temperature (lower x-axis). The multiplicative shift factors used in the shifting are shown on the figure. The upper x-axis gives the time axis for the superposed data at 108°C. 52
Figure 32 (Left). Oxygen consumption rate results for Samuel Moore CSPE versus aging time at the indicated aging temperatures. 52
Figure 33 (Right). Oxygen consumption results for Samuel Moore CSPE obtained by integrating the results from Figure 32. 52
Figure 34 (Left). Time-temperature superposition at 37°C (lower x-axis) of the integrated oxygen consumption results from Figure 33. The multiplicative shift factors are shown on the figure. 53
Figure 35 (Right). Arrhenius plot of the shift factors for elongation for nine different CSPE jackets and the shift factors for oxygen consumption for two different CSPE jackets (all data normalized at 100°C). 53
Figure 36 (Left). Tensile elongation results for a Rockbestos CP cable jacketing material. 55
Figure 37 (Right). Time-temperature superposition of the elongation results from Figure 36 at an 80°C reference temperature (lower x-axis). The multiplicative shift factors used in the shifting are shown on the figure. The upper x-axis gives the time axis for the superposed data extrapolated to 25°C. 55
Figure 38 (Left). Time-temperature superposition at 25°C (lower x-axis) of the integrated oxygen consumption results for Rockbestos CP jacket [14]. The multiplicative shift factors are shown on the figure. 55
Figure 39 (Right). Arrhenius plot of the shift factors for elongation and oxygen consumption for the Rockbestos CP jacket (all data normalized at 80°C). 55
Figure 40 (Left). Tensile elongation results for an Okonite CP cable jacketing material. 56
Figure 41 (Right). Time-temperature superposition of the elongation results from Figure 40 at an 24°C reference temperature. The multiplicative shift factors used in the shifting are shown on the figure. 56
Figure 42. Arrhenius plot of the shift factors for elongation for the Okonite CP jacket. 57
Figure 43. Scan of Brandrex XLPO insulation material at 5°C/min under Ar. [53]. 58
Figure 44 (Left). Elongation versus time at the indicated temperatures for Brandrex XLPO insulation cable insulation material. 59
Figure 45 (Right). Time-temperature superposed elongation results at a reference temperature of 99°C for the 99°C and 109°C data of Brandrex XLPO cable insulation. 59

Figure 46 (Left). Time-temperature superposition of the oxygen consumption results for Brandrex XLPO insulation using the empirically derived shift factors shown on the figure. 59
Figure 47 (Right). Arrhenius plot of the O_2 consumption shift factors for Brandrec XLPO insulation from the elongation results in Figure 45 and the oxygen consumption results from Figure 46 59
Figure 48. DSC scan of the Rockbestos XLPO cable insulation at 5°C/min under Ar [54]. All three conductor colors have the same DSC trace. 60
Figure 49 (Left). Elongation versus time at the indicated temperatures for black-colored Rockbestos XLPO insulation cable insulation material. 61
Figure 50 (Right). Elongation versus time at the indicated temperatures for green-colored Rockbestos XLPO insulation cable insulation material. 61
Figure 51 (Left). Elongation versus time at the indicated temperatures for red-colored Rockbestos XLPO insulation cable insulation material. 61
Figure 52 (Right). Time-temperature superposed elongation results for the black Rockbestos XLPO insulation at a reference temperature of 124°C from Figure 49. 61
Figure 53 (Left). Time-temperature superposed elongation results for the green Rockbestos XLPO insulation at a reference temperature of 124°C from Figure 50. 62
Figure 54 (Right). Time-temperature superposed elongation results for the red Rockbestos XLPO insulation at a reference temperature of 124°C from Figure 51. 62
Figure 55. Arrhenius plot of the shift factors derived for the three colors of the Rockbestos XLPO insulation. 62
Figure 56 (Left). Time-temperature superposition of the oxygen consumption results for green Rockbestos XLPO insulation using the empirically derived shift factors shown on the figure. 63
Figure 57 (Right). Arrhenius plot of the O_2 consumption shift factors for green Rockbestos XLPO insulation from the elongation results in Figure 53 and the oxygen consumption results from Figure 56. 63
Figure 58. DSC scans of four different EPR cable insulation materials at 5°C/min under Ar [54]. 65
Figure 59. Arrhenius plots of the times required for the elongation to drop to 50% absolute for six EPR cable insulation materials. 65
Figure 60 (Left). Time-temperature superposition of the oxygen consumption results for Anaconda Durasheeth EPR insulation using the empirically derived shift factors shown on the figure. 66
Figure 61 (Right). Arrhenius plot of the shift factors for oxygen consumption from Figure 60. 66
Figure 62 (Left). Combined environment data for Okonite CP jacket. The dose to 50% elongation is plotted versus dose rate with the aging temperature in °C of the experiment indicated by the numbers adjacent to the data points. Data plotted as triangles are in the region where DLO effects are important. 68
Figure 63 (Right). Time-temperature dose-rate superposition of the data from Figure 62 using the DED approach. 68

Figure 64. Time-temperature dose-rate superposition of data from six CSPE jacket materials at a reference temperature of 50°C (bottom x-axis) using the DED approach based on the shift factor data from Figure 35. 69
Figure 65 (Left). Same figure as Figure 64 except top x-axis is set for the time scale appropriate to 40°C. 70
Figure 66 (Right). Same figure as Figure 64 except top x-axis is set for the time scale appropriate to 70°C. 70
Figure 67 (Left). Oxygen consumption for CSPE to reach 100% elongation versus dose rate at 50°C. 71
Figure 68 (Right). Estimates of $\phi[O_2]_{ref}$ versus combined environment aging conditions at five different aging temperatures for CSPE jacket materials. 71
Figure 69 (Left). Time-temperature dose-rate superposition of the Rockbestos Firewall III CP jacket results (filled circles) added to the Okonite results from Figure 63. The bottom x-axis corresponds to the predictions at 50°C whereas the top x-axis relates to predictions at 25°C. 72
Figure 70 (Right). Estimates of $\phi[O_2]_{ref}$ versus combined environment aging conditions at five different aging temperatures for a Rockbestos CP cable jacketing material. 72
Figure 71 (Left). Combined environment data for Brandrex XLPO insulation. The dose to 100% elongation is plotted versus dose rate with the aging temperature in °C of the experiment indicated by the numbers adjacent to the data points. ... 74
Figure 72 (Right). Time-temperature dose-rate superposition of the data from Figure 71 using the DED approach. 74
Figure 73. Combined environment oxygen consumption rate results for Brandrex XLPO insulation at ~38 Gy/h versus the aging temperature. 74
Figure 74 (Left). Oxygen consumption for Brandrex XLPO to reach 100% elongation versus dose rate at 50°C. 75
Figure 75 (Right). Estimates of $\phi[O_2]_{ref}$ versus combined environment aging conditions at three different aging temperatures for a Brandrex XLPO cable insulation material. 75
Figure 76 (Left). Combined environment data for Anaconda Flameguard FR/EP insulation. The dose to 100% elongation is plotted versus dose rate with the aging temperature in °C of the experiment indicated by the numbers adjacent to the data points. 76
Figure 77 (Right). Time-temperature dose-rate superposition of the data from Figure 76 using the DED approach. 76
Figure 78. Estimates of $\phi[O_2]_{ref}$ versus combined environment aging conditions at three different aging temperatures for the Anaconda Flameguard EPR cable insulation material. 77
Figure 79. Comparison of P_{Ox} coefficient results for six different elastomeric sealing materials. 78
Figure 80 (Left). P_{Ox} results for a commercially formulated CSPE from ref. [106]. 79
Figure 81 (Right). P_{Ox} results for a commercially formulated CP from ref. [106]. 79
Figure 82 (Left). P_{Ox} results for two XLPO cable insulation materials. 79
Figure 83 (Right). P_{Ox} results for four EPR cable insulation materials. 79

Figure 84 (Left). Estimated profiles for oxygen concentration and oxidation rate across the Rockbestos cable under typical “worst-case ambient aging conditions..... 82
Figure 85 (Right). Estimated profiles for oxygen concentration and oxidation rate across the Anaconda or AIW cables under typical “worst-case ambient aging conditions. 82
Figure 86 (Left). Estimated profiles for oxygen concentration and oxidation rate across the Rockbestos cable under sequential 150°C aging conditions..... 83
Figure 87 (Right). Estimated profiles for oxygen concentration and oxidation rate across the Rockbestos cable under sequential 4500Gy/h plus 25°C aging conditions. 83
Figure 88 (Left). Estimated profiles for oxygen concentration and oxidation rate across the Anaconda cable under sequential 150°C aging conditions. 84
Figure 89 (Right). Estimated profiles for oxygen concentration and oxidation rate across the Anaconda cable under sequential 3600Gy/h plus 25°C aging conditions. 84
Figure 90. Estimated profiles for oxygen concentration and oxidation rate across the AIW cable under sequential 121°C aging conditions..... 85
Figure 91 (Left). Estimated profiles for oxygen concentration and oxidation rate across the 1/C Samuel Moore cable under sequential 121°C aging conditions. 86
Figure 92 (Right). Estimated profiles for oxygen concentration and oxidation rate across the 1/C Samuel Moore cable under sequential 7500Gy/h plus 25°C aging conditions. 86
Figure 93. Estimated profiles for oxygen concentration and oxidation rate across the 1/C Okonite cable under sequential 150°C aging conditions. 87
Figure 94 (Left). Estimated profiles for oxygen concentration and oxidation rate across the 1/C Okonite cable under the indicated combined environment aging conditions. 89
Figure 95 (Right). Estimated profiles for oxygen concentration and oxidation rate across the 3/C Samuel Moore cable under the indicated combined environment aging conditions..... 89
Figure 96 (Left). Estimated profiles for oxygen concentration and oxidation rate across the 3/C Rockbestos Firewall III cable under the indicated combined environment aging conditions..... 90
Figure 97 (Right). Estimated profiles for oxygen concentration and oxidation rate across the 3/C Brandrex cable under the indicated combined environment aging conditions. 90
Figure 98. Estimated profiles for oxygen concentration and oxidation rate across the 2/C BIW cable under the indicated combined environment aging conditions. 91
Figure 99 (Left). Estimated profiles for oxygen concentration and oxidation rate across the 3/C Brandrex cable under the indicated combined environment aging conditions using $\beta = 1$ for the XLPO insulation..... 94
Figure 100 (Right). Estimated profiles for oxygen concentration and oxidation rate across the 3/C Brandrex cable under the indicated combined environment aging conditions using $\beta = 20$ for the XLPO insulation..... 94

Figure 101 (Left). Estimated profiles for oxygen concentration and oxidation rate across the 3/C Samuel Moore Dekoron Polyset cable under the indicated combined environment aging conditions. 95
Figure 102 (Right). Estimated profiles for oxygen concentration and oxidation rate across the 3/C Rockbestos Firewall III cable under the indicated combined environment aging conditions. 95
Figure 103. Estimated profiles for oxygen concentration and oxidation rate across the 1/C Okonite cable under the indicated combined environment aging conditions. 96
Figure 104. Combined environment results for Brandrex XLPO at 41°C. 97
Figure 105 (Left). Estimated profiles for oxygen concentration and oxidation rate across the 3/C Brandrex cable under combined environment aging conditions of 41°C plus 30 Gy/h. 98
Figure 106 (Right). Estimated profiles for oxygen concentration and oxidation rate across the 3/C Brandrex cable under combined environment aging conditions of 41°C plus 100 Gy/h. 98

Table of Tables

Page

Table 1. Demonstration of theoretical oxidation estimation for a 2 mm thick insulation material in contact with air (left) ($ß_0$ = 1, $p(O_2)$=13.2cmHg) and inert conditions (right). Radiation exposure is simulated at different dose rates where homogeneity of 1 equals uniform degradation throughout. Radiation oxidation rate and permeability were chosen to be somewhat realistic. 22

Table 2. Estimation of oxidative damage levels corresponding to 100% elongation at a dose rate of 100 Gy/h for stripped Brandrex XLPO insulation aged under air. Most importantly, it shows the transition in failure oxidation levels between 40°C and 60°C (see bold numbers). 29

Table 3. Oxygen Consumption Rate Estimates for CSPE Jacket Materials 54

Table 4. Oxygen Consumption Rate Estimates for Rockbestos Firewall III CP Jacket. 56

Table 5. Oxygen Consumption Rate Estimates for Brandrex XLPO Insulation. 60

Table 6. Oxygen Consumption Rate Estimates for Rockbestos XLPO Insulation. 63

Table 7. Oxygen Consumption Rate Estimates for Anaconda Durasheeth EPR Insulation. 66

Table 8. Estimates of Oxygen Consumed to Reach 100% Elongation for CSPE Jackets. 69

Table 9. Estimates of Oxygen Consumed to Reach 100% Elongation for Brandrex XLPO. 73

Table 10. Estimates of Oxygen Consumed to Reach 100% Elongation for EPR Materials. 76

Table 11. Estimates of POx (ccSTP/cm/s/cmHg) versus Temperature. 79

Table 12. Estimates of $\phi[O_2]_{ref}$, P_{Ox} and their Ratio at 50°C plus 0.5 Gy/h 81

Acronyms

BWR	Boiling water reactor
DBE	Design basis events
CLPO	Cross-linked polyolefin
CLPE	Cross-linked polyethylene
CM	Condition monitoring
CP	Chloroprene
CPT	Control power transformer
CSPE	Chlorosulfonated polyethylene
DED	Dose to equivalent damage
DLO	Diffusion limited oxidation
EPR	Ethylene propylene rubber
EPDM	Ethylene propylene diene comonomer elastomer
eV	Electron volt
FE	Finite element
Gy	Unit for radiation dose, 1Gy = 100 rad
IEEE	Institue of Electrical and Electronics Engineers
ITB	Inverse temperature behavior, where the effective degradation rate is faster as the temperature is lowered
IR	Infrared spectroscopy
JAERI	Japan Atomic Energy Research Institute
LOCA	Loss of coolant accident
MOV	Motor operated valve
NMR	Nuclear magnetic resonance
NPP	Nuclear power plant
OIT	Oxygen induction time, used as a potential CM method
PET	Polyethyleneterephthalate, polyester polymer
PWR	Pressurized water reactor
RT	Room temperature, ambient temperature conditions
SCDU	Surrogate circuit diagnostic unit
SNL	Sandia National Laboratories
TED	Time to equivalent damage
TID	Total integrated dose
XLPO	Cross-linked polyolefin

Note: Wherever dose data are provided in this report, we expect the term ‘dose’ to relate to absorbed energy in the material rather than a nominal exposure dose.

1 Lifetime Prediction of Polymeric Materials in Radiation-Thermal-Oxidative Environments

1.1 Introduction to Accelerated Aging Studies and Lifetime Prediction

In general terms, polymer aging and degradation can be separated into two regimes of distinctly different processes that may occur in parallel or individually as a dominant degradation pathway. The two processes are physical relaxation due to molecular rearrangements subject to slow molecular mobility, and chemistry-driven degradation where the chemical makeup of the material changes due to specific chemical reactions depending on the environment and material constituents (i.e. its chemical make-up).

Physical relaxation behavior (stress relaxation under constant load or strain), will depend on internal stress state as well as applied mechanical load and temperature (as a result of electrical loading or environment, whichever is limiting), where elevated temperature will normally accelerate physical relaxation behavior significantly. Physical degradation processes often depend on the glass transition (T_g) or melting temperature (T_m) of a material, with temperatures above these transitions allowing for significant motion. Further, physical relaxation depends on the structure and makeup of a polymer network, and often even highly cross-linked materials like epoxies may have high T_g, but will slowly relax (mechanical creep) under significant load at RT (room temperature) rather than display immediate brittle fracture. This implies that on a nanoscale, the polymer has mobile chain fragments and larger domains that allow for the bulk material to slowly deform despite the polymer being frozen-in below T_g. Unfortunately, polymers are never ideal and homogeneous in their makeup and therefore relaxation processes are common even at low temperature. Polymers may adjust their state more quickly after processing, but if a material has built-in stress states in the long-term, it may lead to stress-cracking and hence a perceived aging behavior.

Physical relaxation in polymers is an intrinsic feature of molecular mobility, cross-link state or a response to stress buildup due to load, processing, cure or final shape of materials. For example, curable resins often contract somewhat during cure (density increases) associated with their crosslinking reactions. Thermoplastics processed with injection molding, for example, have a tendency to develop a memory effect induced by a flow-driven stress state prior to solidification. In composites, viscous flow and primary orientation stress states may appear in parallel with cure shrinkage, and can result in a more complicated scenario. Physical relaxation occurs virtually in all processed polymers and is accelerated by temperature. Purely physical relaxation phenomena such as creep and stress state adjustments are often called aging processes, but over time may also settle into new equilibrium states. A good example is the compression stress-relaxation behavior of O-ring or seal materials under mechanical load in the absence of thermo-oxidative or chemical attack. From a perspective of commonly encountered degradation in polymers, physical aging processes are often less important than property changes due to chemically-driven reactions, unless the best chemically inert materials are considered in niche applications under mechanical load. In structural applications, mechanical engineers are often more concerned about physical aging if materials with low chemical sensitivity, for example high density polyethylene, PVC (pressure pipes), or composite materials in benign environments are being used.

More important in polymer degradation, and certainly most relevant to the long-term degradation of safety-related cable insulation and jacketing materials under consideration here, are chemically-driven property changes due to thermo-oxidative, radiation (gamma or particulates), hydrolytic, or chemical attack. For example, polyolefins are notoriously sensitive to long-term oxidation, as are cross-linked elastomers containing unsaturation (residual carbon double bonds that are chemically sensitive to further reaction and oxidative aging) normally required for crosslinking reactions. Some good examples are rubber bands and O-rings that harden rapidly even at RT because they contain a high degree of unsaturation; or hoses, belts and similar items in automotive applications. Such materials require antioxidants to protect against thermo-oxidative degradation. Similarly, there are no polymers that are completely resistant to high energy radiation. High energy radiation exposure results in polymer radiation chemistry, where the specific follow-up reactions depend on the polymer type and intermediate free radicals.

Radiation above a few eV of photon energies will penetrate into a polymer and result in indiscriminate radiation chemistry. Chemical bonds will break via generation of free radicals, which in turn will reconfigure themselves, with scission or crosslinking of polymer molecules being the immediate outcome. In the presence of oxygen dissolved within the material, free radicals will combine with the oxygen and facilitate the incorporation of oxidative species that often lead to chain scission and densification as a precursor to embrittlement. It is not always possible to predict the likely behavior of a material under high energy radiation exposure. Extensive "polymer radiation chemistry" studies by experts in this field have been conducted to establish radiation chemical yields for scission and crosslinking behavior for numerous materials [1-6]. These are empirical measurements and while some analogies can be derived or materials can be grouped into classes with similar behaviors, extensive experimental work is required to establish radiation sensitivities as a function of dose rates, doses and environmental conditions (inert or oxidative). Generally, aromatic-based polymers (i.e. epoxies, polyimides, polyether ketones) perform better than aliphatic polymers (i.e. polybutadiene and derivatives, polypropylene), in terms of total radiation doses required for significant mechanical property changes to occur. A good literature base is available to rate the performance of individual polymer types under radiation as a function of total dose. There is no foolproof method available for predicting the underlying types of reactions that polymers may undergo under irradiation besides comparing with previous experimental data.

Often we can observe the relative importance of scission versus crosslinking when exposing the material to radiation under oxygen or nitrogen (inert conditions). In many materials (like polyolefins) inert irradiation may emphasize crosslinking, while scission, or at least the partial generation of low molecular weight chain fragments, is often associated with oxidative radiation chemistry. Most importantly, however, we need to recognize that inert versus oxidative conditions under irradiation are the key drivers to fundamentally different reactions and hence performance-determining criteria. For example, a polymer may do reasonably well under extended irradiation under nitrogen by slowly crosslinking and maintaining mechanical properties, but in comparison may do very poorly when oxygen is present. Oxidative degradation may quickly result in localized densification (incorporation of oxygen), more pronounced scission yields and a more rapid loss of mechanical properties for equal exposure doses. It is important to recognize that some materials may exist where radiation degradation may not significantly depend on inert or oxidative conditions (perhaps some highly cross-linked, mostly aromatic polymers). However, for the majority of polymers and in particular the

materials of interest in this report, we expect very different behaviors under inert versus oxidative conditions.

Throughout this report, we emphasize that as a consequence of highly accelerated radiation exposure, inert or near-inert conditions will often prevail for the insulation material and reduced oxidation typically occurs for the jackets. This implies that such highly accelerated exposures have minimal value for the performance prediction of a material under environments where oxidative conditions and therefore oxidatively driven polymer degradation is predominant.

Finally, a few comments on hydrolytic polymer degradation are necessary, where the polymer is sensitive to cleavage and hence a reduction in molecular weight subject to attack by a small reagent molecule, for example water, acid, alkaline, alcohols, amines, etc. Condensation polymers such as polyamides (Nylon), polyesters, polyurethanes and acid anhydride cured epoxies, for example, are sensitive to hydrolysis as the reverse reaction of their synthesis (esterification). De-esterification leading to chain cleavage is accelerated by stronger pH-levels, both acidic and alkaline, and the presence of moisture. It is important to recognize that even one hydrolysis step can result in a critical loss of molecular weight via chain scission. Useful mechanical properties often depend on maintaining molecular weights. A good example is stress cracking encountered in strongly alkaline washing conditions of PET bottles. Degradation initiates at the surface of the material due to hydrolysis and can quickly result in fracture propagation and mechanical failure. In comparison, cross-linked materials (such as XLPO, EPDM, Hypalon, or Neoprene) that are commonly used for cable insulation or jacketing, are not particularly sensitive to hydrolytic degradation because they usually do not include ester, amide, urethane, or similar functional groups. Silicone polymers, however, can undergo hydrolytic chain scission and crosslinking reactions. For most cable insulation materials the primary sensitivity is oxidative degradation subject to temperature and radiation exposure. Yet, under LOCA conditions (where steam at high temperatures is present), previously degraded materials may become sensitive to hydrolytic chain cleavage reactions involving in-chain ester containing species. Such processes could introduce an additional degradation pathway that may have to be considered for some specific materials. For example, evidence exists indicating that LOCA exposures can degrade oxidatively aged cable materials faster than materials with less or no oxidation [7].

1.2 Discussion of Lifetime Prediction Approaches and Models

There are several approaches used to predict the lifetimes of polymeric materials under thermal [8-21] and radiation environments [22-25]. The most common involves accelerated aging studies where the material of interest is exposed to environments that are more severe than seen in application situations, e.g. higher than ambient temperatures and/or higher radiation dose rates. The primary intent is to speed up the degradation rate. Degradation can be monitored by basic physical property changes such as tensile elongation and strength, elastic modulus, compression set, volume/density changes, creep behavior, or as bulk changes in the chemical makeup of the polymer, for example crosslink state, oxidation level, molecular mobility (for example from NMR molecular relaxation measurements), chain scission, or average molecular weights. Most importantly, all such approaches require the definition of failure for the polymer or an understanding of broad performance-limiting property changes. Accelerated aging studies should not be conducted unless such tests have been considered within pre-defined expectations

of the material and involve clearly understood acceptance criteria. There are generally no constraints in having to use specific degradation monitors, as long as the test method is consistent and does not change with exposure conditions. In fact, depending on what polymers are being investigated, degradation monitors often vary. The most important criterion for such applied testing is the sensitivity of the chosen parameter to aging-induced changes. The more sensitive the aging indicator is, the more meaningful data can be obtained in a given timeframe and also over a larger temperature range or larger range of the determining stress variable. The relationship between the environmental stress level and the degradation rate under accelerated conditions is then determined. With the assumption that this relationship remains unchanged down to ambient stress conditions, the accelerated results are then used to predict by extrapolation the lifetime under ambient or less severe conditions. This approach has been widely used for thermo-oxidative aging environments and usually involves the Arrhenius model, based on the fact that the chemistry underlying degradation often has an Arrhenius dependence on temperature [12]. As a limit to linear Arrhenius extrapolations, however, it has been established that the degradation chemistry underlying thermo-oxidation of many elastomeric polymers shows substantial evidence of non-Arrhenius behavior, reflecting the fact that the dominant reactions often change as a function of aging temperature [8,10-14,26-31]. Therefore, predictions from accelerated aging experiments must be viewed with caution unless they are supported with extensive and carefully analyzed results such as sensitive property measurements at temperatures near or approaching the ambient temperature. One such approach, involving an ultra-sensitive oxygen consumption technique capable of low temperature measurements in the normal extrapolation regime, has been described in several recent papers which emphasize the use of this method at SNL for many years [8,10,12,13,15,16].

A second approach, sometimes referred to as condition monitoring [14,17,32-39], follows the aging of a material under its accelerated or ambient environment by monitoring changes in some degradation parameter and correlating these changes with a key degradation variable that would reflect on the loss of the equipment's safety function (for example the tensile elongation). Correlations obtained under accelerated conditions can then be used to predict material property changes for ambient-aged materials under the assumption that the accelerated correlation remains valid under ambient conditions. If the CM parameter changes in some regular fashion, its time dependence can be used to estimate the remaining time to failure. For instance, if the property being followed decreases linearly with aging time, it is possible to estimate the lifetime of the material by extrapolating linearly to the failure point as defined. This method is still of value even if nonlinear relationships with monotonic changes are observed. Unfortunately, finding such a well-behaved degradation parameter is not always possible implying that direct use of condition monitoring results for predicting a material's remaining lifetime is usually not straightforward. In fact, the worst-case situation occurs when the material exhibits so-called ''induction-time'' behavior where the property changes very little until just before complete failure, when abrupt changes suddenly develop. In such cases, traditional condition-monitoring parameters will not anticipate when failure is about to occur. Condition-monitoring aging models with predictive value cannot be developed using this approach when materials display pronounced ''induction-time'' behavior, as discussed for example in the framework that resulted in the proposed 'Wear-out method' (discussed below) [18,19].

A third approach, the Wear-out method [18,19], in effect represents a combination of the condition-monitoring and accelerated aging approaches, in that it takes samples that have been

aged for various times under low environmental stresses (e.g. at ambient or low temperature aging condition T_a) and completes the aging under accelerated aging conditions (e.g., at the Wear-out temperature T_w). It is based on the concept that in some polymers degradation is mostly cumulative and failure will occur when sufficient damage accumulates. As shown in previous publications [18,19], a particularly simple situation occurs when the time-dependent shape of the degradation curves is the same at the two temperatures. In general, a situation where degradation curves have the same shape independent of the degradation stress level is referred to as a ‘‘stress-independent damage model.’’ For polymers aged in thermally-accelerated environments, a stress-independent damage model corresponds to the concept of time-temperature superposition [18], where the data at two temperatures can be superposed on the time axis by multiplying the times at one of the temperatures by a constant multiplicative factor [8,10-13,15,16,40,41]. In such cases aging models using incremental or fractional damage data with mathematical relationships can reliably predict lifetimes. When time-temperature superposition is valid, the same trends in degradation curves at lower stress levels will represent the shape of the degradation curve at the Wear-out temperature T_w (i.e. the accelerated condition). Fractional aging times or actual aging times spent at T_a are plotted versus the fractional aging times or the actual aging times required at T_w to reach failure. As discussed in relevant papers it has been shown that a non-predictable situation involving induction-time behavior can in principle be converted into predictive linear plots through the application of the cumulative damage concepts underlying the Wear-out approach [18,19].

1.2.1 Degradation and Lifetime Prediction of Cable and Jacketing Materials

As a good approximation, the degradation of cable and jacketing materials in NPP environments will depend on three important variables: the penetration of the reactive chemical agent into the material, in this case oxygen, and the magnitude and temperature dependence of the resulting radio-oxidatively induced chain scission and crosslinking reactions. As an addition, purely thermo-oxidative degradation at very low dose rates, as always encountered for polymers in the presence of oxygen, will have to be considered. It is clear that the combination of these processes is highly convoluted and the competing reactions in the transition regime between solely thermal- and radiation-dominated degradation will be difficult to predict. In this transition regime, apparent dose rate effects (caused by the transition from radiation-dominated degradation to thermal-dominated degradation) will appear, despite the fact that true dose rate effects may or may not be present. The situation is further complicated by catalytically active impurities, for example, copper traces at the conductor interface, halogenated flame retardant additives and the migration- or radiation-induced loss of antioxidants. Copper facilitates oxidative polymer degradation and hence at the conductor interface additional degradation mechanisms may apply [14,42]. For this reason the cable core conductors are often protected by tin. Halogenated flame retardants could act as a source of halogen free radicals that may interfere with the usual thermo-oxidative degradation pathways; little is known about possible mechanistic implications. Physical loss (migration) and radiation cleavage of antioxidants will represent parallel degradation mechanisms that are outside the thermo-oxidative description, but may add to overall degradation rates. If it wasn’t for thermo-oxidative degradation in the absence of radiation, plus thermally-driven follow-up reactions from limited radiation initiation events, lifetime predictions as a function of dose rate alone might often be reasonably straightforward. It is this low temperature, low dose rate regime that is difficult to predict and requires extensive experimental examination. It is the area of key concern that must be

well-understood for lifetime predictions and margin assessments. Most importantly, the high temperature, high dose rate aging simulations used in qualification testing normally do not provide guidance on degradation rates in actual plant environments as discussed later in this report.

Rather than conducting empirical rapid aging studies using predefined sample numbers, statistical analysis and varying exposure matrices as has been conducted in the past, we believe a much deeper understanding of the degradation pathways is required to develop reliable predictive aging models for these conditions. We require an understanding of the critical fundamental processes, which is one of the goals of this review, and any future work should be focused towards bridging the holes where serious knowledge gaps exist. Without that information, more empirical-based testing of specimens by focusing purely on changes in mechanical properties or LOCA performance of 'aged specimens,' for that matter, will not deliver substantiated predictive capabilities. One example is the aging and lifetime prediction of elastomers, where only oxidation rate-based approaches over a large temperature range conclusively showed that curvature in the Arrhenius plots was due to mechanistic changes as a function of temperature and was critically important for extrapolation [8,9,12-14,16-21,32,33,40,43-54]. Lifetimes at lower temperatures are in fact much shorter than was predicted based on existing engineering testing (i.e. loss of elongation or elasticity for rapidly thermally-aged specimens) [11-13]. Additional pitfalls of aging exposure at high temperatures and/or dose rates are the complications introduced by diffusion limited oxidation (DLO) conditions, where the degradation process may develop into 'inert aging' with limited predictive value [9,10,49]. In summary, such studies emphasized the issues where many other research groups have been missing the key challenges for extrapolations for many years. Up to this point, reliable lifetime prediction centered on more engineering-based approaches, such as compression set, hardness and similar mechanical evaluations did not exist. Understanding the key degradation process will result in more reliable extrapolation models.

To develop reliable extrapolation models and predictive capabilities a solid understanding of the following is required:

(1). **The diffusion of reactive oxygen into the material as a function of temperature**. This is a physical process that as a complicating matter is also expected to depend somewhat on degradation levels since the chemical environment will change and in turn affect the O_2 permeation rate. Penetration of the oxygen reagent will control the degree to which surface initiation or homogenous bulk property changes will develop. Knowing this process allows us to understand the basis for stress cracking and loss of mechanical properties as a function of depth and to establish the degradative differences between qualification tests and plant environments.

(2). **The ingress and importance of moisture for LOCA performance evaluation.** Does the presence of moisture contribute to LOCA failure and under what circumstances? Most cable insulation and jacketing materials are relatively non-polar, i.e. are based on polyethylene and similar hydrocarbon based polymers that will not take up much water. However, this property will change with aging; oxidation products generally are hydrophilic and will facilitate water uptake. While LOCA testing of pre-aged cables in the past has usually been conducted on partially oxidized jackets and un-oxidized or

weakly oxidized insulation (i.e. DLO controlled pre-aging), fully aged specimens with higher levels of oxidation products may be more sensitive to the subsequent LOCA environment [7]. Therefore it is necessary to gain some understanding of the water interaction behavior as part of the polymer degradation process during low dose rate, low temperature exposure and its correlation with LOCA performance while steam is present. This would have direct impact on any margins extracted from the performance of mostly 'inert' pre-aged LOCA specimens by showing why they would not be reliable.

(3). **The dependence of oxidation reactions on temperature to establish activation energies and support degradation models with relevant acceleration factors.** This is the core of any extrapolation model and validates to what degree short exposures at higher temperatures can yield extrapolative meaning at all. It sets the constraints and the framework for any predictive models. It is similar to demonstrating that accelerated aging of elastomers conducted under DLO conditions at high temperatures, which most engineering groups have done for years, is fundamentally unsuitable for lifetime prediction and can only deliver the intended extrapolative capabilities under considerable constraints. Degradation under radio-thermo-oxidative conditions is subject to similar limitations. In fact, it is even more complex, because thermal oxidation and radiation-initiated oxidation compete and the underlying reactions interact. The outcome of not knowing the relevant framework and conducting exposure and aging under little understood conditions is evident in the previous studies under review (see discussion in section 3). Such work does not deliver strong extrapolative value. Extrapolation models must be validated based on applicability under specific exposure conditions, and must show the basis for their claim to deliver useful predictions.

While there is much emphasis in existing studies on activation energies, and different groups may argue about which values may better describe a material under certain conditions or which data taken from a specific test method should be trusted, it is important to realize that such activation energies can only truly describe the temperature regime for which they were determined. No matter what the actual activation energies are, aging models require support for what the <u>activation energies should be in the regime to be extrapolated.</u> Most engineering-based models in polymer degradation fail in this respect and good extrapolative models are rare. A primary reason is that Arrhenius linearity is widely used but seldom verified in the field; similarly questionable are the expectations that accelerated aging studies should follow previously observed behavior for other polymers. Despite dependence on a particular degradation mechanism, we have shown for many materials that these concepts are flawed and can lead to erroneous lifetimes [11]. Most polymers are unique and display different aging signatures, requiring an understanding of how individual materials behave and then customizing aging models to accommodate these trends.

In the worst case of anomalous aging, we examined a material that unexpectedly aged faster at lower temperatures, completely contradictory to common Arrhenius models predicting slower degradation rates as the temperature drops. The reason for this behavior was shown to be a secondary 'damage repair' mechanism that was only active at elevated temperatures and maintained the useful properties under the condition when aging should in fact have occurred most rapidly [53,54]. Existing Arrhenius-based aging

models could not explain the nature of this material and failed completely to describe the aging process. Phenomenological-based aging exposure using common test matrices (such as a few high temperature and dose rate conditions) and basic mechanical testing (tensile elongation as a degradation indicator) at elevated temperatures predicted significant lifetimes for this material under use conditions. Interestingly, precisely the opposite happened, as the material failed rapidly at low temperatures. Only an in-depth analysis of the degradation processes in this cable insulation material could establish the nature of this behavior and demonstrate the inapplicability of traditional aging models and their extrapolations. In polymer degradation and lifetime prediction, a single established aging model or routine accelerated aging study, as applied to differing polymers and as has been conducted for cable and jacketing materials before, will rarely deliver on the goals of valid extrapolation models. In polymer aging currently there is no single approach that fits all situations.

To the best of our knowledge the literature is weak on such a basic understanding of the chain scission and crosslinking reactions and their translation into a performance criterion (i.e. mechanical property or LOCA performance) at oxidative low dose rate, low temperature environments, yet this is critically important. Of course, specimens exposed and aged in higher stress environments will show relative rates of degradation and some activation energies may be established. However, it is important to point out that most previous studies on the degradation of such materials failed to comprehend why extrapolations could be flawed, despite using the established approach of different temperatures or dose rates and an experimental matrix of various exposure conditions. The key point is that "chemistry," after all, is the driving force for the degradation of these materials in the application environment. Engineering-based evaluations using mechanical testing, perhaps conducted within a comprehensive test matrix with degradation indicators involving changes in mechanical properties (T_g, density, or LOCA performance), will be limited to measuring macroscopic property changes. While those measurements are important and must be conducted, we must also be cognizant of the key problem, which is that macroscopic properties are often heavily convoluted and can mask the important underlying trends, resulting in misperceptions of what should be going on in extrapolative regimes. Further, as mentioned before, for materials with pronounced induction time behavior the key to success for lifetime prediction is to better understand the processes prior to failure.

(4). **The connection between degradation chemistry and mechanical or similar property changes.** The nature of the degradation due to chain scission and crosslinking, combined with incorporation of oxidized species, will greatly impact the material's performance. Mechanical property changes and stress fracture, or similarly a dielectric breakdown, are ultimately dependent on chemical changes in the polymer structure. We believe that changes in polymer network properties should be understood and correlated with such mechanical indicators as moduli or tensile elongation to best describe the aging processes and then be used to develop degradation models. We have seen greatly differing behaviors in polymer aging. Some materials accommodate significant chemistry before mechanical properties change significantly while others are extremely sensitive to small amounts of scission or crosslinking. For example, many elastomers (neoprene, nitrile rubbers, EPDM, EPR) can accommodate above 2% oxidation before the property

changes would be defined as failure. In contrast, highly crystalline polyolefins show stress cracking and embrittlement with oxidation levels of less than 0.1%, as the critical tie molecules get easily damaged. In such cases, one could conduct screening tests for embrittlement using common thermal exposure test matrices, study macroscopic damage evolution and linearly extrapolate, believing in the applicability of the Arrhenius relationship. However, without knowing the 'chemistry pathways' for low oxidation levels, variations in their effectiveness (see discussion later on inverse temperature behavior) and their changes towards lower temperatures, any extrapolative models lack a solid basis and cannot be validated. For example, a French research group dealing with failure prediction and aging models for many engineering materials, including water pipes, epoxies and composites, uses kinetic-based degradation models to validate their approaches and gain more reliable predictive capabilities [55-66]. Chemically driven processes almost always precede mechanical failure. Understanding the underlying kinetic variables allows lifetime prediction, rather than having to wait for empirical macroscopic failure in aging studies and then not knowing how to extrapolate.

(5). **The compilation of network chemistry and mechanical property changes, coupled with reaction kinetics and failure definition into predictive aging models.** If reliable aging models with predictive capabilities are to be obtained one must examine the key aging parameters and their reaction basis, their degree of contributions to material changes, as well as the environmental conditions of interest. All of them need to be coupled into a model for the evolution of failure as a function of exposure conditions. Further, understanding the key processes and under what conditions they can be extrapolated should form the basis for any successful model.

1.2.2 Accelerated Aging as Relevant to Cable Lifetime Prediction

As discussed before, under highly accelerative aging environments materials will age under DLO conditions, whereas in plant equivalent environments non-DLO oxidative conditions prevail. Therefore, when plotting overall damage levels (i.e. radiation dose to failure) as a function of dose rate at constant aging temperature, it is clear that such plots will likely combine oxidative conditions at low dose rates with observations for inert behavior at high dose rates (see Figure 12 in the following discussion). An additional complication exists in a sense that the higher dose rate side of such a plot is dominated by radiation degradation, whereas the lower dose rate side is dominated by thermal degradation processes. Extrapolations from right to left (i.e. towards lower dose rates) in such plots are close to impossible or are misleading at best unless the underlying phenomena and transitions are well understood. This will also depend on material-specific features, relevant oxidation and permeation rates, knowledge of E_a and any synergistic behavior between thermal and radiation processes.

However, at moderate dose rates or for materials of appropriate thickness where DLO is not important, consistent oxidative conditions (minimal DLO effects) may apply and plots of dose to equivalent damage (DED) versus dose rate are meaningful presentations, as they demonstrate the transition behavior between thermal and radiation dominated conditions. Some literature refers to such transitions as dose rate effects, but it is important to recognize that one reason for such a "dose rate effect" is the competition between radiation and thermal processes (in addition, true chemical dose rate effects may also occur for certain materials).

Dose to equivalent damage analysis and modeling towards low dose rates

For accelerative combined radiation thermo-oxidative environments the degradation behavior is best displayed in a plot of DED versus dose rates for lifetime prediction purposes. Similarly, time plots can be obtained as time to equivalent damage (TED) versus dose rates. These plots combine the thermal and radiation aging components to result in a presentation of overall damage accumulation. This simplest of models assumes the following:

- Pure parallel reactions for thermal and radiative degradation pathways.
- Total damage accumulation equals sum of thermal and radiative process.
- No synergism, additional dose rate effect, or thermal correction factors.

The definition of variables for this mathematical approach is:

T_f: thermal damage component to failure [mol/g]
k_T: thermal oxidation rate [mol/g-s]
R_f: radiative damage component to failure [mol/g]
k_R: radiative oxidation rate [mol/g-Gy]
t_f: time to failure under combined environments [s]
γ': dose rate [Gy/s]
γ_f: total dose to failure [Gy]
C_f: critical oxidation to failure [mol/g or % oxidation]

The following relationships apply:

$$\gamma_f = \gamma' t_f \qquad T_f = k_T t_f$$

$$\delta = \frac{T_f}{R_f} = \frac{k_T}{k_R \gamma'}$$

$$\frac{R_f}{C_f} = (\delta + 1)^{-1} = \frac{k_R \gamma'}{k_T + k_R \gamma'} \qquad \frac{T_f}{C_f} = \left(1 + \tfrac{1}{\delta}\right)^{-1} = \frac{k_T}{k_T + k_R \gamma'}$$

$$R_f = k_R t_f \gamma' = k_R \gamma_f \qquad C_f = T_f + R_f = t_f (k_T + k_R \gamma')$$

This yields the key equations for DED and TED as function of failure level (C_f), dose rate (γ'), radiation (k_R) and thermal (k_T) degradation rate.

$$\gamma_f = \frac{C_f \gamma'}{k_T + k_R \gamma'}$$ (DED - dose to equivalent failure)

$$t_f = \frac{C_f}{k_T + k_R \gamma'}$$ (TED - time to equivalent failure)

As long as the underlying variables are known it is easy to simulate DED and TED plots versus dose rates for combined radiation-thermal conditions. Let us assume the following parameters for our basic model that simulates degradation for 30 to 90°C (Figure 1, to Figure 3): Note: These variables are chosen to show how combined radiation-thermal degradation can be approached via modeling focused on deconvolution rather than to show the behavior of a particular material or implied aging process.

- An activation energy of Ea = 80 kJ/mol for the thermal process.
- Thermal only lifetime = 50 years at 50°C, corresponds to a rate of 3.17e-13 mol/g-s.
- Radiation damage: 5e5 Gy as the radiative damage criterion defined for failure.
- Radiative oxidation rate of 1e-9 mols/g-Gy, equals 0.5e-3 mols/g or 1.6% oxidation to failure.
- Dose rate γ' [Gy/h].

The TED plot (Figure 1b) shows the interplay of radiative and thermal damage accumulation and how extrapolation of data from high dose rates (linear line) would project very high lifetimes at low dose rates. However, thermal degradation will become dominant and the degradation curves will instead project towards the thermal lifetimes (i.e. the 50 years at 50°C in Figure 1b).

Model for Ea=80 kJ/mol for thermal degradation

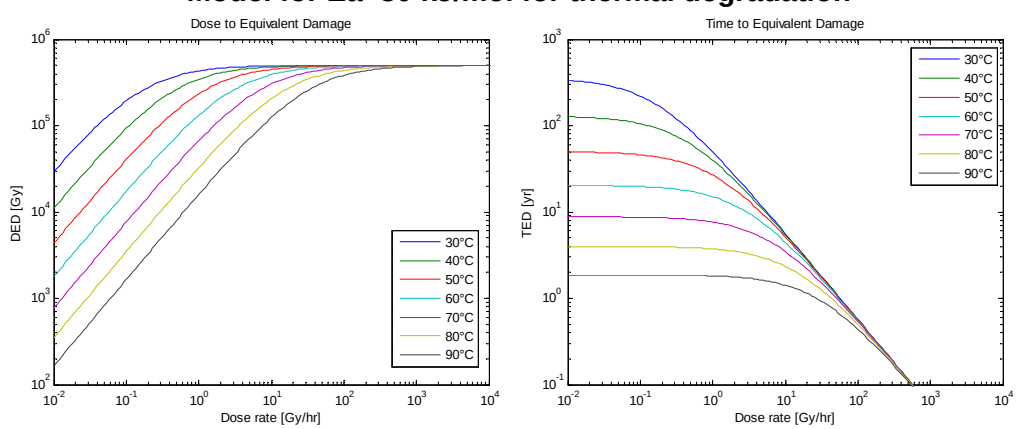

Figure 1a, b. DED and TED plot versus dose rate for E_a = 80 kJ/mol for a theoretical set of parameters defined above.

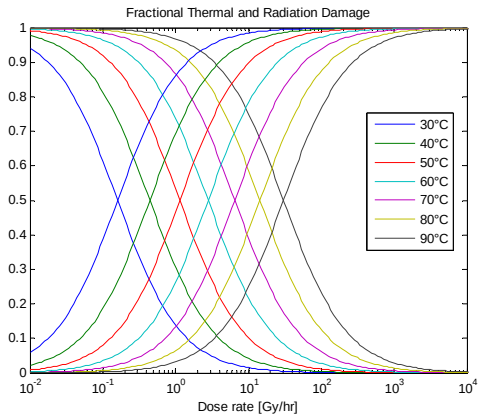

Figure 2. Corresponding fractional degradation, i.e. the thermal (predominant at low dose rates) and radiative components (at high dose rates) of the combined degradation process.

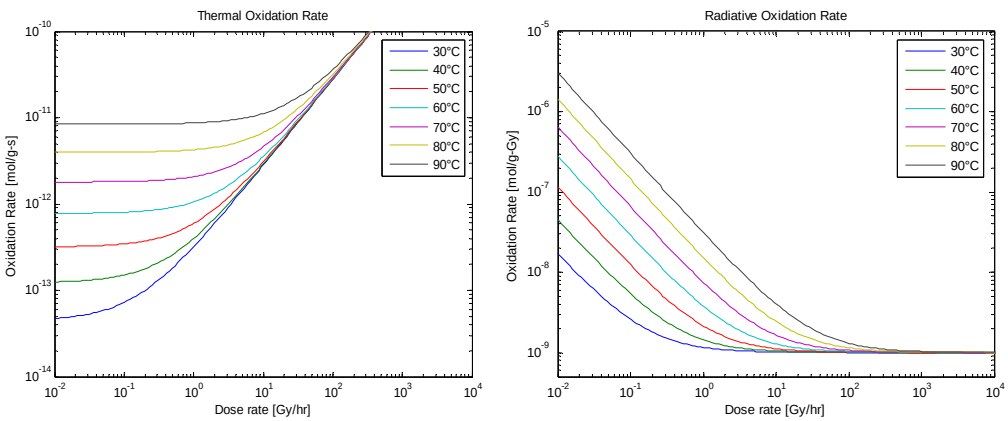

Figure 3a, b. The effective oxidation rate for the combined degradation process. For 50°C at low dose rates (left Figure) the rate approaches 3.17e-13 mol/g-s, i.e the thermal only conditions . For high dose rates (right Figure) the rate settles on 1e-9 mol/g-Gy as defined for the situation that was modeled.

It is also possible to display the fractional contributions of the thermal or radiation process as a function of dose rate (see Figure 2). Further, the embedded effective oxidation rates can be expressed either in thermal or radiation equivalent rates, as shown in Figure 3. It is easy to imagine the generation of a suitable model if oxidation rates at a number of temperatures and dose rates, and at least one failure definition were experimentally available. Below are the examples of a model using the same parameters, but instead with an E_a of 50 or 100 kJ/mol (Figure 4 to Figure 7). Any other parameters can be similarly modified, with for instance the model plots shown for a radiative oxidation rate of 1e-8 mol/g-Gy (Figure 8 and Figure 9) and a failure dose of 1e5 Gy (Figure 10 and Figure 11). Such models can provide significant guidance on the nature of the degradation behavior in these combined environments. For example, as shown in Figure 11, this model would imply mostly radiation degradation for dose rates above 15 Gy/h and temperatures below 70°C, but would imply 75% thermal degradation at 0.37 Gy/h and 50°C. Such models can be easily expanded to accommodate dose rate or synergistic effects (essentially by adding damage effectiveness parameters for specific combinations of input

variables), different E_a values for radiation and thermal reactions and changes in oxidation level for equal damage with temperature.

There is an opportunity for the development of new analytical models for better understanding and predictions of the situation in combined environments. These models should aid in the deconvolution of complex dose to equivalent damage (DED) and effective oxidation rate data trends from combined thermal radiation environments thereby establishing the individual signatures of thermal and radiation degradation pathways. We propose using such models for reverse fitting approaches that should enable deconvolution and predictions based on multi-parameter fits. They should accommodate deviations from linear Arrhenius behavior or constant DED failure-level assumptions, as well as simulate dose rate effects and changes in oxidation levels for equal damage as a function of temperature (i.e. inverse temperature effects).

Model for same parameters but Ea=50 kJ/mol for thermal degradation

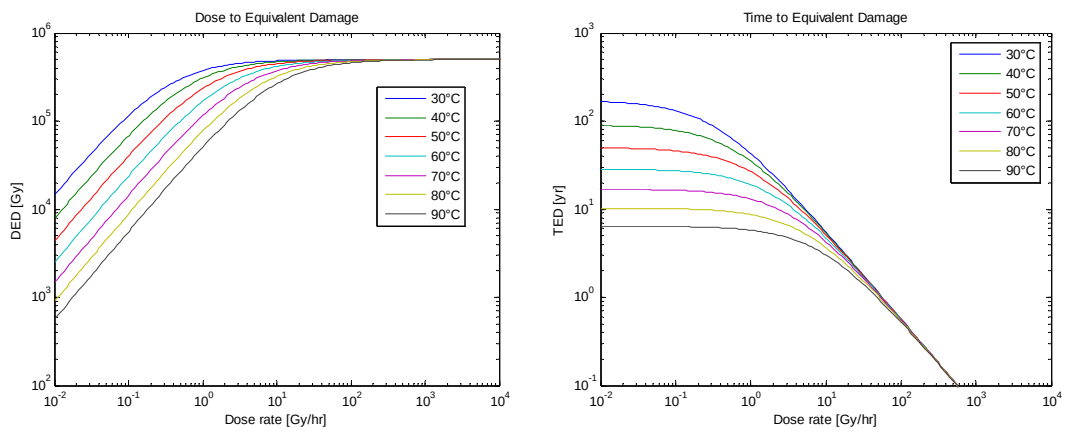

Figure 4a, b. DED and TED plot versus dose rate for E_a = 50 kJ/mol for a theoretical set of parameters discussed above.

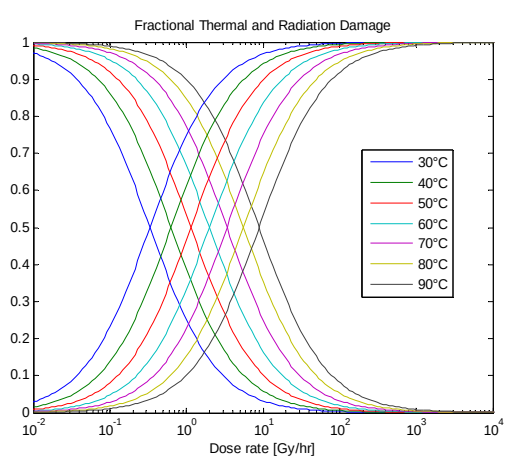

Figure 5. Corresponding fractional degradation, i.e. the thermal (predominant at low dose rates) and radiative components (at high dose rates) of the combined degradation process.

Model for same parameters but Ea=100 kJ/mol for thermal degradation

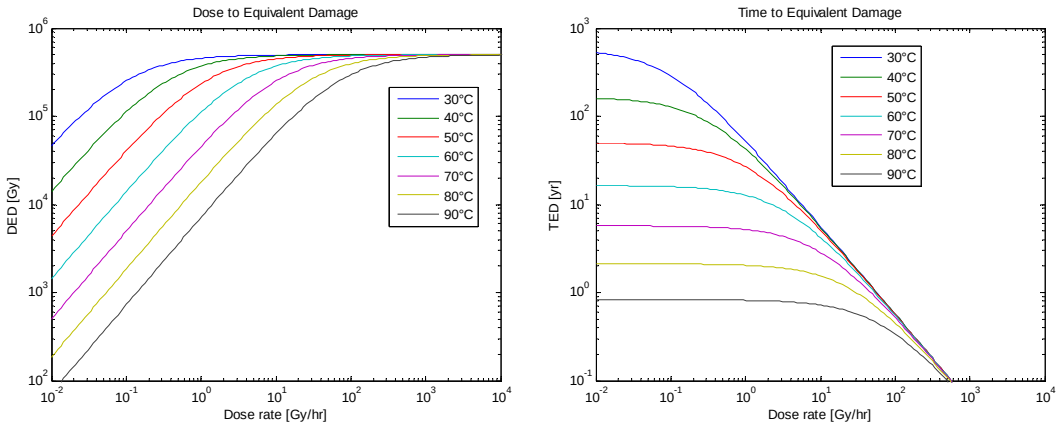

Figure 6a, b. DED and TED plot versus dose rate for E_a = 100 kJ/mol for a theoretical set of parameters discussed above.

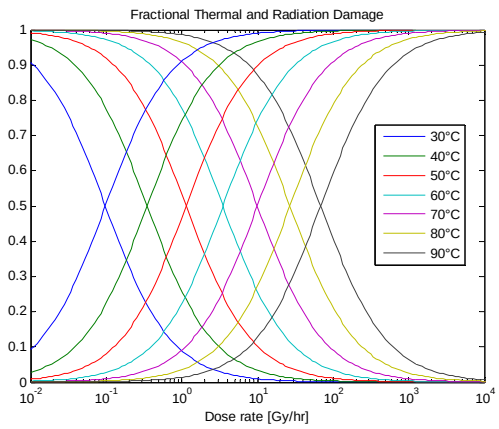

Figure 7. Corresponding fractional degradation, i.e. the thermal (predominant at low dose rates) and radiative components (at high dose rates) of the combined degradation process.

Model for same parameters with Ea=80 kJ/mol for thermal degradation and a radiative oxidation rate of 1e-8 mol/g-Gy

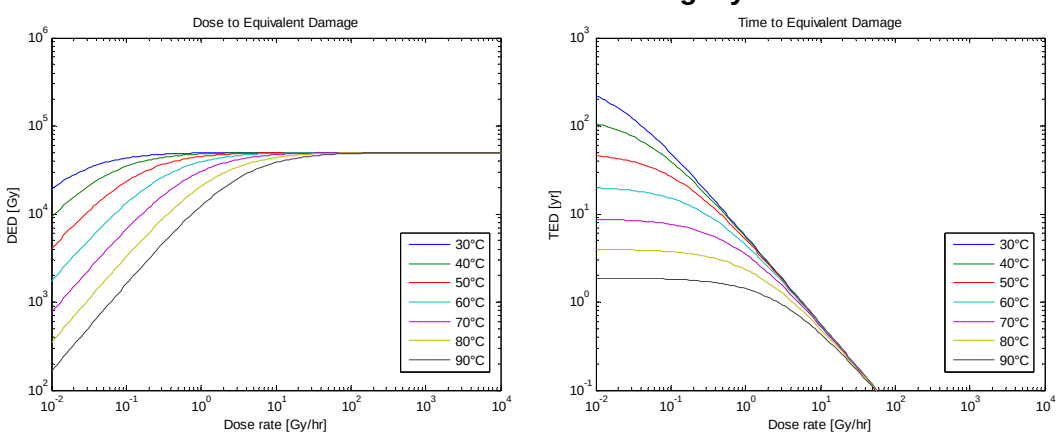

Figure 8a, b. DED and TED plot versus dose rate for E_a = 80 kJ/mol for the theoretical set of parameters discussed above, but a radiative oxidation rate of 1e-8 mol/g-Gy.

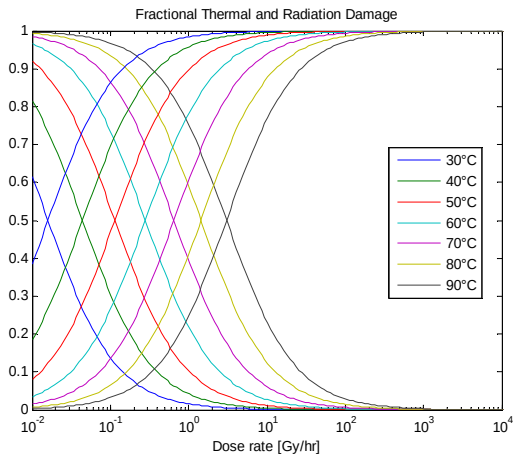

Figure 9. Corresponding fractional degradation, i.e. the thermal (predominant at low dose rates) and radiative components (at high dose rates) of the combined degradation process.

Model for same parameters with Ea=80 kJ/mol for thermal degradation and failure defined as 1e5 Gy

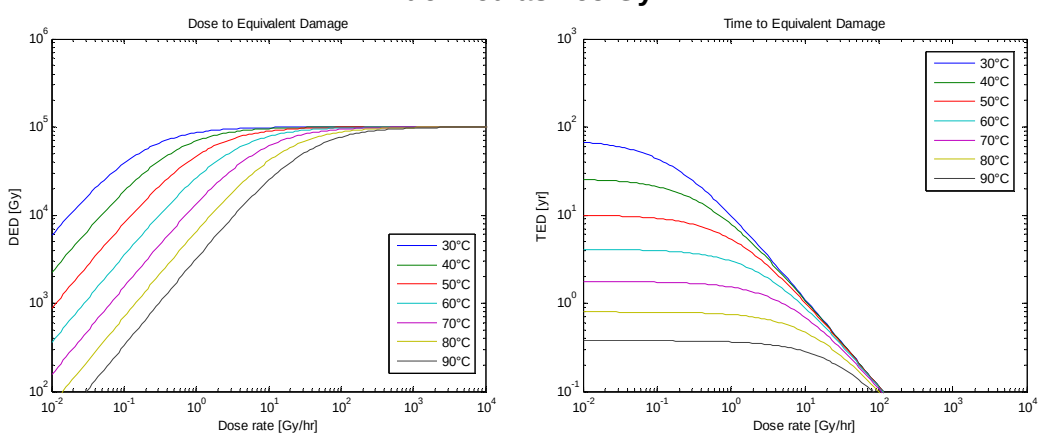

Figure 10a, b. DED and TED plot versus dose rate for E_a = 80 kJ/mol for the theoretical set of parameters discussed above, but with failure defined as 1e5 Gy. At 50°C with an identical thermal rate of 3.17e-13 mol/g-s failure at thermal only conditions will therefore occur at 10 years. Note: Oxidative failure will now occur at 0.32% oxidation consistent with a 5 times lower total dose for identical radiative oxidation rate of 1e-9 mols/g-Gy.

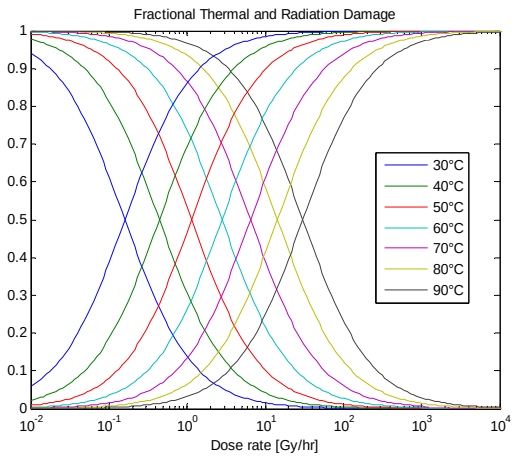

Figure 11. Corresponding fractional degradation, i.e. the thermal (predominant at low dose rates) and radiative components (at high dose rates) of the combined degradation process.

1.3 Performance Predictions from Highly Accelerated Qualification Conditions versus Actual Conditions Encountered in the Plant

The focus of the IEEE Std. 323-1974 [67] was to qualify materials by successfully passing LOCA performance simulations under successive short-term high dose rate, thermal steam, and boric acid spray environments. There could have been a perception that a material passing these requirements would then be qualified for long term operation, since it could handle a large radiation dose and high temperature plus steam environments. However, the IEEE Std. 323-1974 document expresses caution in many respects and did not address qualification for extended operation in poorly understood 'aging environments'. For example, in excerpts the document states:

> "It is based on awareness by the IEEE that the ability of Class IE equipment to perform its safety related function might be affected by changes due to natural, operational, and environmental phenomena over time (aging). It was not the intent that aging must be applied to all Class IE equipment, but rather that aging must be considered in the same manner as environmental parameters. The need for aging of particular equipment should be determined based on an evaluation of the specific design and application. If aging is needed, a further determination must be made as to whether accelerated aging techniques can be applied to the equipment and yield valid results that may be correlated to real time, ongoing qualification.
>
> Optionally (and particularly where the state-of-the-art is limiting), aging as part of the qualification program may be addressed by operating experience, analysis, combined, or ongoing qualification as detailed in Section 5.2, 5.3, 5.4 and 5.5.
>
> Qualified life shall be determined from the time dependent effects of the environmental influences by quantitatively demonstrating that the performance characteristics of the equipment meet or exceed the design specifications of the equipment after a design basis event, preceded by a time period during which the equipment is subjected to its normal design environment. The maximum time period of normal environment for which the quantitative analysis is valid shall be the maximum life for which the equipment can be qualified by analysis.
>
> The qualification methods described thus far may yield a qualified life of equipment that is less than the anticipated installed life of the equipment. When this occurs, an on-going qualification

program may be implemented. Two methods for achieving this are: (1) aging and testing of identical equipment. The objective of aging is to put samples in a condition equivalent to the end-of-life condition. If previous aging of various devices exists, it can be utilized provided these data are applicable and justifiable in regard to the service conditions that are required by the performance specifications of the device to be type tested.

On-going qualification. Some equipment may have a qualified life less than the required design life of a nuclear power generating station. There are two recommended methods of long term qualification (see Section 5.5): (1) Equipment of the same type as that which has been type tested and installed in a station shall be placed in an environment that accelerates the aging under controlled conditions. When it is determined that the equipment has reached the required design life of the station, it shall be removed from the accelerated life environment and type tested. The installed equipment may be considered adequate for the design life of the station if the equipment that was subjected to the accelerated life environment passes the type test (2) Additional identical equipment shall be installed in a nuclear generating station in locations where service conditions equal or exceed those of the equipment to be qualified. This equipment shall be removed after a planned period less than the previously qualified life and subjected to a qualification test similar to that performed prior to its installation. This test must include additional accelerated aging. Successful completion of this type test extends the qualified life of the installed equipment. This procedure shall be repeated until the qualified life equals the required installed life of the equipment."

The committee preparing the IEEE Std. 323-1974 recognized that long-term aging processes would be part of plant environmental exposure, but did not deal with the consequences of such material changes besides stating that materials qualification should be addressed by additional operating experience and analysis as part of ongoing qualification requirements, and that additional accelerated aging studies allowing for performance verification should be conducted (however, specific environmental details are not provided). Further, we believe that a single rapid accelerated test method, as applied in IEEE Std. 323-1974, for lifetime simulation of a multitude of materials is often not feasible, since specific design types (here materials) and specific environment sensitivities would have to be addressed individually. For example, for some materials there may be some value in extrapolations of aging and LOCA performance, but for other materials, like those that display inverse temperature behavior or are mostly dependent on oxidative degradation pathways, any extrapolations would be erroneous (one of the essential messages in this report). The IEEE Std. 323-1974 does not properly address the developing aging issues and its impact on the definition of design life. One of the likely reasons of course is the lack of knowledge of the complexity of polymer degradation processes in the 1970's.

Considering that ongoing aging issues were identified, but no technical guidance was provided on how to deal with them, we conclude that IEEE Std. 323-1974 cannot provide the basis for re-qualification of most materials beyond initial design life criteria. We also conclude that any additional margins applied within a test protocol according to IEEE Std. 323-1974 (i.e. extra temperature, pressure, radiation or similar stress variable) will likely neither quantify extra operational margins for lifetime extension purposes, nor successfully compensate for long-term aging effects, unless avenues for extrapolations and a clear understanding of the specific degradation pathways, sensitivities to DLO processes and inverse temperature effects is available for specific cable insulation and jacketing materials.

An underlying issue of highly accelerated conditions for lifetime simulation is also the huge margin in terms of the relevant acceleration factor. Plant conditions have been characterized as

0.6 Gy/h (60 rad/h), for a total integrated dose (TID) of 0.2-0.4 MGy (20-40 Mrad) over 40 years, followed by ~1.5 MGy (150 Mrad) for a LOCA event. A dose rate of 0.6 Gy/h equates to 5.3 kGy/y or 0.26 MGy (26 Mrad) for 50 years. If this dose were to be deposited within a two week time period as part of an accelerated test, an extrapolation factor of 50x52/2 = 1300 times would have to be implied. Even if accelerated testing were to be applied over a longer six month period, it would still constitute an acceleration factor of 100 for a 50 year lifetime. Mechanistic changes will likely interfere when such high acceleration factors are under consideration.

We therefore conclude that neither the IEEE Std. 323-1974 qualification testing nor similar highly accelerated exposure conditions can precisely predict extended plant performance. The most important factor is the transition to essentially inert aging conditions for most cable insulations during the highly accelerated test versus the oxidative conditions encountered during actual plant operation. Of course, one of the key questions remains. At which point does this divergence prohibit predictive aging? Based on other 'polymer degradation studies' we believe that as long as accelerated aging conditions are chosen which will simulate oxidative degradation with relative homogeneous degradation profiles and hence would match mechanistic conditions in the plant, it should be possible to develop models for lifetime prediction purposes [8,10,12,13,16,52]. Perhaps margins could be established if LOCA performance data existed for 'pre-aged' specimens with successive increases in oxidation levels or any other damage pictures that would correlate with the features of damage accumulation during plant conditions. Therefore, further research should focus on aging phenomena, LOCA performance and potential remaining margins for non-DLO oxidatively aged cables involving specimens that will mimic plant aging conditions.

In brief reference to IEEE Std. 383-2003, we recognize that this standard attempted to emphasize the complexity of some polymer degradation processes. Limitations of simple accelerated aging studies were seen in material specific features, such as diffusion limited oxidation (DLO), dose rate or any other synergistic effects that would complicate extrapolations. However, besides stating that appropriate aging tests should be applied within 'methods that shall be used with due consideration to cost, time, and complexity', no detailed guidance on how to specifically address these issues for meaningful lifetime prediction purposes was included. The problem remains that if unknown aging behavior existed, such behavior would likely not be incorporated into standard qualification testing. Nevertheless, this standard does imply that material-specific behavior and aging anomalies must be taken into account and documented to validate qualification. It also implies that generic testing approaches have limits.

1.4 Comments on Margin Assessments

The above discussion emphasizes an important issue: Can accelerated qualification conditions be mechanistically so different in comparison with actual aging conditions that they preclude any meaningful prediction for remaining margins? The answer here is yes, which is certainly not unexpected in light of the fact that the IEEE Std. 323-1974 qualification scenario does not sufficiently focus on the issues of long-term aging during extended plant operations and was an approximate approach to address initial qualified life. Whenever substantial differences in the nature of the aging behavior between accelerated LOCA testing and plant aging conditions exist, margins assessments cannot be established. Any efforts of doing so would in fact imply

correlations for which no scientific basis exists. Further, they imply performance that may not exist.

As shown later in a discussion of the aging behavior at plant equivalent conditions, there is sufficient evidence that oxidation is usually homogeneous. Unfortunately, most previous aging and LOCA studies did not succeed in accommodating these important differences. Some previous LOCA experiments confirmed that cable failure at lower dose rates can in fact occur at lower total doses. While such effects are often described and interpreted as dose rate effects, they are in fact usually driven by the competition between oxidative and inert aging conditions (DLO effects) and/or the transition from radiation-domination towards thermal-domination. True dose rate effects can only be established if other possible mechanistic variations, such as DLO, are anticipated and prevented in any highly accelerated aging study. Using similar terminology for fundamentally very different aging behavior is an issue that complicates data interpretation throughout the existing literature. One avenue forward is to engage in further research which should focus on aging phenomena, condition monitoring, LOCA performance and potential remaining margins for non-DLO oxidatively aged cables.

For example, if LOCA failure occurs at lower total doses when the dose rate is lowered, this may suggest that lowering the dose rate further would result in even lower total doses to failure. While such approaches may yield very conservative assessments and extrapolations, they nevertheless show that such extrapolations are misleading. Ultimately, once more or less homogeneous oxidation conditions are reached the dose rate becomes less important and there would be a nearly consistent dose level that equates to material failure for a range of dose rates [23]. If however, one would investigate much lower dose rates (levels that are not normally probed with LOCA testing), the situation will be more complicated as radiative and thermal degradation processes start competing and a thermal component as an equivalent dose will creep into the calculations. This is demonstrated in Figure 12 where the dose to failure depends strongly on dose rate and temperature. In such a case, assuming that a failure dose of 5e5Gy is valid towards even lower dose rates would imply overly optimistic lifetimes.

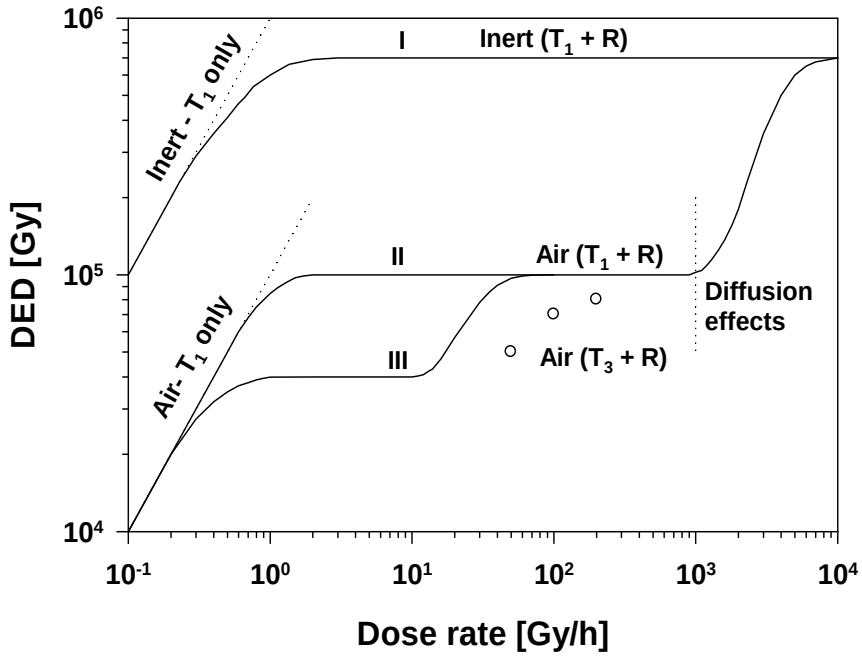

Figure 12. Hypothetical results illustrating the types of dose-rate effects which can occur in radiation-aged polymeric materials: the dose to equivalent damage (DED) is plotted versus the dose rate (R). The curve labeled Inert (T_1 + R) gives results for samples aged in inert atmospheres at temperature, T_1, this curve must asymptotically approach the isochrone (labeled Inert – T_1 only) appropriate to inert aging in a thermal-only environment. The curves with air substituted for inert have identical meaning for aging in air environments. At high dose rates, diffusion-limited oxidation effects can become important, resulting in the eventual approach of the air results to the inert results (Figure reproduced from [23]).

The question is, under what circumstances could carefully conducted LOCA performance testing then yield margin data? If consistent samples with varying oxidation levels are prepared that mimic plant degradation features (extent of oxidation and homogeneity aspects), it should be possible to establish remaining margins. For example, let us assume we prepare nearly homogenously aged specimens at low dose rates with 1, 2, 3, or 4% oxidation levels. If LOCA performance testing yields satisfactory results for 1, 2, or 3%, but a failure for 4%, one would have established a critical oxidation damage level; in this case a conservative number would be 3%. If an understanding of oxidation rates under plant conditions exists and it turns out that it requires about 40 years to reach 2% oxidation, this would then imply another 50% performance margin for 3% or an extra 20 years.

As shown later, the existing aging data are insufficient to confidently determine the remaining operational margins for these materials. This does not imply that the existing 40 year old materials would necessarily fail if LOCA conditions occurred, but rather that meaningful statements about the current conditions and anticipated LOCA performance cannot be provided. The non-availability of critical data for current aging state, LOCA behavior, and lifetime prediction purposes, however, does imply major challenges for any requalification or extended operation of these materials.

1.5 Accelerated Aging Studies and LOCA testing: The Key Message from other Studies

The original statement of work for this review required us to examine the key conclusions of a number of relevant documents and determine whether the existing data could be used to establish remaining margins for extended reliable operation of cable insulation and jacketing materials. These documents include two additions (IEEE Std. 323-1974 plus NUREG/CR-6202) and are:

SAND91-1776, Aging, Condition Monitoring, and Loss of Coolant Accident (LOCA) test class 1E cables, prepared by Sandia National Laboratories for the US Department of Energy August 1992. (NUREG/CR-5772 Vol.1-3) [68-70].

NUREG/CR-6384, Literature Review of Environmental Qualification of Safety-Related Electric Cables, Prepared by Brookhaven National Laboratory, April 1996. [71]

SAND05-7331, Nuclear Energy Plant Optimization (NEPO): Final Report on Aging and Condition Monitoring of Low-Voltage Cable Materials, prepared by Sandia National Laboratories for the U.S. Department of Energy, November 2005. [14]

JNES-report 2009, Japanese Nuclear Energy Safety Organization. Assessment of Cable Aging for Nuclear Power Plants, prepared by JNES July 2009. [72]

IEEE Std. 323-1974, IEEE Standard for qualifying class IE equipment for nuclear power generating stations [67].

NUREG/CR-6202, Long-Term Aging and Loss-of-Coolant Accident (LOCA) Testing of Electrical Cables, U.S./French Cooperative Research Program, Nelson, C. F.; Gauthier, G.; Carlin, F.; Attal, M.; Gaussens, G.; Le Tutour, P.; Morin, C.,", IPSN 94-03, SAND 94-0485, 1996. [73].

We conclude as demonstrated throughout this report and particularly evident in the quantification attempts discussed in Section 4, that remaining margins cannot be established using the existing literature. A large degree of uncertainty exists in understanding the aging state of 40-year-old materials and any correlations between this aging state and LOCA performance. The original LOCA qualification testing and subsequent accelerated aging plus LOCA studies were mostly conducted under rapid accelerated aging conditions resulting in materials with mostly 'inert' aging processes in the interior insulation materials. This means that complete oxidative damage in these situations is limited to the surfaces of the cable jackets. This situation is in stark contrast with the aging behavior observed and implied for low dose rate, low temperature plant conditions, where oxidation is much more homogeneous in nature. The heterogeneous degradation expected under highly accelerated aging conditions could be compared to a material that has a severely degraded skin, but is otherwise not significantly changed in its properties. Since LOCA high dose rate radiation exposure also incurs mostly heterogeneous degradation, we are concerned that pre-aged materials of heterogeneous nature may pass LOCA performance, but could fail if they had been more uniformly aged. Since the aging conditions over decades are very different from those that were mostly applied in the accelerated aging studies, we conclude that the existing aging data are insufficient to confidently determine the remaining operational margins for these materials. However, this does not imply that the existing 40-year-old materials would necessarily fail if LOCA conditions occurred, but rather that unambiguous statements

about the current conditions and anticipated LOCA performance cannot be provided. Since suitable margins cannot be predicted we are also faced with major challenges for any re-qualification or extended operation of these materials.

Below is an example of the variations in oxidation behavior that exist between radiation degradation conducted at high and low dose rate conditions for a 2 mm thick insulation material that is exposed to air on the left side and to inert conditions on the right (i.e. solid conductor core). The relevant aging characteristics for a polymeric material that would resemble an XLPO insulation material are provided in Table 1 and the resulting degradation profiles under a range of dose rate conditions excluding a thermal component are presented in Figure 13. At high dose rate conditions the degradation is severely diffusion limited and the oxidation is limited to the surface; the total amount of oxidized material is a fraction of that generated at low dose rate conditions. The material experiences mostly inert radiation degradation which will translate very differently into mechanical or other property changes in comparison with oxidative degradation. Low dose rate conditions result in nearly uniform oxidation throughout the material. For demonstration purposes we assume a radiation dose exposure of 0.5 MGy (50 MRad) deposited under different dose rate conditions at 10 kGy/h, 1kGy/h, 10 Gy/h and 1 Gy/h. Exposure times are therefore 50 h, 500 h, 5.7 and 57 years. A radiative oxidation rate of 1e-9 mols/g-Gy, plus specific permeability and beta-factor ($ß_0$; linking O_2 partial pressure and oxidation rate) were chosen to result in a realistic demonstration of DLO effects for dose rate dependent degradation profiles. At this oxidation rate and total dose condition the surface (non-DLO) will oxidize to 1.6 weight % of oxygen incorporation.

Table 1. Demonstration of theoretical oxidation estimation for a 2 mm thick insulation material in contact with air (left) ($ß_0$ = 1, p(O_2)=13.2cmHg) and inert conditions (right). Radiation exposure is simulated at different dose rates where homogeneity of 1 equals uniform degradation throughout. Radiation oxidation rate and permeability were chosen to be somewhat realistic.

Exposure dose rate	10 kGy/h	1 kGy/h	10 Gy/h	1 Gy/h
Oxidation rate [mol/g/Gy]	1.0E-09	1.0E-09	1.0E-09	1.0E-09
Time to 0.5 MGy (50 MRad)	50 h	500 h	5.7 y	57 y
Oxidation rate [mol/g/s]	2.78E-09	2.78E-10	2.78E-12	2.78E-13
O2 permeability [ccSTP/cmHg-s-cm]	1.0E-10	1.0E-10	1.0E-10	1.0E-10
Oxidation at surface [weight %]	1.6	1.6	1.6	1.6
Homogeneity of degradation	0.023	0.074	0.680	0.963

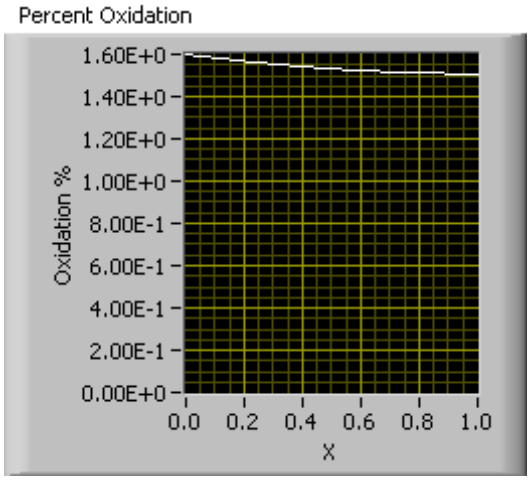

Nearly flat profile at 1 Gy/h, oxidation throughout the material

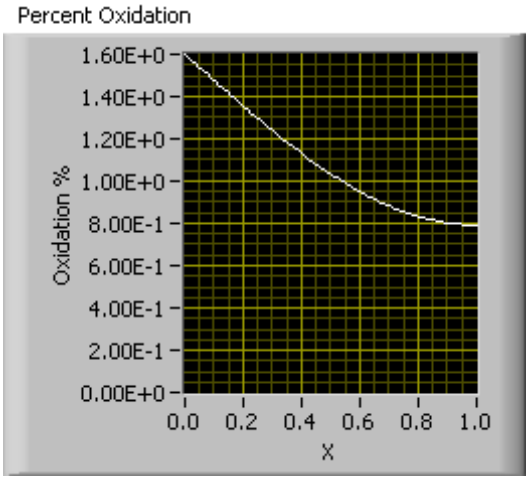

Beginnings of heterogeneity at 10 Gy/h

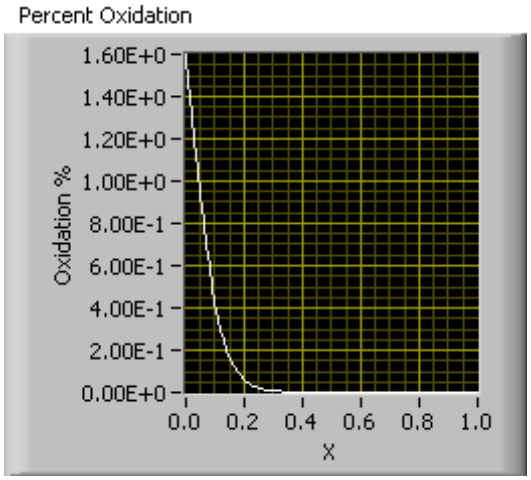

Significant heterogeneity at 1 kGy/h

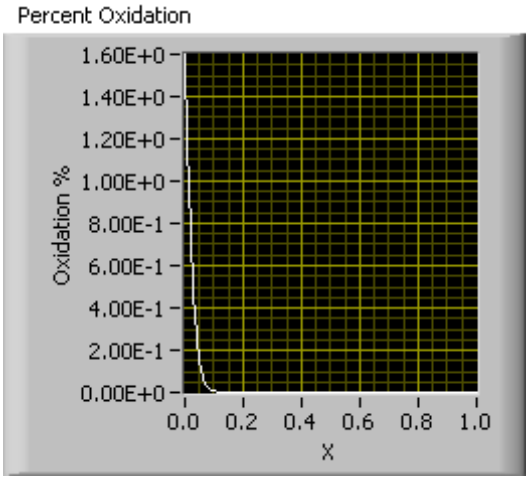

Oxidation is limited to surface at 10 kGy/h

Figure 13. Visualization of different oxidation degradation profiles as a function of dose rate for equal deposited doses (0.5 MGy) where x equals normalized position (thickness of 2 mm) and oxygen is present on the left side of the specimen. At low dose rates the material is uniformly oxidized. At the high dose rate of 10 kGy/h the oxidation is limited to the surface, the total amount of oxidized material across the specimen is less than 2.5% of that generated at 1 Gy/h. At 10 and 1 kGy/h the material is mostly irradiated under inert degradation conditions, i.e. no oxidation effects occur within the interior.

The current literature does not provide for good correlations between the accumulated plant material natural aging state and LOCA performance. There are perceived correlations only between various types of exposure (high temperature, high dose, etc.), reminiscent of the various accelerated aging tests that have been conducted and expected to have delivered some type of 'pre-age,' and subsequent LOCA testing [68-73]. What such previous tests offer in terms of extrapolative and qualification surety remains open, as they compare oxidative, with partial oxidative and inert aged conditions. For today's aged plant materials the existing literature certainly does not allow for margins in LOCA performance to be established, since the required experiments have not been documented.

We believe one reasonable way forward for coupling plant aging situations with LOCA performance is achieved in basic terms via:

- A better understanding of the degradative processes that apply during plant aging.
- Confirmation of predominant oxidative aging behavior as currently perceived.
- Generation of homogeneously aged specimens with different oxidation levels.
- Testing of LOCA performance of such specimens as a function of oxidative damage levels.

Such approaches would establish the underlying correlations between the primary aging state and LOCA behavior. Unless we move beyond the perception that it is sufficient exposing materials to rapid, high radiation levels with subsequent LOCA testing and acquiring pass or fail data, we will not be in a position to judge the remaining margins of existing infrastructure with regard to LOCA performance. We need to better understand how cable and insulation materials have degraded over decades of power plant operation and how this natural aging history relates to LOCA performance if an accident occurred within the projected service life.

1.6 Wear-out Aging Study to assist in Margin Determination

It is important to first briefly focus on condition monitoring and point out potential weaknesses in this approach. Pure condition monitoring approaches are intended to rely on some sensitive parameter that can be probed in a material and via calibration curves linked with age, previous aging history and/or critical aging parameters (e.g., tensile elongation). A good hypothetical example would be a material that hardens while it ages. Let us assume at temperature condition X a linear correlation exists between age and surface modulus, for instance probed with an indenter (which, incidentally, also probes material modulus below the surface although with diminishing importance as the depth into the material increases). If one further establishes that the original material has a modulus of 10 MPa and perhaps 20 MPa relates to material failure (perhaps defined for example by tensile elongation reaching a certain value), then a measured modulus of 15 MPa may suggest 50% aging history or 50% remaining lifetime, as long as the linear age-property relationship applies. Hence, if it took 10 years to reach 15 MPa, then the total lifetime would be expected as 20 years. It is clear that this simplistic example relies on the correlation between age and modulus property change. Linear relationships are great to work with, but unfortunately in material aging they often do not exist. Let us expand our example and assume that over 15 years the modulus only changes from 10 to 13 MPa, but over the last 5 years changes more dramatically from 13 to 20 MPa. As long as the critical age-property relationship has been determined ahead of time predictions could be made. The question is then this: can these correlation curves be established via accelerated aging tests or would data have to be acquired for 20 years at the aging condition itself? The usual approach is to derive the correlations using accelerated tests out to failure and then assume the same correlation will prevail for the ambiently aged materials. Such an assumption clearly needs confirmation, something that has not been achieved for most studies to date. Let us now expand our example further: what if the material displayed severe induction time behavior in its property changes? For example, if it takes 19 years at this aging condition to change from 10 to 11 MPa, but over the last 1 year the modulus changes drastically from 11 to 20 MPa. If measurements of around 11 MPa were taken at an age of 18 years, one may be inclined to assume plenty of life remains, as 11 MPa is safely below the 20 MPa failure modulus. Nevertheless, in this case the material

would be close to imminent failure. It demonstrates that unless a precise age-property correlation at the relevant aging condition is given, such margin predictions can be challenging or in the worst case misleading. Condition monitoring requires significant knowledge of the material aging behavior and the effects of acceleration on the derived correlations between the CM parameter and degradation in order to offer suitable predictive value.

Condition monitoring also requires property changes that can be probed with suitable techniques and offer a reasonable dynamic range to distinguish between aging states. In the past, CM techniques investigated include mechanical property tests like indenter hardness ("non-destructive"), surface modulus from modulus profiling, torsion behavior, density changes or NMR relaxation time changes on small milligram test specimens, oxygen induction time, infrared spectroscopy, solubility and swelling behavior, dielectric spectroscopy or changes in electrical properties. Any of these condition monitoring parameters must be correlated with age and aging condition (i.e. temperature and dose rate) to establish remaining margins in materials. Since tensile elongation is usually considered the best degradation parameter and often used to define "failure" (50% absolute is commonly used), many CM parameters are correlated to elongation results in order to estimate the value of the CM parameter corresponding to "failure". Extensive aging data sets and good resolution of a specific method with age and/or elongation must exist for this approach to be useful. Further, a condition monitoring property may be useful for material A but not material B. Since we are dealing with various material types in NPP applications, no general options for condition monitoring methods exist as of to date. Condition monitoring methods do not cover all materials, particularly when inverse temperature effects or degradation with strong induction time behavior is involved. An alternative methodology exists in the so called 'Wear Out approach' introduced by Sandia, where the behavior under additional aging conditions becomes the condition indicator in itself [14,18,19].

One approach for conducting aging studies and obtaining some predictive guidance from the history of field samples is given in what we call the 'Wear-Out approach'. It amalgamates the concepts of condition monitoring with additional aging of pre-aged specimens. The principle is based on cumulative material damage by establishing a correlation between the state of field samples and behavior in accelerated aging studies. The basic approach is simple and involves the following requirements:

- It is implied that any aging history in a material will result in some type of signature or material property change, simply speaking as some degree of damage or just age.

- A partial aging history thereby relates to a partial property change of some type and a partial change in its future aging behavior.

- An existing partial change in a material can be quantified using reasonably accelerated aging tests by probing the remaining lifetime.

- Inverse correlations between partial 'pre-aging' states and remaining fractional lifetimes in accelerated testing can be established.

Using the 'Wear-Out approach' we determine the condition or pre-aging state of a material not just via a specific condition monitoring technique but rather via the behavior of a 'pre-aged'

material in accelerated aging studies. Fractional behavior in an accelerated aging test is thereby correlated with an existing fractional age or fractional remaining lifetime. In essence, we use the remaining aging behavior of pre-aged or field exposed samples as a condition monitor. Pre-age and remaining lifetimes are thereby correlated with fractional performance in additional aging tests, hence the term 'Wear-Out Aging' approach.

The 'Wear-out Aging' method involves a combination of condition-monitoring to reach a specific failure point and accelerated aging, and relies on samples that have been aged to a certain condition under low environmental stresses, e.g. at low temperature and low dose rate [14,18,19]. Aging to reach a predefined failure criterion is then completed under some moderate accelerated aging conditions, e.g. at the wear-out temperature and/or wear-out dose rate. It is based on the concept that polymer degradation is of intrinsic cumulative nature and failure will occur when sufficient damage has been accumulated irrespective of differences in the exposure level. Obtaining incremental and fractional damage data trends coupled with underlying knowledge of the relationships of aging state versus exposure condition can predict remaining lifetimes. This approach can deal with materials which show induction time behavior, in fact sudden drastic property changes are ideal as they define a good failure point in time. Ideally, materials that will qualify for wear-out aging should show some measurable property change on small samples and unless induction time behavior applies with expected simultaneous 'failure in parallel properties', the wear-out property in turn will require some correlation with a performance of interest, i.e. mechanical (elongation) or LOCA.

Whether we use condition monitoring, wear-out aging, or any other lifetime prediction avenues, all of these approaches have one key requirement, namely the definition of failure for a particular environment and performance expectation. Even if condition monitoring or 'Wear-Out' approaches are applied to existing aged materials, the question of LOCA performance in relation to whatever margins may exist in other properties, such as hardness, OIT, or remaining life in any similar property, remains open. Since we are dealing with radiation thermal degradation processes, any wear-out aging studies would also have to involve combined temperature and radiation exposure. For Wear-Out studies involving materials with inverse temperature behavior, such as XLPO insulation, great care would have to be applied in how to conduct additional wear-out aging studies. Significant increases in temperature would have to be considered as problematic; perhaps the only option would be additional radiative exposure at similar low temperature conditions as were relevant during previous aging.

Finally it should be noted that attempted correlations of CM techniques with mechanical degradation (e.g., elongation) based on accelerated aging exposures can be significantly influenced by DLO effects. If the accelerated aging is carried out at high temperatures and/or dose rates, the materials being examined may have important DLO effects implying that the material properties depend strongly on position in the material cross-section. Most CM techniques are correlated to elongation results which are typically unaffected by DLO effects since cracks that start at the sample surface (at equilibrium with the surrounding air atmosphere) quickly propagate through the material leading to failure. On the other hand, typical CM techniques such as density, OIT, torsion behavior, swelling and solubility sample the entire sample cross-section and will therefore be influenced by DLO effects. Another CM technique, the indenter, also probes material modulus below the surface although with diminishing importance as the depth into the material increases. Thus any such correlations determined will

depend upon the importance of DLO effects. Since these derived (DLO-influenced) correlations are meant to be applied to field-aged samples where DLO effects are absent, such correlations can be totally misleading. The only correlations that can be trusted are either based on true surface measurements at air-exposed surfaces or determined under slow enough accelerated conditions such that DLO effects are minimal. True surface measurements are potentially available from techniques that profile the sample cross-section or truly sample the surface.

1.7 Complications Introduced by Inverse Temperature Behavior

Of particular concern for lifetime predictions are situations where the classical behavior of lower degradation rates with lower temperatures does not hold. Due to the nature of accelerated aging tests, which under normal circumstances cover only short time frames and therefore only a few test temperatures, any deviations from expected Arrhenius behavior can be easily missed. This dilemma originates from the fact that comprehensive meaningful material aging studies require time and funding (an ongoing issue in many areas of materials performance), but that short term studies provide no more than indications of the trends over the temperature range investigated. These limited studies have an intrinsically high degree of uncertainty in predicted lifetimes or margins. While extrapolations are often believed to follow linear Arrhenius behavior with temperature, we have obtained more and more evidence over the last 20 years that this is usually not the case with numerous materials showing a drop in Arrhenius activation energy as the temperature is reduced [8,10-14,17,21,45,52]. In fact, no general trends in 'polymer aging science' exist that could predict which materials should display reasonable Arrhenius behavior and which materials should not. It is an area of ongoing research, and all we are conscious about are the factors that contribute to mechanistic variations in the aging process. For semi-crystalline materials these could be morphological transitions; in most polymers changes in molecular mobility as a function of T_g or T_m could influence the lateral activity of free radicals, the active intermediates in radio-thermo oxidative degradation. Changes in their recombination, initiation and termination efficiencies will affect chain scission and crosslinking reactions and hence the development of different types of polymer structural damage features. Chain scission and crosslinking is the driving force in polymer degradation under irradiation and its translation into mechanical or physical property changes is highly complex. It is clear that significant changes in these two reactions as a function of temperature will relate to varying amounts of 'total degradation chemistry' being responsible for physical damage to develop differently, i.e. loss of elongation, elasticity, brittleness or electrical performance as a function of primary polymer chain damage.

The worst-case scenario for lifetime predictions is the situation where a significant mechanistic transition in the aging behavior may occur towards lower temperatures, the range where extrapolations should normally provide guidance for performance. Such changes may result in much faster degradative damage accumulation, than would be implied based on short term, higher temperature aging studies. In the extreme case for radiation exposures, aging may proceed more rapidly as the temperature is lowered. We have described such behavior as an <u>anomalous or inverse temperature aging behavior</u> [53,54]. Unless extensive data sets are available covering a large temperature range and including partial aging at the temperatures to be extrapolated to, precise predictions or margins cannot be established. Where evidence for inverse temperature behavior exists, more fundamental aging studies are required and must include approaches towards understanding the early stages of degradation, i.e. development of

fractional damage and its dependence on dose rate and combined oxidation rates. However, if changes in total oxidation levels are involved, there is no perfect approach dealing with this situation unless critical damage levels are already known.

Interestingly, qualification tests or screening of materials performance are often based on a few data points obtained from highly accelerating temperatures. This is seen in the engineering tests discussed throughout this report here and also exemplified in the IEEE Std. 323-1974 test. Much of the work summarized in the Brookhaven reports or in the Japanese work has not addressed the issues of significant extrapolation requirements [72,74] Their conclusions and lifetime predictions are based on the belief that linear Arrhenius behavior is the paramount aging model and 'must' be valid for margin assessments. Unfortunately, this work does not take into account that primary damage levels for equal loss of performance, may in itself, depend on temperature. Further, none of these studies have dealt with inverse temperature effects and their consequences for operational margins and lifetime prediction. Likewise, the IEEE Std. 323-1974 qualification testing does not address inverse temperature phenomena (which were published in 1996 and 1998 [53,54] and unknown at the time when the standard was written), and prevents any further operational margins to be established for any materials that 1) may have unusual non-Arrhenius aging behavior, 2) are subject to inverse temperature effects or 3) where performance changes differ between oxidative and inert aging condition.

An important study with detailed evidence of inverse temperature behavior for a Brandrex XLPO cable insulation in radio thermo-oxidative environments was published in 1996 [53]. In a follow-up study, additional generic trends indicative of inverse temperature behavior were also reported for the Brandrex XLPO and other cable insulation materials including another XLPO (Rockbestos), an XLPE (GE Vulkene) and an EPR (Eaton Dekoron) [54]. Virtually every XLPO and XLPE material has crystallinity with evidence of crystalline melting at intermediate temperatures (~60°C to 80°C and above). Since all three of the XLPO and XLPE materials that we have studied (Brandrex, Rockbestos and GE Vulkene) showed evidence of inverse temperature effects, we might expect that most other XLPO/XLPE insulations might have such effects. On the other hand, some EPR materials are crystalline (the Eaton Dekoron EPR) and others (e.g., an Anaconda Flameguard EPR) are rubbery with little indication of crystalline melting. Studies of these two materials indicate that the former has inverse temperature effects whereas the latter does not [75]. This again strongly suggests that the presence of crystallinity is an important indicator of likely inverse temperature effects.

Examination of two important data sets for the Brandrex XLPO are presented in Figure 14, i.e. the oxidation rates at 38 Gy/h dose rate combined with various temperatures ranging from 22°C to 110°C (left figure) and the available DED failure data as defined for 100% residual elongation versus various combinations of dose rates and temperatures (right figure). These data were obtained for stripped Brandrex XLPO insulation where the cable jacket and copper conductor had been removed before aging, with air available at both the external and internal surface. Strong inverse temperature effects are evident at 22°C and 40°C in the right hand plot since at a constant aging dose rate (e.g., 100 Gy/h), degradation occurs much faster than at 60°C. For aging above 60°C, degradation proceeds in the expected fashion where increases in temperature lead to faster degradation.

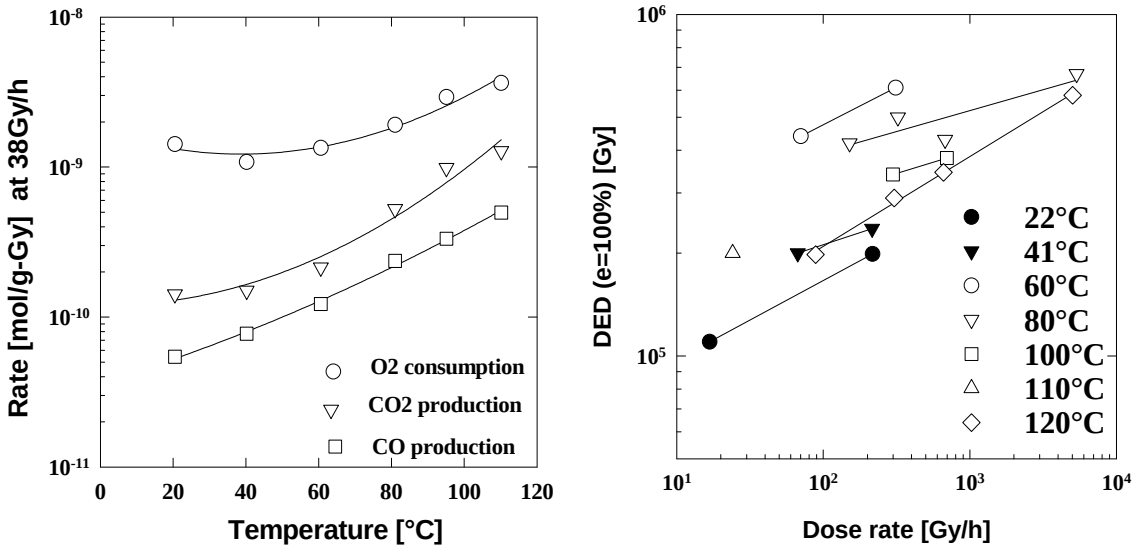

Figure 14. Oxidation rates and DED properties for Brandrex XLPO insulation material.

Table 2 uses results from these two figures to provide estimates of the doses, times and weight percent oxidation for the elongation to reach 100% at 100 Gy/h plus various aging temperatures ranging from 25°C to 110°C. The results show the profound effects caused by inverse temperature behavior. For example, three times less oxidation is required at 25°C than at 110°C to reach 100% elongation.

Table 2. Estimation of oxidative damage levels corresponding to 100% elongation at a dose rate of 100 Gy/h for stripped Brandrex XLPO insulation aged under air. Most importantly, it shows the transition in failure oxidation levels between 40°C and 60°C (see bold numbers).

	25°C	**40°C**	**60°C**	**80°C**	**95°C**	**110°C**
Ox. rate at 38 Gy/h [mols/g/Gy]	1.4E-09	1.1E-09	1.3E-09	1.9E-09	2.9E-09	3.6E-09
Est. ox. rate at 100 Gy/h [mols/g/s]	3.9E-11	3.1E-11	3.6E-11	5.3E-11	8.1E-11	1.0E-10
DED (100% elo.) at 100 Gy/h [Gy]	1.7E+05	2.1E+05	4.7E+05	4.0E+05	2.3E+05	2.0E+05
Time to 100% elongation [h]	1.7E+03	2.1E+03	4.7E+03	4.0E+03	2.3E+03	2.0E+03
Oxidation at surface [weight %]	**7.6E-01**	**7.4E-01**	**2.0E+00**	**2.4E+00**	2.1E+00	2.3E+00

Since low dose rate data were not available from this study, a crude estimate assuming linear extrapolation of the reported DED data would predict failure at ~50 kGy for RT and ~80 kGy at 41°C for a dose rate of 0.6 Gy/h. This would imply lifetimes as defined for 100% elongation of 83,000 h at RT and 133,000 h at 40°C, or 10 to 15 years. At a third of the applicable dose rate (i.e., 0.2 Gy/h) such lifetime predictions may fall within 30 to 45 years. These numbers are related to the assumption of an NPP environmental dose rate of 0.2 to 0.6 Gy/h at 40C and total integrated dose of 200 kGy to 400 kGy (20-40 Mrad, followed by additional ~200 Mrad for LOCA). The inverse temperature behavior implies significant property changes for much lower

total doses, namely 50 kGy at RT. A total dose of 400 kGy at 0.2 Gy/h would require 230 years, yet 50 kGy for failure according to limited DED trends would be reached within ~30 years.

It is important to recognize that such extrapolations are currently subject to a high degree of uncertainty, since DED data for dose rates of less than 20 Gy/h at low temperatures have not been measured. The trends, however, are obvious and must be considered. The inverse temperature behavior of relatively fast degradation rates observed for these materials has considerable consequences for the lifetime prediction and any re-qualification attempts. The highly accelerated tests imply margins for plant environments that do not exist based on preliminary low dose rate/low temperature data.

Most importantly, the observed inverse temperature behaviors apparent in the DED plot, plus the above calculations show that the fundamental tenet of lifetime prediction, namely the assumption of equal chemical degradative damage for equal physical property changes, is NOT always valid (see Table 2). There has long been speculation that microscopic heterogeneity occurring in the chemical degradation processes on the molecular level may result in a temperature dependence of the oxidation levels for equal loss of physical properties. The origin of such phenomena is related to changes in molecular mobility that results in similar chemical damage potentially being more localized or concentrated. Hence, at lower temperatures similar amounts of chemical damage could be more effectively translated into physical property degradation. Such processes are difficult to probe and only extensive and careful long term, low dose rate experiments would be able to demonstrate these processes in detail. At this point, there is evidence that these XLPO materials can absorb above 2% oxidative damage at elevated temperatures to result in 100% residual elongation, but only 0.7% at RT to 40°C (see bold numbers in Table 2). This represents a critical transition in the degradation process for these materials as the temperature approaches ambient conditions.

Assessing margins or predicting lifetimes must take these observations into account. Since we currently lack the required data sets, only additional aging studies focusing on these trends could provide some degree of certainty for this phenomenon or at minimum an empirical descriptive framework. It is currently not established on how to best perform accelerated aging studies when inverse temperature effects apply. The existing data demonstrate that inverse temperature effects are coupled with a change in the correlation between chemical and physical damage, hence precision data on chemical degradation must be compared with a physical performance test. Significant additional research is required to understand the exact origin and implications of such phenomena. Ultimately, this may provide options for better lifetime prediction and margin assessments. None of the other reports (Brookhaven and Japan) [72,74] have dealt with these important issues, despite the first evidence for inverse temperature effects having been reported in the mid-1990s and the fact that these issues are highlighted in IAEA "Assessment and management of ageing of major nuclear power plant components important to safety: In-containment instrumentation and control cables Volume II, International Atomic Energy Agency, IAEA-TECDOC-1188, 2000 [76]," IEC "Determination of long-term radiation ageing in polymers - Part 2 : Procedures for predicting ageing at low dose rates, International Electrotechnical Commission, IEC 1244-2, 1996 [77]," and Brookhaven documents "Subudhi, M. Literature Review of Environmental Safety-Related Qualification of Electric Cables, NUREG/CR-6384 BNL-NUREG-52480 Vol 1, 1996.,p. 4-87 [71]."

2 Literature Review of Previous LOCA Testing Approaches and Recommendations

This section focuses on a literature based evaluation of previous LOCA testing methods, their limitations and consequences for performance assessments and lifetime prediction. It involves an evaluation of the issues associated with 'pre-aging' and preparation of more suitable 'pre-aged specimens', and provides recommendations for future LOCA testing to be conducted as part of an additional experimental program.

Electrical cables used in the operation of safety equipment in a nuclear power plant must be able to transmit power, control signals and data during design basis events (DBE) such as a loss-of-coolant accident (LOCA). The US NRC requires by 10 CFR 50.49 that Class 1E electric cables used to energize, monitor or control safety related equipment be qualified for use in nuclear power generating stations. The qualification process requires the simulation of normal operation aging followed by a postulated LOCA environment, which includes exposure to additional radiation, high temperature steam and chemical (PWR) or water (BWR) sprays. The general requirements and guidelines for qualifying Class 1E are described in IEEE Std. 323-1974 including the temperature, pressure, radiation and chemical exposures required. The IEEE Std. 383-1974 [78] provides additional details on the qualification parameters for cables including radiation dose, maximum dose rates for simulating a normal 40 year operation life and the cable performance tests required during and after the LOCA simulation. Many nuclear power plants are now approaching the end of 40 year operation licenses and seeking 20 year renewals. These renewals will require qualification of the Class 1E cables for up to a 60 year service life. At issue is whether there is adequate margin in the earlier qualification testing to justify these qualification extensions.

Another purpose of this literature review is to evaluate previous LOCA testing methods of pre-aged specimens, and if needed, provide recommendations for more appropriate LOCA testing and preparation of more suitable pre-aged specimens to be conducted as part of a proposed experimental program. This section of literature review focuses on the pertinent LOCA testing portions of the four reports specified in the statement-of-work (SOW) as well as one additional report found to be relevant.

The four reports specified in the statement of work are:

NUREG/CR-6384, M. Subudhi, "Literature Review of Environmental Qualification of Safety-Related Electric Cables", BNL-NUREG-52480 Vol. 1, Prepared by Brookhaven National Laboratory, April 1996 [71].

SAND91-1776, M. J. Jacobus, "Aging, Condition Monitoring, and Loss of Coolant Accident (LOCA) test of class 1 E cables", prepared by Sandia National Laboratories for the U. S. Department of Energy, August 1992. (NUREG/CR-5772) [68-70].

JNES-SS-0903, T. Yamamoto and T. Minakawa, "The Final Report of the Assessment of Cable Aging for Nuclear Power Plants", prepared by the Japanese Nuclear Energy Safety Organization, July 2009 [72].

SAND05-7331, K.T. Gillen, R.A. Assink, and R. Bernstein, "Nuclear Energy Plant Optimization (NEPO) Final Report on Aging and Condition Monitoring of Low-Voltage Cable Materials", prepared by Sandia National Laboratories for the U.S. Department of Energy, November 2005 [14]. Note that SAND05-7331 pertains to state-of-the-art issues concerning pre-aging of cables and not LOCA testing *per se* so this report was not drawn upon for the LOCA testing portion of the literature review.

The additional report is:

SAND94-0485, C.F. Nelson, G. Gauthier, F. Carlin, M. Attal, G. Gaussens, P. Le Tutour, and C. Morin, "Long-Term Aging and Loss-of-Coolant Accident (LOCA) Testing of Electrical Cables: U.S./French Cooperative Research program", NUREG/CR-6202, IPSN-94-03, Sandia National Laboratories, October 1996 [73].

2.1 LOCA Testing Overview

NUREG/CR-6384 presents a thorough review of a large body of literature with substantial chapters on aging characterization, LOCA testing and condition monitoring methods. As this Section of the current report concerns LOCA testing, the discussion is limited to the chapter on LOCA testing and those parts of the other chapters germane to LOCA testing.

LOCA testing was conducted in the studies covered by SAND94-0485, JNES-SS-0903, and SAND91-1776. The Class 1E equipment qualification process is generally conducted in a sequence of steps. First the cables are subjected to thermal and radiation exposures that produce changes in the polymeric insulation and jacketing that is equivalent to the expected normal operation service life in the power plant. The aging is typically accelerated by a factor ranging from 100 to 1000. The IEEE Std. 383-1974 [78] specifies that thermal aging will be conducted at a minimum of three temperatures "…including 136°C and two or more others at least 10°C apart…" and evaluated "...using the Arrhenius technique or other method of proven validity to simulated installed life." The cables should also "…be subjected in air to gamma radiation from a source such as ^{60}Co to a dosage of $5x10^7$ rad (0.5 MGy) at a rate not greater than $1x10^6$ rad per hour 10 kGy/hr)." No temperature is specified for the aging irradiation exposure.

According to IEEE Std. 383-1974 [78] the aged cables are then to be subjected to a mandrel-bend-voltage-withstand test where the cables are coiled on a mandrel with a diameter of approximately 20 times the overall cable diameter and immersed in tap water. While immersed the specimens should withstand for 5 minutes a potential of 80 Vac or 240 Vdc per mil of insulation thickness. This test was not conducted in any of the three studies under review.

In the next step, the pre-aged cables are subjected to an additional, final dose of radiation and a prescribed program of superheated/saturated steam and chemical sprays that simulate a LOCA. The IEEE Std. 323-1974 [67] Appendix A specifies a total additional accident dose of 150 Mrads (1500 kGy) for PWR LOCAs with details on the dose delivery with time (which extents out to one year) and 26 Mrad (260 kGy) for BWR LOCAs with no further details. No temperature is specified for the LOCA irradiation exposure. For most the studies considered in this review the PWR accident exposure was implemented since this qualifies the cable for use in both PWR and BWR plants. Typically, the PWR accident dose is applied at a constant rate over a relatively

short period of time. The IEEE Std. 383-1974 limits the dose rate to 1 Mrad/hr (10 kGy/hr) unless "the LOCA profile requires a greater dose rate" [78].

The IEEE Std. 323-1974 Appendix A also provides details on the steam exposure profiles for PWR and BWR reactors (as well as a combined PWR/BWR example) including details on the spray exposures [67]. IEEE Std. 383-1974 specifies that during the thermal portion of the LOCA exposure the cables are to be operated under rated voltage and load [78]. The cable must function electrically throughout exposure to the LOCA environmental extremes. In SAND94-0485 the cables were energized with 110 Vdc but no current; cable failure during LOCA testing was indicated by opening of a 1A fuse. Near-continuous insulation resistance measurements predicted cable failure. In JNES-SS-0903 the cables were energized with the rated voltage but no current. The cables were monitored for electrical shorts and leakage current. In SAND91-1776, the cables were energized in the U.S. portion of the study. During aging and accident irradiation non-coaxial cables were energized with 50 Vdc and 300 mA current and coaxial cables were energized with 600 Vdc and no current. During the accident steam exposure all cables were energized with 50 Vdc and no current to allow for near-continuous insulation resistance measurements. A major conclusion of the NUREG/CR-6384 literature review is that failure of a cable during LOCA testing is ill defined and suggests "…simulating the performance of cables using actual electrical loads (e.g., power cables with small motors, control cables with SOVs, and instrumentation cables with transmitters or RTDs)."

Cable fire testing at Sandia has resulted in the development of sophisticated cable monitoring equipment available for LOCA testing that can accomplish the recommended monitoring function [79]. The electrical response behavior of selected cables can be monitored using the surrogate circuit diagnostic unit (SCDU). Wherein a cable under test is connected to simulated control/instrument circuits representative of those used to control and monitor typical nuclear plant safe shutdown components. Motor operated valve (MOV) control circuits, set up with different circuit conditions, can be implemented to assess the effects of control power transformer (CPT) ratings, multiple or single voltage sources, and circuit grounding (grounded and ungrounded) on the manifestation of specific cable failure modes and their likelihoods. Circuit voltages and currents can be monitored continuously during a LOCA test to provide information on the timing and nature of observed failures in each cable.

Finally, after the LOCA exposure the cables are evaluated for acceptable performance by repeating the mandrel-bend-voltage-withstand test described above except now using a larger mandrel 40 times the cable diameter. This final performance test was conducted as part of the studies described in SAND91-1776 and JNES-SS-0903 but not SAND94-0485. In SAND91-1776 failure was taken as leakage of more than 20 mAac. This final performance test is described in the IEEE Std. 383-1974 [78] standard as more severe than exposure to two cycles of the thermal environment. After the LOCA irradiation and thermal exposure the cables are brittle. SAND91-1776 describes the extensive damage done to the cable jackets during the handling of the cables where most of the jacketing had completely fallen off. A major conclusion of the NUREG/CR-6384 literature review is that the post-LOCA mandrel bend test requires evaluation for relevance because it may impart unrealistic stresses on the cables that induce failure in otherwise functioning cables.

2.2 LOCA Testing Issues

The pertinent issues identified in NUREG/CR-6384 in rough order of importance are radiation dose-rates during LOCA tests, presence of oxygen during LOCA tests, simultaneous versus sequential environmental exposure, effect of aging method on LOCA simulation, acceleration of the post-transient LOCA environment, superheat versus saturated steam conditions, beta versus gamma radiation exposure, and chemical sprays during LOCA tests. Of these, the last three, concerning the type of steam exposure, the type of radiation exposure and the effect of chemical sprays were not considered to be of great importance in NUREG/CR-6384 and so are not discussed any further here.

2.2.1 Radiation dose-rates during LOCA tests

Radiation dose-rate effects are perhaps the most serious issue confronting Class 1E electrical cable qualification efforts. As discussed in great detail in Section 3 of this report, radiation dose-rate effects can often be attributed to diffusion limited oxidation (DLO). If oxygen cannot diffuse into the polymer fast enough to keep dissolved oxygen concentration within the polymer stable during irradiation then DLO conditions exist. Irradiation damage to the bulk polymer under DLO conditions is significantly less severe because oxidation is biased toward the surface. While especially significant for accelerated pre-aging of cables, dose-rate effects due to DLO also operate during the LOCA irradiation step.

Appendix A of IEEE Std. 323-1974 provides guidance on the time dose signature of a PWR LOCA. The dose rate during the first hour is 40 kGy/hr and for the next eleven hours 15 kGy/hr. After 30 days the total dose delivered is 0.55 MGy and the rate has dropped to 0.31 kGy/hr. The total dose after 6 months is 1.1 MGy and the total dose required after one year is 1.5 MGy and the final dose rate is 0.09 kGy/hr. Two thirds of the total LOCA dose is delivered at 0.12 kGy/hr over an eleven month period.

Two Japanese studies discussed in NUREG/CR-6384 clearly demonstrate the effect of LOCA dose rate. In the first study (ref. 5.17) [80] Japanese EPR and CSPE cables were subjected to two dose rates (temperature was not stated in NUREG/CR-6384 but ambient is typical of Japanese studies). The first dose rate was 9.3 kGy/hr (near the 10 kGy/hr limit allowed in IEEE Std. 383-1974 [78]) to a total dose of 1.55 MGy while the other dose rate was 0.55 kGy/hr to a total dose of 1.19 MGy. Even though the cables exposed at the lower dose rate received a lower total dose the rate of degradation was twice as high. The presence of air during the LOCA enhanced the effect. This is not unexpected and consistent with our knowledge on DLO effects present at such high dose rates. At the lower dose rate more oxidative damage has a chance to build up resulting in failure at an overall lower total dose.

In the second study (ref. 5.18) [81], five different Japanese cable materials (EPR, SR, Hypalon, XLPE and Chloroprene) were irradiated at different dose rates (0.45 to 10 kGy/hr) in air at room temperature and the elongation was measured as a function of total dose (pre-aging plus accident) up to 2.0 MGy. Samples aged to 1.5 MGy were subjected to a LOCA steam spray and elongation was measured as function of time up to 280 hours. During the irradiation all of the materials responded similarly in that they lost most (85 to 95%) of their elongation with little evidence of dose rate effect except for the XLPE material. However, during steam exposure at

120°C the response of each material was significantly different and dose rate effects were much more evident, again suggestive of significant DLO situations. The low dose rate EPR material degraded more significantly than the material irradiated at high dose rates. For the XLPE material, steam exposure improved elongation and there was little evidence of dose rate effects. The other materials degraded in elongation with evidence of dose rate effects. That is, the material exposed at lower dose rates to the same level of total dose (1.5 MGy) were more degraded by the subsequent steam exposure. In essence, such DLO effects (the underlying cause of physical dose rate effects) are variable with individual materials.

Two sets of materials were irradiated under more oxidizing conditions. One was conducted at room temperature at a moderate dose rate (4.2 kGy/h) in pure oxygen. The other was conducted in air at 70°C rather than room temperature. While degrading similarly with the other conditions tested during irradiation, the enhanced oxidation cases were the most degraded during the steam exposure, for EPR and Hypalon, two materials with significant dose rate response. The enriched oxygen effect was most pronounced for the EPR material with the elongation ratio falling below 1% after only 20 hours of subsequent steam exposure. NUREG/CR-6384 reports that in this study the volume resistivity of EPR and to a lesser extent XLPE decreased significantly for samples irradiated at the lower dose rates. This was attributed to unstable oxidized species formed during irradiation that had little effect on tensile properties. However, during the LOCA steam exposure the oxidized species decomposed resulting in mechanical degradation. The formation of these oxidized species during irradiation can be limited by oxygen diffusion (as discussed in the Section 3) resulting in degradation profiles with extensive oxidation limited to surface material.

In SAND94-0485, four cables (U.S. 2 conductor EPR with Hypalon jacket, French 3 conductor EPR with Hypalon jacket, U.S. 3 conductor XLPE with Hypalon jacket and French PE coax) were aged and LOCA tested. The aging was performed at low dose rates (0.002 kGy/hr to 0.10 kGy/hr) to total doses ranging from 14 to 210 kGy. The aging was performed at two temperatures (40°C and 70°C) with air flow over times up to five years. The lowest 0.002 kGy/hr dose rate was performed in a research reactor and was considered to be about ten times above realistic containment conditions. The LOCA irradiation for complete cables pre-aged to 84 kGy was performed at 70°C with air flow at a dose rate of 0.80 to 0.90 kGy/hr for an additional accident dose of 0.60 MGy. The steam exposure included air and generally followed French qualification procedures which utilize lower peak steam temperatures, and less aging and accident irradiation than typical in U.S. qualification programs.

A dose rate effect was observed that was similar to the effect seen in the Japanese studies discussed above. In general, for a given total dose the degradation was greater for lower dose rates and the amount of degradation decreased as the dose rate increased. This apparent dose rate effect operates down to very low dose rate levels in air. At 40°C, the degradation of the cables irradiated at 2 Gy/hr in a research reactor was very similar to the cables irradiated at 5 Gy/hr using Co-60 sources indicating a lower limit for dose rate effects in air.

Most LOCA test programs administered the LOCA irradiation at a constant rate over a relatively short period of time. In SAND 91-1766 the LOCA irradiation was conducted at ambient temperature and a dose rate of 6 kGy/hr to a total dose of 1.1 MGy over an eight day period. Note that the 1.1 MGy total dose corresponds to the six month duration of the simulated steam

exposure. In JNES-SS-093 the LOCA irradiation was conducted at ambient temperature and a dose rate of <10 kGy/hr to a total dose of 1.5 MGy over approximately a seven day period. In SAND 94-0485 the LOCA irradiation was delivered at 70°C over a 30 day period at a dose rate of 0.8 to 0.9 kGy/hr to a total dose of 0.60 MGy.

2.2.2 Dose rate recommendation

The dose rate for LOCA irradiation should be kept near levels expected in an actual accident. Our recommendation is that the dose rate for LOCA irradiation be delivered at ambient temperature in the presence of air at the high levels expected during the first day of an actual accident (or as high a dose rate possible in the irradiation facility). Due to observed dose rate responses the dose delivered at these high rates will not be as damaging as it would if delivered at a lower rate but this is the prototypic reality of the accident environment. The remainder of the total dose should be delivered at ambient temperature in the presence of air over a 30 to 90 day period. The much lower dose rate required still represents an accelerated aging step so DLO conditions may still be an issue.

2.2.3 Simultaneous vs. sequential testing and air flow during LOCA

In an actual LOCA, cables located inside containment would be exposed simultaneously to radiation, oxygen (unless containment is inert with nitrogen), and superheated and saturated steam impingement. Past programs for qualification of these cables have followed both simultaneous and sequential approaches for aging and accident simulation. Historically, due to cost and other practical considerations, most cable qualifications have been conducted with sequential exposure approaches for both aging and LOCA.

A typical sequential qualification test regiment consisted of the following sequential steps:

(1). thermal aging equivalent to the design life of the power plant (typically 40 yrs)

(2). gamma radiation exposure simulating both normal design life exposure (500 kGy) plus the LOCA exposure (typically 1500 kGy for PWR) both at ambient temperature.

(3). steam/chemical spray exposure simulating the thermal portion of the LOCA

The radiation exposure for a sequential qualification test regiment (both aging and LOCA) is typically conducted with the test chamber underwater in a pool at ambient temperature. The radioactive sources are placed symmetrically around the test chamber. All manipulations of the sources are conducted beneath the water which provides a high degree of shielding and operational safety. During the LOCA steam exposure the test chamber is located in open air.

A typical simultaneous qualification test regiment consisted of the following sequential steps:

(1). combined accelerated thermal and radiation aging (500 kGy at elevated temperatures)

(2). combined radiation (additional 1500 kGy), steam and chemical spray exposure in the LOCA simulation

The simultaneous thermal and radiation aging qualification is achieved by controlling the temperature of the cables inside the test chamber with electric heaters during the underwater radiation exposure. The radiation exposure for a simultaneous LOCA test requires open air irradiation which requires a more sophisticated facility in order to be conducted safely and hence is generally more costly. Using the facilities presently available at Sandia, the facility charge for open air irradiation is ten times greater than the facility charge for in-pool irradiation.

Although a simultaneous testing approach is obviously more realistic, arguments are made in NUREG/CR-6384 that sequential testing is more conservative because the cables are more degraded by the complete radiation exposure (at low or ambient temperature) before being subjected to the steam exposure in the final thermal portion of the LOCA test. This is expected to depend on the type of polymer under investigation.

As summarized in NUREG/CR-6384, there have been a number of studies conducted to determine the difference between the simultaneous and sequential approaches to cable qualification with three of the more recent also considering the impact of air being included during the LOCA test (ref. 5.13, 5.14, and 5.15 in NUREG/CR-6384) [82-84]. It is important to note that the results of these types of cable characterization studies are prone to scatter, when testing a range of different insulating materials there are always exceptions and cables made with the same materials by different manufacturers can differ significantly in behavior. Generally (but not always), simultaneous LOCA testing without air flow was the least degrading approach and was considered unacceptable. Simultaneous LOCA testing with air flow, and sequential LOCA testing with or without air flow were roughly equivalent although simultaneous tests with air are generally the most degrading. Because sequential tests were considered more conservative, substantially less expensive than simultaneous test and have been shown to be equivalent or provide only slightly different results, most qualification programs have been conducted sequentially and air has not been injected during the LOCA steam test. (NUREG/CR-6384)

In the more recent studies conducted at Sandia (SAND94-0485 and SAND91-1776) and the most recent study conducted in Japan (JNES-SS-0903) a hybrid test regiment was used that consisted of the following sequential steps:

(1). combined accelerated thermal and radiation to simulate the desired normal aging period with air flow (at elevated temperatures required by IEEE Std. 383-1974 [78])

(2). additional gamma radiation exposure simulating the LOCA exposure with air flow (ambient or elevated temperatures)

(3). steam/chemical spray exposure simulating the thermal portion of the LOCA (with or without air flow)

The accelerated aging was conducted simultaneously with flowing air to minimize depletion of oxygen in the atmosphere thereby reducing any diffusion limited oxidation effects caused by such depletion. The LOCA radiation dose was applied next at ambient temperature in SAND91-1776 and JNES-SS-0903 and at 70°C in SAND94-0485. Finally the cables were subjected to the steam exposure. There was no air flow during the LOCA steam exposure in

SAND91-1776 and JNES-SS-0903. There was air flow during the LOCA steam exposure in SAND94-0485.

2.2.4 LOCA test sequence recommendation

The hybrid test regiment as used in SAND94-0485 is recommended for further LOCA testing. The LOCA would be conducted sequentially. The accident irradiation would be conducted at ambient temperature just after aging. Again, ample air flow would be used to minimize oxygen diffusion limits. Air would also be injected during the steam exposure sequence of the LOCA simulation to better represent the actual conditions expected inside containment during a LOCA. A simultaneous LOCA is not being recommended for a number of reasons. As discussed above, the difference between a simultaneous and sequential LOCA simulation is not great but the cost of a simultaneous LOCA test is at least an order-of-magnitude greater than a sequential LOCA test.

A final consideration concerns the irradiation geometry differences between simultaneous and sequential LOCA testing. In sequential LOCA testing the irradiation is performed underwater in a pool. The cobalt sources can be arranged in an axially symmetric fashion around the test vessel to evenly irradiate all the cables. The total dose delivered to any location on any given cable can be determined with a high degree of confidence. A simultaneous LOCA test would be conducted inside of a specially designed room that allows the cobalt sources to be raised out of the pool into the air. The sources may not be positionable in an axially symmetric fashion but rather irradiation may need to be from the side of the test vessel. This asymmetric irradiation requires that the test vessel be rotated during the live steam exposure test. While this is possible, the end result may be that the cables are not irradiated as uniformly as in the sequential test where axially symmetric irradiation is more easily implemented.

2.2.5 Oxygen enrichment for aging acceleration

The dose rate for accelerated aging and LOCA irradiation should be as low as practical to minimize or mimic prototypic DLO conditions. Very low dose rates that eliminate DLO (~5 Gy/hr for a typical 3 conductor cable but dependent on the cable materials, the cable configuration and material thicknesses) would require excessive exposure times to reach a desired total dose. Oxygen enrichment is a potential method for mitigating DLO and effecting moderate aging acceleration during irradiation that has never been seriously studied. Increasing the oxygen concentration would accomplish two things. Oxidation reaction rates (both thermal and radiological) would be moderately accelerated and permeation rates of oxygen into the polymer would be increased. In order to mitigate DLO conditions the increase in the oxygen permeation rate would need to more than counter the increase in oxidation rates. The greatly enhanced damage for EPR cables in the one LOCA irradiation conducted under pure oxygen at room temperature (ref. 5.18 in NUREG/CR-6384) [81] suggests encouragement. Implementation of this approach would require the use of an already existing thermo-oxidative degradation model that accommodates increased oxygen concentrations through the application of a parameter labeled β (see section 3.3), which enables a correlation between O_2 partial pressure and oxidation rate. For values of β that are small compared to unity, the oxygen permeability rate and the oxidation rate increase equally as the surrounding oxygen pressure is increased implying that the importance of DLO effects will not change as oxygen pressure is

increased. In the opposite extreme where β is much greater than unity, the oxidation rate will not be affected by an increase in oxygen partial pressure so that the importance of DLO will be reduced by the square root of the increase in partial pressure. In between these two limits, the effect of partial pressure changes will be intermediate. Thus it is clear that an extensive series (temperature and dose rates) of oxygen consumption measurements versus oxygen partial pressure for each material considered will be extremely helpful in determining the utility of utilizing oxygen overpressure techniques because these measurements will lead to estimates of the β parameter. The potential advantage would then be the ability to confidently use higher dose rates to accelerate aging and LOCA irradiation without DLO problems. The only other means to eliminate DLO problems is to lower aging dose rates to ~5 Gy/hr which will require ~10 year exposures and conduct LOCA irradiation exposures over a 6 to 12 month time frame.

2.3 Summary

The recommended LOCA testing program would utilize the U.S. test chambers and roughly follow the U.S. test procedures described in SAND 94-0485. The U.S. LOCA test procedures followed sequential exposures of the cables to radiation and steam. The irradiation step was conducted at 70°C with a constant dose rate and air flow (perhaps with enriched oxygen) over a 30 day period. The subsequent steam exposure is also conducted with air flow over a 14 day period. The recommended changes to this LOCA testing regiment pertain to the irradiation step. The irradiation should be conducted at ambient temperature with air flow at an elevated dose rate that mimics the dose rate postulated for the first 24 hours of the LOCA (e.g. IEEE Std. 323-1974 Appendix A). The dose rate would then be reduced to provide the desired total dose over a 30 to 90 day period. As this still represents an accelerated aging step, DLO conditions may still be an issue. The use of oxygen enriched air may provide a means to accommodate higher dose rates without DLO issues but additional research is needed to develop this technique.

If DLO conditions can be largely minimized or eliminated during cable aging and accurately represented during LOCA irradiation then prototypic cable damage will be more precisely reproduced. However, since the integrated oxidative damage across the cable or jacketing diameter is expected to be greater than achieved in previous studies, more cable failures can be expected, especially as a result of the final mandrel-bend-voltage-withstand test. IEEE Std. 383-1974 [78] admits this is a severe test and NUREG/CR-6384 concludes this test is overly severe. As recommended in NUREG/CR-6384, a better approach for evaluating expected cable performance during an actual LOCA is to monitor realistic cable operation during a LOCA simulation. Properly aged cables, although more severely damaged, may still pass a realistic cable operation evaluation during a LOCA simulation.

INTENTIONALLY LEFT BLANK

3 Estimates of Margins in Past and Future Aging Simulations of Safety-related Cables

3.1 Introduction

The original qualifications of low voltage cables for nuclear power plant applications were based on the application of IEEE Std. 323-1974 [67]. In order to simulate 40 years of low-voltage cable aging under ambient plant conditions, the approach was to use sequential thermal aging at very high temperatures followed by radiation exposures at very high dose rates as summarized on p. 2-11 in a recent Brookhaven document [74]. Over the past 30 years or so, much information concerning proper aging techniques has been published. These studies show that the procedures used in the original qualifications based on IEEE Std. 323-1974 do not address numerous potential pitfalls that can impact degradation and lifetime simulations. These include:

(1). The presence of dose-rate effects for radiation aging [22-25,72,85-87]

(2). Differences occurring for combined radiation-thermal aging dependent upon whether sequential thermal followed by radiation occurs or the opposite sequence occurs or whether the exposure is combined [88]

(3). The assumption of Arrhenius behavior when non-Arrhenius is often found [8,11-13,21,26,28-31,89,90]

(4). Significant reductions in aging rates that occur due to diffusion-limited-oxidation (DLO) when aging is accelerated by large amounts [91-95] and

(5). The presence of so-called “inverse temperature” effects wherein degradation for a given dose-rate environment can sometimes occur more rapidly as the combined environment aging temperature is lowered [53,54,75].

Many of the original qualifications conducted at extremely high acceleration rates were thought to provide significant margins in terms of the qualification conditions utilized. In light of the advances in knowledge that have occurred, one important purpose of this report is to re-examine the historic sequential qualifications to determine whether such margins exist. In addition, we examine more recent simultaneous simulations [68-70] carried out at more moderate acceleration conditions to estimate the margins represented by these experiments. The modeling and calculations also allow us to suggest the best accelerated aging conditions to use for any future attempts at simulating the aging expected under ambient nuclear power plant aging conditions. We also describe areas where research could lead to more confident margin predictions.

3.2 Effects of Oxidation on Cable Degradation

According to Henry’s Law, when a material is surrounded by a gaseous environment (e.g., air), each constituent gas of the air at equilibrium will have a dissolved concentration in the material based on the product of the solubility coefficient S for that gaseous component in the material of interest times the partial pressure p of that surrounding gas. In other words, for a surrounding air

atmosphere containing oxygen with a reference partial pressure p_{ref}, the dissolved oxygen concentration throughout the material at equilibrium will be given by:

$$[O_2]_{eq} = [O_2]_{ref} = Sp_{ref} \tag{1}$$

When cables slowly age in air during their ambient lifetime exposures to radiation and thermal environments, the dominant degradation reactions will typically involve reactions with the dissolved oxygen. As dissolved oxygen is used up by degradation chemistry, it is re-supplied by diffusion processes from the surrounding air atmosphere. However, if the degradation reactions use up oxygen faster than it can be re-supplied by diffusion effects, the dissolved oxygen concentration will decrease. This can lead to so-called diffusion-limited oxidation (DLO) where decreases in the degradation reaction rates result. The most critical oversight in the early cable aging simulations was not recognizing that the highly accelerated aging conditions used can lead to such rapid oxidation rates that important DLO effects occur. We will verify that this is the case but first we want to show evidence for the importance of oxidation to cable material degradation by comparing degradation results for oxygen-containing environments with those appropriate to inert gas aging environments.

We first show results for thermal-only aging environments. Figure 15 shows elongation versus aging time results for an Okonite chloroprene (CP) cable jacket aged at 150°C both in air and in nitrogen [14]. Given the logarithmic time axis, the aging in the oxygen containing environment occurs more than an order of magnitude faster than aging in the absence of oxygen. Results for a Samuel Moore Dekoron chlorosulfonated polyethylene (CSPE) jacket that was aged at 138°C in both air and argon are shown in Figure 16 [14]. It is again clear that aging in the oxygen-containing environment leads to faster degradation than that occurring in an inert argon environment. Another example is shown in Figure 17 for an Anaconda Flameguard ethylene propylene rubber (EPR) cable insulation aged at 150°C where again the presence of oxygen leads to a much more rapid degradation [14].

This latter material is particularly interesting since it is affected by copper-catalyzed oxidation. This effect occurs for some unprotected insulations when copper salts from the adjacent copper conductor diffuse into the adjoining surface of the insulation either during the high-temperature extrusion process that is used during manufacture or during long-term applications. The importance of copper-catalysis for this material was described in an earlier publication [42]. In this study an un-aged insulation that had its copper conductor removed was aged at various temperatures and the aging monitored by following tensile properties. Figure 18 shows elongation results versus aging time for this material. Since DLO effects are not expected to be important for this material when aged separately from its jacket and conductor at 101°C, we expected to have uniform oxidation across its entire cross-section. This was not the case as evidence by density profiling results shown in Figure 19.

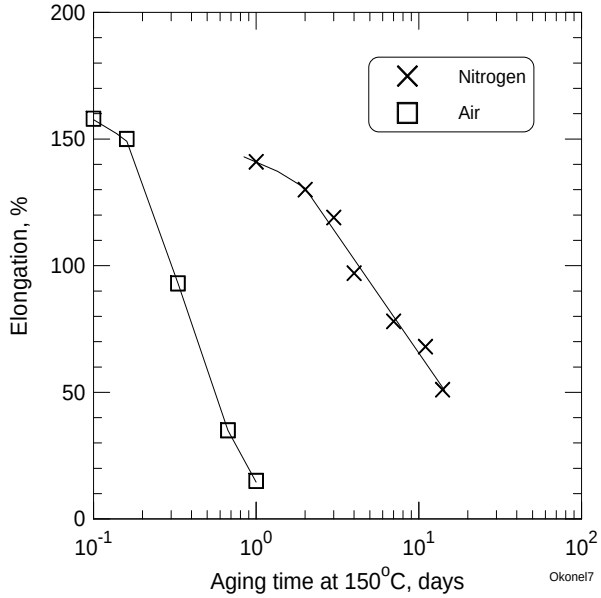

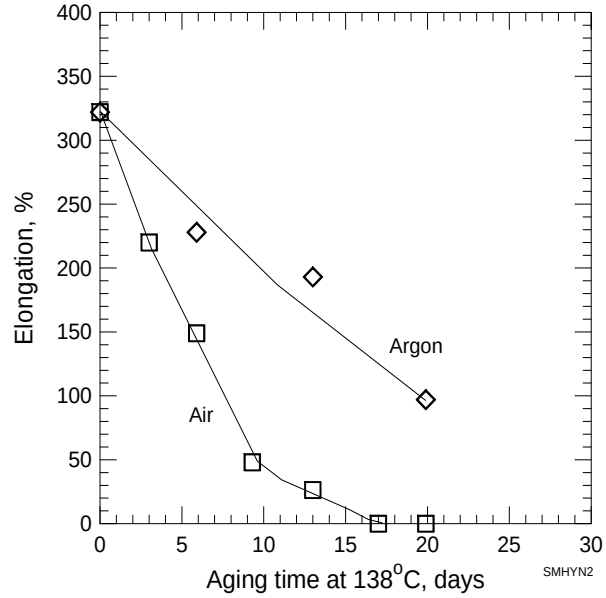

Figure 15 (Left). Comparison of elongation results versus aging time at 150°C for an Okonite chloroprene (CP) jacket in an oxygen-containing environment (air) versus aging under inert conditions.

Figure 16 (Right). Comparison of elongation results versus aging time at 138°C for a Samuel Moore Dekoron chlorosulfonated polyethylene (CSPE) jacket in an oxygen-containing environment (air) versus aging under inert conditions (surrounding atmosphere of argon).

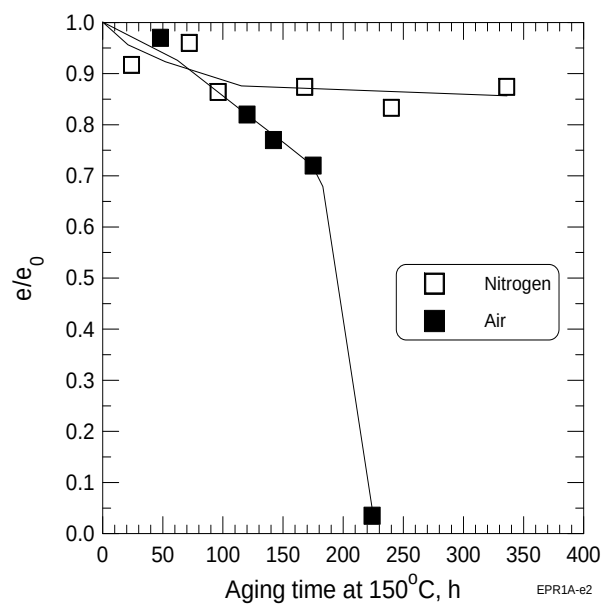

Figure 17. Comparison of elongation results versus aging time at 150°C for an Anaconda Flameguard ethylene propylene rubber (EPR) insulation in an oxygen-containing environment (air) versus aging under inert conditions.

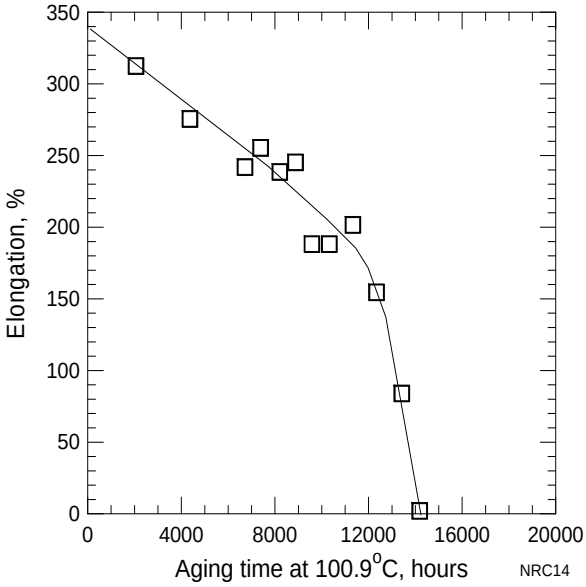

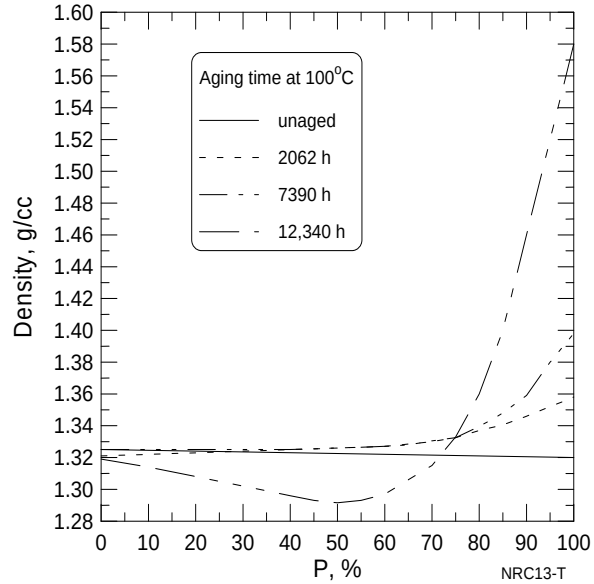

Figure 18 (Left). Tensile elongation results versus aging time at 100.9°C in air for an Anaconda Flameguard ethylene propylene rubber (EPR) insulation.

Figure 19 (Right). Density profile results for the Anaconda Flameguard ethylene propylene rubber (EPR) insulation after the various indicated aging times at 100.9°C.

Density profiling involves taking thin slices across the cross-section of a material and measuring their densities in a density gradient column. For the results shown in Figure 19 the x-axis represents the percentage of the distance from the outside surface of the insulation (0%) to the inside surface that used to be adjacent to the copper-conductor (100%). The density profile for unaged material is shown by the solid almost horizontal line at ~1.32 g/cc. It is normally found that oxidation leads to increases in the density of a material [34]. The results shown in Figure 19 indicate that noticeable density increases occur at the inside surface after only 2062 hours which is early in the aging (Figure 18). This increase gets larger after 7390 hours (~half way through the degradation) and even larger near the end of the degradation at 12,340 hours. Based on a number of analytical tests that showed large copper concentrations near the inside surface of the unaged sample, we identified this aging mechanism as copper-catalyzed oxidation [42].

Not surprisingly, thermal aging in the absence of oxygen totally eliminates the copper-catalyzed oxidation effect as shown in Figure 20 (previously unpublished). Although the air-aging results again show important copper-catalyzed oxidation, aging in nitrogen totally eliminates the large increases observed at the inside surface.

We can therefore conclude from the results for aging in thermal-only environments that the presence of dissolved oxygen during the aging can have a profound influence on the rate of mechanical degradation. Therefore if DLO effects are important during accelerated aging simulations, the dominant degradation chemistry may be eliminated or reduced.

We now show comparisons of air-aging and inert aging for materials aged in radiation environments. Such data are in fact quite limited but we were able to find some results for the two most important insulation materials, XLPO and EPR. Results for Brandrex XLPO [53] are

shown in Figure 21 where it is clear that the presence of oxygen leads to a much quicker degradation rate.

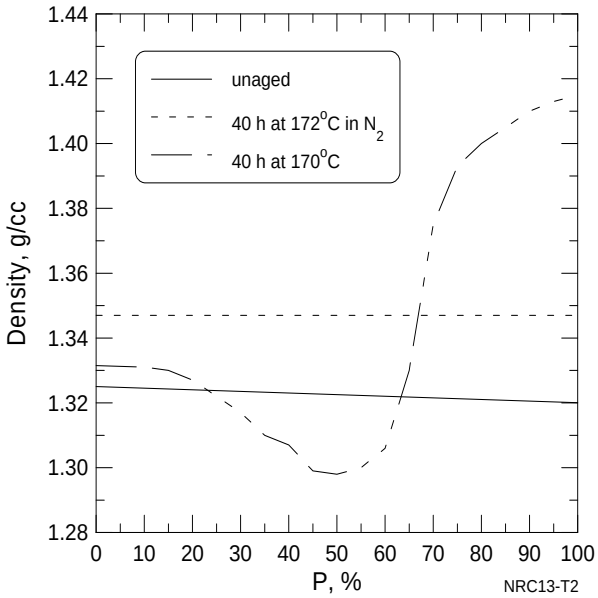

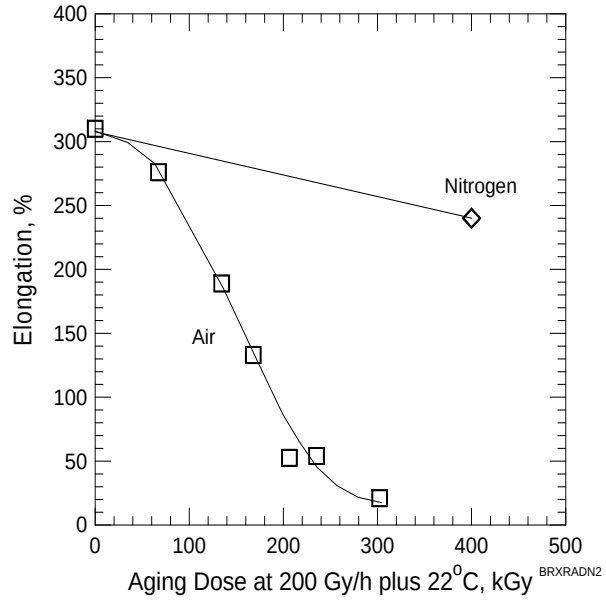

Figure 20. (Left) Density profile results for the Anaconda Flameguard ethylene propylene rubber (EPR) insulation after the various indicated aging times at ~170°C comparing aging in air versus aging in nitrogen.

Figure 21. (Right) Elongation results versus total aging dose for a Brandrex XLPO cable insulation aged at 200 Gy/h plus 22°C in air and in nitrogen.

Results for the Anaconda Flameguard EPR material are more interesting as seen for normalized elongation data in Figure 22 and normalized tensile strength data in Figure 23 (previously unpublished). In this instance there is little difference between air and inert aging for elongation data. However, the tensile strength results indicate that differences in chemistry are operative. The drop in tensile strength for air aging implies that scission processes are dominating cross-linking processes whereas this is not the case for inert aging. Additional evidence for large changes in chemistry is evident from density profiling results comparing radiation aging in air versus radiation aging in nitrogen for this material. These results (previously unpublished) are plotted in Figure 24 and indicate that the air-aging involves copper-catalyzed oxidation near the inside surface whereas nitrogen aging totally eliminates this degradation mechanism.

It should be clear from the results shown in this section that the presence or absence of oxygen during aging simulations can have significant effects on the degradation chemistry and on the rate of mechanical degradation of important cable materials.

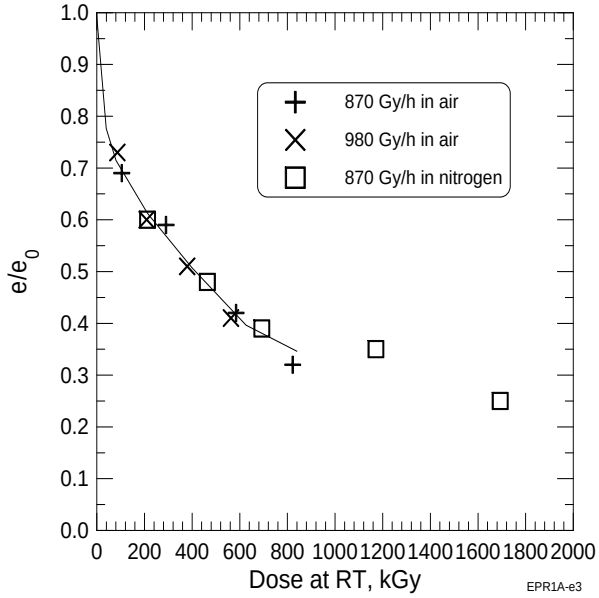

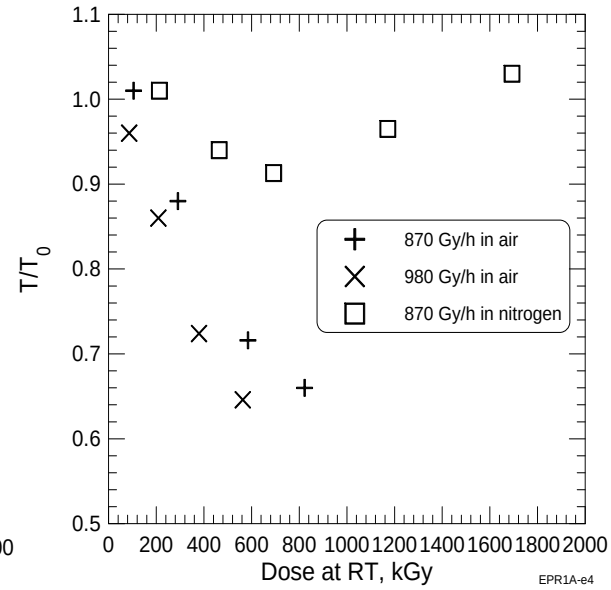

Figure 22. (Left) Normalized elongation results versus total aging dose for an Anaconda Flameguard EPR cable insulation aged under the indicated radiation aging conditions.

Figure 23. (Right) Normalized tensile strength results versus total aging dose for an Anaconda Flameguard EPR cable insulation aged under the indicated radiation aging conditions.

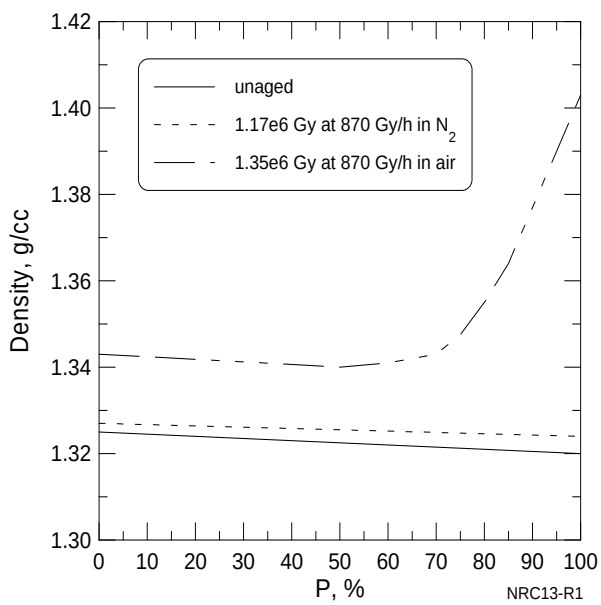

Figure 24. Density profile results for the Anaconda Flameguard ethylene propylene rubber (EPR) insulation after radiation aging at 870 Gy/h in air versus aging in nitrogen.

3.3 Diffusion-Limited Oxidation (DLO) Modeling

As demonstrated, the concentration of dissolved oxygen in a material during aging can have a large impact on the degradation chemistry and degradation rates. Therefore it becomes critical to be able to estimate the oxidation profile across cables (e.g., amount of oxidation versus cross-sectional position) when they are subjected to accelerated and ambient aging conditions. This involves modeling of DLO effects. Since this subject is extensively covered in several publications [91-95], only a brief summary will be included here. The theoretical modeling for a simple sheet material starts by utilizing the best chemical kinetic schemes thought to represent the aging chemistry occurring for both thermal and radiation aging which leads to the following expression for the rate of oxidation where $[O_2]$ represents the dissolved oxygen concentration in the material and C_1 and C_2 are constants involving the underlying rate constants governing the chain of reactions leading to degradation.

$$\phi[O_2] = \frac{dO_2}{dt} = \frac{C_1[O_2]}{1 + C_2[O_2]} \qquad \text{(Eq. 2)}$$

When the dissolved oxygen concentration is at equilibrium with the oxygen partial pressure (reference conditions) in the surrounding air atmosphere (p_{ref}), then Equation (2) plus Equation (1) lead to:

$$\phi[O_2]_{ref} = \frac{dO_2}{dt} = \frac{C_1[O_2]_{ref}}{1 + C_2[O_2]_{ref}} = \frac{C_1[O_2]_{ref}}{1 + C_2 S p_{ref}} = \frac{C_1[O_2]_{ref}}{1 + \beta_{ref}} \qquad \text{(Eq. 3)}$$

$$\beta_{ref} = C_2[O_2]_{ref} = C_2 S p_{ref} \qquad \text{(Eq. 4)}$$

When DLO effects occur, the oxygen concentration dissolved in the polymer $[O_2]$ will decrease below its equilibrium reference value at the air-exposed surface. By combining Equations (2) and (4), the oxidation rate corresponding to this reduced dissolved oxygen concentration is given by:

$$\phi[O_2] = \frac{dO_2}{dt} = \frac{C_1[O_2]}{1 + C_2[O_2]} = \frac{C_1[O_2]}{1 + \beta \frac{[O_2]}{[O_2]_{ref}}} \qquad \text{(Eq. 5)}$$

In the case of large β_{ref} values, the rate of oxidation will drop very slowly as the dissolved oxygen concentration is reduced by DLO effects. On the other hand, the same equation indicates that in the opposite limit, when β_{ref} is very small, the oxidation rate will drop linearly with the drop in dissolved oxygen concentration. These effects can be seen in the results shown in Figure 25. This figure shows how the oxidation rate drops relative to the drop in internal dissolved oxygen concentration as a function of the β_{ref} value at the air-exposed surface. As discussed, a low value of β_{ref} (0.1) leads to an approximately linear drop in rate versus dissolved oxygen concentration, whereas a very large value of β_{ref} (1000) leads to very little drop until extreme drops in dissolved oxygen concentration are reached. Thus, the higher the value of β_{ref}, the less

impact DLO effects will generally have on the material as it ages. This is important since β_{ref} is one of the parameters needed for the modeling and measurements or estimates of this parameter are scarce. Generally speaking, the evidence appears to indicate that β_{ref} is close to unity for thermal-aging exposures [15,94]. For radiation-aging exposures, there is some limited evidence that the values of β_{ref} may be somewhat higher in the range of 10 to 30 [92,93,95]. For our simulations below, we will show how values of β_{ref} from 1 to 20 affect the conclusions. This is one area of research where some careful measurements would be helpful and these may be available through the use of the Respirometer approach [96].

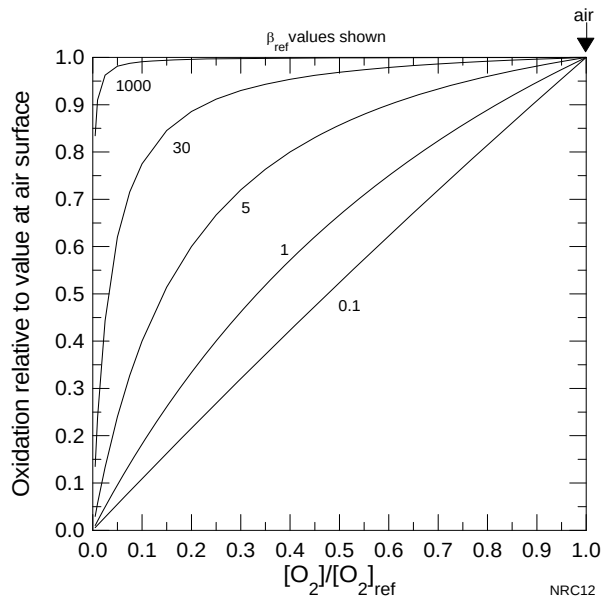

Figure 25. Oxidation relative to the reference oxidation rate at the air-exposed surface plotted against the reduction in the dissolved oxygen concentration for the values of β_{ref} indicated on the plot.

When the expression for consumption given by Equation (3) is combined with a standard diffusion expression, steady-state oxidation profiles can be derived for sheet material of thickness L exposed to air on one side only in terms of the parameter β_{ref} and a second geometric parameter α (a parameter that combines sample thickness with rate coefficients and diffusivity) given by:

$$\alpha = \frac{C_1 L^2}{D} \qquad \text{(Eq. 6)}$$

The resulting profiles for the relative oxygen concentration and the relative oxidation rate across samples when β_{ref} = 1 at various values of α are shown in Figure 26 and Figure 27, respectively. For this reasonably low value of β_{ref} the oxidation profiles have similar shape to the oxygen concentration profiles although they drop with distance a bit slower. Results for β_{ref} = 30 are shown in Figure 28 and Figure 29. Comparing these two figures shows how the higher value of β_{ref} leads to a reduction in the rate of drop in the oxidation profile relative to the drop in oxygen concentration as the latter is reduced as well as a change in the shape of the oxidation profile.

Although the plots are shown as a function of β_{ref} and α, it turns out [91-95] from the theory that profile shapes can be derived from the knowledge of 1) the oxygen permeability coefficient P_{Ox}, 2) the oxygen consumption rate at the air-exposed surface $\phi[O_2]_{ref}$ and 3) β_{ref}.

The DLO calculations are for a single sheet of material. Cables are more complex since they have more complex (e.g., cylindrically-based) geometries and typically involve two different materials (jacket and insulation) each having differing values for their oxygen consumption rates, their oxygen permeability coefficients and potentially their β_{ref} values. It turns out that for a typical 3-conductor cable with a 1.5 mm thick jacket and 0.9 mm thick insulations, the average (centerline) circumferential length around the outside jacket is reasonably close to the sum of the average (centerline) circumferential lengths around the three insulations. This means that as a first approximation, we can treat this situation as two parallel sheets of material (1.5 mm thick jacket next to a 0.9 mm thick insulation). Given the long lengths of cable, we will assume that air can only get inside the cable by diffusing through the jacket. For our sheet model, this implies that air will be available on the outside surface of the jacket and no air source exists on the inside surface of the insulation. The reason we set up the model as outlined is that we have an existing reaction-diffusion model that handles parallel sheet materials having differing degradation and permeability parameters. (Note: DLO modeling at SNL has been accomplished with different software applications; a BASIC module is called LAMX2 [97]). This allows us to derive reasonable estimates without having to develop finite element analyses codes in order to attack the multitude of cable sizes, cross-sections and configurations that exist in a typical nuclear power plant. For slightly more accuracy, it might be appropriate in the future to develop more rigorous finite element codes that can handle complex cable geometries.

In order to use modeling software (for example the SNL LAMX2 [97] program or similar approaches), we need, for each of the two layers, values for 1) the oxygen permeability coefficient P_{Ox}, 2) the oxygen consumption rate at the air-exposed surface $\phi[O_2]_{ref}$ and 3) β_{ref} Additional required data are either readily available (the material density ρ and the material thickness L) or have no effect on the calculations (the oxygen solubility coefficient S). The next several sections of this report will be devoted to obtaining the best estimates available for the consumption rates and the permeability coefficients. These derived values will then be used to estimate the importance of DLO effects for various cables under “worst-case” ambient aging conditions and under various accelerated aging environments (e.g., the early sequential aging qualifications under highly accelerated aging conditions and Jacobus’ more moderately accelerated combined environment exposures [68-70]).

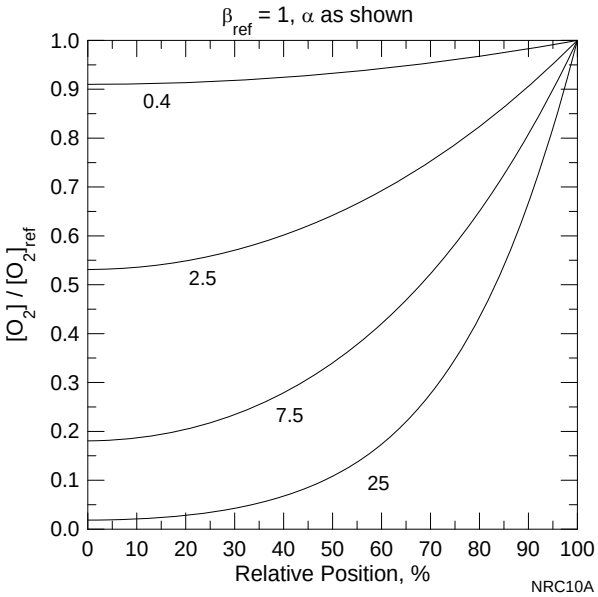

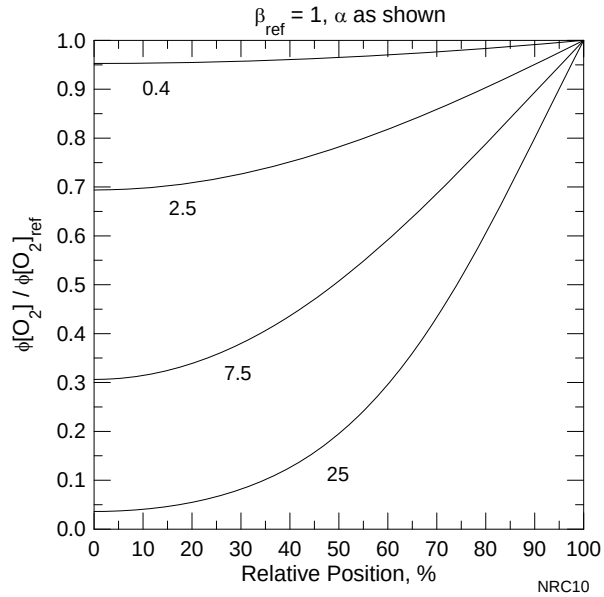

Figure 26 (Left). Relative dissolved oxygen concentration versus relative position across sheet samples with air on one side and β_{ref} = 1 under air partial pressure conditions. Curves are shown for various values of α.

Figure 27(Right). Relative oxidation rate versus relative position across sheet samples with air on one side and β_{ref} = 1 under air partial pressure conditions. Curves are shown for various values of α.

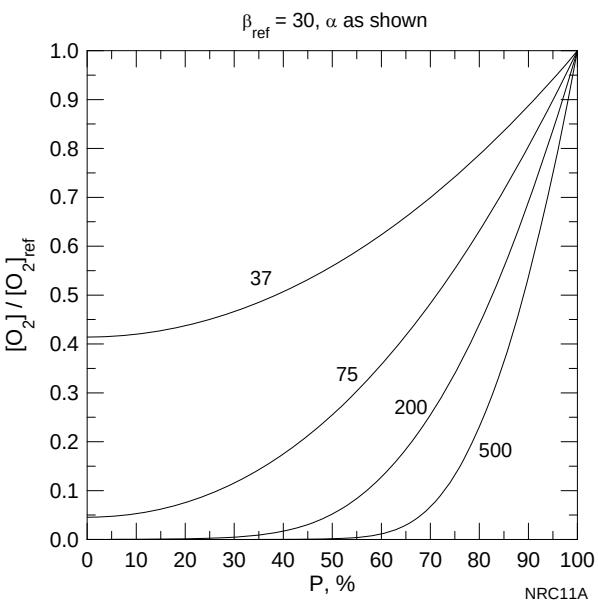

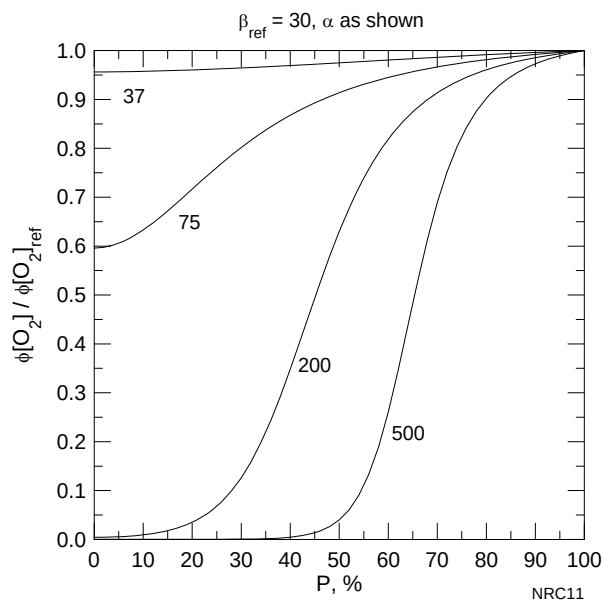

Figure 28 (Left). Relative dissolved oxygen concentration versus relative position across sheet samples with air on one side and β_{ref} = 30 under air partial pressure conditions. Curves are shown for various values of α.

Figure 29 (Right). Relative oxidation rate versus relative position across sheet samples with air on one side and β_{ref} = 30 under air partial pressure conditions. Curves are shown for various values of α.

3.4 Estimates of Oxidation Rate for Thermal Aging Conditions

Since the qualification aging was usually done sequentially with thermal exposure followed by radiation exposure, any modeling of such aging would need to be done sequentially. As shown in Table 2.3 of reference [74], the Rockbestos cable (CP jacket and XLPO insulation) experienced thermal aging conditions of around 1100 hours at 150°C. The same Table indicates cables containing CSPE jackets and EPR/EPDM insulations are often exposed under similar thermal temperature (150°C but for a shorter duration of 1 to 3 weeks) or under a lower 121°C for 1 week. Based on the need to estimate the importance of DLO effects for the above sequential thermal-aging simulations, we will make estimates of $\phi[O_2]_{ref}$ versus aging temperature for CSPE and CP jackets plus EPR and XLPO insulations in this section.

3.4.1 Chlorosulfonated Polyethylene (CSPE) Jackets

Tensile elongation results [14,73] for a Samuel Moore CSPE jacket are shown in Figure 30. These results are time-temperature superposed at a temperature of 70°C (the lower x-axis gives the time scale at 70°C) in Figure 31. The multiplicative shift factors a_T, used at each temperature for the shifting procedure, are shown on the figure. The upper x-axis shows the time scale appropriate to aging at 108°C. At this temperature it takes ~133 days for the elongation to drop to 100%. Since we would like to know the amount of oxygen consumption corresponding to degradation reaching this level and the highest temperature used for oxygen consumption measurements was 108°C, this information will be used below. Oxygen consumption measurements at temperatures ranging from 108°C to 37°C have been carried out on this material and are shown in Figure 32. Since the data at the highest temperature of 108°C does not go out to 133 days, we extrapolate the 108°C results out to 133 d as shown by the dashed line on the figure. These data are then integrated, leading to the consumption versus aging time results shown in Figure 33. Finally the integrated results (Figure 33) are time-temperature superposed at a reference temperature of 37°C (lower x-axis) with the results shown in Figure 34. From the upper x-axis (corresponding to 108°C), we see that reaching 100% elongation corresponds to an oxygen absorption of ~7.5e-4 mol/g.

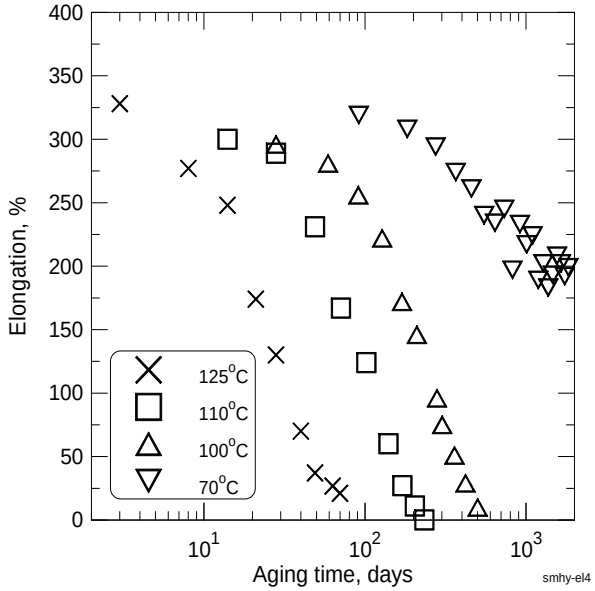

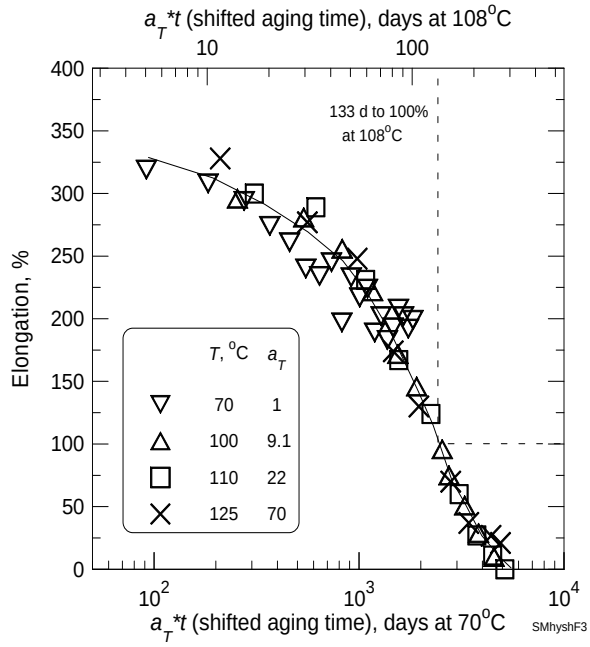

Figure 30 (Left). Tensile elongation results for a Samuel Moore CSPE cable jacketing material.

Figure 31 (Right). Time-temperature superposition of the elongation results from Figure 30 at a 70°C reference temperature (lower x-axis). The multiplicative shift factors used in the shifting are shown on the figure. The upper x-axis gives the time axis for the superposed data at 108°C.

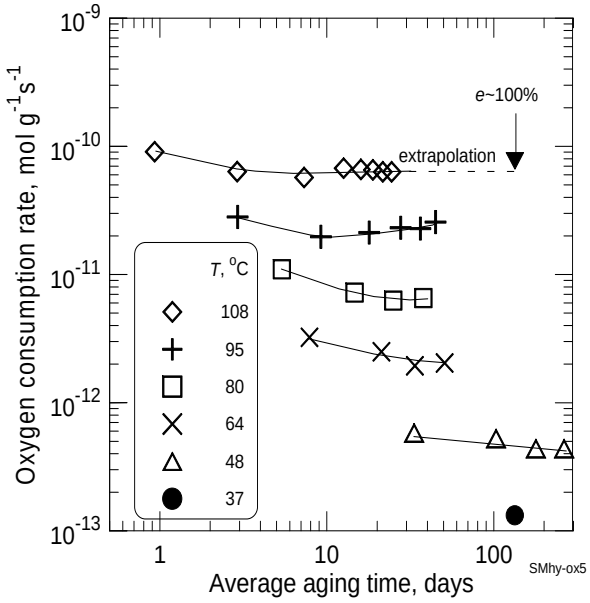

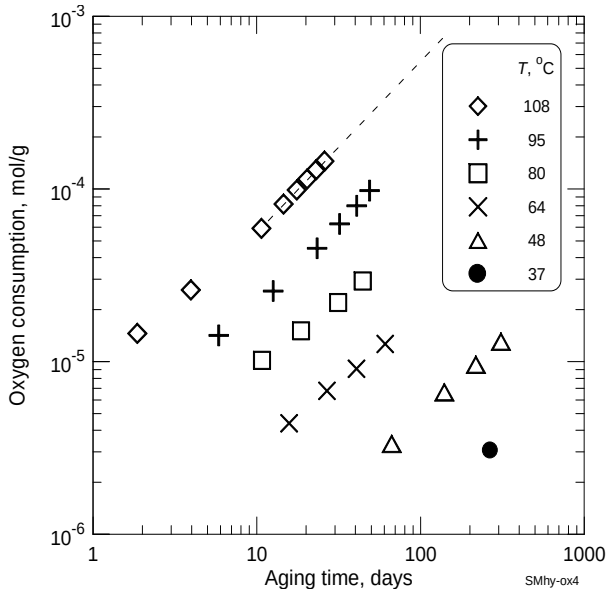

Figure 32 (Left). Oxygen consumption rate results for Samuel Moore CSPE versus aging time at the indicated aging temperatures.

Figure 33 (Right). Oxygen consumption results for Samuel Moore CSPE obtained by integrating the results from Figure 32.

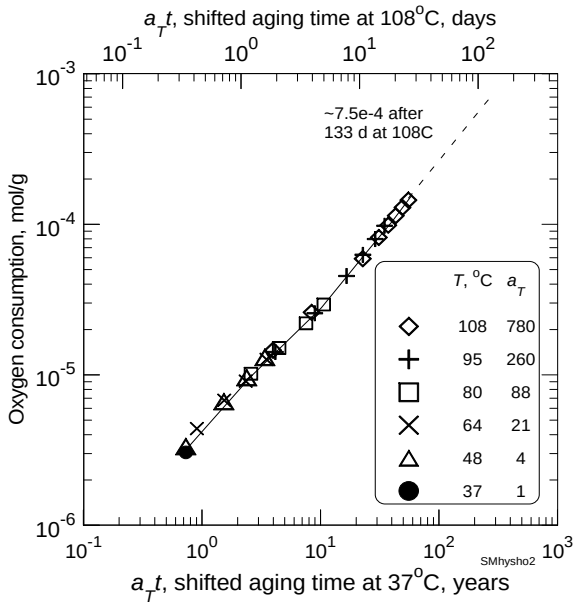

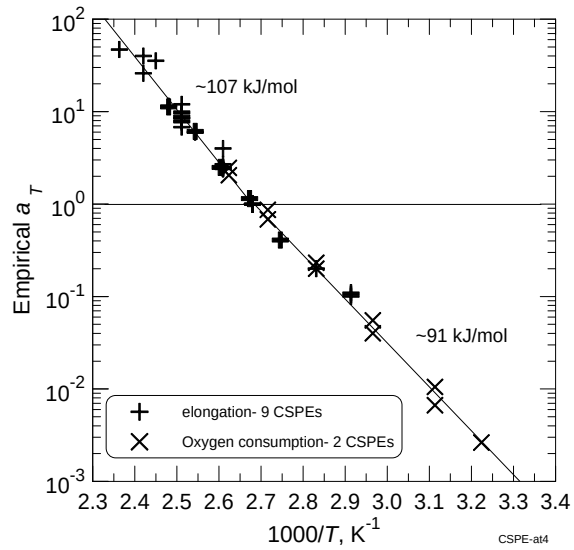

Figure 34 (Left). Time-temperature superposition at 37°C (lower x-axis) of the integrated oxygen consumption results from Figure 33. The multiplicative shift factors are shown on the figure.

Figure 35 (Right). Arrhenius plot of the shift factors for elongation for nine different CSPE jackets and the shift factors for oxygen consumption for two different CSPE jackets (all data normalized at 100°C).

From the elongation (Figure 31) and oxygen consumption results (Figure 34) we have derived shift factors for this material. It turns out that under oven-aging conditions, elongation results have been carried out on eight additional CSPE jacketing materials and oxygen consumption results on one additional CSPE material. All of these materials degrade at fairly similar rates [14]. In addition, when the shift factors for all nine materials are combined on one Arrhenius plot (normalized to 100°C), very little spread occurs in the results as shown in Figure 35. This indicates that the Arrhenius plots for nine different materials are quite similar. From these results we also note that the data is non-Arrhenius with a small drop in E_a from ~107 kJ/mol above 100°C to ~91 kJ/mol below this temperature. The observation of a drop in E_a as the aging temperature is reduced is now quite commonly observed because data is now generated over a large enough temperature range to see such effects [8,11-13,21,26,28-31,89,90]. In the early days of aging, experiments were often confined to three or four closely separated high temperatures where it would have been difficult to pick up changes in Arrhenius slope. A systematic French study examined an industrial CSPE material prepared from Hypalon 40 using dielectric and dynamic mechanical techniques [98]. Nice linear degradation results from 90°C to 135°C led to Arrhenius behavior with an E_a of 95±10 kJ/mol which offers additional evidence backing the elongation and oxygen consumption results.

Since we concluded that 133 d at 108°C causes a substantial drop in elongation to 100% and that ~7.5e-4 mol/g of oxygen corresponds to this drop, we can calculate the average oxygen consumption rate $\phi[O_2]_{ref}$ at 108°C as 6.5e-11 mol/g/s. Estimates of $\phi[O_2]_{ref}$ at other temperatures are easily obtained by utilizing the E_a results from Figure 35 and are summarized in Table 3.

Table 3. Oxygen Consumption Rate Estimates for CSPE Jacket Materials

***T*, °C**	**150**	**121**	**108**	**100**	**50**
$\phi[O_2]_{ref}$, mol/g/s	1.86e-9	2e-10	6.5e-11	3.15e-11	3.4e-13

With the results from Figure 35 in mind, it is interesting to look at the simulations used in historic qualifications such as those summarized in Table 2.3 of ref. [74]. For the Samuel Moore cable comprising a CSPE jacket and an EPDM insulation, the thermal part of the sequential aging simulation used 168 h at 121°C to simulate 40 years at 58°C based on an assumed E_a of 131 kJ/mol, a very different value from the results shown in Figure 35. Using the much more accurate E_a values from Figure 35 shows that, for the CSPE jacket, 168 h at 121°C corresponds to ~5 years at 58°C instead of 40 years. The AIW cable (CSPE/EPR) used 168 h at 121°C to simulate 40 years at 50°C based on an assumed E_a of 114 kJ/mol. Using the more accurate E_a values from Figure 35 shows that 168 h at 121°C corresponds to ~11 years at 50°C. The Anaconda cable (CSPE/EPR) used 168 h at 150°C to simulate 40 years at 69°C based on an assumed E_a of 114 kJ/mol. Using the more accurate E_a values from Figure 35 shows that 168 h at 150°C corresponds to ~16 years at 69°C. If the ambient aging temperature is a more realistic 50°C, 168 h at 150°C would correspond to ~105 years at 50°C. However, as will be shown below, aging at 150°C will lead to substantial DLO effects so if the ambient aging temperature were in fact 50°C, there would still be a significant problem with the 150°C simulation.

3.4.2 Chloroprene (CP) Cable Jackets

Tensile elongation results [14] for a Rockbestos Firewall III CP jacket are shown in Figure 36. These results are time-temperature superposed at a temperature of 80°C in Figure 37. The multiplicative shift factors a_T, used at each temperature for the shifting procedure, are shown on the figure. At 80°C it takes ~410 days for the elongation to drop to 50%. Since we would like to know the amount of oxygen consumption corresponding to degradation reaching this level we examine the time-temperature superposed oxygen consumption data for this material. These results are shown in Figure 38 where the bottom axis corresponds to shifting to 25°C and the top axis corresponds to an 80°C time scale. Since the data does not go out to 410 days at 80°C, we extrapolate the results as shown by the dashed line on the figure. Based on this procedure, we estimate that reaching 50% elongation corresponds to oxygen absorption of ~6.8e-4 mol/g.

From the elongation (Figure 37) and oxygen consumption results (Figure 38) results we have derived shift factors for this material and these are normalized to 80°C and plotted on an Arrhenius plot in Figure 39. Similar to the CSPE results we notice curvature in the Arrhenius plot with an E_a of ~96 kJ/mol above 80°C dropping to ~76 kJ/mol near room temperature.

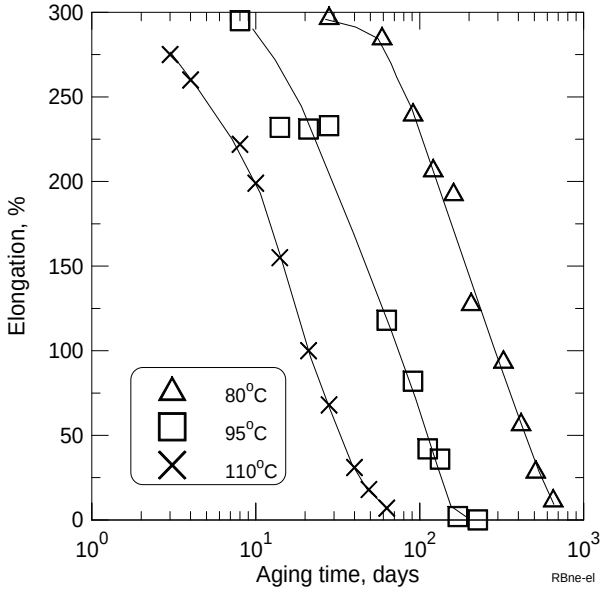

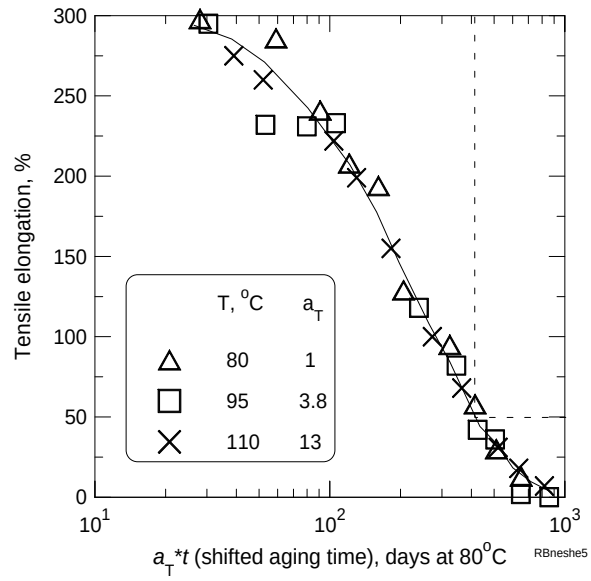

Figure 36 (Left). Tensile elongation results for a Rockbestos CP cable jacketing material.

Figure 37 (Right). Time-temperature superposition of the elongation results from Figure 36 at an 80°C reference temperature (lower x-axis). The multiplicative shift factors used in the shifting are shown on the figure. The upper x-axis gives the time axis for the superposed data extrapolated to 25°C.

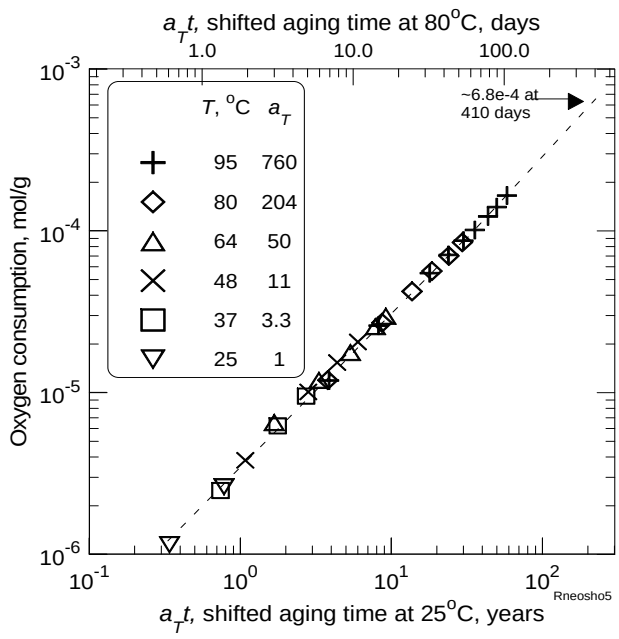

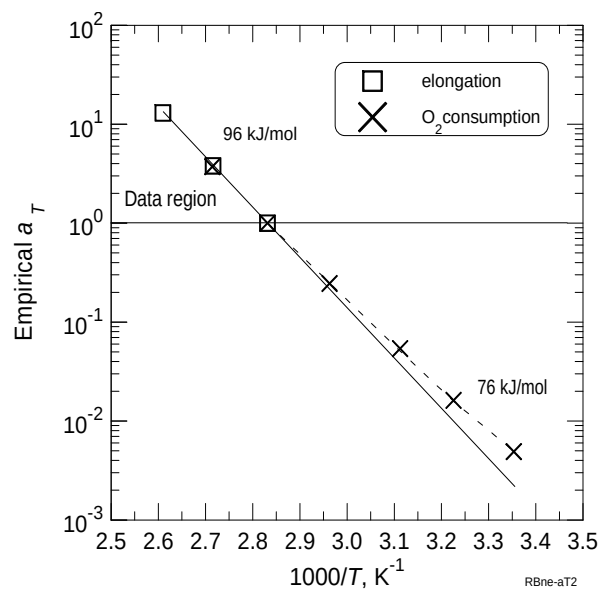

Figure 38 (Left). Time-temperature superposition at 25°C (lower x-axis) of the integrated oxygen consumption results for Rockbestos CP jacket [14]. The multiplicative shift factors are shown on the figure.

Figure 39 (Right). Arrhenius plot of the shift factors for elongation and oxygen consumption for the Rockbestos CP jacket (all data normalized at 80°C).

Extensive data [13,14] taken on a second chloroprene cable jacket manufactured by Okonite shows somewhat faster mechanical degradation rates as seen by comparing the elongation results given in Figure 40 with those given for the Rockbestos Firewall III CP jacket (Figure 36). For the Okonite material, we also had very long-term data for samples aged at ~24°C for up to 24 years. When these results are time-temperature superposed (Figure 41) and the resulting shift factors plotted on an Arrhenius plot (Figure 42), we again see the non-Arrhenius character of the results. We also note that the higher temperature E_a value (89 kJ/mol) and the lower temperature value (71 kJ/mol) are very close to those found for the Rockbestos Firewall III CP jacket above (96 and 76 kJ/mol, respectively).

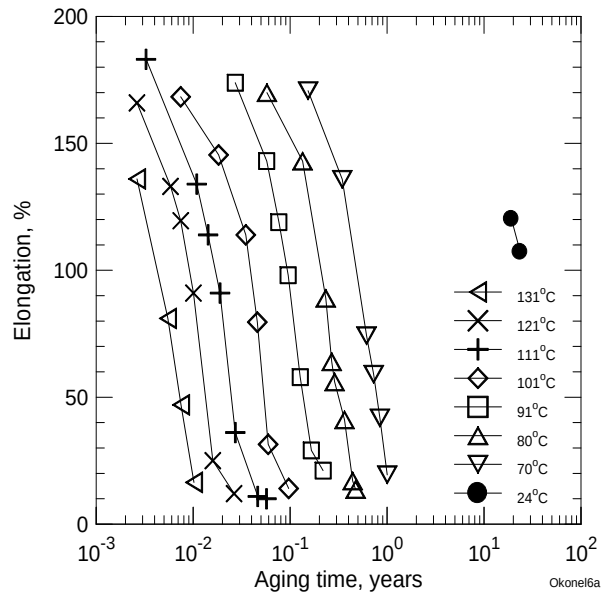

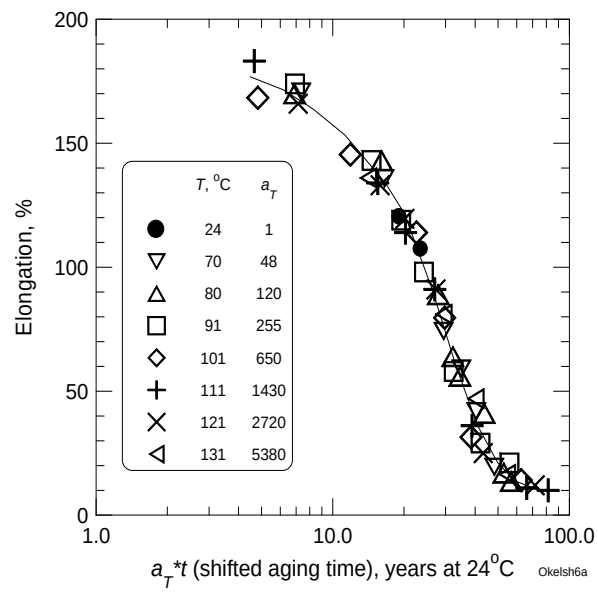

Figure 40 (Left). Tensile elongation results for an Okonite CP cable jacketing material.

Figure 41 (Right). Time-temperature superposition of the elongation results from Figure 40 at an 24°C reference temperature. The multiplicative shift factors used in the shifting are shown on the figure.

Since we concluded for the Rockbestos Firewall III CP jacket that 410 d at 80°C causes a substantial drop in elongation to 50% and that ~6.8e-4 mol/g of oxygen corresponds to this drop, we can calculate that the average oxygen consumption rate $\phi[O_2]_{ref}$ at 80°C is 1.92e-11 mol/g/s. Estimates of $\phi[O_2]_{ref}$ at other temperatures are easily obtained by utilizing the results from Figure 39 and are summarized in Table 4.

Table 4. Oxygen Consumption Rate Estimates for Rockbestos Firewall III CP Jacket.

***T*, °C**	**150**	**100**	**80**
$\phi[O_2]_{ref}$, mol/g/s	4.3e-9	1.1e-10	1.92e-11

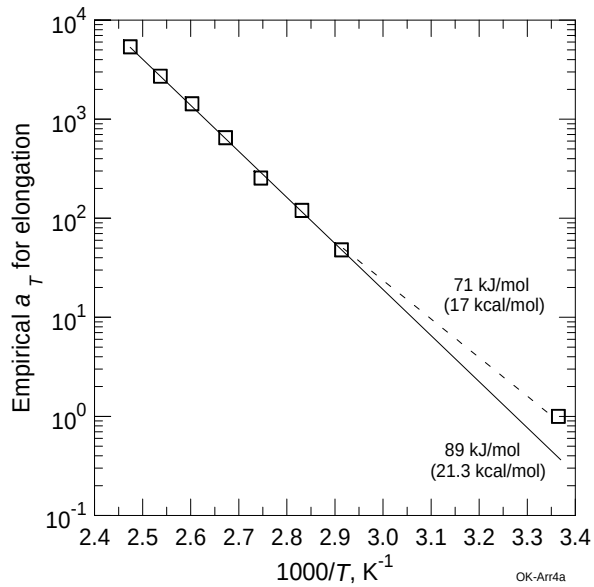

Figure 42. Arrhenius plot of the shift factors for elongation for the Okonite CP jacket.

With the Rockbestos Firewall III CP jacket Arrhenius results from Figure 39 in mind, it is interesting to look at the simulations used in historic qualifications of a Rockbestos Firewall III CP/XLPE cable summarized in Table 2.3 of ref. [74]. The thermal part of the sequential aging simulation claimed that 850 hours at 150°C simulated 40 years at 90°C based on an assumed E_a of 128 kJ/mol, a very different value from the results shown in Figure 39 for the recently-studied Rockbestos Firewall III CP jacket. Using the much more accurate E_a values from Figure 39 shows that 850 h at 150°C corresponds to ~9 years at 90°C instead of 40 years. If the ambient aging temperature is a more realistic 50°C, 850 h at 150°C would correspond to ~350 years at 50°C. However, as will be shown below, aging at 150°C will lead to substantial DLO effects so if the ambient aging temperature were in fact 50°C, there would still be a significant problem with the 150°C simulation.

3.4.3 Crosslinked Polyolefin (XLPO) Cable Insulation Materials

XLPO cable jacketing materials are typically semi-crystalline with complex crystalline melting point behavior. For instance, Figure 43 shows the Differential Scanning Calorimeter (DSC) scan of a Brandrex XLPO cable insulation material. The major crystalline melting point is around 120°C with a secondary peak around 90°C. Because of the robustness of XLPO materials in thermal environments, most accelerated aging studies are done in the temperature range above 120°C. This implies that the Arrhenius analyses are done for completely amorphous material. Unfortunately aging can be quite different with differing E_a values below 120°C since the material is partially crystalline in this region. Since ambient aging typically occurs at a maximum temperature of ~50°C, Arrhenius analyses of accelerated aging results taken above the melting point and subsequent extrapolation of the high-temperature Arrhenius behavior across the melting point region can be problematic. Since our recent studies [14] involved aging exposures of 10 years or more, we were able to access temperatures below the main melting point. Figure 44 shows our tensile elongation results at four different aging temperatures. Two of the temperatures (152°C and 125°C) were above the main crystalline melting point, whereas the other two aging temperatures (109°C and 99°) were below the melting point. Since the results

are plotted versus the log of the aging time and the shapes of the degradation curves are clearly different above and below 120°C, this indicates a change in chemical degradation pathway, not unexpected when crossing a crystalline melting point. When differing shapes occur (a more rapid drop-off rate at the two highest temperatures), it is not possible to achieve time-temperature superposition by multiplicative shifting of the data. However, the results at 109°C and 99°C do have similar shapes and can therefore be time-temperature superposed with good overlap as seen in Figure 45. From these data, we can see that it takes ~500 weeks (9.6 years) of aging at 99°C to reach 100% elongation. Like many XLPO cable insulations, this is clearly a robust material.

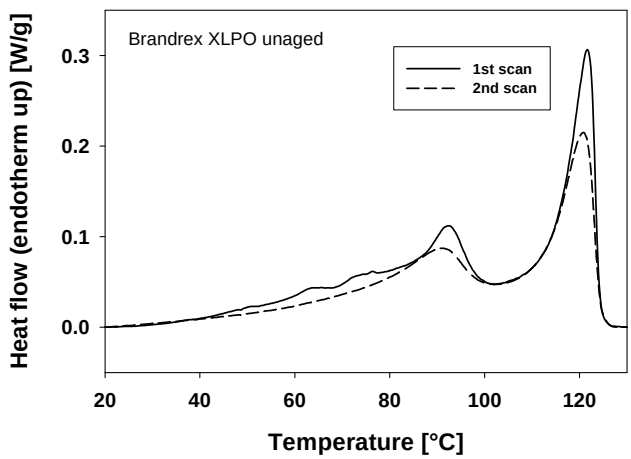

Figure 43. Scan of Brandrex XLPO insulation material at 5°C/min under Ar. [53]

To derive an estimate of the Arrhenius E_a value to use for extrapolations down to ambient conditions, we obtained [14] oxygen consumption rate results at seven aging temperatures over a wide temperature range (48°C up to 138°C). The results were integrated and time-temperatures superposed at a reference temperature of 48°C (lower x-axis) as shown in Figure 46. Using the empirically derived shift factors (normalized at 99°C) for elongation (Figure 45) and oxygen consumption (Figure 46), an Arrhenius plot shown in Figure 47 was constructed. From this figure an E_a of ~72 kJ/mol appears to represent aging below the main melting point. Although the mechanical degradation mechanism changes above 120°C, it appears that the underlying oxygen consumption reactions do not since the oxygen consumption shift factors above 120°C follow the same Arrhenius line. Since we saw earlier (Figure 45) that 500 weeks at 99°C corresponded to the elongation decreasing to 100%, we utilize the 72 kJ/mol E_a to create the 99°C time scale for the superposed oxygen consumption results. This is shown as the upper x-axis on Figure 46. From this time scale, we see that 30 weeks of aging at 99°C corresponds to an oxygen absorption of 4.7e-5 mol/g. This calculates out to an average rate at 99°C of 2.59e-12 mol/g/s. With an E_a of 76 kJ/mol, this leads to estimates for $\phi[O_2]_{ref}$ at selected temperatures shown in Table 5. If the 2.59e-12 mol/g/s rate holds over 500 weeks at 99°C, the total oxygen consumption corresponding to the elongation reaching 100% would be 7.8e-4 mol/g. It is also interesting to note that 500 weeks at 99°C is equivalent to ~330 years at 50°C implying a very long thermal life at 50°C for this material.

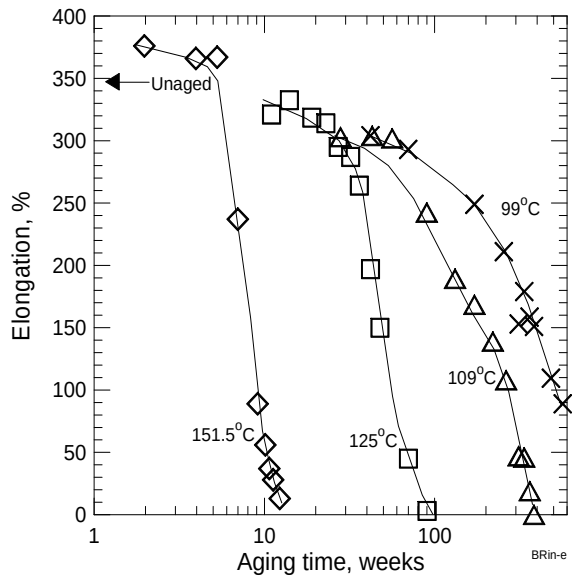

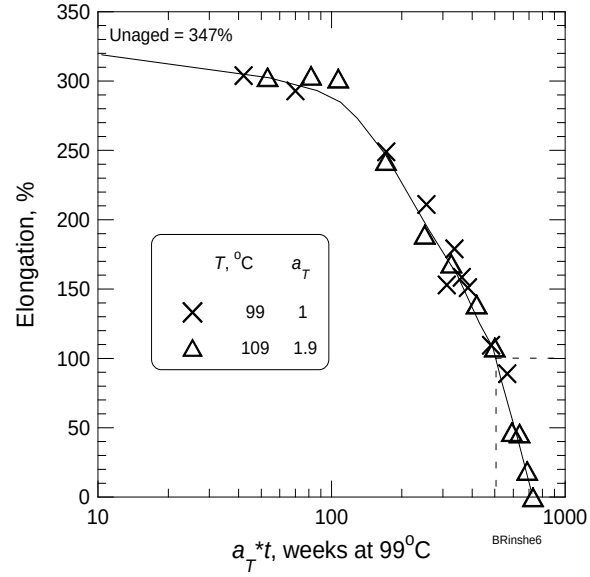

Figure 44 (Left). Elongation versus time at the indicated temperatures for Brandrex XLPO insulation cable insulation material.

Figure 45 (Right). Time-temperature superposed elongation results at a reference temperature of 99°C for the 99°C and 109°C data of Brandrex XLPO cable insulation.

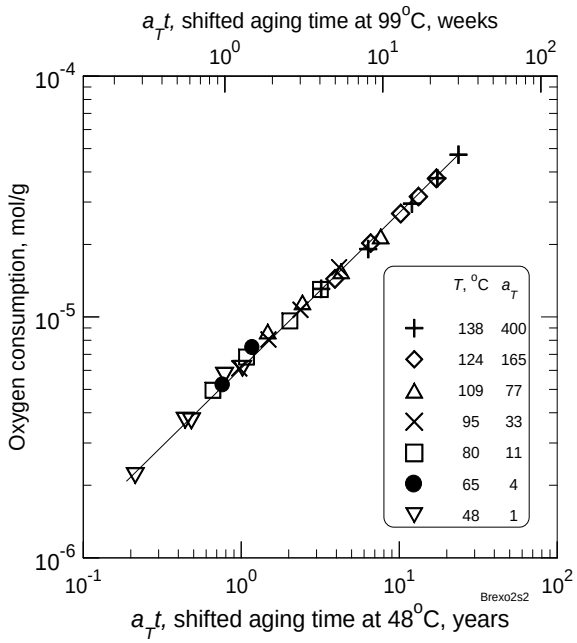

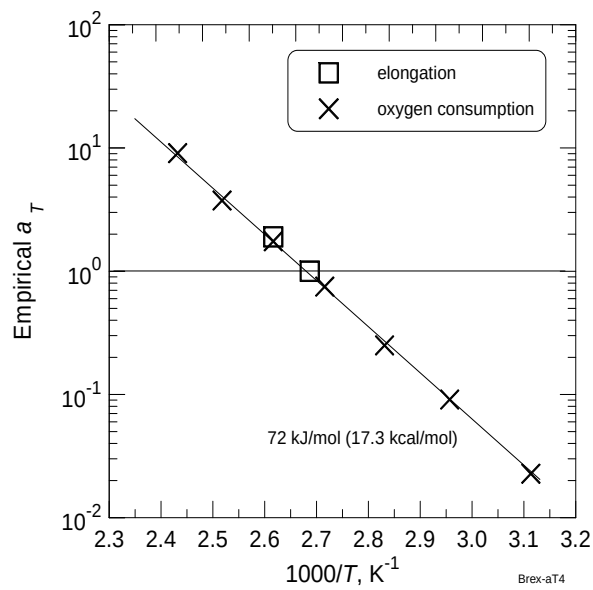

Figure 46 (Left). Time-temperature superposition of the oxygen consumption results for Brandrex XLPO insulation using the empirically derived shift factors shown on the figure.

Figure 47 (Right). Arrhenius plot of the O_2 consumption shift factors for Brandrec XLPO insulation from the elongation results in Figure 45 and the oxygen consumption results from Figure 46

Table 5. Oxygen Consumption Rate Estimates for Brandrex XLPO Insulation.

***T*, °C**	**150**	**100**	**50**
$\phi[O_2]_{ref}$, mol/g/s	4.4e-11	2.75e-12	7.5e-14

Tensile elongation and oxygen consumption results were also obtained for an XLPO cable insulation removed from a Rockbestos Firewall III cable [14]. The DSC scan for this material, shown in Figure 48, indicates that the major crystalline melting peak is at ~120°C with additional peaks at around 111°C and 100°C. Elongation results were measured versus oven aging time for three different color insulations at aging temperatures of 151.5°C, 138°C, 124°C and 109°C. The results for the three different colors are shown in Figure 49, Figure 50 and Figure 51. From these results, sufficient data exists for time-temperature superposition only at the three higher temperatures, all of which are above the main melting peak. The time-temperature superposition procedure leads to the superposed results shown in Figure 52, Figure 53 and Figure 54 where the shift factors used for the superposition are shown on the figures. There are some minor differences in the rates of degradation dependent on the insulation color, an often observed phenomenon [99]. When the shift factors from these figures are plotted on an Arrhenius plot (shown in Figure 55), it is seen that the Arrhenius E_a value is ~130 kJ/mol from 124°C to 151.5°C. Since these results reflect totally amorphous material (above the main melting point), it says little about the E_a value expected below the melting point. In fact, there is evidence on the elongation plots that the E_a value does drop below 120°C. On all three figures (Figure 49, Figure 50 and Figure 51) we plot dashed curves where the expected results would occur at 109°C if the 130 kJ/mol (31 kcal/mol) E_a continued below 124°C. Although the actual 109°C data (filled diamonds on the figures) is not sufficient for analyses, it is falling much faster than a 130 kJ/mol E_a would predict. This is indicative of a drop in E_a below the main melting point.

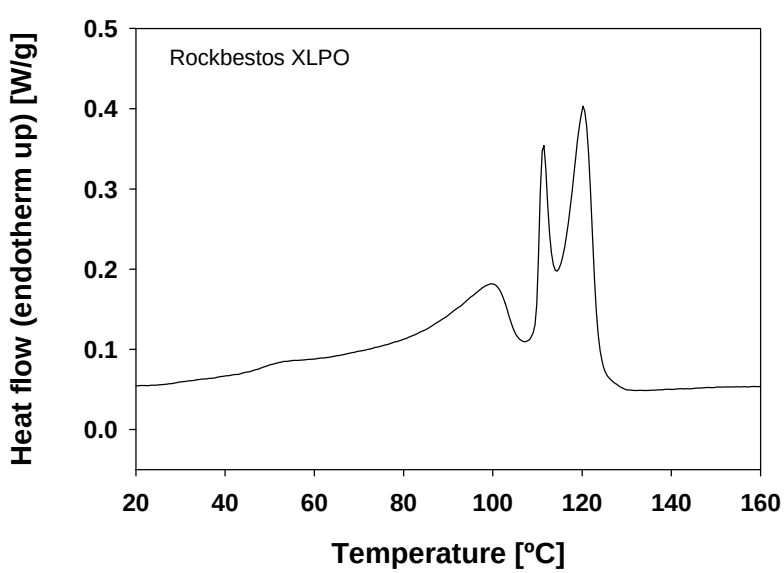

Figure 48. DSC scan of the Rockbestos XLPO cable insulation at 5°C/min under Ar [54]. All three conductor colors have the same DSC trace.

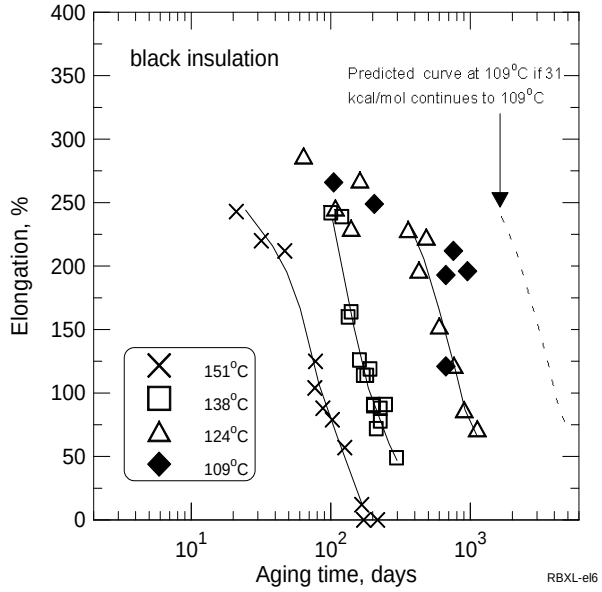

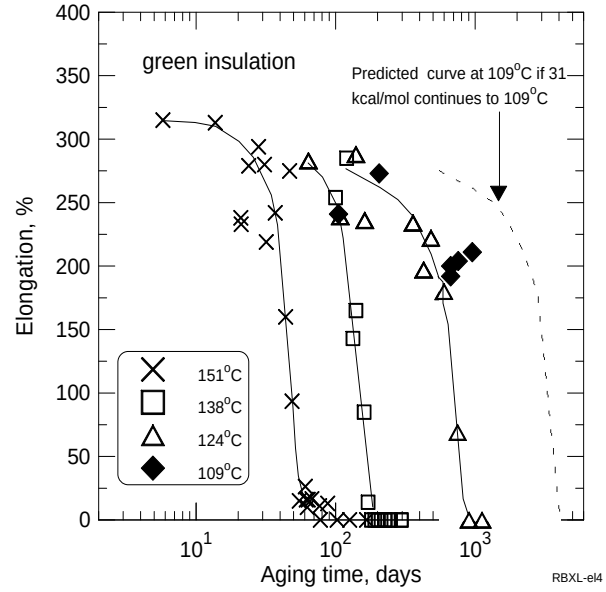

Figure 49 (Left). Elongation versus time at the indicated temperatures for black-colored Rockbestos XLPO insulation cable insulation material.

Figure 50 (Right). Elongation versus time at the indicated temperatures for green-colored Rockbestos XLPO insulation cable insulation material.

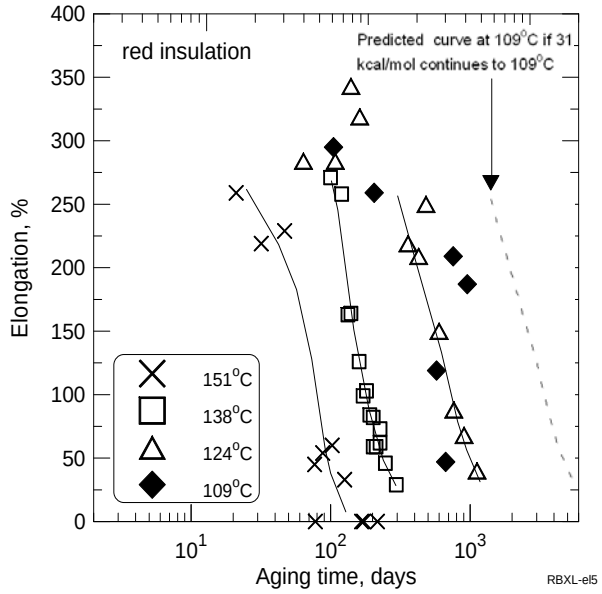

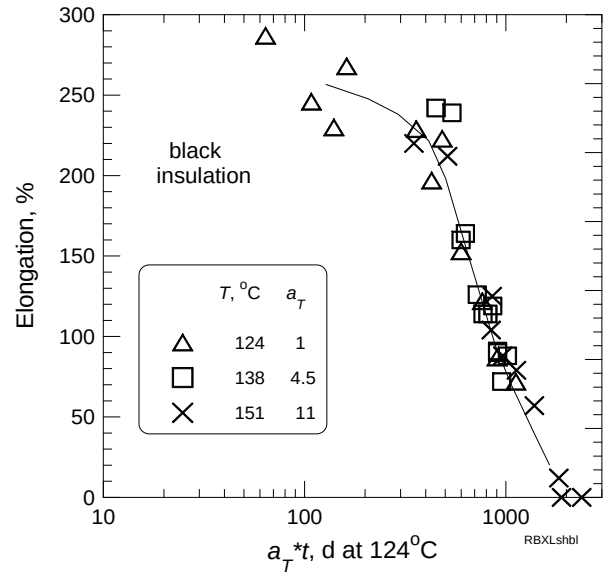

Figure 51 (Left). Elongation versus time at the indicated temperatures for red-colored Rockbestos XLPO insulation cable insulation material.

Figure 52 (Right). Time-temperature superposed elongation results for the black Rockbestos XLPO insulation at a reference temperature of 124°C from Figure 49.

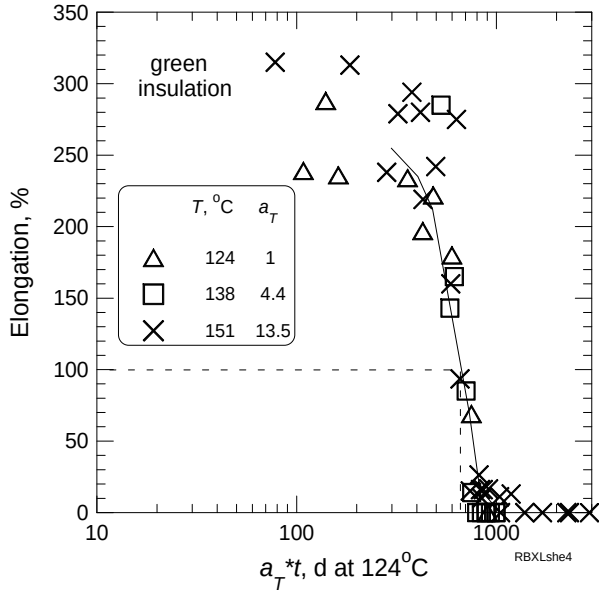

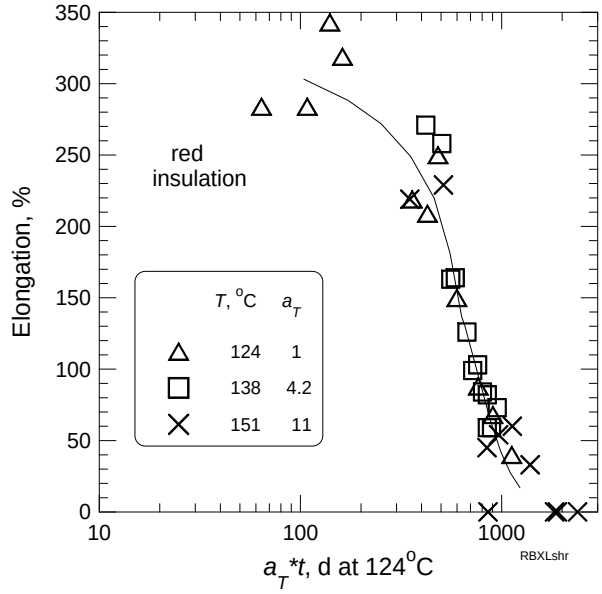

Figure 53 (Left). Time-temperature superposed elongation results for the green Rockbestos XLPO insulation at a reference temperature of 124°C from Figure 50.

Figure 54 (Right). Time-temperature superposed elongation results for the red Rockbestos XLPO insulation at a reference temperature of 124°C from Figure 51.

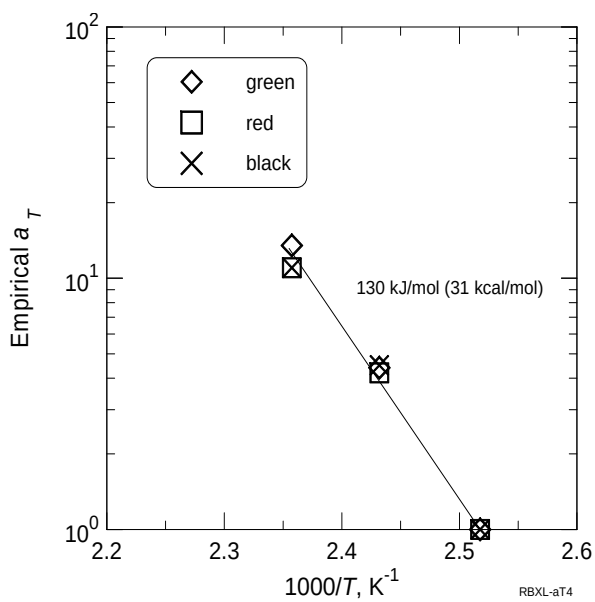

Figure 55. Arrhenius plot of the shift factors derived for the three colors of the Rockbestos XLPO insulation.

Oxygen consumption measurements were conducted at temperatures ranging from 48°C to 138°C on the green insulation [14]. After integrating, they were time-temperature superposed at a reference temperature of 48°C (bottom x-axis) as shown in Figure 56. Using the empirically derived shift factors (normalized at 124°C) for elongation (Figure 53) and oxygen consumption (Figure 56) of the green insulation, an Arrhenius plot shown in Figure 57 was constructed. This figure shows that an E_a of ~98 kJ/mol appears to represent aging below the main melting point

compared to ~135 kJ/mol above the melting point. By utilizing the 98 kJ/mol E_a appropriate from 48°C to 124°C, we constructed the time axis appropriate to 124°C as the top x-axis on Figure 56. From this time scale, we see that 54 days of aging at 124°C corresponds to an oxygen absorption of 7.6e-5 mol/g. This calculates out to an average rate at 124°C of 1.63e-11 mol/g/s. With the shift factor results shown on the Arrhenius plot (Figure 57), this leads to estimates for $\phi[O_2]_{ref}$ at selected temperatures shown in Table 6. At 124°C, the dashed lines in Figure 50 indicate that it takes ~660 days to reach 100%. If the 1.63e-11 mol/g/s rate holds over 660 weeks at 124°C, the total oxygen consumption corresponding to the elongation reaching 100% would be 9.3e-4 mol/g. It is also interesting to note that 660 days at 124°C is equivalent to ~1600 years at 50°C implying a very long thermal life at 50°C for this material.

Table 6. Oxygen Consumption Rate Estimates for Rockbestos XLPO Insulation.

***T*, °C**	**150**	**100**	**50**
$\phi[O_2]_{ref}$, mol/g/s	1.97e-10	2.43e-12	1.79e-14

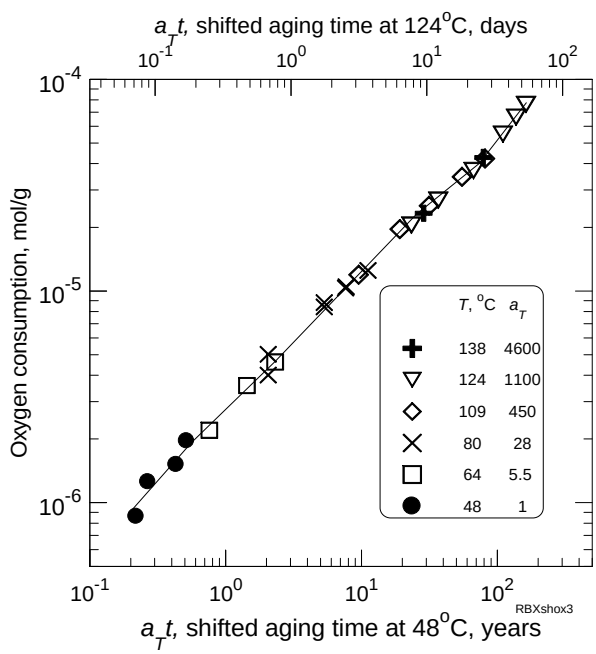

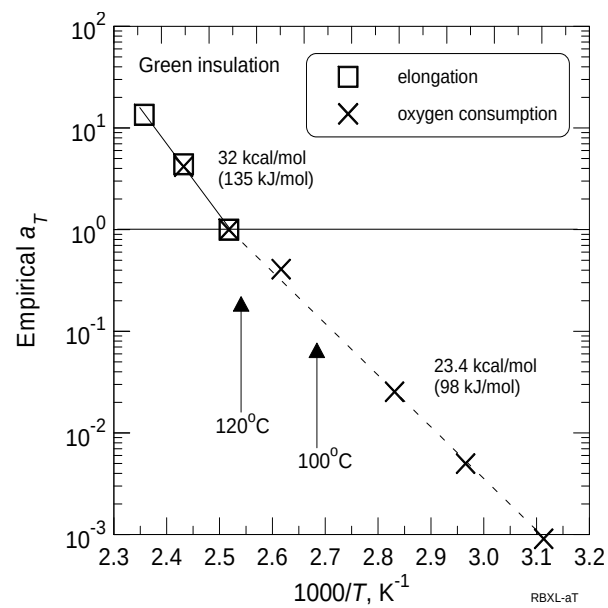

Figure 56 (Left). Time-temperature superposition of the oxygen consumption results for green Rockbestos XLPO insulation using the empirically derived shift factors shown on the figure.

Figure 57 (Right). Arrhenius plot of the O_2 consumption shift factors for green Rockbestos XLPO insulation from the elongation results in Figure 53 and the oxygen consumption results from Figure 56.

With the Rockbestos Firewall III XLPO insulation Arrhenius results from Figure 57 in mind, it is interesting to look at the simulations used in historic qualifications of a Rockbestos Firewall III CP/XLPE cable summarized in Table 2.3 of ref. [74]. The thermal part of the sequential aging simulation claimed that 850 hours at 150°C simulated 40 years at 90°C based on an assumed E_a

of 128 kJ/mol, a very different value from the results shown in Figure 57 for the recently-studied Rockbestos Firewall III CP jacket. Using the E_a value obtained from oxidation rate measurements (see Figure 57) shows that 850 h at 150°C corresponds to ~19 years at 90°C instead of 40 years. If the ambient aging temperature is a more realistic 50°C, 850 h at 150°C would correspond to ~1100 years at 50°C. However, as will be shown below, aging at 150°C will lead to substantial DLO effects so if the ambient aging temperature were in fact 50°C, there would still be a significant problem with the 150°C simulation.

3.4.4 EPR/EPDM Cable Insulation Materials

Some EPR/EPDM materials are semi-crystalline while others are true elastomers (no crystallinity). In our past studies we have examined five different EPR/EPDM cable insulations under thermal aging conditions [14]; Figure 58 shows DSC scans for four of these materials. These results indicate that the two Anaconda insulations are rubbery whereas the Okonite EPR and the Eaton Dekoron Elastoset EPR have crystallinity. Arrhenius plots of the time to reach 50% absolute elongation for our five EPR materials and an additional EPR material studied by Anandakumaran and Stonkus [100] are shown in Figure 59. All of the six materials give reasonably linear Arrhenius plots and the lifetimes to 50% elongation vary over a range of approximately a factor of 4. The Anaconda Flameguard EPR materials have the shortest lifetimes at every temperature, an observation that might be related to the fact that copper-catalyzed oxidation was implicated in their degradation chemistry [42]. However, even for this material a linear extrapolation of the Arrhenius line (E_a ~106 kJ/mol) indicates a lifetime to 50% elongation of approximately 300 years at 50°C. Therefore, from a thermal-only perspective, EPR insulations appear to represent robust materials. Figure 59 shows that the other materials have even longer lifetimes than the Anaconda Flameguard materials under accelerated aging conditions and have similar Arrhenius slopes thereby implying even longer 50°C lifetimes. However, it should be noted that the two materials with crystallinity (Okonite EPR and Eaton Dekoron Elastoset EPR) were aged at a minimum of 109°C (above the transitions shown in Figure 58), there would be high degree of uncertainty to extrapolate data from these two materials to 50°C since this would entail extrapolating across the crystalline melting point. For this reason, we will concentrate our discussions in this report on the Anaconda Flameguard and Anaconda Durasheeth materials. We have oxygen consumption results for the Anaconda Durasheeth material which we use to make estimates of $\phi[O_2]_{ref}$ versus aging temperature. When we make estimates in the next section of this report of $\phi[O_2]_{ref}$ under combined radiation plus temperature results, we will utilize combined environment aging results obtained on the Anacconda Flameguard material.

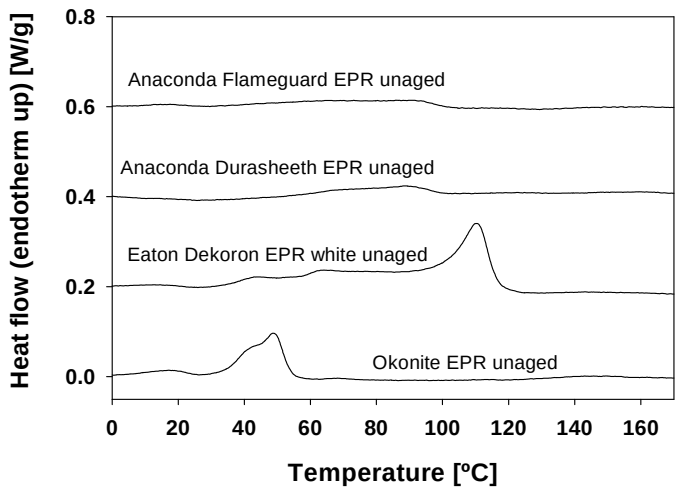

Figure 58. DSC scans of four different EPR cable insulation materials at 5°C/min under Ar [54].

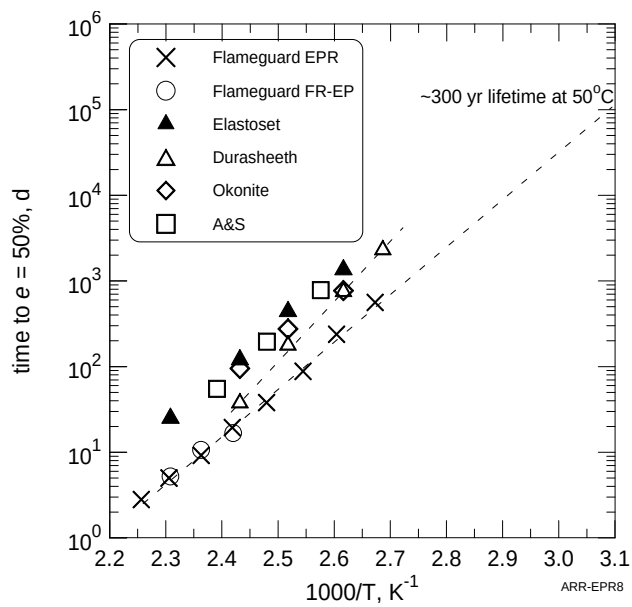

Figure 59. Arrhenius plots of the times required for the elongation to drop to 50% absolute for six EPR cable insulation materials.

Figure 60 shows the time-temperature superposed oxygen consumption results for the Anaconda Durasheeth EPR cable insulation at a reference temperature of 52°C. The shift factors used in the superposition are shown on this figure and these shift factors are incorporated in the Arrhenius plot given in Figure 61. The Arrhenius results imply linear behavior with an E_a of 100 kJ/mol. The results from Figure 60 indicate total oxygen absorption of 1.46e-4 mol/g for 192 years of aging at 52°C implying an average value for $\phi[O_2]_{ref}$ of 2.41e-14. Using this value together with an E_a of 100 kJ/mol leads to estimates for $\phi[O_2]_{ref}$ at selected temperatures shown in Table 7. Since the latter stages of aging (e.g., when elongation reaches 100%) for this material have a different E_a value from the early stages, we do not attempt to estimate the total oxygen consumed that corresponds to the elongation dropping to 100% for this material.

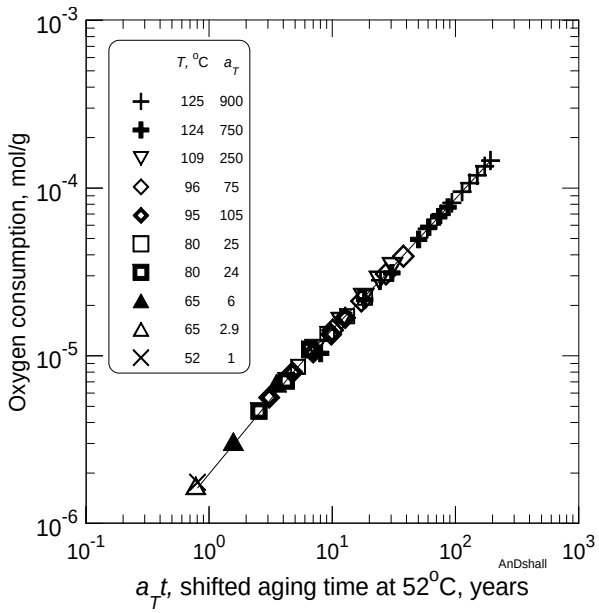

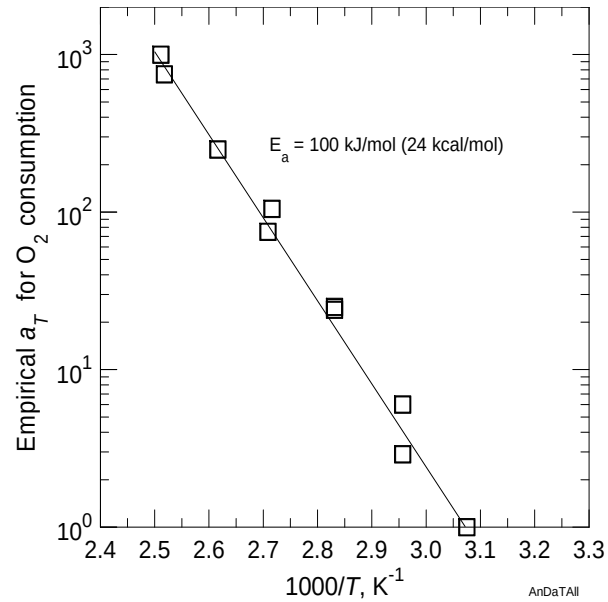

Figure 60 (Left). Time-temperature superposition of the oxygen consumption results for Anaconda Durasheeth EPR insulation using the empirically derived shift factors shown on the figure.

Figure 61 (Right). Arrhenius plot of the shift factors for oxygen consumption from Figure 60.

Table 7. Oxygen Consumption Rate Estimates for Anaconda Durasheeth EPR Insulation.

***T*, °C**	**150**	**121**	**100**	**50**
$\phi[O_2]_{ref}$, mol/g/s	1.31e-10	1.6e-11	2.87e-12	1.92e-14

It is again interesting to use the results to look at the simulations used in historic qualifications such as those summarized in Table 2.3 of ref. [74]. Since our Anaconda Flameguard elongation results led to an E_a of 106 kJ/mol and the Anaconda Durasheeth EPR oxygen consumption results implied an E_a of 100 kJ/mol, we will use 103 kJ/mol for our updated analyses. For the Samuel Moore cable comprising a CSPE jacket and an EPDM insulation, the thermal part of the sequential aging simulation [74] used 168 h at 121°C to simulate 40 years at 58°C based on an assumed E_a of 131 kJ/mol. Substituting 103 kJ/mol, 168 h at 121°C corresponds to ~8 years at 58°C instead of 40 years. The AIW cable (CSPE/EPR) used 168 h at 121°C to simulate 40 years at 50°C based on an assumed E_a of 114 kJ/mol. Using 103 kJ/mol indicates that 168 h at 121°C corresponds to ~19 years at 50°C. The Anaconda cable (CSPE/EPR) used 168 h at 150°C to simulate 40 years at 69°C based on an assumed E_a of 114 kJ/mol. With 103 kJ/mol, 168 h at 150°C corresponds to ~20 years at 69°C. If the ambient aging temperature is a more realistic 50°C, 168 h at 150°C would correspond to ~165 years at 50°C. However, as will be shown below, aging at 150°C will lead to substantial DLO effects so if the ambient aging temperature were in fact 50°C, there would still be a significant problem with the 150°C simulation.

3.5 Estimates of Oxidation Rate for Combined Radiation plus Thermal Aging Conditions

Sequential radiation aging at very high dose rates was used for many of the early historic cable qualifications (Table 2.3 of reference [74]). More recent combined environment simulations were done at much lower dose rates and fairly moderate aging temperatures [68-70]. In order to estimate the importance of DLO effects and therefore estimate the margin associated with such exposures, we need to make estimates of $\phi[O_2]_{ref}$ under combined environment aging conditions as a function of aging dose rate and aging temperature. These estimates will then allow us to design the proper aging conditions to use for upcoming simulations. In general there is not a lot of $\phi[O_2]_{ref}$ data available under combined radiation plus thermal conditions and it is clear that this is one area where some effort should be made to enhance the quality and quantity of such data. However there are enough results available such that some simple new ideas can be tested that will be shown below to lead to reasonable initial estimates of the desired data.

The approach starts with the best available model for analyzing and extrapolating combined environment aging results, the dose to equivalent damage (DED) approach. This approach is one of the two approaches (DED and superposition of time-dependent data) recommended by the IAEA [76] and the IEC [77]. The superposition of time-dependent data approach is strictly empirical with three adjustable parameters and has been shown to suffer from numerous flaws[75]. The DED approach does not have any adjustable parameter and can be rigorously tested by observing whether the modeling leads to reasonable superposition [14,22-25,75]. It assumes that if you utilize thermal-only aging results and determine the appropriate thermal E_a value, that coupling an increase in temperature corresponding to an increase in thermal aging rate by a factor X with a dose rate increase by the same factor X leads to an overall increase in the combined environment degradation rate by the same factor X. An example of combined environment results for the Okonite CP jacket material is shown in Figure 62 where the dose required for the elongation to decrease to 50% is plotted versus the combined environment dose-rate and temperature (the latter in °C noted by the numbers next to the data points). These data are then time-temperature dose-rate shifted using the DED model assumptions to a give the dose rate dependence at a selected reference temperature using the thermal aging shift factor from the thermal-aging analysis (Figure 42) coupled with an identical dose-rate shift factor. The results of this procedure (Figure 63) justify the assumptions underlying the approach since they show excellent superposition without the use of any adjustable empirical parameter. In this instance even the data influenced by DLO effects superimpose. This is due to the fact that oxidation at the air-exposed surfaces of this material are at equilibrium. Thus the surface degradation is not affected by DLO effects. It turns out that significant hardening occurs as oxidation progresses so the surface hardens without being influenced by whether DLO effects are important or not in the interior regions of the material. This hardening is where cracks initiate during tensile testing and the initiated cracks immediately propagate through the material. Therefore DLO effects do not lower the rate at which the elongation degrades. With the above background we can now examine the four materials of interest with the goal of developing $\phi[O_2]_{ref}$ estimates versus radiation dose rate and temperature.

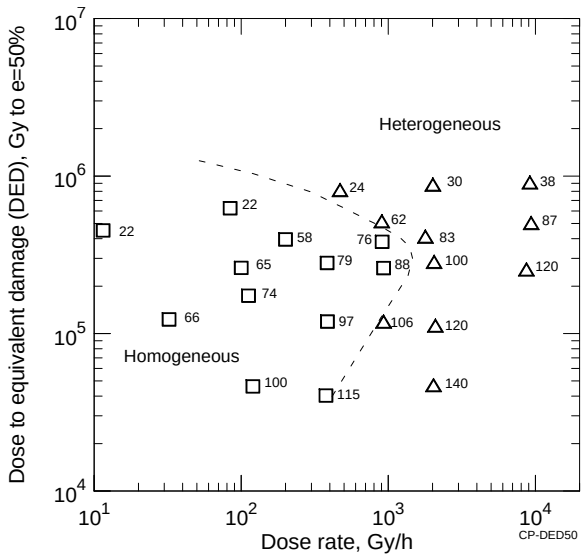

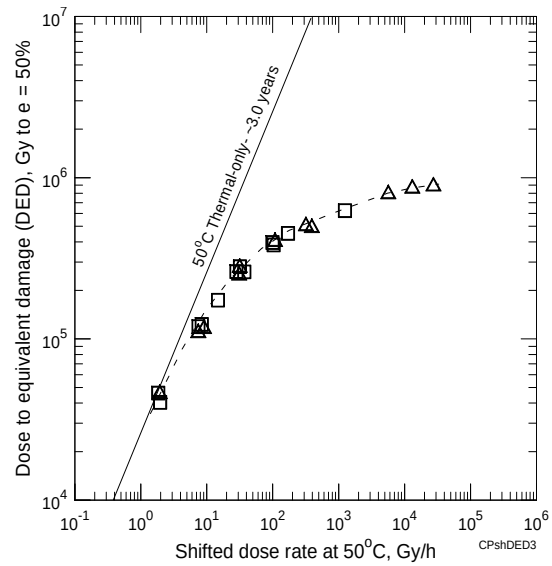

Figure 62 (Left). Combined environment data for Okonite CP jacket. The dose to 50% elongation is plotted versus dose rate with the aging temperature in °C of the experiment indicated by the numbers adjacent to the data points. Data plotted as triangles are in the region where DLO effects are important.

Figure 63 (Right). Time-temperature dose-rate superposition of the data from Figure 62 using the DED approach.

3.5.1 Chlorosulfonated Polyethylene (CSPE) Jackets

We showed earlier (Figure 35) that 9 different CSPE cable jacketing materials had very similar Arrhenius behavior for their thermal aging shift factors of elongation and oxygen consumption. We have also generated combined environment aging data on six of these CSPE samples. When all of these data from the six materials are time-temperature dose rate shifted to indicate the dose rate dependence appropriate at a 50°C reference temperature (bottom x-axis) utilizing the DED approach [14], the results show remarkable superposition as evidenced by Figure 64. Very limited $\phi[O_2]_{ref}$ data have been generated for combined radiation plus temperature exposures of CSPE cable jacketing materials. Early data came from Japanese experiments on a commercial and a model formulation where they found $\phi[O_2]_{ref}$ to be equal to 5.0e-10 mol/g/Gy and 3.2e-10 mol/g/Gy respectively in air at 25°C and 2e3 Gy/h [101,102]. If we take our time-temperature dose rate shifted results of Figure 64 and show the dose rate scale appropriate to 25°C as the top x-axis, we can go out to 2e3 Gy/h aging conditions and estimate that 1.3e6 Gy is required for the elongation to reach 100%. At a consumption rate of 5e-10 mol/g/Gy, this implies a total oxygen consumption of 6.5e-4 mol/g to reach 100%. At 3.2e-10 mol/g/Gy, the estimated total consumption to reach 100% elongation would be 4.2e-4 mol/g.

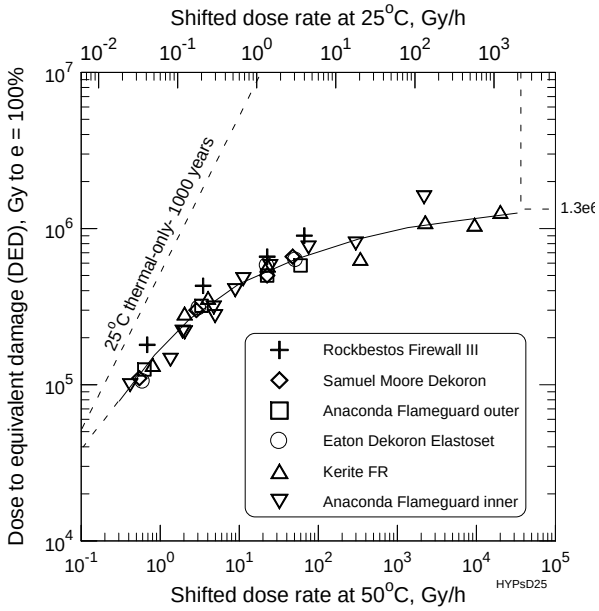

Figure 64. Time-temperature dose-rate superposition of data from six CSPE jacket materials at a reference temperature of 50°C (bottom x-axis) using the DED approach based on the shift factor data from Figure 35.

More recent data was reported by Calmet and co-workers [103] who measured oxygen consumption rates for both the CSPE jacket and the EPR insulation of a 3/C CSPE/EPR French nuclear cable. Measurements were taken at 40°C in combination with 5 Gy/h (2.04e-9 mol/g/Gy) and 750 Gy/h (6e-10 mol/g/Gy) dose rates as well as at 70°C in combination with 5 Gy/h (3.7e-9 mol/g/Gy), 20 Gy/h (2.35e-9 mol/g/Gy) and 750 Gy/h (6.7e-10 mol/g/Gy) dose rates. Analyzing these conditions in the same fashion as we did for the early Japanese results, we create the dose rate dependencies (upper x-axes) appropriate to 40°C and 70°C on Figure 65 and Figure 66, respectively and then obtain in the same fashion the total oxygen consumed to reach 100% elongation (noted on the figures). All of the results are summarized in Table 8.

Table 8. Estimates of Oxygen Consumed to Reach 100% Elongation for CSPE Jackets.

T, °C	Dose rate, Gy/h	$\phi[O_2]_{ref}$, mol/g/Gy	Dose to e=100%, Gy	Mol/g to e=100%
25	2e3	4.1e-10	1.3e6	5.3e-4
40	5	2.04e-9	5e5	10.2e-4
40	750	6e-10	1.05e6	6.3e-4
70	5	3.7e-9	1.4e5	5.2e-4
70	20	2.35e-9	2.9e5	6.8e-4
70	750	6.7e-10	7.2e5	4.8e-4

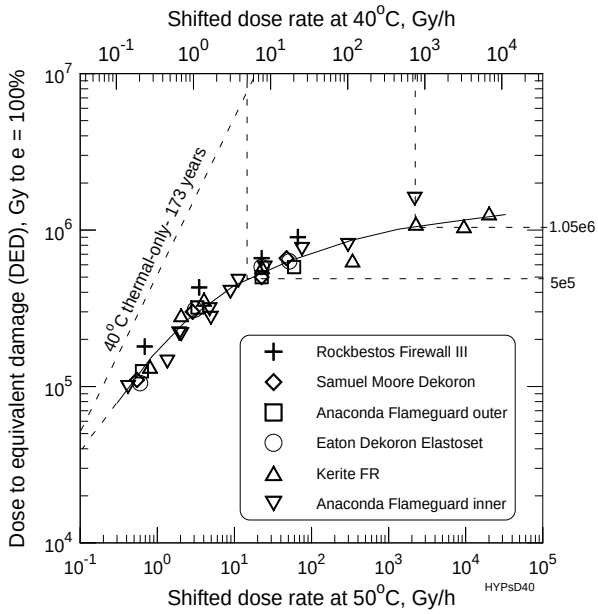

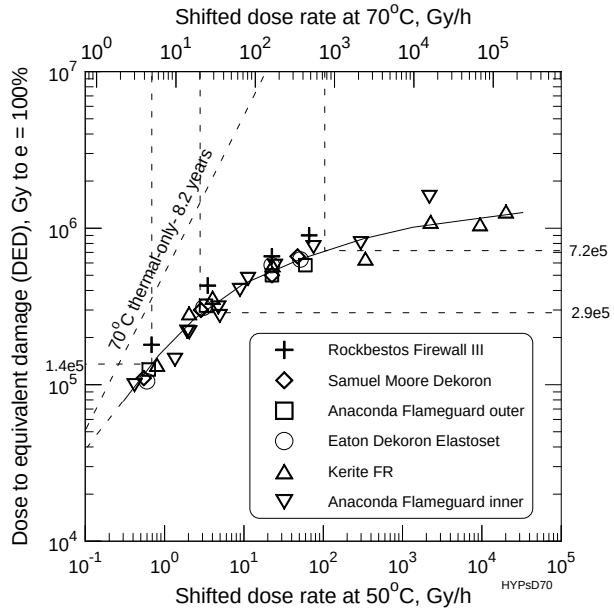

Figure 65 (Left). Same figure as Figure 64 except top x-axis is set for the time scale appropriate to 40°C.

Figure 66 (Right). Same figure as Figure 64 except top x-axis is set for the time scale appropriate to 70°C.

When the results are examined at 50°C (lower x-axes on Figure 64, Figure 65 and Figure 66), we obtain the oxygen consumption results to 100% elongation versus the dose rate at 50°C with the results shown in Figure 67. At low dose rates, thermal effects dominate whereas at high dose rates, radiation effects dominate. Although the results show some scatter, it is clear that no discernible trend with dose rate is obvious. Thus we can speculate that ~6.4±2.5e-4mol/g of oxygen is required to reach 100% elongation regardless of whether the degradation is dominated by radiation effects (high dose rate exposures), temperature (low dose rate exposures) or influenced by both environments. Earlier we estimated that 7.5e-4 mol/g of oxygen was required during pure thermal-only aging to reduce the elongation to 100%, a value consistent with the above conclusions. These observations imply that the amount of mechanical degradation is correlated with the amount of oxidation that occurs regardless of where in the radiation-temperature two-dimensional space one exists, a conclusion that might be expected. This observation offers additional evidence for the DED approach since it is based on a simple connection between radiation and thermal aging. Finally it allows us to use DED generated curves together with the assumption that the oxygen absorbed anywhere on the curve is a constant value (we choose 7e-4 mol/g to reach 100%) as a method of generating values of $\phi[O_2]_{ref}$ versus aging dose rate and temperature. This simple assumption together with the DED results for CSPE materials (Figure 64) allow us to generate the desired data which is given for several aging temperatures in Figure 68. Since the curves come from the DED approach, any two temperature curves are related by a shift upwards and to the right by the same multiplicative factor which is equal to the thermal shift factor relating the two temperatures. Thus predictions at any other desired temperatures are easily generated.

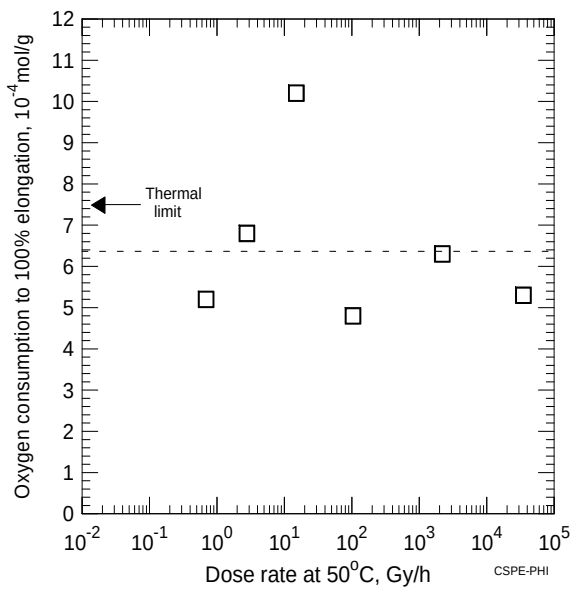

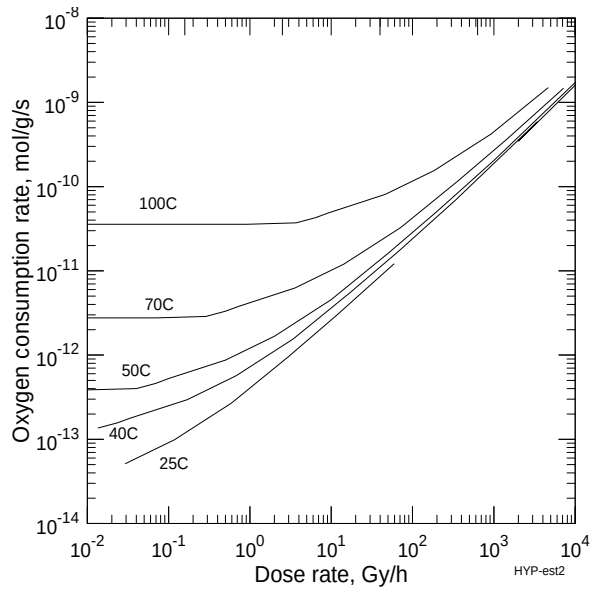

Figure 67 (Left). Oxygen consumption for CSPE to reach 100% elongation versus dose rate at 50°C.

Figure 68 (Right). Estimates of $\phi[O_2]_{ref}$ versus combined environment aging conditions at five different aging temperatures for CSPE jacket materials.

3.5.2 Chloroprene (CP) Cable Jackets

In our earlier discussion above on the DED approach, we showed time-temperature dose-rate superposed predictions at 50°C for the Okonite CP cable jacket material (Figure 63). More limited combined environment results were obtained and analyzed using the DED approach for the Rockbestos Firewall III CP jacket [14]. The predicted results for a drop in elongation to 50% from these analyses are shown in Figure 69 (filled circles) which also repeats the results for the Okonite CP jacket material from Figure 63. Since the Rockbestos material was superior from a thermal aging point of view, the results diverge in the low dose-rate thermal limit. However as radiation becomes the dominant degradation phenomenon at higher dose rates, the results for the two materials become similar. Based on this observation we crudely approximate the expected behavior of the Rockbestos at dose rates higher than the data range with a dashed extension curve that approximates the shape of higher dose-rate results for the Okonite material.

The only literature results of oxygen consumption in radiation environments that we could find for chloroprene cable jacketing materials were published in 1986 [101,102]. These studies looked at a commercially formulated material and a specially formulated material under air at a dose rate of 2e3 Gy/h at 25°C. The $\phi[O_2]_{ref}$ measurements gave 5e-10 and 6.9e-10 mol/g/Gy. Using the shift factors found for the Rockbestos material (Figure 39), we can add the dose rate scale appropriate to 25°C to Figure 69 (top x-axis). By going out to 2e3 Gy/h on this axis, we estimate that 1.1e6 Gy is required at 25°C and this dose rate to reach 50% elongation. Coupling this result with the average $\phi[O_2]_{ref}$ result of ~6e-10 mol/g/Gy leads to an estimated total consumption of 6.6e-4 mol/g to reach 50% elongation in the radiation-dominated region. Earlier we estimated that 6.8e-4 mol/g of oxygen consumption was required to reach 50% elongation in the thermal-only limit for this material. Therefore, similar to the situation for CSPE jackets, the

evidence appears to suggest an equal amount of oxygen absorption (to 50% elongation) in the thermal-dominated region and in the radiation-dominated regime. We therefore assume that 6.8e-4 mol/g is appropriate over the entire spectrum of combined environments for this material. This leads to the estimated $\phi[O_2]_{ref}$ results versus dose rate at several selected temperatures shown in Figure 70.

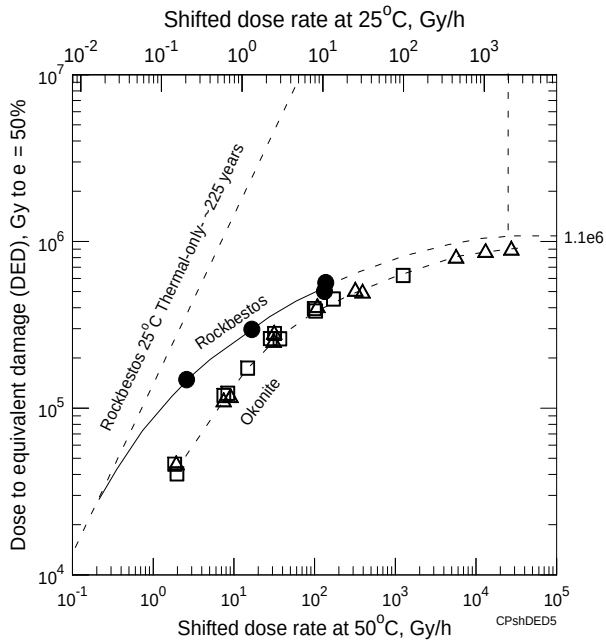

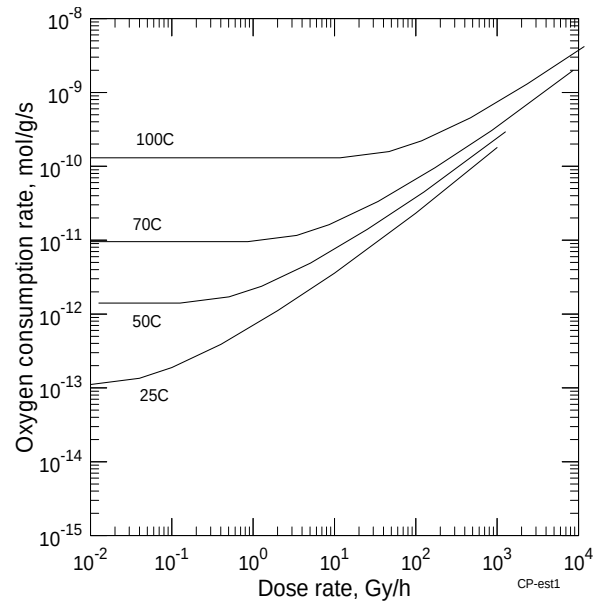

Figure 69 (Left). Time-temperature dose-rate superposition of the Rockbestos Firewall III CP jacket results (filled circles) added to the Okonite results from Figure 63. The bottom x-axis corresponds to the predictions at 50°C whereas the top x-axis relates to predictions at 25°C.

Figure 70 (Right). Estimates of $\phi[O_2]_{ref}$ versus combined environment aging conditions at five different aging temperatures for a Rockbestos CP cable jacketing material.

3.5.3 Crosslinked Polyolefin (XLPO) Cable Insulation Materials

Combined environment results for the Brandrex XLPO cable insulation material are shown in Figure 71. These results exhibit very strange behavior. Normally for combined environment exposures, raising the aging temperature at a constant dose rate leads to faster degradation and this is the case for temperatures of 60°C and higher. However, this is not the case for aging temperatures of 41°C and 22°C (filled squares on the figure) where faster degradation occurs then at higher temperatures. This effect is referred to as the "inverse-temperature effect" and has been documented and studied in great detail [53,54]. Inverse temperature effects are observed for several XLPO and EPR materials [54] usually at temperatures below ~50°C. For the higher temperature exposures, the DED approach often leads to reasonable superposition except for the anomalous inverse temperature data. This is observed for the Brandrex material which is time-temperature dose-rate superposed at 50°C (lower x-axis) as seen in Figure 72. Oxygen consumption results under combined environment conditions comprising a dose rate of ~38 Gy/h coupled with six different temperatures ranging from 20°C to 110°C have been obtained on this material are these results are plotted on Figure 73. These results also have anomalous behavior

since the consumption rate is found to increase as the aging temperature is lowered from 40°C to 20°C. With the above in mind, we concentrate our initial efforts on estimating the oxygen consumption rates in combined environments having temperatures of 50°C and above. Using the approach for the CSPE and CP jacketing materials, we determine the dose required to lower the elongation to 100% under the conditions used for the oxygen consumption experiments. For instance, at 39 Gy/h plus 110.2°C, the $\phi[O_2]_{ref}$ is equal to 3.64e-9 mol/g/Gy. Shifting the dose rate axis to 110.2°C in Figure 72 (upper x-axis) leads to an estimate that 2.1e5 Gy is required to reach 100% elongation under these aging conditions. In a similar fashion, data was generated for the other higher temperature combined environment results shown in Figure 73. The results are summarized in Table 9. The last column gives the dose rate results appropriate at 50°C. For the present material there appears to be a slight downward trend in the amount of oxygen absorbed to reach 100% as the chemistry moves from temperature-dominated to radiation dominated. This is seen in Figure 74 where the amount of oxygen required to reduce the elongation to 100% is plotted versus dose rate at a reference temperature of 50°C (last two columns of Table 9). To obtain estimates of $\phi[O_2]_{ref}$ versus aging temperature and dose rate we utilize the DED results from Figure 72 coupled with the results from Figure 74. We restrict our estimates to temperatures of 50°C and higher to avoid the inverse temperature effects occurring at lower temperatures. At each temperature, the results shown (Figure 75) are approaching the radiation dominated region at the highest doses modeled. Thus we expect the results at the three temperatures to come together and display fairly linear behavior at higher dose rates. This is crudely modeled by the dashed line extensions of the data. The only use of such high dose rate extrapolations will be in simulating early sequential radiation aging simulations. It will be shown below that any errors in such extrapolations will not affect these simulations since DLO effects will virtually eliminate oxidation in cables containing XLPO insulations covered by CP (or CSPE) jackets.

Table 9. Estimates of Oxygen Consumed to Reach 100% Elongation for Brandrex XLPO.

T, °C	Dose rate, Gy/h	$\phi[O_2]_{ref}$, mol/g/Gy	Dose to e=100%, Gy	Mol/g to e=100%	Dose rate for 50°C, Gy/h
60.6	38	1.34e-9	4.2e5	5.6e-4	16
81	37	1.91e-9	3.2e5	6.1e-4	3.5
95.1	37	2.93e-9	2.6e5	7.6e-4	1.36
110.2	39	3.64e-9	2.1e5	7.6e-4	0.57
50 (T-only)				7.8e-4	0.01

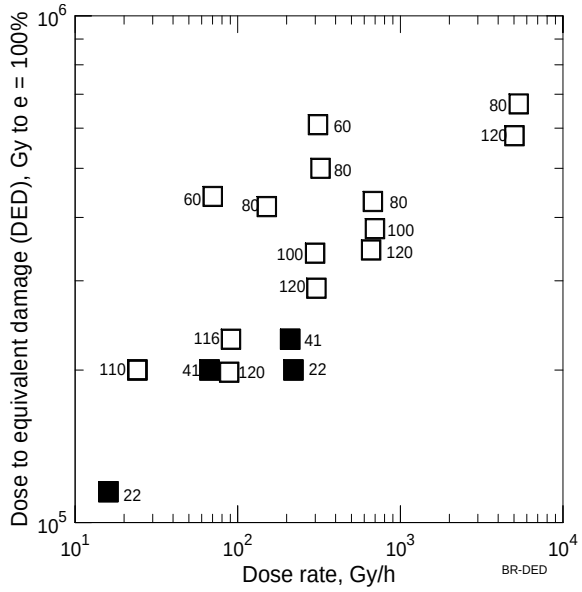

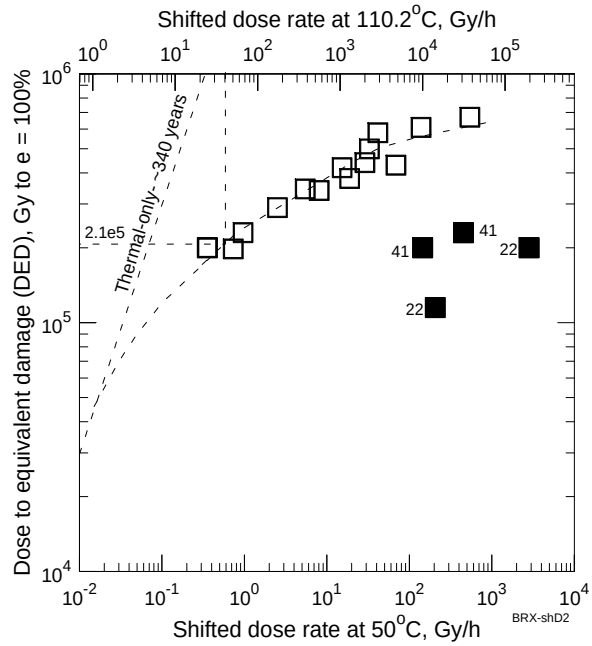

Figure 71 (Left). Combined environment data for Brandrex XLPO insulation. The dose to 100% elongation is plotted versus dose rate with the aging temperature in °C of the experiment indicated by the numbers adjacent to the data points.

Figure 72 (Right). Time-temperature dose-rate superposition of the data from Figure 71 using the DED approach.

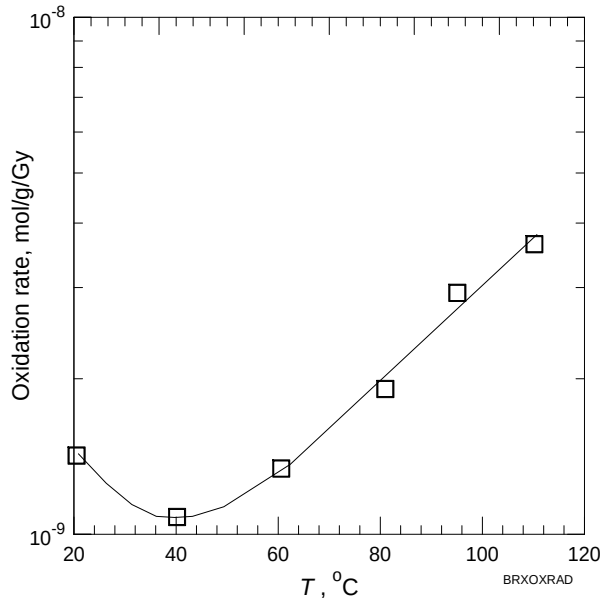

Figure 73. Combined environment oxygen consumption rate results for Brandrex XLPO insulation at ~38 Gy/h versus the aging temperature.

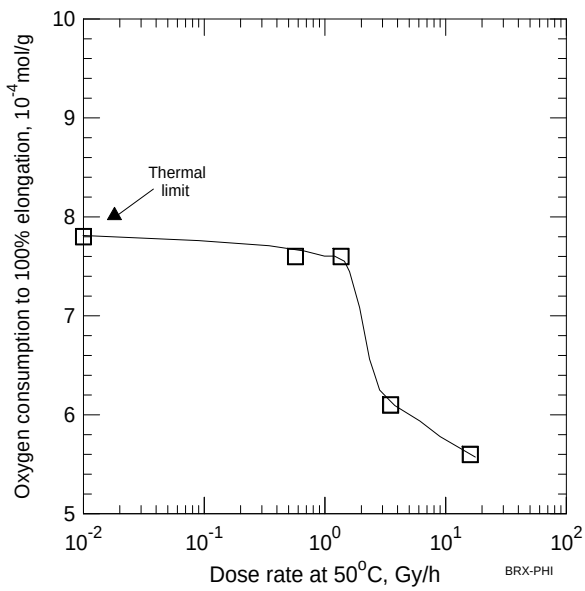

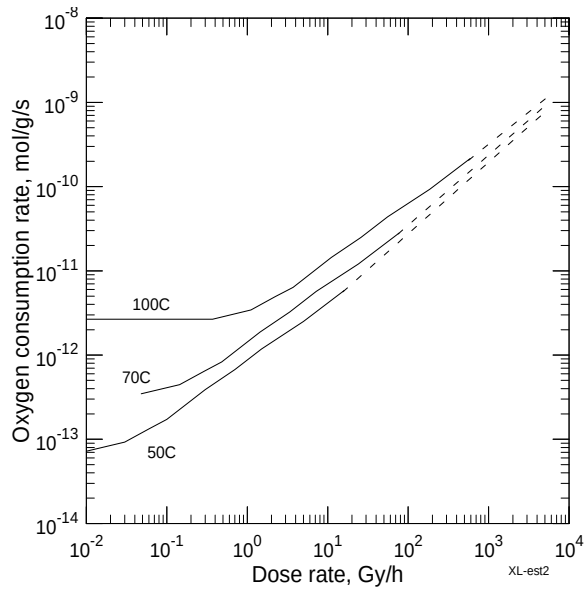

Figure 74 (Left). Oxygen consumption for Brandrex XLPO to reach 100% elongation versus dose rate at 50°C.

Figure 75 (Right). Estimates of $\phi[O_2]_{ref}$ versus combined environment aging conditions at three different aging temperatures for a Brandrex XLPO cable insulation material.

3.5.4 EPR/EPDM Cable Insulation Materials

Extensive combined environment exposures were conducted on the Anaconda Flameguard EPR cable insulation material by following the tensile properties versus aging time in each combination of dose rate and temperature [104]. In addition, Reynolds and co-workers [86] reported results for the same material [86]. The results from both studies showing the dose required for the elongation to drop to 100% are plotted versus dose rate in Figure 76 with the aging temperature in °C noted by each data symbol [75]. These results are time-temperature dose-rate shifted to a 50°C reference temperature according to the DED model utilizing the appropriate E_a value of 106 kJ/mol (from Figure 59). The results are shown in Figure 77 where the lower x-axis represents the dose rates appropriate for 50°C combined conditions. Oxygen consumption results for EPR materials under combined radiation plus temperature conditions are available from several sources. These include Japanese results taken at room temperature (25°C assumed) plus 2000 Gy/h [102], French results at 40°C plus 5 Gy/h and 750 Gy/h and at 70°C plus 5 Gy/h, 20 Gy/h and 750 Gy/h [103], and results taken on a Parker E740-75 EPR sealing material [93]. In addition we obtained results (previously unpublished) at 680 Gy/h and 25°C for the actual Anaconda Flameguard EPR material. We can analyze for the DED value appropriate to all of these combined environment aging conditions using the same approach outlined above. For instance, for the 70°C French conditions (5 Gy/h, 20 Gy/h and 750 Gy/h), we use the 106 kJ/mol E_a to create the dose rate scale appropriate for 70°C aging (top x-axis of Figure 77). We can then find the DED value appropriate to the three dose rates of interest at 70°C as indicated by the dashed lines on the figure. By using this same procedure for the other combined environment aging conditions of interest, we obtain the results summarized in Table 10. There is some scatter in the estimated consumption necessary to reach 100% elongation but this is not unexpected given the fact that the oxygen consumption rates of several different EPR materials

are being used for analyses on combined environment processed results of the Anaconda Flameguard EPR. The average total consumption estimated to reach 100% elongation is 2.3e-4 mol/g. Since the one measurement on the Anaconda Flameguard EPR is 2.0e-4 mol/g, we use this value to generate the estimates of the consumption rates versus dose rate and temperature. These results are given on Figure 78.

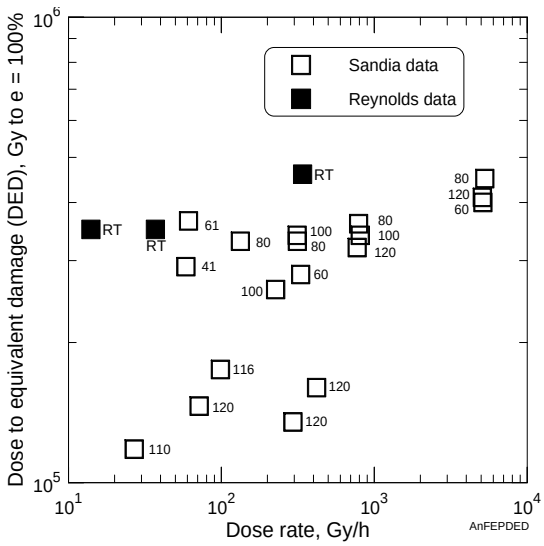

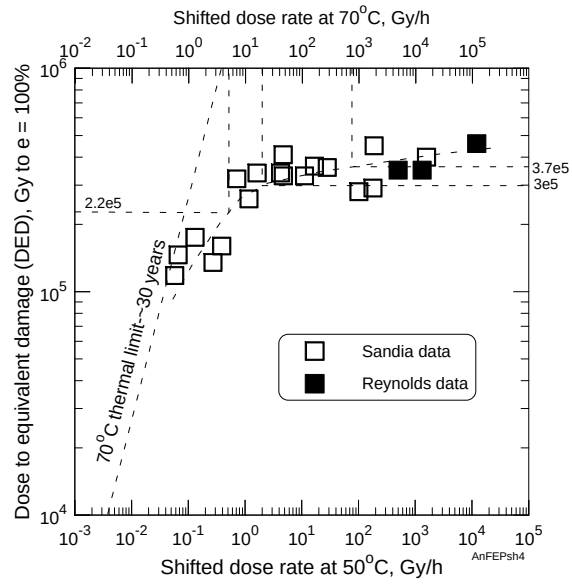

Figure 76 (Left). Combined environment data for Anaconda Flameguard FR/EP insulation. The dose to 100% elongation is plotted versus dose rate with the aging temperature in °C of the experiment indicated by the numbers adjacent to the data points.

Figure 77 (Right). Time-temperature dose-rate superposition of the data from Figure 76 using the DED approach.

Table 10. Estimates of Oxygen Consumed to Reach 100% Elongation for EPR Materials.

Source	T, °C	Dose rate, Gy/h	$\phi[O_2]_{ref}$, mol/g/Gy	Dose to e=100%, Gy	Mol/g to e=100%	Dose rate for 50°C, Gy/h	Ref.
French EPR	40	5	9.1e-10	3.4e5	3.1e-4	1.43	[103]
French EPR	40	750	5.1e-10	4.2e5	2.1e-4	214	[103]
French EPR	70	5	1.2e-9	2.2e5	2.6e-4	49	[103]
French EPR	70	20	8.1e-10	3e5	2.4e-4	197	[103]
French EPR	70	750	5.18e-10	3.7e5	1.9e-4	7386	[103]
JAERI EPR	25	2000	6.5e-10	4.4e5	2.86e-4	75	[102]
E740-75	70	1240	5e-10	3.8e-5	1.9e-4	1.22e4	[93]
E740-75	70	120	5.1e-10	3.5e5	1.78e-4	1180	[93]
E740-75	70	2090	6.3e-10	3.8e5	2.4e-4	2.06e4	[93]
Flameguard	25	680	4.6e-10	4.4e5	2.0e-4	25.4	-

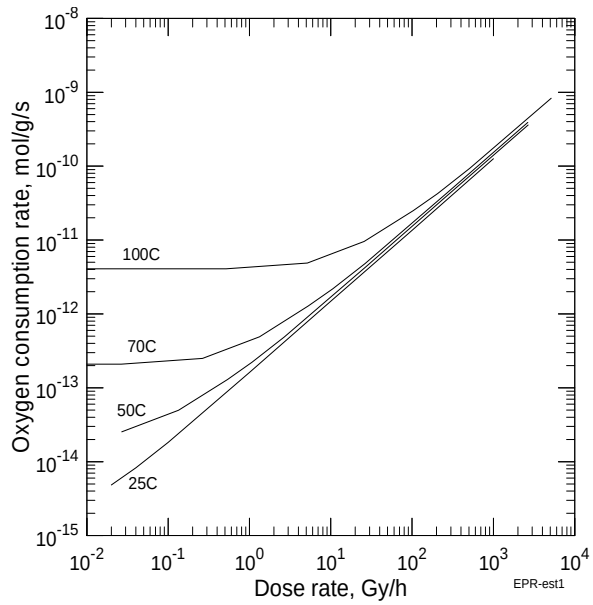

Figure 78. Estimates of $\phi[O_2]_{ref}$ versus combined environment aging conditions at three different aging temperatures for the Anaconda Flameguard EPR cable insulation material.

3.6 Estimates of P_{Ox} under Thermal Aging Conditions

Since early simulations of cable aging used sequential thermal aging up to 150°C (Table 2.3 of ref. [74]), we need estimates of oxygen permeability coefficients (P_{Ox}) up to this temperature to model the importance of DLO effects for these simulations. Until recently very few such measurements were carried out at such high temperatures. Typically P_{Ox} measurements have been carried out over a small temperature range near room temperature and the data were assumed to follow linear Arrhenius behavior, if estimates at higher temperatures were needed. Unfortunately it turns out that P_{Ox} values are not found to be Arrhenius, a phenomenon that is again difficult to observe if data are taken over a limited temperature range. Attempts at taking P_{Ox} measurements at high temperatures resulted in strange behavior where the P_{Ox} values appeared to reach a maximum as the temperature was increased and then began to decrease as the temperature was raised further. Several years ago we solved this apparent dilemma by showing that the anomalous behavior was caused by the presence of oxidation reactions at the higher temperatures [105]. By modeling these reactions, we were able to extract high temperature results and show that the P_{Ox} results were non-Arrhenius when examined over an extended temperature range. Typical results for six different elastomeric sealing materials are shown in Figure 79 which shows that non-Arrhenius behavior occurs for all of these materials [105].

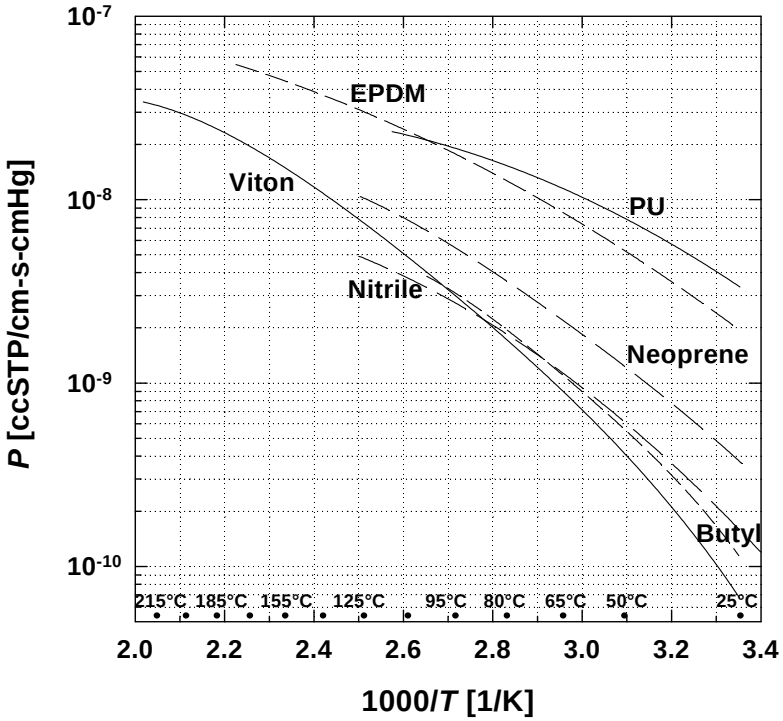

Figure 79. Comparison of P_{Ox} coefficient results for six different elastomeric sealing materials.

Unfortunately measurements at higher temperatures have not been made on CP and CSPE cable jackets and EPR and XLPO cable insulations. However, measurements have been taken or reported at lower temperatures for all four types of cable materials. Using these results, it is possible to make rough estimates at temperatures up to 150°C by assuming that the shape of the permeability curves on an Arrhenius plot resembles the "average" shape seen for the six elastomers in Figure 79.

Figure 80 and Figure 81 show results obtained at JAERI for a commercially-formulated CSPE material and a commercially-formulated CP material, respectively [106]. Even with the limited temperature range of 21°C to 50°C for the JAERI data, a slight amount of the expected curvature can be seen for both materials. These data are extrapolated to 150°C using the dashed curves that approximately represent the average curvature found for the six previously studied elastomers. Figure 82 gives results for an ITT Suprenant Exane II XLPO cable jacketing material [104] and for a General Electric Vulkene Supreme XLPE cable jacketing material (previously unpublished). The results are again extrapolated up to 150°C in the usual fashion. Figure 83 gives P_{Ox} results for four different EPR/EPDM materials, three from the JAERI Report [106] and Sandia results for the Anaconda Flameguard EPR cable insulation material [104]. For this material we extrapolate from the Anaconda results since this is an actual cable insulation sample and data from this material was used to generate other parameters of interest to the DLO calculations that will be done in the next section of this report. Using these four permeability coefficient plots we can make temperature-dependent estimates of the P_{Ox} values for the four types of material and such values at selected temperatures are summarized in Table 11.

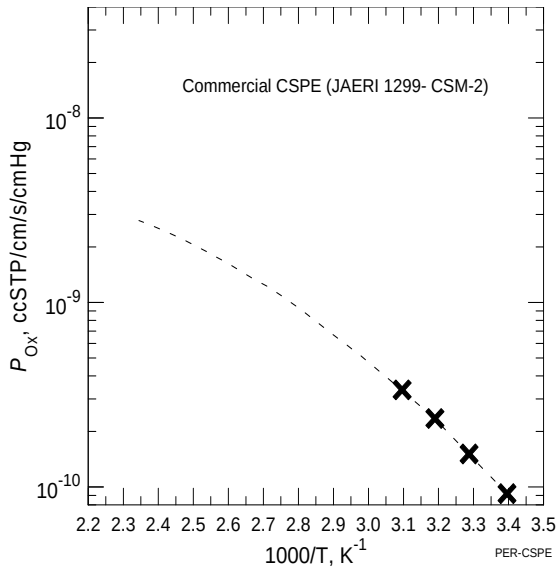

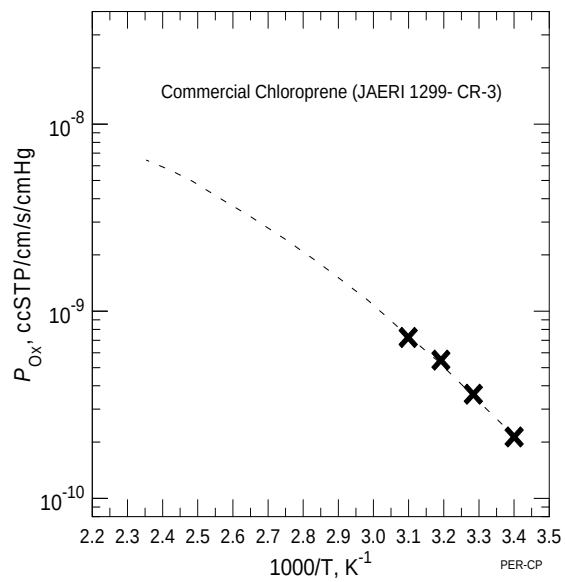

Figure 80 (Left). P_{Ox} results for a commercially formulated CSPE from ref. [106].

Figure 81 (Right). P_{Ox} results for a commercially formulated CP from ref. [106].

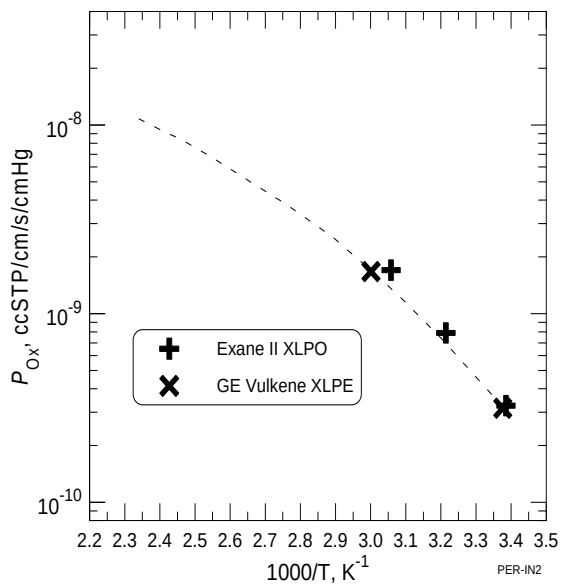

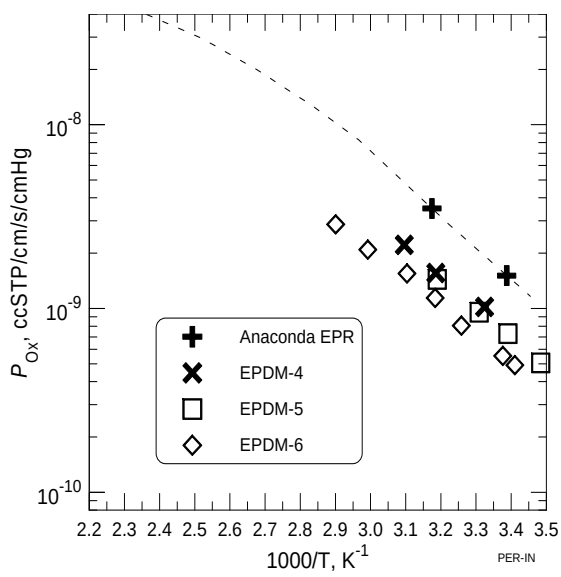

Figure 82 (Left). P_{Ox} results for two XLPO cable insulation materials.

Figure 83 (Right). P_{Ox} results for four EPR cable insulation materials.

Table 11. Estimates of POx (ccSTP/cm/s/cmHg) versus Temperature.

T, °C	25	50	100	121	150
EPR	1.7e-9	5e-9	2e-8	2.9e-8	4e-8
XLPO	3.6e-10	1.2e-9	4.7e-9	7e-9	1.05e-8
CP	2.65e-10	7.3e-10	3e-9	4.4e-9	6.25e-9
CSPE	1.12e-10	3.35e-10	1.33e-9	1.9e-9	2.7e-9

3.7 Estimates of the Importance of DLO for Selected Aging Conditions

We have now generated for the four materials of current interest estimates of (1) the oxygen consumption rate ($\phi[O_2]_{ref}$) versus thermal aging temperature, (2) the oxygen consumption rate ($\phi[O_2]_{ref}$) under combined radiation plus temperature conditions versus dose rate and temperature and 3) the oxygen permeability coefficient (P_{Ox}) versus aging temperature. Combining these with other variables (geometry, β) will allow us to estimate the importance of DLO effects for typical "worst-case" ambient aging conditions found in existing nuclear power plants. The results will also allow estimates of DLO effects for cable aging simulations under various simulated aging conditions such as the early sequential high acceleration qualification approaches [74] and more recent, more moderate acceleration simulations under combined radiation plus thermal environments [68-70]. Finally, we will use the estimates to suggest combined environment aging conditions to utilize for future experiments currently under consideration.

Before initiating the calculations in this section, it should be noted and obvious from the previous sections of this report that some uncertainty exists in the estimates of $\phi[O_2]_{ref}$ and P_{Ox}. This is caused by several factors. First of all, for any generic type of material (e.g., CSPE jackets), one expects differences to exist in the $\phi[O_2]_{ref}$ and P_{Ox} values dependent on the particular commercial formulation. Since past experimental data is often sparse, we typically obtained our estimates by combining data from several sources that had studied differing commercial formulations. In addition, we were often forced to extrapolate data (e.g., P_{Ox} results to 150°C) when no actual data existed in the range of interest. This implies that the numbers used in the calculations for a particular cable may be off by a factor of perhaps two or more. We will show below that this uncertainty will not have a profound effect on many of the upcoming conclusions concerning ambient aging and high acceleration sequential simulations (Table 2.3 of ref. [74]). However, there will be moderate effects caused by the uncertainties when examining the more moderate aging conditions used by Jacobus [68-70] and the planned conditions for future simulations. Thus it would be potentially useful to obtain some additional data to fill in some obvious holes in the existing data. For instance, given the limited amount of oxygen consumption data that exists in combined radiation plus thermal environments, it would be helpful to obtain such data on commercial materials of interest. Similarly, obtaining P_{Ox} results up to higher temperatures for key materials would be recommended. Also recommended would be estimates of the β parameter under combined environments by doing oxygen consumption measurements versus O_2 partial pressure.

There are numerous cable configurations used in nuclear power plants [e.g., single conductor, multi-conductor with an outside jacket, multi-conductor with individual jackets (bonded or non-bonded) plus an outside jacket, etc.]. In addition, the geometries of each type will differ in terms of conductor sizes, material thicknesses, etc.). With this in mind, we will concentrate our analyses on the cables listed in Table 2.1 of ref. [74] since these cables represent a cross-section of the cable types currently used in nuclear power plants.

3.8 Estimation of DLO Effects under Long-Term Ambient Nuclear Power Plant Aging Conditions

Worst case ambient aging conditions for safety-related cables vary from plant to plant and plant location to plant location. With this in mind we will arbitrarily select a worst case environment to be 50°C plus 0.5 Gy/h. The importance of DLO effects depend upon the ratio of the consumption rate to the permeability coefficient (the higher the ratio, the more important DLO) and the thickness of the materials (the thicker the materials, the more important DLO). We will therefore begin our modeling on the cables from reference [74] having the thickest overall dimensions for jacket plus insulation and the highest ratio of oxygen consumption rate to permeability coefficient. Table 2.1 of reference [74] shows that the multi-conductor cables from Rockbestos (45 mil CP jacket, 30 mil XLPE insulation), AIW and Anaconda (both with 60 mil of outer plus inner CSPE jacket, 30 mil of EPR insulation) represent the thickest materials. Based on our estimates, we summarize the appropriate values of $\phi[O_2]_{ref}$ and P_{Ox} at 50°C plus 0.5 Gy/h plus the ratio of the two quantities for the four materials of interest in Table 12. We will model both of these cable types for the three conductor configuration.

Table 12. Estimates of $\phi[O_2]_{ref}$, P_{Ox} and their Ratio at 50°C plus 0.5 Gy/h

Material	CP	XLPO	CSPE	EPR
$\phi[O_2]_{ref}$, mol/g/s	1.7e-12	5.4e-13	9e-13	1.2e-13
P_{Ox}, ccSTP/cm/s/cmHg	7.3e-10	1.2e-9	3.35e-10	5e-9
Ratio= $\phi[O_2]_{ref}/P_{Ox}$	2.3e-3	4.5e-4	2.68e-3	2.4e-5

For a typical 3-conductor cable, the average (centerline) circumferential length around the outside jacket is reasonably close to the sum of the average (centerline) circumferential lengths around the three insulations (or around the insulation and around its inner jacket if it exists). This means that as a first crude approximation, we can treat the cable geometry as two parallel sheets of material, the first of thickness equal to the jacket (plus the inner jacket if it exists), the second of thickness equal to that of the insulation. Given the long lengths of cable, we will assume that air can only get inside the cable by diffusing through the jacket(s). For our sheet model, this implies that air will be available on the outside surface of the jacket(s) and no air source exists on the inside surface of the insulation. The reason we set up the model as outlined is that we have an existing reaction-diffusion program that handles such a situation [97]. This allows us to test our ideas without having to develop finite element analyses codes in order to attack the multitude of cable sizes, cross-sections and configurations that exist in a typical nuclear power plant. If slightly more accurate simulations are desired in the future, such codes can be developed.

In order to use the LAMX2 program [97], we need the $\phi[O_2]_{ref}$ and P_{Ox} values given in Table 12 plus the oxygen solubility coefficient (S), the material density ρ and a value for the oxidation parameter β. The results are not sensitive to the value of S so we use an S value equal to 0.001 We will assume typical densities [14] for these materials (1.5 g/cc for CP and CSPE, 1.3 g/cc for

EPR/EPDM and XLPO). The β value will be set equal to 1 at a reference oxygen partial pressure of 16 cmHg (sea-level oxygen partial pressure) for all materials. Where appropriate, other values of β will be modeled to show the effect of changing β.

We first model the Rockbestos 3/C cable with the results shown in Figure 84. *P* on the x-axis denotes the percentage of the distance from the inside surface of the insulation to the outside surface of the jacket with the vertical line denoting the interface between jacket and insulation. The numbers under XLPO and CP denote the parameters used in the simulation (starting with thickness and proceeding downwards to $\phi[O_2]_{ref}$ (mol/g/s), P_{Ox} (ccSTP/cm/s/cmHg), solubility, density (g/cc) and β). Both the oxygen concentration and the oxidation rate are plotted versus position and it is clear that DLO effects are essentially absent under typical "worst-case" ambient aging conditions (50°C plus 0.5 Gy/h) for this cable. Modeling for the AIW and Anaconda 3/C cables is shown in Figure 85. In this case, the insulation is oxidized to ~97% of equilibrium and the jacket averages ~98% of equilibrium so DLO effects are not important for these cables under ambient conditions. For the ambient simulations of the remaining cables in Table 2.1 of reference [74], DLO effects would be even less important since their thicknesses are smaller than the two situations modeled in this section. <u>We therefore conclude that DLO effects are unimportant for the decades-long exposures occurring to typical cables under ambient nuclear power plant aging conditions. This means that oxidation proceeds at its equilibrium level throughout all of the cable cross-sections typically encountered.</u> Since we saw earlier that oxidation chemistry typically dominates degradation when oxygen is available, any accelerated simulations must sufficiently reproduce the oxidation degradation mechanism. Thus the simulations must minimize the importance of DLO effects.

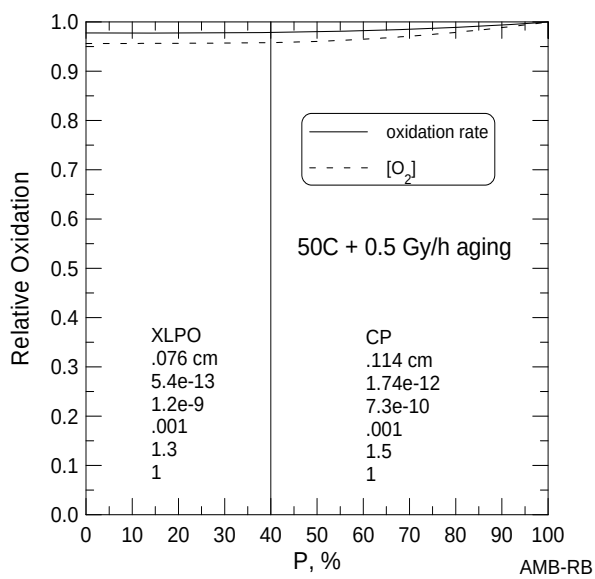

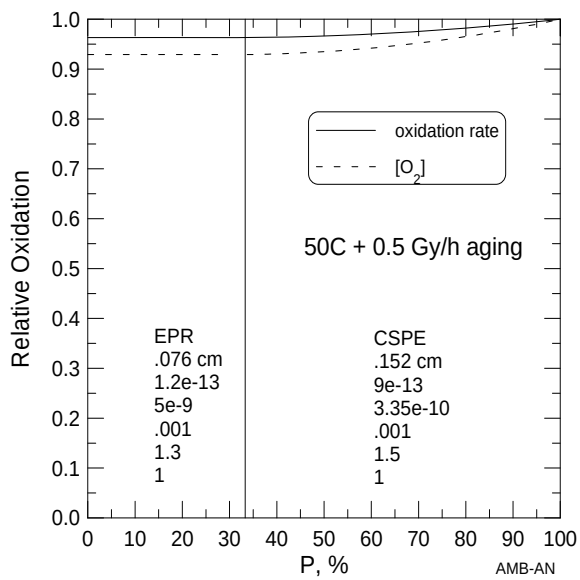

Figure 84 (Left). Estimated profiles for oxygen concentration and oxidation rate across the Rockbestos cable under typical "worst-case ambient aging conditions.

Figure 85 (Right). Estimated profiles for oxygen concentration and oxidation rate across the Anaconda or AIW cables under typical "worst-case ambient aging conditions.

3.9 Estimation of DLO Effects under the High Acceleration Sequential Aging Conditions used in Historic Qualifications

We now examine the importance of DLO effects for the sequential simulations that were used on the cables described in reference [74] which were summarized in Table 2.3 of this reference. The 3/C Rockbestos cable was aged at 150°C followed by aging in an average radiation environment of 4500 Gy/h (we assume at room temperature of 25°C). For the 150°C exposure, we obtain the estimated $\phi[O_2]_{ref}$ values from Tables 4 and 6 and the estimated P_{Ox} values from Table 11. The results of the modeling, shown in Figure 86, indicate that DLO effects are extremely important at 150°C aging conditions. The oxidation of the jacket starts at equilibrium at the outside surface of the jacket but quickly drops to ~1% of equilibrium at the inside surface of the jacket, averaging perhaps 30% of the non-DLO affected oxidation. Almost no oxidation (~1% of equilibrium) occurs across the XLPO insulation. For the follow-up sequential radiation exposure at 4500 Gy/h and 25°C, we obtain the estimated $\phi[O_2]_{ref}$ values from Figure 70 for the CP material (~7e-10 mol/g/s) and Figure 75 for the XLPO material (~6e-10 mol/g/s); estimated P_{Ox} values are obtained from Table 11. The modeling results are given in Figure 87 and again indicate significant DLO effects with essentially zero oxidation in the XLPO insulation. Thus we can conclude that the aging simulation was basically worthless because the dominant degradation mechanism (oxidation) was not replicated.

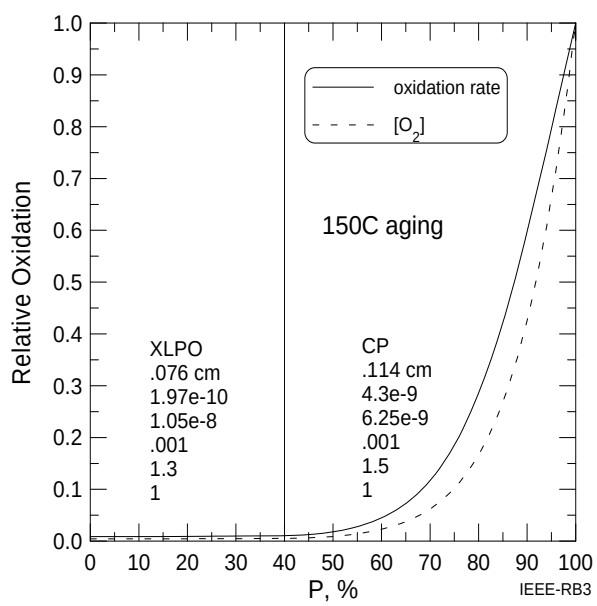

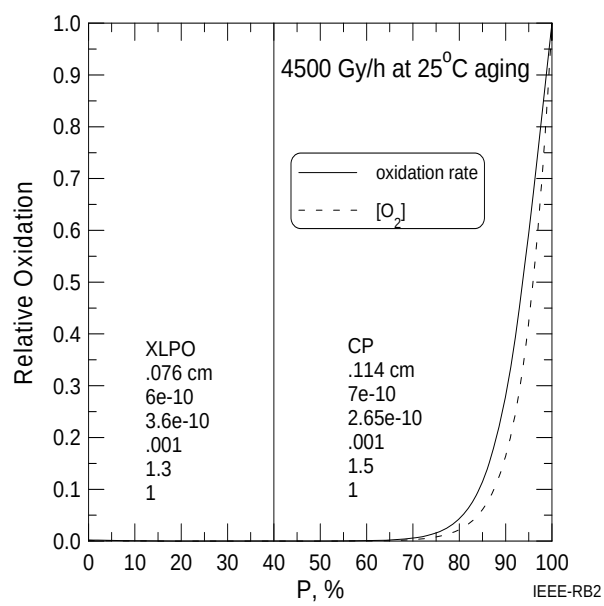

Figure 86 (Left). Estimated profiles for oxygen concentration and oxidation rate across the Rockbestos cable under sequential 150°C aging conditions.

Figure 87 (Right). Estimated profiles for oxygen concentration and oxidation rate across the Rockbestos cable under sequential 4500Gy/h plus 25°C aging conditions.

The 3/C Anaconda CSPE/EPR cable was aged at 150°C followed by sequential radiation aging at 3600 Gy/h (we assume at room temperature of 25°C). For the 150°C exposure, we obtain the estimated $\phi[O_2]_{ref}$ values from Tables 3 and 7 and the estimated P_{Ox} values from Table 11. The results of the modeling, shown in Figure 88, indicate that DLO effects are extremely important at 150°C aging conditions and that essentially zero oxidation occurs in the EPR insulation. For the sequential radiation exposure at 3600 Gy/h and 25°C, we obtain the estimated $\phi[O_2]_{ref}$ values from Figure 68 for the CP material (~5.6e-10 mol/g/s) and Figure 78 for the EPR material (~4.5e-10 mol/g/s); estimated P_{Ox} values are obtained from Table 11. The modeling results are given in Figure 89 and again indicate significant DLO effects and essentially zero oxidation in the EPR insulation, indicating that the earlier sequential qualification missed the dominant degradation mechanism (oxidation) and therefore does not represent actual conditions and is of no value for margin determination.

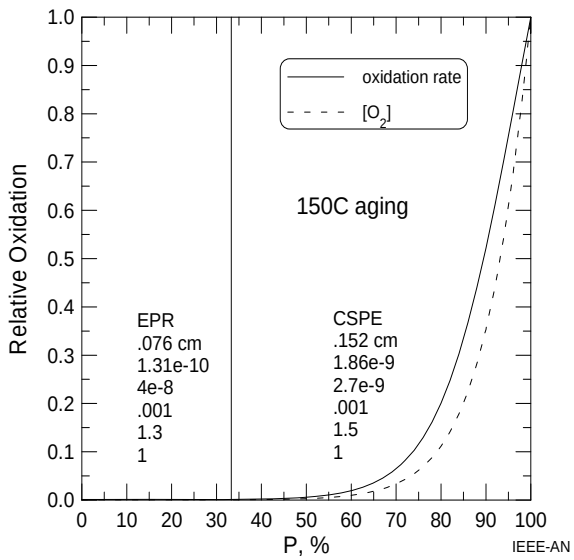

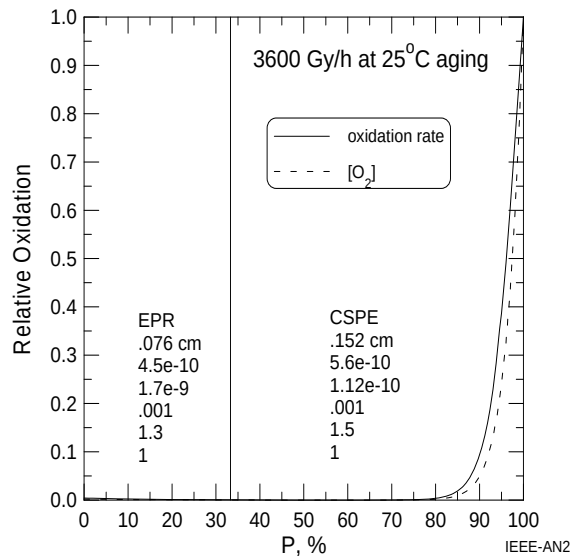

Figure 88 (Left). Estimated profiles for oxygen concentration and oxidation rate across the Anaconda cable under sequential 150°C aging conditions.

Figure 89 (Right). Estimated profiles for oxygen concentration and oxidation rate across the Anaconda cable under sequential 3600Gy/h plus 25°C aging conditions.

The 3/C AIW CSPE/EPR cable has similar geometry to the Anaconda CSPE/EPR cable. It was aged sequentially at 121°C followed by radiation aging at 5500 Gy/h. Since the radiation aging conditions are at a higher dose rate than that used for the Anaconda radiation exposure, DLO effects will be even more significant than those shown for the Anaconda material in Figure 89. However, the lower thermal aging temperature leads to a somewhat lower importance of DLO effects during this part of the aging sequence. This can be seen by modeling the 121°C aging conditions using results from Tables 3 and 7 plus P_{Ox} estimates from Table 11. The results, shown in Figure 90, indicate that the EPR insulation ages at ~18% of the equilibrium (no DLO effects) oxidation rate. In an earlier section of this report we showed that the use of a more rigorously derived E_a value of 103 kJ/mol for EPR implies that 168 h at 121°C used in qualification [74] corresponds to ~19 years at 50°C. Thus DLO effects (18% of equilibrium oxidation) imply that the 19 years is reduced to ~3.4 years of effective oxidation at 50°C. By adding this conclusion to the observation that the radiation part of the sequential aging of the

AIW cable leads to essentially zero oxidation of the EPR insulation, we conclude that the aging simulation of this cable does not represent actual conditions and is of no value for margin determination.

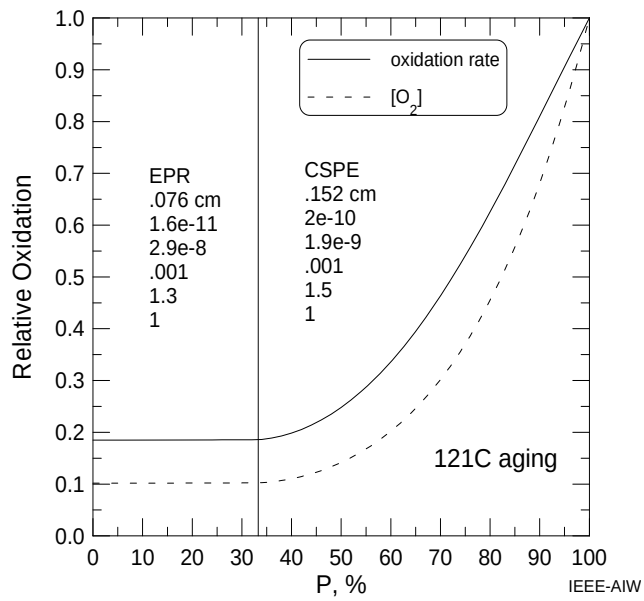

Figure 90. Estimated profiles for oxygen concentration and oxidation rate across the AIW cable under sequential 121°C aging conditions.

There are several 1/C cables (Anaconda, Samuel Moore and Okonite) described in Table 2.1 of reference [74] whose smaller overall thicknesses imply smaller DLO effects. The Samuel Moore 1/C had the thinnest components, comprising a 20 mil EPDM insulation covered by a 10 mil CSPE jacket. This cable was thermally aged for 168 h at 121°C. Using the 121°C $\phi[O_2]_{ref}$ values from Tables 3 and 7 plus the P_{Ox} values at 121°C from Table 11, DLO modeling results in the oxidation profile shown in Figure 91. In this instance, because of the very small thicknesses of the materials and the relatively low aging temperature of 121°C, DLO effects are small. The CSPE jacket is oxidized at ~98% of its equilibrium value and the EPR insulation is ~95% oxidized. In an earlier section of this report we showed that the use of a more rigorously derived E_a value of 103 kJ/mol for EPR implies that 168 h at 121°C used in qualification corresponds to ~19 years at 50°C. Thus DLO effects (95% of equilibrium oxidation) imply that the 19 years is reduced to ~18 years of effective oxidation at 50°C. The sequential radiation aging of this material involved 2.5e5 Gy at 7500 Gy/h. Assuming a temperature of 25°C, the appropriate estimates for $\phi[O_2]_{ref}$ of EPR and CSPE come from Figure 78 and Figure 68, and are 9e-10 and 1.1e-9 mol/g/Gy, respectively and the P_{Ox} values from Table 11. The DLO modeling of these conditions leads to the results shown in Figure 92. These results indicate that little oxidation occurs in the EPDM insulation even for this cable that comprises the smallest overall thickness of any of the cables shown in reference [74]. Therefore, the accelerated sequential simulation of the 1/C Samuel Moore cable resulted in oxidation from the thermal exposure equivalent to ~18 years at 50°C plus essentially zero oxidation from the radiation exposure.

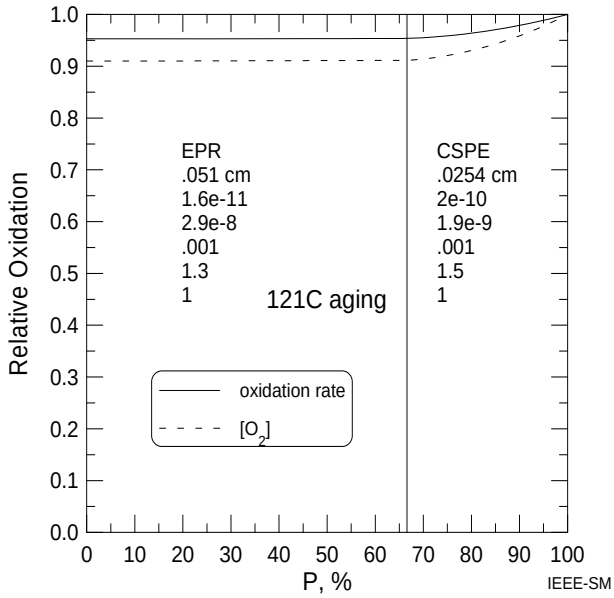

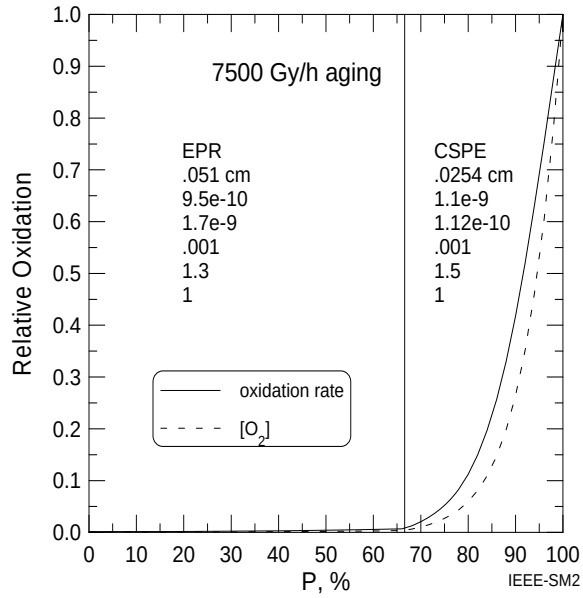

Figure 91 (Left). Estimated profiles for oxygen concentration and oxidation rate across the 1/C Samuel Moore cable under sequential 121°C aging conditions.

Figure 92 (Right). Estimated profiles for oxygen concentration and oxidation rate across the 1/C Samuel Moore cable under sequential 7500Gy/h plus 25°C aging conditions.

Both the Anaconda 1/C cable and the Okonite 1/C cable had 30 mil EPR insulation and 15 mil CSPE jackets and both were thermally aged at 150°C (168 h for the Anaconda cable, 504 hours for the Okonite cable). Modeling of this exposure condition led to the results shown in Figure 93 where DLO effects in the EPR insulation indicate that it is ~44% oxidized. Using the thermal Ea value estimated above for EPR materials (103 kJ/mol), we concluded that 168 h at 150°C was equivalent to ~165 years at 50°C so 504 hours exposure is equivalent to ~500 years at 50°C. Therefore 44% oxidized samples could be considered to be equivalent to ~73 years and 220 years aging at 50°C, respectively. On first glance, one might conclude that these results (especially the Okonite 504 hour exposure) might indicate some margin in the thermal aging part of the sequential aging exposure. However, two other factors need to be considered. First of all, modeling of the radiation exposure conditions will result in the observation of zero oxidation in the EPR insulation (both the EPR and the CSPE are 50% thicker than these materials in the 1/C Samuel Moore which showed essentially zero oxidation of the EPR (Figure 92). In addition, Figure 77 shows that radiation plays an important role under ambient aging conditions (0.5 Gy/h plus 50°C).

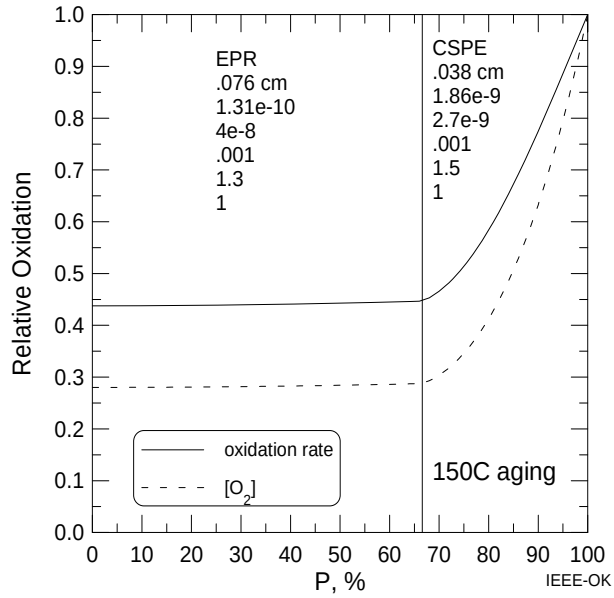

Figure 93. Estimated profiles for oxygen concentration and oxidation rate across the 1/C Okonite cable under sequential 150°C aging conditions.

One interesting observation that can be made from all of the DLO modeling results is that in every instance the profile of oxygen concentration and therefore oxidation for the insulation (EPR or XLPO) part of the cable cross-section is essentially flat. This means that the importance of DLO in the insulation is basically determined by how much the oxygen concentration drops off from the outside jacket surface to the inside jacket surface. This is because the jacket materials (CP or CSPE) are more sensitive to oxidation under the environment conditions used in the aging and the P_{Ox} values for the insulations are greater than those for the jackets (Table 11).

Based on the modeling of the importance of DLO effects under the aging and geometric conditions summarized for several representative, sequentially-aged cables [74], we conclude that the oxidation of the insulation materials was typically small or non-existent. Since oxidation chemistry normally dominates the mechanical degradation of cable materials and this chemistry was reduced or absent for the insulations, no margin can be determined by these early attempts at simulating cable aging as a part of cable qualifications. Further research is needed to better understand the aging phenomena, LOCA performance and potential remaining margins for non-DLO oxidatively aged cables.

From a radiation aging point-of-view, it is interesting to note that the IEEE recognized in 1993 the issues surrounding the importance of making sure that DLO effects were unimportant during accelerated radiation aging exposures for electrical insulation materials. This recognition resulted in IEEE Std. 775-1993, a standard that has been subsequently withdrawn [107]. Table 1 of this Standard gives estimates of the room temperature radiation dose rates necessary to have minimal DLO effects for various generic material types of several sheet thicknesses. Since these "critical dose rate" results refer to sheets with air on both sides of the sheet, they must be reduced by a factor of 4 for sheets with air on one side. For 1.5 mm thick samples of CSPE (hypalon) and CP (neoprene) exposed to air on one side of the sheet, the calculations lead to maximum dose rates of 33 Gy/h and 15 Gy/h, respectively. For 1-mm thick samples, the estimates are 75 Gy/h and 33 Gy/h, respectively.

3.10 Estimation of DLO Effects under the Combined Environment Conditions used by Jacobus [68-70]

Now that we have concluded that the early sequential aging simulations of cables under highly accelerated aging conditions did not appropriately represent the oxidation chemistry that occurs under long-term ambient aging exposures, we next examine more recent combined environment exposures that were done under less accelerated aging conditions. In particular, we will look at the extensive study conducted by Mark Jacobus in the early 1990s [68-70] that looked at several cables containing the materials of interest (CP and CSPE jackets plus EPR and XLPO insulations). Our goal is to use the LAMX2 modeling [97] to determine the importance of DLO effects for these studies and to apply the DED model to estimate the ambient 50°C conditions (e.g., years and dose rate) simulated by the combined accelerated conditions utilized in Jacobus' studies. Jacobus exposed whole cables to combined radiation plus thermal environments for 3-month, 6-month and 9-month time periods meant to represent 20-year, 40-year and 60-year exposures under ambient aging conditions of 55°C and 1.14 Gy/h with an assumed thermal E_a of 111 kJ/mol. After determining the importance of DLO effects for his studies, we will assume an ambient temperature of 50°C and use the thermal E_a values for the various materials to determine the aging conditions (dose rate and time) simulated by these studies.

The first cable examined is the 1/C Okonite Okolon (30 mil EPR insulation, 15 mil CSPE jacket) aged for 9 months at 100°C plus 84 Gy/h. Using Figure 78 and Figure 68 plus Table 11, we obtain the parameters of interest and generate the appropriate DLO profile shown in Figure 94. Small DLO effects are appropriate for this cable with the oxidation of the insulation and jacket representing approximately 87% and 94% of equilibrium, respectively. Therefore 9 months of EPR insulation aging represents ~0.87 (9 months) ~ 7.8 months of homogeneous oxidation. Using the DED model, the appropriate E_a of 103 kJ/mol gives a shift factor of 170 between 100°C and 50°C. Therefore 7.8 months of 100°C plus 84 Gy/h is equivalent to 110 years of 50°C plus 0.49 Gy/h. Thus for this 1/C cable, significant margin of almost a factor of 2 exists if 60 years at 50°C plus 0.5 Gy/h is chosen as the ambient aging condition. Since the E_a for the CSPE is 91 kJ/mol from 100°C down to 50°C which corresponds to a shift factor of 93, the 9 month exposure at 100°C corresponds to 0.94 (9 months) (93) = 787 months or 66 years at 84Gy/h/93 = 0.9 Gy/h. This also represents margin due to the higher dose rate and the longer time period.

Most of the other cables examined in the Jacobus study were 3/C cables where the larger thicknesses lead to more important DLO effects with less evidence of margin. For instance, the 3/C Samuel Moore Dekoron Polyset cable (30 mil XLPO insulations, 45 mil CSPE jacket) was aged for 9 months at 100°C plus 79 Gy/h. Using Figure 75 and Figure 68 plus Table 11, we obtain the parameters of interest and generate the appropriate DLO profile shown in Figure 95. Moderate DLO effects are appropriate for this cable with the oxidation of the insulation and jacket representing approximately 35% and 65% of equilibrium, respectively. Therefore 9 months of XLPO insulation aging represents ~0.35 (9 months) ~ 3.2 months of homogeneous oxidation. Using the DED model, the appropriate E_a of 72 kJ/mol gives a shift factor of 36 between 100°C and 50°C. Therefore 3.2 months of 100°C plus 79 Gy/h is equivalent to ~10 years of 50°C plus 2.2 Gy/h. Thus there is lack of margin in time although there is a factor of ~4 margin in dose rate. For the CSPE jacket, the shift factor of 93 implies 9 months of 100°C plus 79 Gy/h is equivalent to 0.65(0.75 year)(93) ~ 45 years at 50°C plus 0.85 Gy/h.

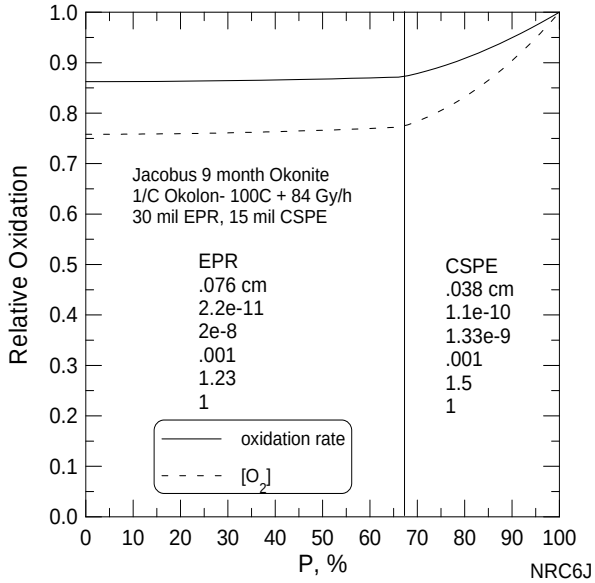

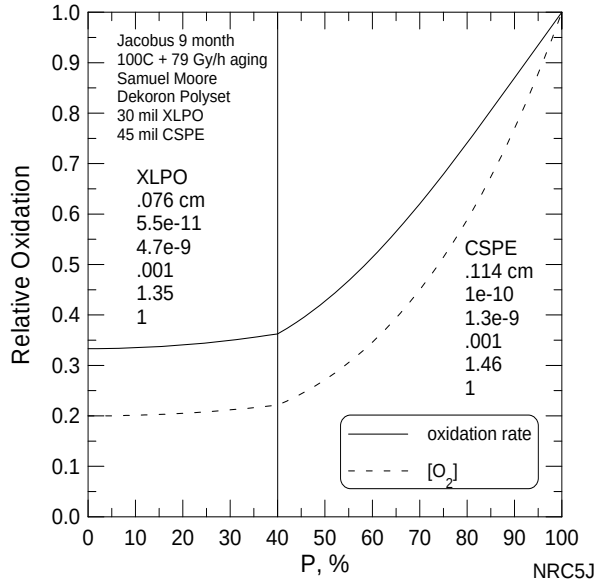

Figure 94 (Left). Estimated profiles for oxygen concentration and oxidation rate across the 1/C Okonite cable under the indicated combined environment aging conditions.

Figure 95 (Right). Estimated profiles for oxygen concentration and oxidation rate across the 3/C Samuel Moore cable under the indicated combined environment aging conditions.

The 3/C Rockbestos Firewall III cable (30 mil XLPO insulations, 45 mil CP jacket) was aged for 9 months at 100°C plus 84 Gy/h. Using Figure 75 and Figure 70 plus Table 11, we obtain the parameters of interest and generate the appropriate DLO profile shown in Figure 96. Moderate DLO effects are appropriate for this cable with the oxidation of the insulation and jacket representing approximately 44% and 70% of equilibrium, respectively. Therefore 9 months of XLPO insulation aging represents ~ 44% of 9 months or ~ 4 months of homogeneous equilibrium oxidation. Using the DED model, the appropriate E_a of 72 kJ/mol gives a shift factor of 36 between 100°C and 50°C. Therefore 4 months of 100°C plus 84 Gy/h is equivalent to ~12 years of 50°C plus 2. Gy/h. Thus there is again a lack of margin in time although there is a factor of ~4 times higher dose rate over the 12 year equivalent time period. The simulated dose of 2 Gy/h over 12 years could be considered to be comparable to 48 years at 0.5 Gy/h in the absence of dose rate effects. For the CP jacket, the shift factor of 93 implies 9 months of 100°C plus 84 Gy/h is equivalent to 0.7(0.75 year)(93) ~ 49 years at 50°C plus 0.9 Gy/h (in the absence of dose rate effects, the radiation could be equivalent to 88 years at 0.5 Gy/h). Thus for the 3/C Rockbestos Firewall III cable, Jacobus' aging conditions suggest that some amount of margin is being approached and arguments for margin could probably be justified for slightly reduced accelerated aging conditions over slightly longer aging times.

The 3/C Brandrex cable (30 mil XLPO insulations, 60 mil CSPE jacket) was aged for 9 months at 100°C plus 68 Gy/h. Using Figure 75 and Figure 68 plus Table 11, we obtain the parameters of interest and generate the appropriate DLO profile shown in Figure 97. Due to the larger cross-sectional dimensions, DLO effects are more significant for this cable with the oxidation of the insulation and jacket representing approximately 23% and 57% of equilibrium, respectively. Therefore 9 months of XLPO insulation aging represents ~0.23 (9 months) ~ 2.1 months of homogeneous oxidation. Using the DED model, the appropriate E_a of 72 kJ/mol gives a shift

factor of 36 between 100°C and 50°C. Therefore 2.1 months of 100°C plus 68 Gy/h is equivalent to ~6.6 years of 50°C plus 1.9 Gy/h. Thus there is again a lack of margin in time although there is a factor of ~4 margin in dose rate (in the absence of dose rate effects, the radiation could be equivalent to 25 years at 0.5 Gy/h). For the CSPE jacket, the shift factor of 93 implies 9 months of 100°C plus 68 Gy/h is equivalent to 0.57(0.75 year)(93) ~ 40 years at 50°C plus 0.73 Gy/h.

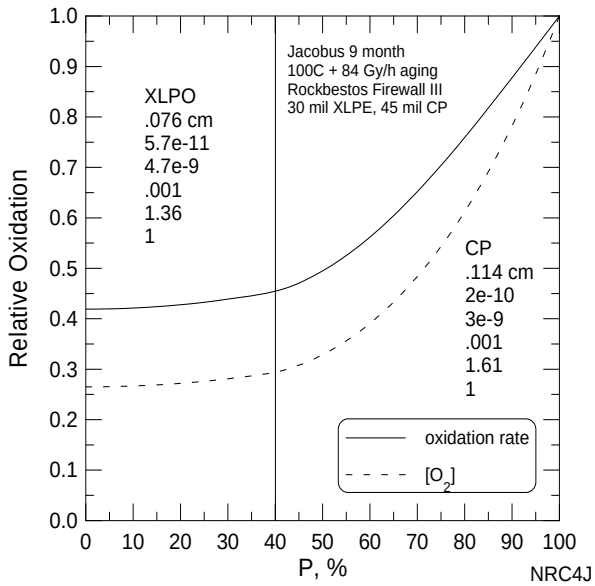

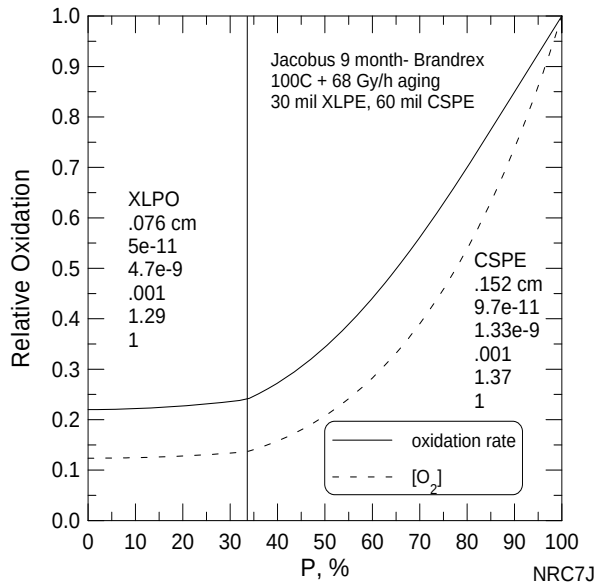

Figure 96 (Left). Estimated profiles for oxygen concentration and oxidation rate across the 3/C Rockbestos Firewall III cable under the indicated combined environment aging conditions.

Figure 97 (Right). Estimated profiles for oxygen concentration and oxidation rate across the 3/C Brandrex cable under the indicated combined environment aging conditions.

The final Jacobus cable exposed to a 9-month environment of 100°C plus 82 Gy/h was a BIW 2/C cable (30-mil EPR insulation, 15 mil CSPE individual jacket, 60 mil CSPE outside jacket). Using Figure 78 and Figure 68 plus Table 11, we obtain the parameters of interest and generate the appropriate DLO profile shown in. Combining the two CSPE thicknesses to 75 mil overall implies that this material should have the most important DLO effects of the Jacobus cables and the modeling results shown in Figure 98 back up this expectation. The oxidation of the insulation and jacket represent approximately 13% and 47% of equilibrium, respectively. Therefore, 9 months of EPR insulation aging represents ~0.13 (9 months) ~ 1.2 months of homogeneous oxidation. Using the DED model, the appropriate E_a of 103 kJ/mol for EPR gives a shift factor of 170 between 100°C and 50°C. Therefore 1.2 months of 100°C plus 82 Gy/h is equivalent to ~17 years of 50°C plus 0.48 Gy/h. Thus for this 2/C cable, no margin occurs. Since the E_a for the CSPE is 91 kJ/mol from 100°C down to 50°C which corresponds to a shift factor of 93, the 9 month exposure at 100°C corresponds to 0.47 (0.75 years) (93) ~ 33 years at 0.88 Gy/h.

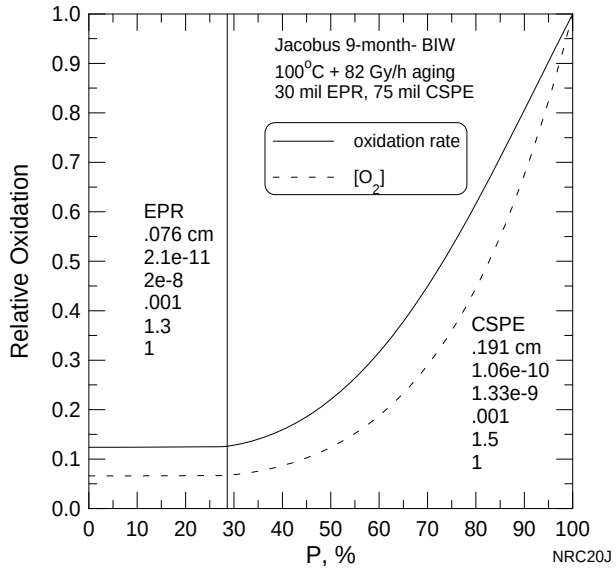

Figure 98. Estimated profiles for oxygen concentration and oxidation rate across the 2/C BIW cable under the indicated combined environment aging conditions.

It is again interesting to note for the Jacobus modeling that in every instance the profile of oxygen concentration and therefore oxidation for the insulation (EPR or XLPO) part of the cable cross-section is close to flat. This again means that the importance of DLO in the insulation is basically determined by how much the oxygen concentration drops off from the outside jacket surface to the inside jacket surface. This is because the jacket materials (CP or CSPE) are more sensitive to oxidation under the combined environment conditions used in the aging and the P_{Ox} values for the insulations are greater than those for the jackets (Table 11).

The analyses of the Jacobus aging conditions indicates that 1/C cables with relatively thin insulations and jackets appear to have margin in their simulation of 60 years at 50°C plus 0.5 Gy/h. The results for the jacketing materials of the 2/C and 3/C cables indicate moderate DLO effects and aging that simulates on the order of 30 to 50 years (shy of the goal of 60 years) at 50°C plus ~0.8 Gy/h (60% margin over goal of 0.5 Gy/h). Thus, the jackets come reasonably close to simulating the desired conditions. The insulations, on the other hand, appear to simulate approximately 6 to 17 years at 50°C plus 0.5 to 2.3 Gy/h. These results suggest that lowering of the dose rate during the simulation (DLO will be reduced) plus lengthening the exposure times might do a better job of simulating ambient aging conditions.

Finally, it should be pointed out that recent work at JNES [72] used slightly more accelerated conditions (100°C plus 100 Gy/h) than those used by Jacobus for pre-LOCA aging of 3/C cables comprising 0.8 mm thick EPR insulations together with 1.5 mm thick CSPE or CP jackets. Comparing their aging conditions and material thicknesses with those of Jacobus discussed above, it is clear that conclusions for the JNES simulations should be similar to those made for Jacobus' 2/C and 3/C cables if similar activation energies apply. It should be noted, however, that they assume a very low Arrhenius activation energy of 15 kcal/mol (63 kJ/mol) for their EPR materials. If true, the DED approach would conclude that their simulations underestimated the aging time at 50°C and simulated an increased dose rate at that temperature.

3.11 Development of Combined Environment Aging Conditions for Future Experiments

We would now like to develop combined environment aging conditions for future experiments that have a reasonable chance of having margin with respect to a chosen set of worst case ambient conditions (for example 60 years at 50°C plus 0.5 Gy/h). In selecting aging conditions, several complications occur. In an ideal world, all of the materials would have identical E_a values and no DLO effects would be present. This would allow one to select a single set of accelerated aging conditions that would result in all four materials of interest being equivalently aged to the exact same ambient aging conditions of interest (e.g., 60 years at 50°C plus 0.5 Gy/h). Unfortunately this is not the case since important DLO effects are often present and the E_a values differ. As noted earlier in this report, the eight CSPE jackets have reasonably similar E_a values between 50°C and 100°C of 91 kJ/mol (Figure 35), the two CP jackets are also similar with the Rockbestos CP averaging 91 kJ/mol between 50°C and 100°C (Figure 39). The EPR insulations are all reasonably close to each other with a typical E_a averaging about 103 kJ/mol between 50°C and 100°C (Figure 59). However for the XLPO insulations, we concluded that the Brandrex had an E_a of 72 kJ/mol (Figure 47) whereas the Rockbestos had an E_a of 98 kJ/mol (Figure 57). Since our combined environment data was taken on the Brandrex XLPO material (Figure 71), we utilized 72 kJ/mol for our analyses of XLPO materials. If we had Rockbestos combined environment results, the DED analyses would involve the higher E_a value of 98 kJ/mol which would lead to differing accelerated simulation conditions.

In addition to differences in E_a values, DLO effects reduce the effective oxidation to a greater extent in the insulations relative to the jackets. Therefore one must compromise in choosing aging conditions such that the cable material of higher E_a value will typically be over-aged in order to achieve aging in the second material that comes close to simulating ambient conditions. In addition, if the experimental arrangement involves aging all of the cables in a single aging container, the aging conditions will by necessity be designed based on the material with lowest E_a value (e.g., the XLPO with an E_a of 72 kJ/mol); otherwise this material will be severely under-aged.

Another issue concerns the value of β chosen for the simulations; as we will show below, higher β values for the insulation material will tend to reduce the importance of DLO effects and therefore improve the conservatism of the simulations. Another improvement in the DLO simulations would be to replace the parallel sheet model with the actual complex cylindrical geometries appropriate to cable cross-sections. This would require finite element codes to be developed that are appropriate to the many cable geometries used in plants. In general this will lead to small to moderate reductions in the importance of DLO effects and further improve the conservatism of the simulations. One final complication concerns materials that show inverse temperature effects [53,54] (usually at ~40°C and below) since these are not amenable to the DED modeling approach [75].

With all of these complications in mind and assuming only a single chamber will be used for all of the cables being tested, we will now attempt to select optimum accelerated aging conditions. Based on the discussions above of the simulations carried out by Jacobus, we conclude that his aging conditions were reasonably close to achieving this goal. With this in mind, we choose to slightly modify his conditions in several ways to achieve better simulations. Instead of 9 months

at 100°C plus ~80 Gy/h, we select 2 years of aging at 100°C plus 30 Gy/h. This increases the effective aging times at 50°C by a factor of 24/9 ~2.67 times while keeping the total dose during exposure ~ constant. This condition was chosen with the goal of trying to have some margin for the lowest E_a material (the Brandrex XLPO insulation with an E_a of 72 kJ/mol). Materials with higher E_a values would then typically be over-aged and therefore contain margin.

Since we do not know which cables will be used for the future aging-LOCA simulation program, we will utilize as examples four of the cables used by Jacobus in his program. These include the 3/C Brandrex cable, the 1/C Okonite cable, the 3/C Samuel Moore Dekoron Polyset cable, the 3/C Rockbestos Firewall III cable. The DLO modeling results at 100°C plus 30 Gy/h for the Brandrex CSPE/XLPO cable are shown in Figure 99. As usual the jacket determines the importance of DLO effects in the insulation. Since 60 mil worth of CSPE jacket thicknesses represent commonly observed CSPE cable configurations (e.g., a 60 mil jacket or a 15 mil individual jacket with a 45 mil overall jacket), this DLO simulation is a reasonable initial situation to examine. For this simulation, the average oxidation of the CSPE jacket and the XLPO insulation are ~64% and 37% of equilibrium values, respectively. Therefore, 2 years of CSPE aging represents ~0.64 (2 years) ~ 1.28 years of homogeneous oxidation. Using the DED model, the appropriate E_a of 91 kJ/mol for CSPE gives a shift factor of 93 between 100°C and 50°C. Therefore, 1.28 years of 100°C plus 30 Gy/h is equivalent from the DED modeling approach to ~119 years of 50°C plus 0.32 Gy/h. This result for the CSPE jacket should give some margin since the equivalent time is twice the desired 60 years and the total effective integrated dose of 30 Gy/h for 1.28 years is 3.4e5 Gy, approximately 30% greater than the 2.6e5 Gy that would occur at 0.5 Gy/h for 60 years. For the XLPO insulation with its low E_a (for Brandrex XLPO) of 72 kJ/mol, the shift factor of 37 implies that the 2 years of aging at 100°C plus 30 Gy/h corresponds to 2(0.37)(37) = 27 years of homogeneous oxidation at 50°C plus 0.81 Gy/h. In this case, the time is approximately half the desired 60 years and the total effective dose is 0.74 years at 30 Gy/h or 1.95e5 Gy, less than the desired 2.6e5 Gy. This combination of half the time with ~75% of the desired dose clearly does not represent margin in the simulation.

Earlier in this report we mentioned that higher β values are often found for aging in radiation dominated environments. When such values are appropriate, the drop in oxidation with a drop in the dissolved oxygen concentration [O_2] is less severe (Figure 25) which results in reduced DLO effects. We can show the impact of a higher value of β by repeating the modeling shown in Figure 99 except increasing the β value for the XLPO to 20 since the aging of this material is dominated by radiation effects at 100°C plus 30 Gy/h (Figure 75). The results shown in Figure 100 indicate that the XLPO has an average oxidation of ~75% of its equilibrium value. This would imply that the 2 year exposure would correspond to 0.75(2)(37) ~ 56 years at 50°C plus 0.81 Gy/h. Again this comparison shows that experimental measurements of β values for aging in radiation environments would be useful for estimating the margin involved in accelerated simulations.

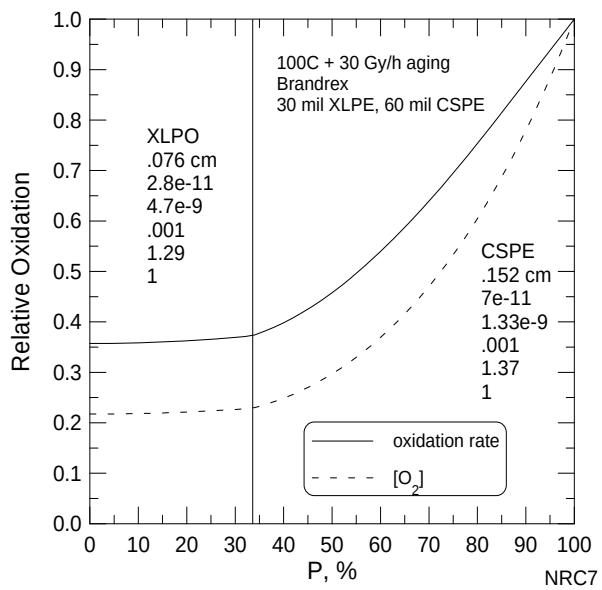

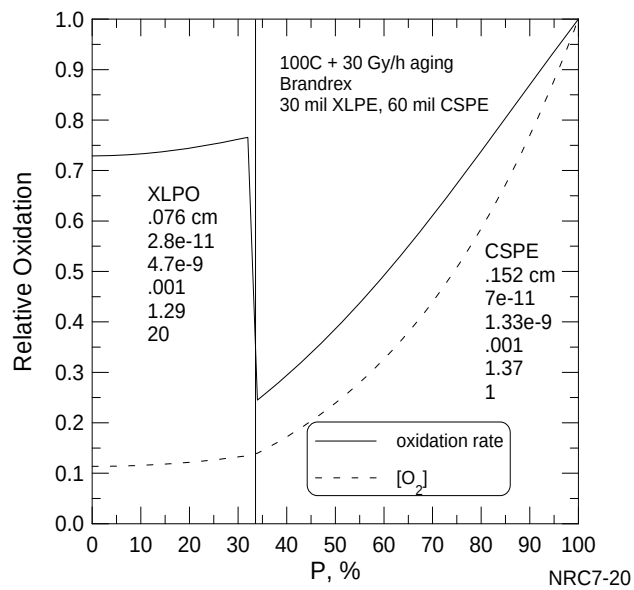

Figure 99 (Left). Estimated profiles for oxygen concentration and oxidation rate across the 3/C Brandrex cable under the indicated combined environment aging conditions using β = 1 for the XLPO insulation.

Figure 100 (Right). Estimated profiles for oxygen concentration and oxidation rate across the 3/C Brandrex cable under the indicated combined environment aging conditions using β = 20 for the XLPO insulation.

We next examine the Samuel Moore Dekoron Polyset XLPO/CSPE cable and the Rockbestos XLPO/CP cable both of which comprise a 30 mil insulation plus a 45 mil jacket. Since the jackets are thinner than the 60 mil jacket for the Brandrex cable, we expect reduced DLO effects. This is confirmed by the DLO modeling shown in Figure 101 and Figure 102, respectively. For the Dekoron Polyset (Figure 101), the average oxidation of the CSPE jacket and the XLPO insulation are ~73% and 51% of equilibrium values, respectively. Therefore 2 years of CSPE aging represents ~0.73 (2 years) ~ 1.46 years of homogeneous oxidation. Using the DED model, the appropriate E_a of 91 kJ/mol for CSPE gives a shift factor of 93 between 100°C and 50°C. Therefore, 1.46 years of 100°C plus 30 Gy/h is equivalent to ~136 years of 50°C plus 0.32 Gy/h. This result for the CSPE jacket should give some margin since the equivalent time is more than twice the desired 60 years and the total integrated effective dose of 30 Gy/h for 1.46 years is 3.84e5 Gy, approximately 50% greater than the 2.6e5 Gy that would occur at 0.5 Gy/h for 60 years. For the XLPO insulation with its low E_a (for Brandrex XLPO) of 72 kJ/mol, the shift factor of 37 implies that the 2 years of aging at 100°C plus 30 Gy/h corresponds to 2(0.51)(37) = 38 years of homogeneous oxidation at 50°C plus 0.81 Gy/h. In this case, the time is approximately 2/3 the desired 60 years although the total effective dose is 1.02 years at 30 Gy/h or 2.68e5 Gy is similar to the desired dose of 2.6e5 Gy. Since radiation dominates the degradation of XLPO at 50°C plus 0.5 Gy/h (Figure 75), this combination might represent a reasonable simulation.

DLO modeling of the Rockbestos cable (Figure 102) indicates that the average oxidation of the CP jacket and the XLPO insulation are ~75% and 58% of equilibrium values, respectively. Since the average E_a of the Rockbestos CP jacket from 50°C to 100°C is ~91 kJ/mol, similar

calculations to those done above indicate that the CP jacket is aged to the equivalent of 140 years at 50°C plus 0.32 Gy/h (more than twice the desired aging time and 50% greater than the desired aging dose). The XLPO conditions correspond to 43 years at 50°C plus 0.81 Gy/h (3/4 of the desired time and ~16% greater than the desired dose). For both of these latter two XLPO insulations, an increase in β will lead to increases similar to those found above for the Brandrex cable. It should also be noted that the actual E_a for the Rockbestos XLPO (98 kJ/mol) is higher than the Brandrex E_a (72 kJ/mol) used in the analyses. A higher E_a would increase the simulation time but without combined environment aging data for the Rockbestos XLPO to analyze using the DED modeling approach, we are forced to utilize the Brandrex results.

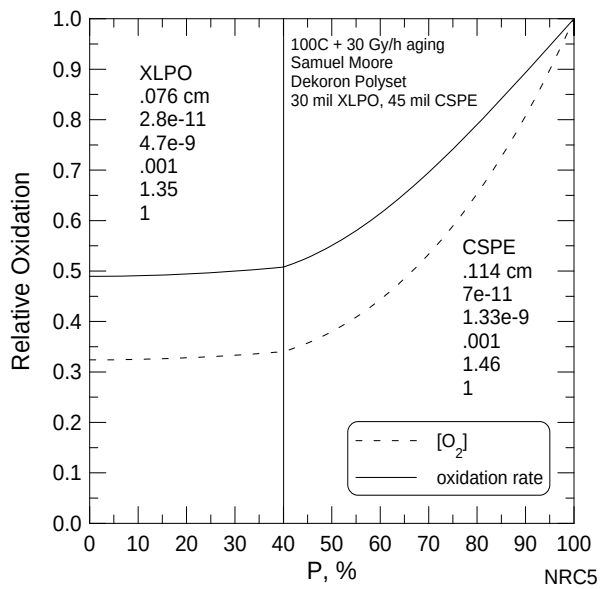

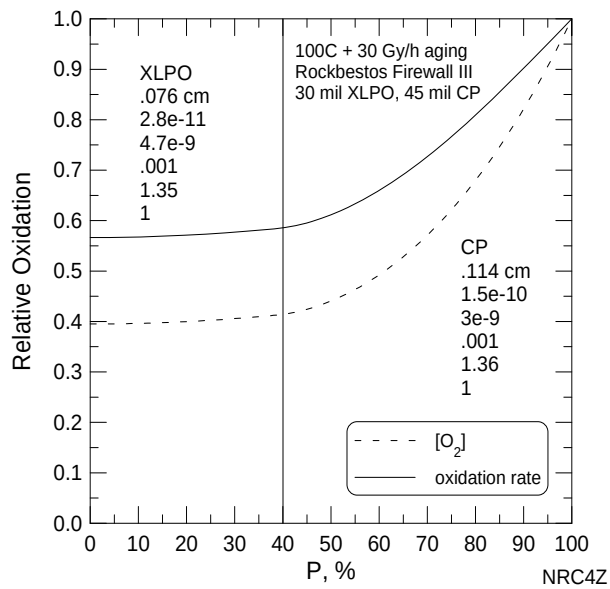

Figure 101 (Left). Estimated profiles for oxygen concentration and oxidation rate across the 3/C Samuel Moore Dekoron Polyset cable under the indicated combined environment aging conditions.

Figure 102 (Right). Estimated profiles for oxygen concentration and oxidation rate across the 3/C Rockbestos Firewall III cable under the indicated combined environment aging conditions.

Our final DLO modeling at 100°C plus 30 Gy/h is for the 1/C Okonite Okolon EPR/CSPE cable. Since this 1/C cable represents very thin materials (30 mil EPR, 15 mil CSPE), we would expect less important DLO effects and this is confirmed by the modeling shown in Figure 103. The average oxidation of the CSPE jacket and the EPR insulation are ~94% and 97% of equilibrium values, respectively. Since the shift factor for CSPE is 93, the CSPE would be aged to the equivalent of 0.97(2)(93) ~ 180 years at 50°C plus 0.32 Gy/h or three times the desired 60 years and twice the desired integrated dose. For the EPR insulation (E_a ~ 103 kJ/mol so a shift factor of 192 from 100°C to 50°C), aging would be equivalent to 0.94(2)(192) ~ 380 years at 50°C plus 0.16 Gy/h or 6 times the desired time and twice the desired integrated dose. Therefore, if one is forced to choose a single aging condition for all cables, the resulting conditions (heavily influenced by the material with lowest E_a) can lead to significant over-aging for materials with higher E_a values.

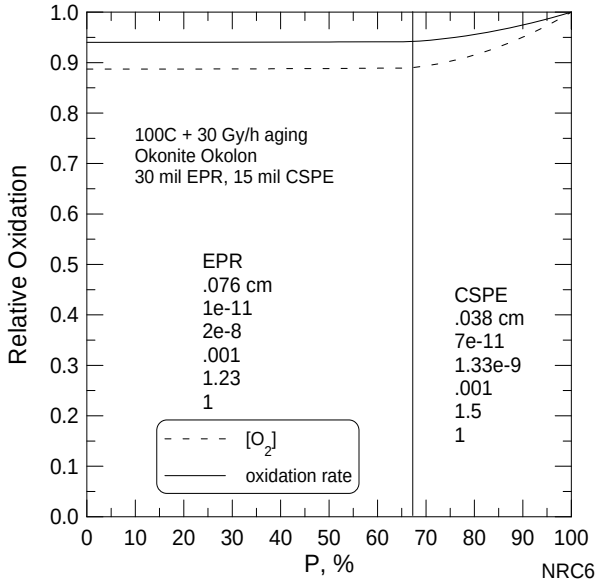

Figure 103. Estimated profiles for oxygen concentration and oxidation rate across the 1/C Okonite cable under the indicated combined environment aging conditions.

3.12 Inverse Temperature Effects

As described earlier for the Brandrex XLPO insulation material, inverse temperature effects are often observed in combined environment exposures at temperatures less than ~50°C (Figure 71). In such instances, the rate of mechanical degradation at a constant radiation dose rate will increase as the combined environment aging temperature is reduced. Inverse temperature effects have been noted for several XLPO and EPR/EPDM cable insulations but have not been noted for other XLPO and EPR/EPDM cable insulations. In particular, evidence for inverse temperature effects is documented for a Brandrex XLPO, a Rockbestos XLPO, an ITT Exane II XLPO and an Eaton Dekoron EPR [28,29,30]. On the other hand, no evidence for inverse temperature effects has been noted for a Dekoron Polyset XLPO [104], an Anaconda Flameguard FR/EP [104] or an Okonite EPR insulation [14]. When inverse temperature effects occur, it is impossible to analyze low temperature results using the DED approach as shown from the results for the Brandrex XLPO material shown in Figure 72. This implies that accelerated aging simulations of low temperature conditions (e.g, 40°C plus 0.5 Gy/h) cannot be done in the usual fashion using DED modeling.

Although we will introduce one possible approach in this section of the report, research on inverse temperature materials is clearly lacking and would be one of the most important areas to devote future research funds. Our suggested approach involves looking at the dose rate dependence at temperatures in the inverse temperature regime. In other words, if we were interested in ambient aging at 41°C and 0.5 Gy/h, we would want to generate combined environment data at 41°C versus dose rate and extrapolate these results to 0.5 Gy/h. For instance, we take the preliminary 41°C results for this material from Figure 71 and plot them on Figure 104. More experimental data is needed before we could confidently extrapolate these results to 0.5 Gy/h and other lower dose rates. However, for the sake of showing our suggested approach, we will assume a linear extrapolation denoted by the dashed curve. This linear extrapolation allows us to estimate the dose rate effect from any accelerated dose rate at 41°C to

any selected ambient dose rate at 41°C. For instance, suppose we select 30 Gy/h as our accelerated aging conditions. Under 30 Gy/h plus 41°C, Figure 104 shows that ~1.8e5 Gy are required for the elongation to reach 100%. If the desired ambient condition were 0.5 Gy/h, the figure gives ~1.2e5. Therefore, the dose rate effect is 1.8 divided by 1.2 or a factor of 1.5. This implies that if one were trying to simulate 60 years at 0.5 Gy/h plus 41°C (a total dose of 2.63e5 Gy) with accelerated conditions of 30 Gy/h plus 40°C, you would need to go to a dose of 1.5(2.63e5)~3.95e5 Gy which would require 1.5 years at the accelerated conditions. For simulating ambient dose rates of 0.25 Gy/h and 0.1 Gy/h, the results from Figure 104 give 1.0e5 Gy and 9e4 Gy, respectively to reach 100% elongation yielding dose rate multiplicative factors (relative to 30 Gy/h) of 1.8 and 2.0, respectively. With 60 year doses of 1.31e5 Gy and 5.26e4 Gy, respectively, the doses and time required for simulation at 30 Gy/h are 2.365 Gy (0.9 years) and 1.05e5 Gy (0.4 years), respectively.

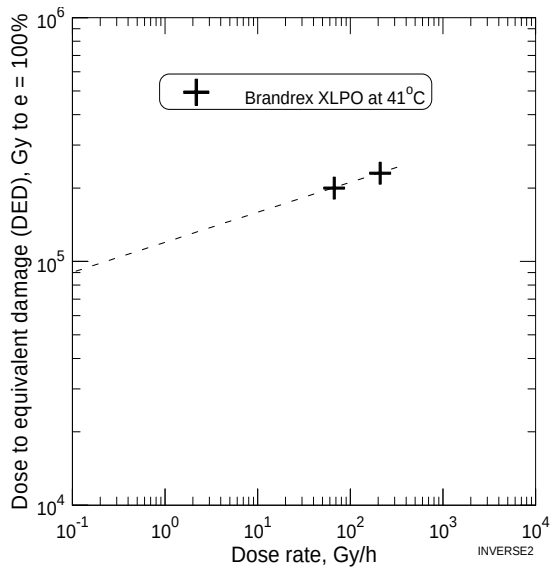

Figure 104. Combined environment results for Brandrex XLPO at 41°C.

The calculations above refer to the XLPO insulation. Meanwhile the same accelerated aging conditions occur for the CSPE jacket material. From Figure 65 using the top x-axis (40°C is close enough to 41°C for this example), we see that 0.1 Gy/h, 0.25 Gy/h, 0.5 Gy/h, and 30 Gy/h correspond to ~7e4 Gy, 1.4e5 Gy, 2e5 Gy and 7e5 Gy, implying dose rate effects factors of 10, 5 and 3.5 from 0.1, 0.25 and 0.5 Gy/h to 30 Gy/h, respectively. When these factors are multiplied times the three 60 year doses appropriate to 0.1 Gy/h (5.26e4 Gy), 0.25 Gy/h (1.31e5 Gy) and 0.5 Gy/h (2.63e5 Gy), we determine that 2 years, 2.5 years and 3.5 years, respectively of 30 Gy/h are required.

The above calculations do not account the possible presence of DLO effects occurring at 30 Gy/h plus 41°C. For the Brandrex XLPO material, Figure 73 indicates a 41°C $\phi[O_2]_{ref}$ value of 1.1e-9 mol/g/Gy which gives at 30 Gy/h, $\phi[O_2]_{ref}$ = 9.2e-12 mol/g/s. The $\phi[O_2]_{ref}$ value for CSPE is ~ 9e-12 mol/g/s from Figure 68. Permeability coefficient estimates are 8e-10 ccSTP/cm/s/cmHg for XLPO (from Figure 82) and 2.4e-10 ccSTP/cm/s/cmHg for CSPE (from Figure 80). With these estimates, we are able to model the oxidation profiles in the usual fashion with the results shown in Figure 105. DLO effects enter with the oxidation percentages averaging ~38% for the XLPO insulation and ~65% for the CSPE jacket. This means that the times required for the

60 year simulations are longer by a factor of 1/0.38 ~ 2.6 for the XLPO insulation and a factor of 1/0.65 ~ 1.54 for the CSPE jacket. Thus instead of 1.5 years, 0.9 years and 0.4 years at 30 Gy/h to simulate 0.5 Gy/h, 0.25 Gy/h and 0.1 Gy/h of XLPO aging, the times are ~4 years, 2.4 years and 1.05 years, respectively. Instead of 3.5 years, 2.5 years and 2 years at 30 Gy/h to simulate 0.5 Gy/h, 0.25 Gy/h and 0.1 Gy/h of CSPE aging, the times are 5.4 years, 3.8 years and 3.1 years. Thus, if aging is done at 30 Gy/h and 41°C for 2.4 years, this reasonably simulates 0.25 Gy/h plus 41°C for the insulation but only simulates ~60(2.4/3.8) ~ 38 years of the jacket. In earlier accelerated aging simulations more severe aging usually occurred in the jackets compared to the insulation since the jackets tended to degrade faster in most environments. In the present example, the inverse temperature effects lead to a reversal where reasonable simulation of the aging of the insulation leads to jacket aging that is less than needed for simulation.

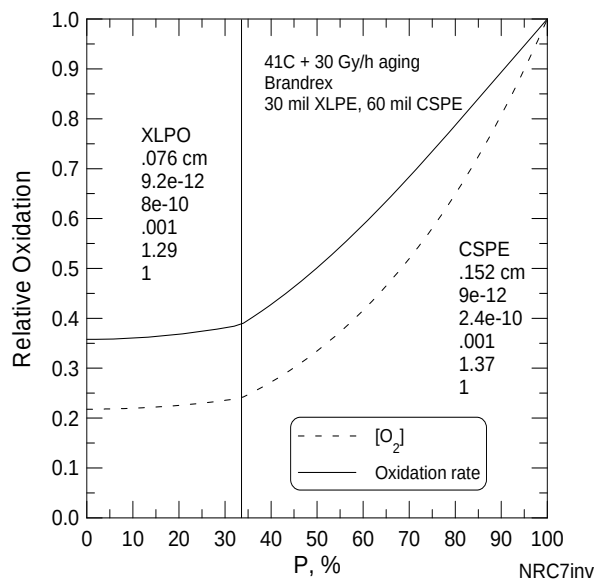

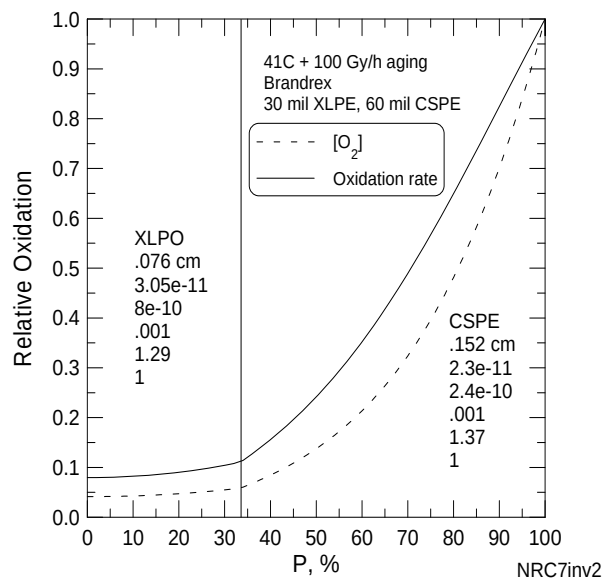

Figure 105 (Left). Estimated profiles for oxygen concentration and oxidation rate across the 3/C Brandrex cable under combined environment aging conditions of 41°C plus 30 Gy/h.

Figure 106 (Right). Estimated profiles for oxygen concentration and oxidation rate across the 3/C Brandrex cable under combined environment aging conditions of 41°C plus 100 Gy/h.

If higher β values were appropriate for the Brandrex XLPO, the DLO effects would be reduced and the times necessary for simulation would also be reduced. In addition, full finite element modeling of the actual geometry would also lead to reduced DLO effects and a further reduction in time. This again underscores the need for more work deriving actual β values and an effort to improve the parallel sheet modeling by developing finite element codes appropriate to the real cross-sectional geometry of the cables.

A reaction to the above example would be to suggest that higher dose rates at 41°C could be used to reduce the aging times required for simulation. Unfortunately this does not occur because an increase in dose rate increases the values for $\phi[O_2]_{ref}$ without changing the P_{Ox} values, leading to more important DLO effects (Figure 106). The increases in the importance of DLO effects more than compensates for the reductions in time caused by using higher dose rates. For example, if we increase the accelerated dose rate from 30 to 100 Gy/h (an increase by a factor of

3.33, the percentage oxidation in the XLPO drops from 38% to ~9% (Figure 106), a reduction by a factor of 4.2.

3.13 Conclusions of Margin Assessments

Some of the major conclusions of this analysis are:

(1). When oxygen is present during the aging of important materials used in nuclear power plant safety-related electrical cables, oxidation reactions normally dominate the degradation chemistry.

(2). Diffusion-limited oxidation (DLO) effects are very significant at the high dose rates and high temperatures historically used in cable qualification schemes based on IEEE Std. 323-1974 and IEEE Std. 383-1974 [67,78]. In particular, under the radiation aging conditions normally used (~3000 to 7000 Gy/h), DLO effects totally eliminate oxidation in most insulation materials.

(3). Since DLO effects are typically absent under normal ambient NPP aging conditions, implying that oxidation chemistry dominates the degradation of cable materials, historic simulations based on IEEE Std. 323-1974 and IEEE Std. 383-1974 [67,78] usually did not probe the chemistry of relevance to the ambient aging occurring in the insulation materials. For the jacketing materials, the simulations led to greatly reduced oxidation levels except at the air-exposed jacket surface.

(4). The preferred accelerated model for simulating ambient aging involves the DED approach. However, this approach is not applicable to insulation materials experiencing "inverse-temperature" effects. For such materials, an approach based on dose-rate extrapolations at a constant aging temperature is proposed.

(5). To achieve more realistic aging simulations, much longer aging times must be applied. Even using 2 years for the simulations can be marginal for certain cables.

(6). Better estimates of the proper simulation aging conditions would be available if more measurements were made addressing 1) thermal activation energies at low temperatures using oxygen consumption approaches, 2) oxygen consumption values versus dose rate in radiation environments, 3) experimental β values, especially in radiation environments again using oxygen consumption approaches and 4) the importance of inverse-temperature effects.

(7). Other possible studies that could prove useful include 1) permeability coefficient studies on actual cable materials from RT up to 100°C and 2) 2-D finite element modeling of actual cable cross-sections.

INTENTIONALLY LEFT BLANK

4 Recommendations for New Research Activities

4.1 Approach towards Additional Aging Studies

We recommend an additional research effort on the aging behavior of cable insulation and jacketing materials used in nuclear power plant applications with the emphasis on lifetime prediction and margin assessments of installed infrastructure. The study should focus on yielding the required material parameters that are relevant for describing the aging behavior and assist the development of suitable aging models for a range of polymers under low temperature, low dose rate degradation environments. The key goal should be a better understanding of aging processes that would allow the development of predictive aging models for better margin assessments. It should also enable informed decisions on short-term meaningful accelerated aging tests for the preparation of suitably 'pre-aged specimens' for LOCA performance qualification.

All cable and jacketing materials are subject to degradation in oxidative thermal radiation environments. Additional work is necessary since most of the existing studies have deficiencies in one or more important areas such as 1) assuming Arrhenius behavior when it often does not hold, 2) aging under conditions where important DLO effects exist and 3) not considering the potential influence of inverse temperature effects.

Margin assessments and re-qualification of cables that rely on studies that clearly tested or qualified cable assemblies under significant DLO conditions should be approached with caution. Further research and testing is needed to enhance our ability to perform margin assessments specifically for cables that were re-qualified utilizing studies that tested or qualified cable assemblies under DLO conditions. Accelerated high temperature, high dose rate conditions, as used in the IEEE Std. 323-1974 and similar previous test methodologies [72,74], will provide some indications for the 'inert' radiation sensitivity and longevity of a material under such conditions, but cannot be considered for guidance in situations where the actual aging environment is known to be different, i.e. predominant oxidative conditions. Our knowledge of polymer aging has evolved throughout the decades after which the original qualifications were conducted. Making any predictions of the current actual state of materials (i.e. fractional aging state or % lifetime remaining and related margin evaluations) based on original qualification testing, or similarly accelerated aging studies, would be challenging; it would disregard existing knowledge about the shortcomings in such studies and would offer no more than unsubstantiated interpretation.

Future work may not find significant levels of performance limits or shortcomings in now more than 40-year-old cables, and it could well be that sufficient margins exist for continued operations of existing cable assemblies. However, such guidance must originate from aging models and accelerated testing approaches that a) rely on a deeper understanding of the material behavior and b) use models that simulate the environment that a cable will experience in the plant. The science of polymer aging and lifetime prediction has developed to the point that it has been shown repeatedly that basic Arrhenius-based extrapolations using a few highly accelerated data points are misleading not just because of potential Arrhenius curvature, changes in activation energy, or any material transitions throughout the extrapolation range. The tenet of appropriate accelerated aging tests and their extrapolations dictates that the accelerated tests must

mimic the expected degradation pathways for which extrapolations are to be made. As shown in Section 3 of this report, based on DLO assessments using known or best estimates of the oxidation describing parameters (oxidation rate for radio-thermal conditions, oxygen permeability, β-factor, dose rate dependencies and cable geometries), we have demonstrated that IEEE Std. 323-1974 and similar studies [72,74] do not succeed in this respect.

It is important to establish the nature of the predominant aging mechanism, namely radio-thermal-oxidative degradation encountered in the cable materials of interest. The oxidation rate kinetics as a function of dose rate, temperature, and physical material properties (permeation, β-factor dependency) must be evaluated and the data used to establish the basis for predictive extrapolations using the Arrhenius approach for temperature-dominated environments and the DED approach for combined radiation plus thermal environments [22-25]. Also included will be modeling of the oxidation chemistry and the physical distribution of oxidative damage in the material cross-sections (DLO modeling). The physical processes of oxygen permeation and its translation into actual oxidation rates as a function of radial position in a circular cable material will need to be established. Models based on existing 1D linear sheet codes will have to be geometrically modified, as we expect that circular geometries and more complicated cable assemblies combining multiple conductors and jacketing materials will result in more confident predictive capabilities. Finite element models will therefore need to be developed and will require significant updates of the existing DLO models used for linear geometries.

The combination of the underlying chemical and physical processes as a function of temperature, dose rate, and total dose should be used to understand the material's aging behavior and develop suitable accelerated aging methodologies that yield anticipated performance data. This will be critical for the generation of better 'pre-aged' LOCA specimens. Predictions from accelerated testing should be compared with wear-out observations and aging state assessments of material samples collected from actual field applications. The ultimate goal is a workable model that relies on meaningful predictive aging tests and yields a perspective on current aging state and guidance for performance predictions as part of existing margin assessments. Understanding the underlying radio-thermal-oxidative degradation framework coupled with suitable accelerated aging tests to prepare appropriate or at least well-understood LOCA test specimens, and predictive aging models for low dose rate, low temperature environments would be an enabling capability of tremendous value to provide reasonable assurance for the continued safe operation of nuclear power plants. Science-based models that could predict the remaining margins of existing cable assemblies currently do not exist, yet they are crucial to address the issues emphasized throughout this report.

While our suggestions for future work may appear biased towards a scientific approach, it is important to recognize that phenomenological based aging studies focusing on macroscopic property changes as a function of applied stress environments (here exposure to varying radiation dose rates, total doses and temperature) may certainly deliver aging information and degradation behavior for whatever test matrix may have been selected. However, solid predictive capabilities, a validation of extrapolation regimes towards plant conditions, and the additional goal of a development of suitable accelerated aging protocols for LOCA material preparation/testing needs as the outcome of any study, must have a more solid foundation. We have demonstrated in many polymer aging studies and fundamental R&D activities that it is necessary to understand how a material behaves and establish what the key degradation reactions

and their relative magnitudes are, in order to develop representative aging models and more relevant aging tests. We believe our approach towards additional work should deliver on those goals. Despite numerous engineering-based studies in this field dealing with cable performance, and approximately 40 years after original IEEE Std. 323-1974 based qualification testing, such tests have failed to provide the in-depth scientific framework for the assessment of remaining operating margins. Therefore, further research in this area is needed. Based on the research and developments in polymer aging, the shortcomings of previous accelerated aging approaches are apparent and better predictive aging tests must be implemented to solidify the knowledge gained in this area and to offer appropriate avenues for margin predictions.

4.2 Targets for Aging Model Development and Expected Impact

Future aging efforts should be focused on clear targets that will allow for the underlying material behavior to be established and these properties to be incorporated into predictive models. It should also enable a perspective on how best to prepare 'pre-aged' LOCA samples.

- Acquire historic operational exposure conditions (dose rate, dose and temperature) and obtain guidance from operators for expected future environmental conditions.

- Develop an understanding of the radio-thermal-oxidative degradation pathways of a range of cable insulation and jacketing materials to better predict degradation processes at low temperature and dose rate conditions representative of actual plant conditions.

- Use oxygen consumption techniques to measure oxidation rates, β-factor properties, and their dose rate dependencies at low to mid-range temperature regimes (RT-90°C). Compare the degradation levels of the materials with those encountered under inert conditions. Focus on evidence of inverse temperature behavior for some materials.

- Develop new analytical approaches to obtain oxygen permeation data from measurements on cylindrical insulation samples over a wide temperature range, and use cylindrical FE models to extract the underlying O_2 permeability constant from such measurements.

- Develop primary oxidation models as a function of deposited dose, time and temperature using oxidation rates, β-factor and permeation data for cylindrical geometries and complex cable assemblies. Establish the relevant DLO situations for the conditions of interest. Incorporate such models into predictive codes. This involves developing sophisticated FE Matlab codes for position-dependent oxidation behavior.

- Develop more sophisticated dose to equivalent damage (DED) models that will utilize the proposed new measurements of effective oxidation rates and DED data trends as available from a range of combined thermal radiation environments, particularly at low dose rate conditions, where the transition regime between thermal and radiation dominant conditions is most pronounced. Develop DED models that enable predictions based on multi-parameter best fits or numerical optimization sub-routines that can be applied to comprehensive but often incomplete data sets. These models should yield margins and variance as a function of input uncertainty. They should enable simulations by accommodating deviations from linear Arrhenius behavior or constant DED failure level

assumptions, plus simulate dose rate effects and changes in oxidation levels for equal damage as a function of temperature, thereby introducing so far poorly described but known aging anomalies into predictive codes.

- Confirm correlation in various combined radiation plus temperature environments between mechanical property results and oxygen consumption results at intermediate acceleration conditions so that confident extrapolations can be done using consumption results at lower environmental conditions where mechanical results are not accessible.

- Establish avenues towards linking the underlying oxidative degradation chemistry with the electrical performance of 'pre-aged' specimens in LOCA environments. How much oxidative damage is required for LOCA failure to occur? Compare such trends with material damage produced under inert conditions and explore fundamental difference of aging state and its correlation with LOCA performance.

- Use this knowledge to develop accelerated aging protocols with predictive capabilities for materials performance over extended operation and re-qualification time periods. Explore how remaining margins could be calculated.

- Conduct the work within the overarching goal of understanding the materials degradation process as it affects LOCA performance and provide recommendations on expected lifetimes.

- Explore 'wear-out' aging studies on samples retrieved from service and incorporate the results into margin predictions.

To support the above goals, more suitable characterization methods applicable to these materials will need to be developed. Existing capabilities will need to be optimized to generate specific data sets:

(1). **The measurement of oxygen permeation in the material.** Measuring true oxygen permeation rates through polymers and its defined impact on degradation processes is a needed first step. Permeation rates will need to be determined for a number of materials and as a function of temperature [94,95,105]. This will be complicated by the non-availability of sheet material specimens for the insulation of interest. Permeation rates would need to be obtained from circular specimens stripped from the conductor core. While flux measurements are certainly feasible for small samples using new sensitive detectors, the underlying permeation constant will have to be determined via modeling of cylindrical geometry.

(2). **Oxidation sensitivity:** Since oxidation is the most important factor for the degradation of these materials, we must obtain oxidation rates for a large set of dose rates and temperatures. They should be complimented by data on the beta-factor, the translation between oxygen concentration in the materials and its corresponding rate. Oxidation rates can be measured using sensitive oxygen uptake methods [8,11,15,21,50,108]. Previous work at SNL has demonstrated the dependence of oxidation chemistry on temperature as the basis for validating extrapolation models for many materials

(3). **The analysis of polymer network changes.** An excellent signature of degradation in bulk cross-linked polymers is their swelling behavior and extractable material yields as a function of degradation levels. Using organic solvents, penetration, uptake and quantification of soluble materials provides guidance on overall chemical changes in the material [53,54,109]. Such measurements are easily conducted and good indicators of mechanical changes as polymer network properties directly govern mechanical features. Probing network changes has the added advantage of being more closely related to degradation chemistry and knowing their temperature dependence aids in extrapolations as it delivers guidance on how scission and crosslinking reactions may evolve with temperature.

(4). **The analysis of physical property changes, such as modulus, density, volume change, changes in T_g or LOCA performance as dependent on aging state.** Without establishing a correlation between degradation chemistry and mechanical properties or similar engineering-based properties (DED values), any aging model based on degradation rates will fail to predict useful properties. Micro-modulus profiling has been used extensively to probe mechanical degradation in polymers and allow for correlations with the underlying chemical degradation processes [45,49,93,110,111]. Changes in modulus, T_g, and density are routine analyses that have been used extensively for condition monitoring of polymers in critical applications [10,14,33,34]. Correlations between chemically-driven property changes and mechanical features can be easily obtained. This will aid in the definition of failure levels and can set the basis for the description of the important macroscopic properties changes.

(5). **Moisture diffusion and water solubility.** The penetration and solubility of moisture or similar reagents into polymers can be measured. This can be achieved either with dynamic vapor sorption experiments or basic solubility studies and weight changes. Moisture permeation rate measurements can be equally attractive [112]. However, measurements under saturated steam environments at elevated temperatures will be difficult and likely require some extrapolations.

4.3 Discussion of Required Future Work

The suggestions above call for fundamental work and the development of a more suitable framework for the insulation and jacketing materials' degradative behavior as required for predictive aging purposes. The ultimate deliverables are seen as the most appropriate short-term exposure regime for follow-up LOCA testing, thereby allowing a predictive capability for materials performance under plant environment-driven degradation and operational margins. This target is demanding, requires in-depth knowledge of behavior for a number of materials, and, as we believe, cannot be met by simply screening a few accelerated aging exposure conditions. This has been attempted and conducted within numerous other studies. On the contrary, a good approach towards a predictive aging protocol lies in the understanding of the material's aging sensitivities, its behavior under accelerated exposure (here oxidative conditions, dose rate, total dose and temperature), the nature of degradation mechanisms as a function of temperature (includes activation energies), recognition of competing processes, for example non-homogeneous DLO situations and their individual dominance for influencing lifetime predictions towards use conditions. After extensive studies, such knowledge may provide the basis to

develop accelerated aging frameworks that could provide additional guidance on lifetimes for the intended applications and remaining margins. Better aging protocols for LOCA testing should also be developed.

An important aspect of the research at SNL in materials aging and reliability over the last 20 years has been directed towards developing a better understanding of the variations occurring in degradation processes and polymer aging with temperature. We have shown that extrapolations from limited short-term aging experiments are often futile. For various reasons, the most important being changes in the degradation mechanism and the dominant process, predictions from quick screening tests often do not yield the intended results. For example, a one week test to predict a 20-year lifetime equates to an acceleration factor of ~1000 times. A one-month to 20-year-extrapolation requires an acceleration of ~250 times. With ten degrees of a temperature increase normally accelerating degradation processes by about 2.5 times, based on thermally driven processes alone, a large temperature range must be bridged between test and extrapolation.

For aging processes in combined environments, diffusion of the reagent (i.e. oxygen) and radio-thermo-oxidative driven chemistry greatly depend on temperature, with the individual activation energies of the underlying reactions varying significantly. As a consequence, the dominant processes change with temperature and introduce non-predictability into limited aging studies. We have witnessed significant Arrhenius curvature in the aging data of polymers under complex environments, defeating the long held believe of the usefulness of a few aging data points as a basis for linear extrapolations. Worse yet is the observation that non-Arrhenius behavior usually indicates a drop in activation energy as the temperature is reduced, implying that high temperature extrapolations using the high temperature activation energy will overestimate material lifetimes at low temperatures. Further complications are encountered when trying to couple primary degradation chemistry with stress-strain behavior and similar mechanical performance criteria. Good predictions and aging models have one key requirement: an understanding of the material and the aging processes which are relevant for the intended environment.

For the degradation and performance of cable and jacketing materials in NPP environments discussed here, developing the scientific foundation towards a lifetime prediction and margin assessment approach must incorporate an understanding of the relevant degradation chemistry and physical processes at play. The significance of the following processes should be examined:

- Thermal-only degradation under inert (no oxygen) conditions versus temperature.
- Thermo-oxidative degradation in the absence of radiation versus temperature.
- Thermo-oxidative degradation coupled with radiation for a range of dose rates and temperatures.
- The development of the macroscopic damage levels as a function of material depth.
- A correlation of chemical damage with mechanical properties.

- A clear definition of an engineering-based LOCA performance criterion and state of material at the perceived end of life or knowledge of fractional damage levels.

In summary, we infer that another round of quick accelerated aging studies involving the screening of mechanical property changes or LOCA performance, and perhaps coupled with a limited research budget, cannot deliver on the targets. We believe that such studies have been conducted in the past and have not provided the desired outcome. In addition, condition monitoring studies need to accommodate such issues as DLO and inverse temperature phenomena to answer how oxidatively aged materials may behave under LOCA conditions.

INTENTIONALLY LEFT BLANK

5 Conclusions

The major previous studies and reports related to the performance of polymeric cable and insulation materials under radiation-thermal-oxidative conditions, as encountered during their application in nuclear power plants, have been reviewed. The main goal was to examine the degree to which long-term degradation under these environmental conditions is a concern and whether such evolving oxidative material aging is sufficiently covered within the original cable qualification testing for LOCA (loss of coolant accident) performance. A comparison of the original LOCA qualification approach from the 1970's (i.e. IEEE Std. 323-1974) with the anticipated aging behavior during operation was intended to offer a perspective on any remaining operational margins for lifetime extension purposes. Further, as part of this review, it was important to examine the availability of literature data that describe the oxidative degradation behavior, such as oxidation rate under radiation-thermal conditions, oxygen permeability, and other degradation parameters. Available data were extrapolated where possible to obtain rough estimates for oxidative degradation levels and heterogeneity aspects for the material degradation under low dose rate thermal conditions and compared with the scenario for original LOCA qualification.

There is sufficient evidence in the literature to emphasize that all cable insulation and jacketing materials will experience oxidative degradation under atmospheric radiation-thermal conditions. Less clear is how the accumulation of oxidative damage relates to the loss of useful properties and in particular LOCA performance. For example, for some materials, good correlations exist between a reduction in mechanical properties (i.e. tensile elongation) and oxidation levels (chemical damage) calculated from measured oxidation rates under specific conditions. For other materials, those that more strongly display the induction time behavior, mechanical and other properties may initially be maintained despite oxidation progressing, but after these delay times, failure may then occur more suddenly. (Note however, that in such instances, the failure times at differing aging temperatures or under differing combined radiation plus temperature environments may still be associated with a constant amount of oxidation offering the possibility of predictive capabilities if the oxidation rate is constant versus time or followed versus time.) While the literature offers a good framework on the general nature of how these materials will degrade, the situation is more complex and less established for our understanding of LOCA performance as it pertains to a very specific application and performance expectation.

Some expected oxidative aging levels of cable and insulation materials have been estimated for 40-60 years of plant use using best available data and extrapolations for oxidation rate, permeability, rate dependencies and dose rate effects. Unfortunately, it is not possible to currently relate such predicted "polymer damage levels" to actual LOCA performance. Significant polymer oxidation is expected, but LOCA performance of such aged materials will need to be established. The LOCA performance behavior of nuclear power plant aged materials is difficult to predict for two reasons: Original qualification testing involved aged materials that were so quickly prepared at high dose rate and high temperature conditions that oxidation could only progress at the material surface due to diffusion limited oxidation (DLO) conditions. Subsequent model studies by the research community extended the exposure time for specimen preparation by using lower dose rates and temperatures, but as this review has shown, many materials were still heterogeneously oxidized and their LOCA behavior cannot be correlated with the expected homogenous degradation that will develop under plant conditions. A useful

material degradation framework allowing the prediction of LOCA performance for decades-old NPP aged materials does not exist and further, neither can accurate predictions be made based on the limited availability of specific oxidative aging literature data. Even if it were possible to establish fractional damage levels in terms of oxidation and mechanical property loss for long-term aged materials, for the above reasons, meaningful LOCA predictions could not be provided. Hence, any remaining performance margins as the primary goal of this study cannot be established. Instead, well planned aging studies are required to better understand the situation of materials degradation and its impact on LOCA performance during long-term plant operation.

Suitable avenues for translating the cumulative oxidative material damage to LOCA performance do not exist. LOCA performance is complex and will depend on the nature of polymer constituents and cable assemblies, micro cracks as well as moisture permeation and stress cracking behavior under high temperatures. Thus, LOCA performance cannot be predicted for a specific oxidation level or by knowing previous aging time and dose exposure of test specimens. The best guidance that polymer aging science can offer is to emphasize that the majority of previous LOCA testing did not involve the type of polymer degradation and its spatial distribution throughout the material that is encountered during plant aging. Previous LOCA testing therefore does not simulate the current aging state for many cable materials after decades of use. Previous LOCA testing used "pre-aged" cables that were not sufficiently homogeneously aged, with polymer damage often limited to the surface region of the cable jacket with little or no oxidation occurring in the cable insulation.

The situation is further complicated by the non-availability of accurate polymer aging parameters, such as oxidation rate, oxygen permeability, and similar data for low dose rate, low temperature plant environmental conditions. There may be situations where jacketing materials could provide long-term oxidative protection of cable insulation, but accurate predictions can only be made when additional polymer aging specific data under the expected conditions become available. Additional complexity is introduced by the fact that from an engineering perspective, cable and jacketing materials may appear to be quite similar as simple flexible polymers, but from a polymer science point of view, the materials employed cover a large range of material types and chemical constituents. Oxidative degradation and radiation sensitivity is greatly dependent on the polymer and material makeup, including stabilizers and additives, and processing variations.

Cable insulation and jacketing materials are based on a broad range of polymers. This implies significant performance variations in aging behavior, such that some materials could perform reasonably well, while others may be more susceptible to significant degradation processes and oxidation sensitivity. This may also be evident as variations involving a dependence on temperature. Elastomeric materials (i.e. some EPDMs and EPRs, Neoprene, Hypalon or similar materials) will age differently in comparison with semi-crystalline polymers (XLPOs, XLPEs, and some EPDMs and EPRs with partial cytsallinity), where inverse temperature behavior can be a complicating issue. For these latter materials, dose rate studies at high temperatures did not produce evidence for anomalous behavior. However, more comprehensive extended aging studies under low dose rate, low temperature conditions have shown that such materials unexpectedly displayed significantly shorter lifetimes than anticipated from the higher temperature results. None of the other reports (Brookhaven and Japanese) have dealt with these important issues, despite the first evidence for inverse temperature effects having been reported

in the mid 1990s and the fact that these issues are highlighted in IAEA TECDOC-1188, 2000 [76], IEC 1244-2, 1996 [77] and Brookhaven documents NUREG/CR-6384 BNL-NUREG-52480 Vol 1, 1996.,p. 4-87 [71]. Such effects have major implications for lifetime prediction and currently prevent any margins from being established for such materials. This type of aging behavior was not considered by the original qualification testing.

We also conclude that comparative engineering testing of materials within a single testing standard will not easily resolve the variations encountered in the degradation of these polymers. The highly variable aging behavior of the range of materials employed implies that simple, standardized aging tests cannot deliver the required aging data and performance predictions. In fact, the past reliance on reasonably fast and mostly high dose rate, high temperature tests may have inadvertently prevented the recognition of significant differences for other aging regimes. More intricate material-specific degradation parameters are required to better predict aging state and establish correlations with LOCA performance.

This review has demonstrated significant shortcomings in our collective knowledge on the aging behavior and anticipated LOCA performance of these materials. We expect that oxidatively driven material degradation will occur over 40-60 years of plant use. Resolving the magnitude of these processes and allowing for the development of predictive aging models will require careful new aging studies with a focus on plant equivalent low dose rate, low temperature oxidative conditions emphasizing updated modeling of combined environment aging and the importance of DLO effects. This implies the development of new 2-dimensional FE based models for DLO situations in complex cable assemblies and sophisticated dose to equivalent damage (DED) models that will utilize experimentally available effective oxidation rate measurements and DED data trends from combined radiation thermal environments. Such models could enable predictions based on multi-parameter fits to comprehensive data sets and should accommodate deviations from linear Arrhenius behavior or constant DED failure level assumptions, plus simulate dose rate effects and changes in oxidation levels for equal mechanical property damage as a function of temperature. Systematic aging studies and fundamental work on oxidative material degradation should be supported by an assessment of the 'aging state' of existing plant materials. We recommend to acquire naturally-aged material specimens from NPPs and conduct wear-out aging of field-aged specimens or condition evaluations to possibly obtain fractional damage data and thereby information on remaining aging margins. Future LOCA test experiments should be conducted using well-characterized, oxidatively aged materials with an aging history that would mimic plant environments or samples generated with an aging state slightly above current expectations, i.e. for lifetime extension. This would allow pass or fail criteria to be established as a function of a defined oxidative aging-state. A better understanding of long-term oxidative degradation processes could then allow for predictions on relative LOCA performance and remaining margins. An underlying need of all such approaches is a clear definition of past and future environmental plant conditions, such as exposure dose rate, total dose and temperature.

As a key conclusion of the literature review, the existing aging and LOCA performance data are insufficient to precisely determine the remaining operational margins for these materials. Therefore, further research which should focus on LOCA performance under non-DLO conditions is needed to enhance our ability to perform margin assessments and precisely determine any remaining operational margins. This does not imply that the existing 40-year-old

materials would necessarily fail if LOCA conditions occurred, but rather that statements with reasonable certainty cannot be made about the current conditions and anticipated LOCA performance. Further, the fact that important data for the prediction of current oxidative aging state, LOCA behavior and lifetime extension do not exist implies major challenges for any re-qualification or extended operation of these materials. It is recommended to conduct and model extensive studies of the material aging parameters under low dose rates at temperatures equivalent to actual plant aging conditions in order to prepare appropriately aged specimens that would mimic 40- to 60- year-old materials for LOCA performance confirmation testing. Unless we move beyond the perception that it is sufficient to expose materials to rapid high radiation levels with subsequent LOCA testing and acquiring pass or fail data, we will not be in a position to judge the remaining margins of existing infrastructure with regard to LOCA performance. We need to better understand how cable and insulation materials have degraded over decades of service in power plants and how this aging history relates to remaining margins, service life prediction and the performance of existing equipment to withstand a LOCA situation.

6 Background of our SNL R&D Team

Sandia is a multi-program national laboratory, where our Organic Materials and Characterization Department and Polymer Group are involved in materials development and optimization for demanding defense related applications. We do not manufacture materials in house but rather focus on the underlying scientific issues of materials performance in a supporting role for various internal customers, and often in collaboration with external groups within the DOE complex or suitable industrial partners as Work for Others (WFO). We normally engage in large multi-year research activities that provide opportunities for in-depth research and development tasks with impact and deliverables of interest to the broader materials performance community.

Our research group at Sandia National Labs is uniquely positioned to engage in the performance evaluation and degradation of insulation and jacketing materials with the goal of better understanding their specific aging behaviors and developing accelerated aging protocols for LOCA sample preparation and testing. We offer a research team with a long history and in-depth expertise in the areas regarded critical to the scientific development needs of this project. Our past work on thermal and radiation aging of elastomers in various applications (seals, O-rings, and cable insulation materials for power plant applications), fundamental work on oxidative degradation of polymers and their DLO situations, development of optimized accelerated aging methods and models, development of unique analytical methods for studying degradation and assessments of lifetime prediction methodologies has resulted in major contributions to the field of polymer degradation and performance evaluation. We achieved significant recognition for our collective work by focusing on the underlying reasons why short accelerated aging tests are often futile for predictive purposes, unless the materials are well-characterized and aging anomalies and complicated temperature dependencies are well understood. We introduced rigorous superposition principles for polymer aging and published many examples where aging data may be suitable for performance predictions using Arrhenius relationships, but also where they may be overly optimistic and in fact misleading. Our work is competitive with the best academic groups dealing with materials degradation and we routinely publish and disseminate trends at conferences and scientific meeting, often as invited speakers or keynote addresses. We have engaged with industry representing research institutes like EPRI in the past, assisted ASTM sub groups or working groups on materials performance in radiation environments, or worked with corporate industry on the broader issues of materials performance and reliability science in demanding applications. Two of our scientists have served the polymer degradation community as North American Editors of the International Journal titled “Polymer Degradation and Stability”.

INTENTIONALLY LEFT BLANK

7 References

[1] Chapiro A. Radiation Chemistry of Polymeric Systems: Interscience Publishers, 1962.

[2] Makhlis FA. Radiation Physics and Chemistry of Polymers: Keter Publishing House Jerusalem Ltd., 1975.

[3] Dole M, ed. The Radiation Chemistry of Macromolecules I: Academic Press, 1972.

[4] Dole M, ed. The Radiation Chemistry of Macromolecules II: Academic Press, 1973.

[5] Clegg DW, Collyer AA, eds. Irradiation Effects on Polymers. New York: Elsevier Science Publishing Co., 1991.

[6] Clough RL, Shalaby SW, eds. Radiation Effects on Polymers. Washington, D. C.: ACS Publications #475, 1991.

[7] Gillen KT, Clough RL, Ganouna-Cohen G, Chenion J, Delmas G. The importance of oxygen in LOCA simulation tests. *Nucl Eng Des* 1983;**74**:271.

[8] Gillen KT, Bernstein R, Celina M. Non-Arrhenius behavior for oxidative degradation of chlorosulfonated polyethylene materials. *Polym Degrad Stab* 2005;**87**:335.

[9] Gillen KT, Celina M, Keenan MR. Methods for predicting more confident lifetimes of seals in air environments. *Rubber Chem Technol* 2000;**73**:265.

[10] Gillen KT, Celina M, Bernstein R. Validation of improved methods for predicting long-term elastomeric seal lifetimes from compression stress-relaxation and oxygen consumption techniques. *Polym Degrad Stab* 2003;**82**:25.

[11] Celina M, Gillen KT, Assink RA. Accelerated aging and lifetime prediction: Review of non-Arrhenius behaviour due to two competing processes. *Polym Degrad Stab* 2005;**90**:395.

[12] Gillen KT, Celina M, Clough RL, Wise J. Extrapolation of accelerated aging data-Arrhenius or erroneous? *Trends Polym Sci* 1997;**5**:250.

[13] Gillen KT, Bernstein R, Derzon DK. Evidence of non-Arrhenius behavior from laboratory aging and 24-year field aging of polychloroprene rubber materials. *Polym Degrad Stab* 2005;**87**:57.

[14] Gillen KT, Assink RA, Bernstein R. Nuclear energy plant optimization (NEPO): Final report on aging and condition monitoring of low-voltage cable materials, Sandia National Laboratories, Albuquerque and Livermore, 2005, SAND2005-7331, pp 286.

[15] Wise J, Gillen KT, Clough RL. An ultrasensitive technique for testing the Arrhenius extrapolation assumption for thermally aged elastomers. *Polym Degrad Stab* 1995;**49**:403.

[16] Gillen KT, Bernstein R, Clough RL, Celina M. Lifetime predictions for semi-crystalline cable insulation materials: I. Mechanical properties and oxygen consumption measurements on EPR materials. *Polym Degrad Stab* 2006;**91**:2146.

[17] Gillen KT, Celina M, Bernstein R. Methods for predicting lifetimes and remaining lifetimes of polymers, In: Martin JW, Ryntz RA, Dickie RA, eds. Service Life Prediction, Challenging the Status Quo, Federation of Societies for Coatings Technology, 2005, p 67.

[18] Gillen KT, Celina M. The wear-out approach for predicting the remaining lifetime of materials. *Polym Degrad Stab* 2000;**71**:15.

[19] Gillen KT, Celina M, Bernstein R, Shedd M. Lifetime predictions of EPR materials using the Wear-out approach. *Polym Degrad Stab* 2006;**91**:3197.

[20] Gillen KT, Clough RL, Wise J. Prediction of elastomer lifetimes from accelerated thermal-aging experiments, In: Clough RL, Billingham NC, Gillen KT, eds. Polymer Durability: Degradation, Stabilization, and Lifetime Prediction. Washington, D.C., American Chemical Society, 1996, p 557.

[21] Celina M, Graham AC, Gillen KT, Assink RA, Minier LM. Thermal degradation studies of a polyurethane propellant binder. *Rubber Chem Technol* 2000;**73**:678.

[22] Gillen KT, Clough RL. Time-temperature-dose rate superposition: a methodology for extrapolating accelerated radiation aging data to low dose rate conditions. *Polym Degrad Stab* 1989;**24**:137.

[23] Gillen KT, Clough RL. Predictive aging results in radiation environments. *Radiat Phys Chem* 1993;**41**:803.
[24] Gillen KT, Clough RL. Accelerated aging methods for predicting long-term mechanical performance of polymers, In: Clegg DW, Collyer AA, eds. Irradiation Effects on Polymers. London, New York, Elsevier Applied Science, 1991, p 157.
[25] Gillen KT, Clough RL. A kinetic model for predicting oxidative degradation rates in combined radiation-thermal environments. *J Polym Sci Polym Chem Ed* 1985;**23**:2683.
[26] Richters P. Initiation process in the oxidation of polypropylene. *Macromolecules* 1970;**3**:262.
[27] Gugumus F. Chapter 6: The use of accelerated tests in the evaluation of antioxidants and light stabilizers, In: Scott G, ed. Developments in Polymer Stabilisation. London, Elsevier Applied Science, 1987, p 239.
[28] Bernstein BS, Lee P-N. Oxidative stability of high-density polyethylene cables. *Proc Int Wire Cable Symp* 1975;**24**:202.
[29] Gijsman P, Hennekens J, Vincent J. The influence of temperature and catalyst residues on the degradation of unstabilized polypropylene. *Polym Degrad Stab* 1993;**39**:271.
[30] Rosik L, Kovarova J, Pospisil J. Lifetime prediction of ABS polymers based on thermoanalytical data. *J Therm Anal* 1996;**46**:465.
[31] Gugumus F. Effect of temperature on the lifetime of stabilized and unstabilized PP films. *Polym Degrad Stab* 1999;**63**:41.
[32] Gillen KT, Assink R, Bernstein R, Celina M. Condition monitoring methods applied to degradation of chlorosulfonated polyethylene cable jacketing materials. *Polym Degrad Stab* 2006;**91**:1273.
[33] Gillen KT, Assink RA, Bernstein R. Condition monitoring approaches applied to a polychloroprene cable jacketing material. *Polym Degrad Stab* 2004;**84**:419.
[34] Gillen KT, Celina M, Clough RL. Density measurements as a condition monitoring approach for following the aging of nuclear power plant cable materials. *Radiat Phys Chem* 1999;**56**:429.
[35] Assink RA, Gillen KT, Sanderson B. Monitoring the degradation of a thermally aged EPDM terpolymer by 1H NMR relaxation measurements of solvent swelled samples. *Polymer* 2001;**43**:1349.
[36] Assink RA, Lang DP, Celina M. Condition monitoring of a thermally aged hydroxy-terminated polybutadiene (HTPB)/isophorone diisocyanate (IPDI) elastomer by nuclear magnetic resonance cross-polarization recovery times. *J Appl Polym Sci* 2001;**81**:453.
[37] Assink RA, Celina M, Minier LM. Condition monitoring of a thermally aged elastomer by 1H-NMR T2 relaxation measurements of solvent-swelled samples. *J Appl Polym Sci* 2002;**86**:3636.
[38] Assink RA, Celina M, Gillen KT. Monitoring the condition of thermally aged polymers by NMR relaxation measurements. *Polymer News* 2003;**28**:102.
[39] Assink RA, Celina MC, Gillen KT. Monitoring the condition of aged polymers by NMR relaxtion measurements. *Polym Prepr* 2003;**44**:311.
[40] Gillen KT, Bernstein R, Wilson MH. Predicting and confirming the lifetime of o-rings. *Polym Degrad Stab* 2005;**87**:257.
[41] Assink RA, Celina MC, Elliott JM. Acceleration factors for the oxidative aging of polymeric materials, In: Celina MC, Assink RA, eds. Polymer Durability and Radiation Effects. Washington, D.C., American Chemical Society, 2008, p 26.
[42] Gillen KT, Clough RL, Dhooge NJ. Density profiling of polymers. *Polymer* 1986;**27**:225.
[43] Gillen KT, Celina M, Clough RL, Malone M, Keenan MR, Wise J. New methods for predicting lifetimes in weapons. Part 1: Ultrasensitive oxygen consumption measurements to predict the lifetime of EPDM O-rings, Sandia National Laboratories, 1998, SAND98-1942, pp 38.
[44] Celina M, Minier L, Assink R. Development and application of tools to characterize the oxidative degradation of AP/HTPB/Al propellants in a propellant reliability study. *CPIA Publication* 2000;**697**:471.

[45] Celina M, Wise J, Ottesen DK, Gillen KT, Clough RL. Correlation of chemical and mechanical property changes during oxidative degradation of neoprene. *Polym Degrad Stab* 2000;**68**:171.
[46] Celina M, Gillen KT, Malone GM, Clough RL, Nelson WH. Polymer materials and component evaluation in acidic-radiation environments. *Radiat Phys Chem* 2001;**62**:153.
[47] Celina M, Gillen KT. Superposition and wear-out approaches applied to polymer lifetime prediction. *Polym Prepr* 2001;**42**:367.
[48] Gillen KT, Celina M, Clough RL. Limitations of the Arrhenius methodology, Sandia National Laboratories, Albuquerque, NM, USA., 1998, SAND98-1726C, pp 11.
[49] Gillen KT, Terrill ER, Winter RM. Modulus mapping of rubbers using micro- and nano-indentation techniques. *Rubber Chem Technol* 2001;**74**:428.
[50] Gillen KT, Celina M, Bernstein R. Review of the ultrasensitive oxygen consumption method for making more reliable extrapolated predictions of polymer lifetimes. *Ann Tech Conf Soc Plast Eng* 2004;**62**:2289.
[51] Celina M, Skutnik Elliott JM, Winters ST, Assink RA, Minier LM. Correlation of antioxidant depletion and mechanical performance during thermal degradation of an HTPB elastomer. *Polym Degrad Stab* 2006;**91**:1870.
[52] Celina M, Gillen KT. Advances in Exploring Mechanistic Variations in Thermal Aging of Polymers, In: Martin JWR, Rose A.; Chin, Joannie; Dickie, Ray A. , ed. Service Life Prediction of Polymeric Materials Global Perspectives, Springer, 2009, p 45.
[53] Celina M, Gillen KT, Wise J, Clough RL. Anomalous aging phenomena in a crosslinked polyolefin cable insulation. *Radiat Phys Chem* 1996;**48**:613.
[54] Celina M, Gillen KT, Clough RL. Inverse temperature and annealing phenomena during degradation of crosslinked polyolefins. *Polym Degrad Stab* 1998;**61**:231.
[55] Colin X, Marais C, Verdu J. A new method for predicting the thermal oxidation of thermoset matrices Application to an amine crosslinked epoxy. *Polym Test* 2001;**20**:795.
[56] Colin X, Marais C, Verdu J. Kinetic modelling and simulation of gravimetric curves: application to the oxidation of bismaleimide and epoxy resins. *Polym Degrad Stab* 2002;**78**:545.
[57] Colin X, Verdu J. Thermal ageing and lifetime prediction for organic matrix composites. *Plast Rubber Compos* 2003;**32**:349.
[58] Colin X, Fayolle B, Audouin L, Verdu J. About a quasi-universal character of unstabilized polyethylene thermal oxidation kinetics. *Polym Degrad Stab* 2003;**80**:67.
[59] Colin X, Audouin L, Verdu J. Determination of thermal oxidation rate constants by an inverse method. Application to polyethylene. *Polym Degrad Stab* 2004;**86**:309.
[60] Colin X, Mavel A, Marais C, Verdu J. Interaction between cracking and oxidation in organic matrix composites. *J Comp Mat* 2005;**39**:1371.
[61] Colin X, Verdu J. Strategy for studying thermal oxidation of organic matrix composites. *Comp Sci Tech* 2005;**65**:411.
[62] Rincon-Rubio LM, Colin X, Audouin L, Verdu J. A theoretical model for the diffusion-limited thermal oxidation of elastomers at medium temperatures. *Rubber Chem Technol* 2003;**76**:460.
[63] Fayolle B, Audouin L, Verdu J. Initial steps and embrittlement in the thermal oxidation of stabilized polypropylene films. *Polym Degrad Stab* 2001;**75**:123.
[64] Fayolle B, Audouin L, George GA, Verdu J. Macroscopic heterogeneity in stabilized polypropylene thermal oxidation. *Polym Degrad Stab* 2002;**77**:515.
[65] Fayolle B, Audouin L, Verdu J. A critical molar mass separating the ductile and brittle regimes as revealed by thermal oxidation in polypropylene. *Polymer* 2004;**45**:4323.
[66] Fayolle B, Tcharkhtchi A, Verdu J. Temperature and molecular weight dependence of fracture behaviour of polypropylene films. *Polym Test* 2004;**23**:939.
[67] IEEE Standard for Qualifying class IE Equipment for Nuclear Power Generating Stations, The Institue of Electrical and Electronics Engineers, Inc., 1974, Std. 323-1974, pp 24.

[68] Jacobus MJ. Aging, condition monitoring, and loss-of-coolant accident (LOCA) tests of class 1E electrical cables. Crosslinked polyolefin cables, Sandia National Laboratories, Albuquerque, NM, USA., 1991, NUREG/CR-5772, SAND91-1766/1, pp 189.
[69] Jacobus MJ. Aging, condition monitoring, and loss-of coolant accident (LOCA) tests of class 1E electrical cables: ethylene propylene rubber cables, Volume 2, Sandia National Laboratories, Albuquerque, NM, USA., 1991, NUREG/CR-5772, SAND91-1766/2, pp 228.
[70] Jacobus MJ. Aging, condition monitoring, and loss-of-coolant accident (LOCA) tests of class 1E electrical cables: miscellaneous cable types, Volume 3, Sandia National Laboratories, Albuquerque, NM, USA., 1991, NUREG/CR-5772, SAND91-1766/3, pp 144.
[71] Subudhi M. Literature review of environmental qualification of safety-related electric cables, Brookhaven National Laboratory, Upton, 1996, NUREG/CR-6384, BNL-NUREG-52480, pp 306.
[72] Yamamoto T, Minakawa T. The final report of the project of "Assessment of cable aging for nuclear power plants", Japan Nuclear Energy Safety Organization (JNES), Tokyo, 2009, JNES-SS-0903, pp 325.
[73] Nelson CF, Gauthier G, Carlin F, Attal M, Gaussens G, Le Tutour P, Morin C. Long-term aging and loss-of-coolant accident (LOCA) testing of electrical cables, Sandia National Laboratories, Albuquerque, 1996, NUREG/CR-6202; IPSN 94-03; SAND 94-0485, pp 154.
[74] Lofaro R, Grove E, Villaran M, Soo P, Hus F. Assessment of environmental qualification practices and condition monitoring techniques for low-voltage electric cables, condition monitoring test results, Brookhaven National Laboratory, Upton, 2001, NUREG/CR-6704.
[75] Gillen KT, Bernstein R. Review of nuclear power plant safety cable aging studies with recommendations for improved approaches and for future work, Sandia National Laboratories, Albuquerque and Livermore, 2010, SAND 2010-7266, pp 79.
[76] Assessment and management of ageing of major nuclear power plant components important to safety: In-containment instrumentation and control cables, International Atomic Energy Agency, Vienna, 2000, IAEA-TECDOC-1188, pp 100.
[77] Determination of long-term radiation ageing in polymers- Part 2: Procedures for predicting ageing at low dose rates, International Electrotechnical Commission, 1996, 1244-2, pp 56.
[78] IEEE Standard for Qualifying Class 1E Electric Cables and Field Splices for Nuclear Power Generating Stations, The Institue of Electrical and Electronics Engineers, Inc., 2003, Std. 383-2003, pp 15.
[79] Nowlen SP, Brown JW. Kerite Analysis in Thermal Environments of Fire (KATE-Fire): Test Results Sandia National Laboratory, Albuquerque, 2011, NUREG/CR-7102, SAND2011-6548P.
[80] Ito M, Kusama Y, Yagi T, Okada S, Yoshikawa M, Yoshida K. Progress on qualification testing methodology study of electric cables, In Twelfth Water Reactor Safety Research Information Meeting, October 22-26 1984, NUREG/CP-0058, Vol.5 1985.
[81] Kusama Y, Yagi T, Okada S, Ito M, Yoshikawa M, Yoshida K, Tamura N, Kawakami W. Progress on qualification testing methodology study of electric cables, In Fourteenth Water Reactor Safety Research Information Meeting, October 27-31 1986, NUREG/CP-0082, Vol.3 1987.
[82] Kusama Y, Okada S, Yoshikawa M, Ito M, Yagi T, Nakase Y, Seguchi T, Yoshida K. Methodology study for qualification testing of wire and cable LOCA conditions, In Tenth Water Reactor Safety Research Information Meeting, October 12-15 1982, NUREG/CP-0041, Vol.5 1983.
[83] Yoshida K, Seguchi T, Okada S, Ito M, Kusama Y, Yagi T, Yoshikawa M. Progress on qualification testing methodology study of electric cables, In Eleventh Water Reactor Safety Research Information Meeting, October 24-28 1983, NUREG/CP-0048, Vol.5 1984.
[84] Bustard LD, Chenion F, Carlin C, Alba G, Gaussens G, Le Meur M. The effect of alternative aging and accident simulations on polymer properties Sandia National Laboratories, Albuquerque, 1985, NUREG/CR-4091; SAND84-2291, pp 579.

[85] Gillen KT, Clough RL. Occurrence and implications of radiation dose-rate effects for material aging studies. *Radiat Phys Chem* 1981;**18**:679.
[86] Reynolds AB, Bell RM, Bryson NMN, Doyle TE, Hall MB, Mason LR, Quintric L, Terwilliger PL. Dose-rate effects of the radiation-induced oxidation of electric cable used in nuclear power plants. *Radiat Phys Chem* 1995;**45**:103.
[87] Placek V, Bartonicek B. The dose rate effect and the homogeneity of radio-oxidation of plastics. *Nucl Instrum Methods Phys Res, Sect B* 2001;**185**:355.
[88] Bonzon LL, Wyant FJ, Bustard LD, Gillen KT. Status report on equipment qualification issues, In Research and Resolution Sandia National Laboratories, Albuquerque, 1986, NUREG/CR-4301; SAND85-1309, pp 579.
[89] Howard JB, Gilroy HM. Some observations on the long-term behavior of stabilized polyethylene. *Polym Eng Sci* 1975;**15**:268.
[90] Bernstein R, Gillen KT. Nylon 6.6 accelerating aging studies: II. Long-term thermal-oxidative and hydrolysis results. *Polym Degrad Stab* 2010;**95**:1471.
[91] Gillen KT, Clough RL. Techniques for monitoring heterogeneous oxidation of polymers, In: Cheremisinoff NP, ed. Handbook of Polymer Science and Technology. New York, Marcel Decker, Inc., 1989, p 167.
[92] Gillen KT, Clough RL. Quantitative confirmation of simple theoretical models for diffusion-limited oxidation, In: Clough RL, Shalaby SW, eds. Radiation Effects on Polymers, ACS Series #475. Washington, D.C., ACS, 1991, p 457.
[93] Gillen KT, Clough RL. Rigorous experimental confirmation of a theoretical model for diffusion-limited oxidation. *Polymer* 1992;**33**:4358.
[94] Wise J, Gillen KT, Clough RL. Quantitative model for the time development of diffusion-limited oxidation profiles. *Polymer* 1997;**38**:1929.
[95] Wise J, Gillen KT, Clough RL. Time development of diffusion-limited oxidation profiles in a radiation environment. *Radiat Phys Chem* 1997;**49**:565.
[96] Assink RA, Celina M, Skutnik JM, Harris DJ. Use of a respirometer to measure oxidation rates of polymeric materials at ambient temperatures. *Polymer* 2005;**46**:11648.
[97] Gillen K, Wise J, Jones G, Causa A, Terrill E, Borowczak M. Final Report on Reliability and Lifetime Prediction, Sandia National Laboratories, 2012, SAND 2012-7644, pp 116.
[98] Chailan JF, Boiteux G, Chauchard J, Pinel B, Seytre G. Effects of thermal degradation on the viscoelastic and dielectric properties of chlorosulfonated polyethylene (CSPE) compounds. *Polym Degrad Stab* 1995;**48**:61.
[99] Clough RL, Gillen KT. Investigation of cable deterioration inside reactor containment. *Nucl Tech* 1982;**59**:344.
[100] Anandakumaran K, Stonkus DJ. Assessment of oxidative thermal degradation of crosslinked polyethylene and ethylene propylene rubber cable insulation. *Polym Eng Sci* 1992;**32**:1386.
[101] Arakawa K, Seguchi T, Yoshida K. Radiation-induced gas evolution in chlorine-containing polymer. Poly(vinyl chloride), chloroprene rubber, and chlorosulfonated-polyethylene. *Radiat Phys Chem* 1986;**27**:157.
[102] Seguchi T. Analysis of dose rate dependence on radiation thermal combined aging of polymer materials. Operability of Nuclear Power Systems in Normal and Adverse Environments, Albuquerque, NM, September 29, 1986- October 3, 1986 1986, pp 509.
[103] Calmet JF, Carlin F, Nguyen TM, Bousquet S, Quinot P. Irradiation ageing of CSPE/EPR control command electric cables. Correlation between mechanical properties and oxidation. *Radiat Phys Chem* 2002;**63**:235.
[104] Gillen KT, Clough RL. Aging predictions in nuclear power plants: crosslinked polyolefin and EPR cable insulation materials, Sandia National Laboratories, Albuquerque, NM, USA., 1991, SAND 91-0882, pp 56.
[105] Celina M, Gillen KT. Oxygen Permeability Measurements on Elastomers at Temperatures up to 225°C. *Macromolecules* 2005;**38**:2754.

[106] Seguchi T, Yamamoto Y. Diffusion and solubility of oxygen in gamma -ray irradiated polymer insulation materials, JAERI,Takasaki,Japan., 1986, pp 64.
[107] IEEE Guide for Designing Multistress Aging Tests of Electrical Insulation in a Radiation Environment, The Institue of Electrical and Electronics Engineers, Inc., 1993, Std. 775-1993, pp 16.
[108] Scheirs J, Bigger SW, Billingham NC. A review of oxygen uptake techniques for measuring polyolefin oxidation. *Polym Test* 1995;**14**:211.
[109] Celina M, George GA. Characterization and degradation studies of peroxide and silane crosslinked polyethylene. *Polym Degrad Stab* 1995;**48**:297.
[110] Gillen KT, Clough RL, Quintana CA. Modulus profiling of polymers. *Polym Degrad Stab* 1987;**17**:31.
[111] Celina M, Wise J, Ottesen DK, Gillen KT, Clough RL. Oxidation profiles of thermally aged nitrile rubber. *Polym Degrad Stab* 1998;**60**:493.
[112] Gillen KT, Green PF. Moisture permeation of environmental seals used in weapons, Sandia National Laboratories, Albuquerque, NM, USA., 1992, SAND92-2651, pp 24.

Distribution

1	MS-0899	Technical Library	9536

2 Christopher White and Stephanie Watson
NIST - National Institute of Standards
100 Bureau Drive, Stop 731.04, Building 226
Gaithersburg, MD 20899-8615

1 Sheila Ray
U.S. Nuclear Regulatory Commission
11555 Rockville Pike, Rockville, MD 20852

1	MS-0885	Aselage, Terrence L.	1810
1	MS-0886	Aubert James H.	1819
1	MS-0888	McElhanon, James R.	1835
1	MS-1411	Celina Mathias C.	1819
1	MS-1411	Gillen Kenneth T.	1819
1	MS-1411	Giron, Nicholas H.	1819
1	MS-1411	Quintana, Adam D.	1819
1	MS-0888	Bernstein, Robert	1835
1	MS-0888	White II, Gregory V.	1835
1	MS-0747	Lindgren, Eric R.	6223
1	MS-0747	Gelbard, Fred	6223
1	MS-0747	Sorenson, Ken B.	6223
1	MS-0744	Mattie, Patrick D.	6233

INTENTIONALLY LEFT BLANK

INTENTIONALLY LEFT BLANK

Sandia National Laboratories